Neuroendocrine and metabolic responses to desiccation stress in *Drosophila melanogaster*

A thesis submitted for the degree of Doctor of Philosophy at the University of Glasgow

Elizabeth Cannell

Molecular and Integrative Physiology

Institute of Molecular, Cell, and Systems Biology

College of Medical, Veterinary, and Life Sciences

University of Glasgow, Glasgow

G12 8QQ, UK

November 2015

Abstract

Insects are highly successful and their large numbers lead to economic loss through crop damage and disease transmission. Insecticides provide a valuable tool for control of insect populations. However, as resistance is increasing to existing products, new modes of action are required for the development of novel products. Understanding of the biological mechanisms underlying stress resistance in insects may provide insight into new potential insecticide targets.

Malpighian tubules are critical for epithelial fluid transport and xenobiotic tolerance in insects. The function of Malpighian tubules in desiccation stress tolerance was explored by examining changes in gene expression, protein levels, fluid transport rates, and metabolism following stress exposure. The results indicate a reduction in secretion rate during desiccation that is reflected in accumulation of metabolites that are normally processed and excreted by the tubules.

Moreover, the involvement of *Drosophila melanogaster* diuretic hormones corticotrophin releasing factor-like (DH_{44}) and leucokinin (LK) were examined using genetic manipulations based on the GAL4-UAS system. Highly selective manipulation of the DH_{44}-producing neurons via knockdown of *DH_{44}* and neuronal ablation indicates that suppression of DH_{44} signalling contributes to desiccation tolerance. This result is supported by the finding that knockdown of *DH_{44} receptor 2* in the Malpighian tubule principal cells improves survival during desiccation stress.

Previous work suggests the possibility of interaction between LK and DH_{44} signalling as LK receptor (LKR) is colocalised to the DH_{44} neurons. This hypothesis is supported by the results of this study as selective knockdown of *LKR* and *DH_{44}* in the DH_{44} neurons produced opposing effects on desiccation tolerance. Moreover, knockdown of *DH_{44}* in the DH_{44} neurons or ablation of these neurons resulted in significantly decreased *LKR* expression in the Malpighian tubules.

Finally, a novel role for the Malpighian tubules in starvation tolerance was uncovered by the study, with *LKR* gene expression increasing significantly following starvation. Knockdowns of either *DH44-R2* or *LKR* in the Malpighian

tubules significantly impaired starvation tolerance. Here, a mechanism for this role of renal epithelia in starvation tolerance is proposed.

Table of Contents

List of Tables

List of Figures

Acknowledgement

I would like to express my gratitude to my supervisors Professors Shireen Davies and Julian Dow, for the guidance and ideas that they provided throughout my research project. I would also like to thank Dr. Selim Terhzaz for his suggestions and ideas and for helping me find my feet in *Drosophila* research. Many thanks to the members of the Dow/Davies laboratory who sacrificed their time to teach me technical skills and to the members of the Glasgow Polyomics Facility for answering manifold questions about metabolomics analysis and datasets. My gratitude also extends to my review panel, Dr. Mathis Riehle and Professor Anna Amtmann for their encouraging comments and challenging questions. Finally, I would like to thank the programme directors of the Wellcome Trust four-year Molecular Functions in Disease program, Professor Darren Monckton and Dr Olywn Byron, for giving me the opportunity to pursue my interest in molecular biology and the Wellcome Trust for financing my research.

My thanks extend also to those who supported me outside of the lab, especially my husband Stephan Keune, who has been there for me since the beginning of the project.

Author's Declaration

The research reported within this thesis is my own work except where otherwise stated, and has not been submitted for any other degree.

Material from this thesis has been published (Cannell et al 2016).

Elizabeth Cannell

Abbreviations

µg	Microgram
µl	Microlitre
ATP	Adenosine triphosphate
B	Blank
bp	Base pairs
cAMP	Cyclic adenosine monophosphate
capaR	Capa receptor
cDNA	Complementary DNA
cGMP	Cyclic guanosine monophosphate
C	Celsius
CI	Confidence interval
CMT	Control Malpighian tubules
CRF	Corticotrophin releasing factor
CS	Canton S
C_T	Threshold cycle
CWF	Control whole fly
DAPI	4',6-diamidino-2-phenylindole
d*f*	Degrees of freedom
DH_{31}	Diuretic hormone 31
DH_{44}	Diuretic hormone 44
DH_{44}-F	Diuretic hormone 44 – fluorescent tag
DH44-R1	Diuretic hormone 44 receptor 1
DH44-R2	Diuretic hormone 44 receptor 2
DMT	Desiccated Malpighian tubules
DNA	Deoxyribonucleic acid
dsRNA	Double-stranded ribonucleic acid
DWF	Desiccated whole fly
EDTA	Ethylenediaminetetraacetic acid
ESI	Electrospray ionisation
g	Acceleration equal to gravity
GC	Gas chromatography
GFP	Green fluorescent protein
GPCR	G-protein-coupled receptor
HILIC	Hydrophilic interaction chromatography
HR	Hazard ratio
KEGG	Kyoto Encyclopedia of genes and genomes
LC	Liquid chromatography
LK	Leucokinin
LKR	Leucokinin receptor
LSM	Laser scanning microscopy
M	Molar
M	Mean
min	Minute

ml	Millilitre
mm	Millimetre
mRNA	Messenger ribonucleic acid
MS	Mass spectroscopy
MT	Malpighian tubules
m/*z*	Ratio of mass number to charge number
ng	Nanogram
nm	Nanometre
NMR	Nuclear magnetic resonance
PBS	Phosphate-buffered saline
PBTA	PBS/Triton/Azide
PC1	Principal component 1
PC2	Principal component 2
PCR	Polymerase chain reaction
ppm	Parts per million
r	Radius
RISC	Ribonucleic acid-induced silencing complex
RNA	Ribonucleic acid
RNAi	Ribonucleic acid interference
RNAse	Ribonuclease
RT	Retention time
RT-PCR	Reverse transcription polymerase chain reaction
SD	Standard deviation
SE	Standard error
SEM	Standard error of the mean
SMT	Starved Malpighian tubules
TBE	Tris/Borate/EDTA buffer
TMR	Tetramethylrhodamine
UAS	Upstream activation sequence
v	Volume
V	Volts
V-ATPase	Vacuolar H^+-adenosine triphosphatase
WF	Whole fly
w^h	White honey (fly genotype)
ZIC-HILIC	Zwitterionic hydrophilic interaction liquid chromatography

1 Introduction

Insects are extremely successful, both in terms of their sheer numbers and in their ability to adapt to survive harsh conditions. Because of their numbers, they inflict significant economic damage annually through crop losses and the spread of disease. Consequently, it is important to be able to control insect populations.

Integrated pest management, which depends on the use of mechanical controls, biological controls, and responsible use of pesticides to bring pest populations down to below the economic injury level, requires sufficiently effective insecticide tools in order to manage insect populations. However, there is presently a great need for insecticides employing new mechanisms of action as resistance to existing compounds has increased and changes in policy have resulted in stringent restriction of the use of some of the effective products, particularly in the European market.

Insects are faced with numerous environmental stressors, many of which they have adapted mechanisms to resist. One of the most potent stressors faced by insects is desiccation, due to their high surface to volume ratio. If the mechanisms of desiccation tolerance are understood, it is possible that methods of interfering with them could be developed, laying the foundation for the discovery of novel insecticides.

Survival of desiccation stress has been found to be significantly affected by the Malpighian tubules, a key epithelial tissue for fluid homeostasis, detoxification, immunity, and stress signalling. The secretion rate of Malpighian tubules can be controlled in insects through regulation of diuretic hormones and has been found to be suppressed by desiccation exposure. Changes in diuretic hormone signalling have been found to be associated with desiccation survival, indicating that regulation of these peptides may be an endogenous mechanism of stress tolerance in some insects.

In order to understand the changes underlying Malpighian tubule adaptation during desiccation, the model insect *Drosophila melanogaster* is used. The plethora of transgenic *D. melanogaster* stocks and ease of rearing enables rapid

and precise manipulation of specific cells and tissues, including both the brain and tubules, in an intact organism. The mechanisms of desiccation survival are explored by examining the effect of desiccation on tubule metabolism and by genetically manipulating diuretic hormone signalling pathways while monitoring changes in stress survival.

In particular, this study focuses on the role of corticotrophin releasing factor-like peptide (CRF-like), known as diuretic hormone 44 (DH_{44}) in a number of insects including *D. melanogaster*, in desiccation stress survival and its interactions with the leucokinin (LK) signalling pathway. As the endocrine system of insects becomes better characterised, it is possible that potential points of interference will emerge that can be exploited for the development of insecticides with novel modes of action.

1.1 Insects as pest species

Insects are highly abundant life forms that have adapted to withstand extreme variations in environmental conditions. Their success both in terms of resilience and population size makes them particularly potent disease vectors. Plant and animal diseases transmitted by insects are responsible for substantial GDP losses globally each year (Dhaliwal et al 2015, Oliveira et al 2014). Additionally, biting flies, such as the mosquito *Aedes aegypti*, are responsible for spreading human diseases like dengue fever, both in its usual and life-threatening haemorrhagic forms (Schneider 2000). Dengue virus is a particularly pressing global concern as approximately 40% of the world's population is at risk of contracting dengue virus (World Health Organisation 2012). As temperatures continue to increase globally and international travel remains common, local transmission of dengue fever has spread to Europe and the possibility of an outbreak of dengue fever in Europe now exists.

At present there is no specific treatment or immunization available to combat dengue virus, rather disease control efforts focus on managing *Aedes* populations (World Health Organisation 2012). This approach relies heavily on strategic insecticide spraying, which is expensive and therefore not always economically viable (Ranson et al 2010, Schneider 2000). Moreover, the efficacy of this method is now being hampered by increased insecticide resistance in *Aedes*

populations (Marcombe et al 2011). Consequently, the development of a novel insecticide against *Aedes aegypti* could renew the effectiveness of dengue control efforts, at least until more specific treatments are available against the virus itself. By increasing our understanding of the ways in which flies cope with environmental stress, it is possible that a new mechanism of population control might be uncovered. The variation in the roles and effects of specific neuropeptides in differing insect species could potentially enable the development of insecticides that target pest species, while sparing beneficial ones (Schooley et al 2011). This is particularly important as policy in the European Union has recently shifted towards reducing the availability of existing pesticides (Jess et al 2014).

1.2 *Drosophila melanogaster*

Research using *D. melanogaster* has been on-going for well over a century (Jennings 2011). During much of this time *Drosophila* has served as a genetic and developmental model and has played a role in seminal discoveries in these fields (Dow 2012a). In more recent years, *Drosophila* has emerged as a model organism in many capacities, including as a model for human diseases like Huntington's disease, kidney stones, and inborn errors of metabolism, as well as a model for insect pests and insect disease vectors (Campesan et al 2011, Dow & Romero 2010, Kamleh et al 2008, Schneider 2000). The suitability of *D. melanogaster* as a model organism is enhanced by its published genome, relative ease of lab rearing, and diverse tools for genetic manipulation (Adams et al 2000, Dow 2012a).

In the present day, the selection of *Drosophila* as an organism for research is a profoundly practical one (Dow 2012a). It is easily kept in the lab and can be bred and reared to adulthood in as few as 10 days, requiring only synthetic diet in a small vial (Ashburner 1989). With over a hundred flies emerging from a single mating pair, statistical power or acquisition of biomass is rarely a concern when using *Drosophila*. Even the small size of the tissues provides an advantage over larger organisms – where larger brains might benefit from slicing prior to visualisation, the *Drosophila* brain can be viewed in its entirety using confocal microscopy.

1.2.1 Epithelial tissue

Epithelial tissue performs the critically important role in both insects and higher organisms of delineating and protecting blood vessels and organs through the formation of a cell mono- or multilayer (Guillot & Lecuit 2013). Epithelial tissues comprise the first line of defence against pathogens and maintain unique physiological environments through the control of transport processes across the plasma membrane. As archetypal polarised tissues, epithelia have two surfaces – the one which encounters the external environment, called the basolateral membrane and the apical membrane, which faces internally to the lumen. Epithelial tissues have been studied in *Drosophila*, making use of its tractability as a genetic model (Tepass et al 2001).

1.2.1.1 Malpighian tubules

One epithelial tissue in particular, the Malpighian tubule, has become a model not only for morphogenesis of epithelia in general, but also for transport mechanisms and maintenance of homeostasis, especially in *D. melanogaster* (Beyenbach et al 2010, Dow et al 1994, O'Donnell et al 1996). The Malpighian tubules are the primary fluid transporting, or excretory, organ in insects and are analogous in function to the vertebrate kidney (Beyenbach et al 2010). They carry out critical functions, including regulation of fluid and osmotic homeostasis, detoxification, stress signalling, and immune signalling (Chung et al 2009, Davies et al 2014, Davies et al 2012, Dow 2009, Poupardin et al 2010, Terhzaz et al 2015a, Terhzaz et al 2014). The tubules are furthermore part of the excretory system, which serves to eliminate metabolic waste, as well as excess fluid and solutes (Klowden 2008). The hindgut contributes to water homeostasis, mainly via water adsorption (Luan et al 2015).

The Malpighian tubules are tubular in shape, found in pairs, and joined by a shared ureter, as shown in Figure 1.1. The ureter forms a junction with the alimentary canal into which it secretes (Wessing & Eichelberg 1978). In *Drosophila*, there are two pairs of tubules, one which projects posteriorly into the abdomen, while the other sits anteriorly in the body cavity (Dow & Davies 2003). Transport and signalling functions are performed by both sets of tubules, although differential gene expression suggests that some functions, including

calcium handling and ammonia generation, are specialities of only one of the two tubule pairs (Chintapalli et al 2012).

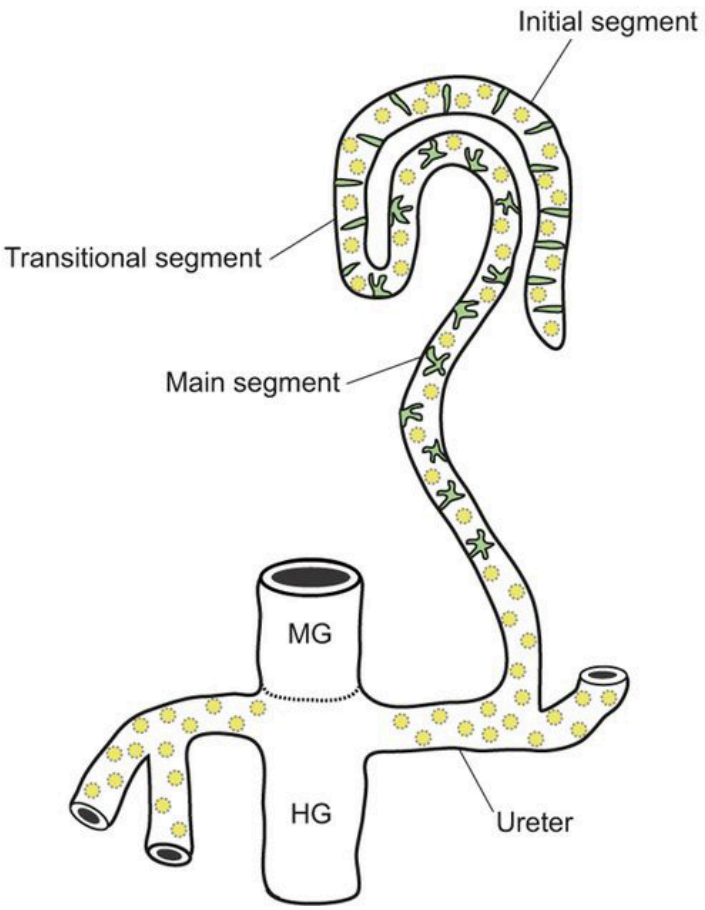

Figure 1.1 The *D melanogaster* Malpighian tubule.
The Malpighian tubules of *D. melanogaster* are formed of three distinct segments plus the ureter, which joins each pair of tubules to the hindgut (HG). Stellate cells are shown in green, with principal cells shown in yellow. MG = midgut. Image from (Denholm et al 2013) used with permission from The Company of Biologists Ltd.

The tubules can be further categorised into three segments based on physiological differences along the length of the tubule pairs. The transitional segment sits between the main segment, which is attached to the ureter, and the initial segment, which forms the blind end of the tubules. The main segment of the tubules is characterised by two distinctive types of cells: stellate (star-shaped) cells and principal cells, which are columnar (Sozen et al 1997). Bar-shaped cells have been observed in the initial segment and may be analogous to stellate cells (Sozen et al 1997).

Regulation of fluid homeostasis by the Malpighian tubules operates primarily through transcellular transport of ions across the epithelium. In *D. melanogaster,* this function is divided between two cell types, with the principal cells specialising in cation transport and the stellate cells transporting anions (O'Donnell et al 1996, O'Donnell et al 1998). Water movement across the tubule epithelium is thought to be driven by the osmotic gradient generated by ion transport, with transcellular pathways supporting fluid movement (Donnell et al 1982, Sofia Hernandez et al 1995). These pathways may be mediated by water channels, or aquaporins, as several aquaporin channel homologues have been found in *D. melanogaster*, with at least one localising to the Malpighian tubule stellate cells (Beyenbach et al 2010, Kaufmann et al 2005).

Cation transport in the principal cells is thought to be primarily driven by a vacuolar H^+-ATPase (V-ATPase) located at the apical membrane of principal cells (Allan et al 2005, Beyenbach et al 2010, Dow et al 1994, Wang et al 2004). By transporting H^+ across this membrane, from the principal cell cytoplasm to the tubule lumen, an electrical gradient is created. The membrane voltage drives movement of K^+ and Na^+ across the basolateral membrane, where the ions are further transported into the lumen. According to the Wieczorek model, this movement is supported by metal-proton exchanging proteins, although the exact identity of these exchangers is not entirely clear (Wieczorek et al 1991). Recent work has identified a Na^+/H^+ exchanger that is highly expressed in *Drosophila* epithelia and which is involved in tubule fluid secretion (Chintapalli et al 2015, Chintapalli et al 2013b, Day et al 2008). The electrical circuit is thought to be completed by the conductance of Cl^- by the stellate cells (Dow 2012b).

Fluid secretion can be stimulated in *Drosophila* by action on a number of receptors located on the basolateral membrane of the tubules. In the stellate cells, the diuretic hormone LK stimulates chloride conductance via intracellular Ca^{2+} signalling (Dow 2012b, Terhzaz et al 1999). This is dependent on a CLC chloride channel that is found both on the basolateral and apical membrane (Cabrero et al 2014). Tyramine, a biogenic amine, can also stimulate chloride shunt conductance in the stellate cells through Ca^{2+} signalling (Blumenthal 2003, Cabrero et al 2013). Resting chloride conductance is not dependent on the CLC chloride channel and may be underpinned by paracellular routes (Cabrero et al 2014).

In the principal cells, intracellular signalling occurs via secondary messengers including calcium, cyclic adenosine monophosphate (cAMP), and cyclic guanosine monophosphate (cGMP), particularly in response to stimulation by neuropeptides (Davies et al 2014). Cyclic nucleotide signalling increases fluid secretion by increasing the membrane potential of the tubules, likely by increasing ATP availability to the V-ATPase (Davies et al 2014, Davies et al 2013, Dow et al 1994). Calcium signalling has multiple effects, influencing V-ATPase function, ion transport, and fluid secretion rates (Davies & Terhzaz 2009). Neuropeptides from the capa peptide family stimulate fluid secretion by the tubules via cGMP and Ca^{2+} signalling in principal cells (Davies et al 2013, Davies et al 1995). Principal cell cAMP signalling is stimulated by neuropeptides DH_{44} and calcitonin-like DH_{31} (Cabrero et al 2002, Coast et al 2001).

1.2.2 Similarity to pest species

As a Dipteran, *Drosophila* is a member of the second largest order of insects, including many important disease vectors and crop pests (Dow 2012a). In particular, *D. melanogaster* is closely related to the soft fruit pest *Drosophila suzukii*, which is currently expanding its presence globally (Chiu et al 2013, Rota-Stabelli et al 2013). The Southeast Asian species invaded the USA mainland, with detection reported in 2008 (Walsh et al 2011). In the same year it was found in Mediterranean countries including Spain and Italy. By 2012 it had spread to most of the European Union countries, including the United Kingdom, and is being recognized as a major threat to soft fruit production (Rota-Stabelli et al 2013). Recent work sequencing the genome of *D. suzukii* has identified homologous genes in *D. melanogaster* for 91.2% of protein-coding genes, indicating that the model organism is well positioned to support the development of new population control strategies (Chiu et al 2013).

Drosophila also shares similarities with disease vectors *Anopheles gambiae*, *Aedes aegypti*, and the tsetse fly, which are responsible for the spread of diseases including malaria, dengue fever, and trypanosomiasis. These similarities include not only genetic homology, but also common physiological features and shared mechanisms of insecticide resistance (Daborn et al 2002, Gilleard et al 2005, Schneider 2000). Many features that could present potential insecticide targets, including diuretic hormone signalling to the Malpighian tubules, are

broadly conserved across insect species within, and to some extent beyond, the Diptera class (Beyenbach et al 2010, Coast et al 2002, Halberg et al 2015). This similarity to economically and ethically important species combined with its genetic tractability, easy laboratory care, and cost effectiveness, places *Drosophila* in a particularly apt position to act as a model organism for pest species to enable understanding of physiological mechanisms that could underlie the development of new approaches to population control.

1.2.3 Genetic toolkit

The variety of genetic tools that have been developed for use with *D. melanogaster* has made it into an outstandingly useful model for functional genomics (Dow 2012a). When these are considered in combination with the ease of rearing *Drosophila* in the lab, it is evident that the fruit fly is a particularly time-efficient and cost-effective organism for physiological research. A wide variety of fly lines carrying different defined constructs or mutations are available from a number of stock centres, including the Bloomington Stock Center and the Vienna *Drosophila* RNAi (ribonucleic acid interference) library.

One of the key facets of the *Drosophila* genetic toolkit is balancer chromosomes. These involve a series of chromosomal inversions paired with phenotypic markers that simultaneously prevent genetic recombination and enable identification of flies carrying the balancer chromosome by simple visual inspection (Dow 2012a). This makes it possible to keep a genetic construct stable and intact even in a heterozygous fly line.

1.2.3.1 Enhancer trapping

P-elements, which are a type of *Drosophila* transposon, are DNA sequences that can move within the genome when they are not repressed by naturally occurring inhibitors. These have been modified for use as a mutagen (Rubin & Spradling 1982). One particular application, called enhancer trapping, involves integrating transgenic P-element constructs containing a reporter gene into the genome downstream of a promoter gene (O'Kane & Gehring 1987). The promoter may then drive expression of the reporter gene, resulting in potentially interesting expression patterns.

1.2.3.2 Heritable RNAi

When double-stranded RNA (dsRNA) is present in *Drosophila*, the Dicer enzyme cleaves it into small interfering RNAs (Bellés 2009). These couple with the RNA-induced silencing complex (RISC) to degrade endogenous RNA transcripts. This process can be used to inhibit gene expression using transgenic P-elements containing a sequence encoding a double-stranded hairpin loop that will produce a dsRNA sequence relating to a particular gene of interest when expressed (Kennerdell & Carthew 2000). This results in reduced transcript levels as Dicer and RISC together degrade the target RNA sequences, which can result in corresponding loss-of-function phenotypes (Bellés 2009).

1.2.3.3 GAL4-UAS System

One application of the enhancer trapping technique is the GAL4-UAS binary expression system (Brand & Perrimon 1993). In *Drosophila,* the yeast transcription factor GAL4 is often positioned near an enhancer sequence for a gene of interest using P-elements. This can result in a wide variety of tissue or cell-specific GAL4 expression patterns. The UAS promoter sequence is activated by GAL4 in yeast, and in *Drosophila,* genetic sequences can be inserted into the genome downstream of the UAS promoter, including sequences coding for dsRNAi, fluorescent proteins like GFP, or the gene *reaper*, which triggers cell apoptosis.

Crossing a fly line containing a GAL4 or 'driver line' that expresses GAL4 in a particular pattern to a fly line with a genetic construct under control of the UAS promoter will cause tissue-specific expression of that construct in the pattern of the driver line (Duffy 2002). This approach can be used for a variety of applications, such as visualisation of a driver line expression pattern, ubiquitous expression of RNAi against a gene of interest, or highly specific ablation of defined groups of cells. Performing these kinds of crosses in *Drosophila* is fairly straightforward as newly emerged and therefore virgin flies can be easily identified by their distinctive physiological appearance. This makes it possible to identify females that have recently emerged and therefore have not yet mated (Ashburner 1989). Thus, virgin females can be easily isolated and used to combine heritable genetic constructs in a defined manner (Dow 2012a).

1.3 Diuretic and antidiuretic hormones

Two different classes of hormones are known to act on the insect excretory system to modify urine production: diuretic hormones act to increase the production of urine, while antidiuretic hormones typically increase the rate of water reabsorption by the hindgut (Coast et al 2002). These hormones are usually produced by neurosecretory cells in the brain and ventral nerve cord ganglia (Coast 2006). After release into the circulation, many of these act at receptors on the Malpighian tubules. Where these receptors are known, they are typically G-protein coupled receptors (GPCR) acting through second messenger cascades including cAMP, cGMP, or Ca^{2+}-mediated signalling (Coast 2006), as described in section 1.2.1.1.

Although several diuretic peptides have been identified and functionally explored in *D. melanogaster*, this study focuses on two in particular, CRF-like, or DH_{44}, and LK. Both of these peptides have additionally been implicated in functions that may not be directly related to their role as a diuretic peptide, as described in the following two sections.

1.3.1 Corticotropin releasing factor-like (DH_{44})

CRF-like peptide, also known as DH_{44} in *D. melanogaster* as it is 44 amino acids long (see Figure 1.2), has been shown to increase fluid production when applied to isolated Malpighian tubules (Cabrero et al 2002). This effect is due to its action on DH44-R2, a GPCR that is localised to the basolateral membrane of principal cells (section 3.2.1.2) in the *D. melanogaster* Malpighian tubule (Cabrero et al 2002, Hector et al 2009). Another DH_{44} receptor has also been identified, DH44-R1 (Johnson et al 2004), however the transcript of this receptor is primarily expressed in the adult brain (Chintapalli et al 2007) and its sensitivity to DH_{44} is two-fold higher than the sensitivity of the tubule to DH_{44} (Hector et al 2009). Additionally, stimulation of DH44-R1 has been shown to increase both cAMP and Ca^{2+} intracellular levels (Hector et al 2009), rather than only cAMP levels, as found when stimulating the tubules with DH_{44} (Cabrero et al 2002). Thus, the function of DH44-R1 seems to be distinct from that of DH44-R2.

NKPSLSIVNPLDVLRQRLLLEIARRQMKENSRQVELNRAILKNV

Figure 1.2 Amino acid sequence of DH_{44}

Amino acid sequence of DH_{44} previously reported in (Cabrero et al 2002). A = alanine, D = aspartate, E = glutamate, I = isoleucine, K = lysine, L = leucine, M = methionine, N = asparagine, P = proline, Q = glutamine, R = arginine, S = serine, V = valine.

DH_{44} also stimulates cAMP phosphodiesterase activity in the tubules, providing a mechanism for signal termination through breakdown of cAMP (Cabrero et al 2002). The cAMP signal appears to be tightly controlled in the Malpighian tubule as it is compartmentalised, a process involving roles for the cAMP exchange protein and protein kinase A (Borland et al 2009, Efetova et al 2013, Houslay 2010). This compartmentalisation may serve to distinguish DH_{44} and DH_{31} signals, as both stimulate cAMP in tubule principal cells (Davies et al 2014).

DH_{44} peptide is produced by neuroendocrine cells in the brain, specifically in three bilateral pairs of cells in the pars intercerebralis with axons extending to the retrocerebral complex of the corpus cardiacum (Cabrero et al 2002). This is similar to a number of other insect species (Vanden Broeck 2001).

1.3.1.1 Functional studies of DH_{44} peptide in *Drosophila*

Consistent with the role of DH_{44} as a diuretic peptide, RNAi knockdown of *DH44-R2* expression impairs survival during osmotic stress (Hector et al 2009). Recent evidence indicates that DH_{44} peptide may have a role in coordinating the response of the excretory system to food intake. Application of DH_{44} to the gut has been found to increase gut contractions, while *D. melanogaster* with mutations of genes *Dh44*, *DH44-R1*, or *DH44-R2* had a reduced rate of excretion when measured in terms of numbers of waste deposits (Dus et al 2015). Moreover, the DH_{44} neurons are activated in response to nutritive sugars, a response that could underlie a coordinated response by the gut and Malpighian tubules to feeding (Dus et al 2015).

Reproductive regulation by the DH_{44} neurons has also been identified in *D. melanogaster*, such that female flies with knockdown of DH_{44} ejected sperm shortly after mating and laid significantly fewer eggs than control flies (Lee et al 2015). This effect was recapitulated by knockdown of brain *DH44-R1*, but not by

knockdown of *DH44-R2*, which is most enriched in expression in the adult Malpighian tubule (Chintapalli et al 2007). This finding is not entirely unprecedented as regulation of feeding and reproduction by a peptide homologous to DH_{44} was found in the desert locust *Schistocerca gregaria* (Van Wielendaele et al 2012). Regulation of reproduction could potentially form part of a coordinated response to nutritional status, with unique roles for each of the two DH_{44} receptors.

DH_{44} neurons receive inputs from the circadian-timing system, which is known to project to the pars intercerebralis (Cavanaugh et al 2014, Hall 2003, Kaneko & Hall 2000). The DH_{44} neurons appear to be involved in rhythms of rest and activity in *D. melanogaster* as these patterns can be disrupted by knockdown of *Dh44* in the DH_{44} neurons, by constitutive activation of the DH_{44} neurons, and by ablation of the DH_{44} neurons (Cavanaugh et al 2014). Although the mechanism underlying this effect has not been clarified, *Dh44* mRNA and DH_{44} protein levels were not found to be associated with circadian rhythm (Cavanaugh et al 2014). Rhythmic locomotion may be associated with feeding and metabolism behaviours, as both of these are regulated by circadian rhythm (Xu et al 2008). The excretory system may likewise be coordinated by circadian rhythm as evidence suggests that the Malpighian tubules have a neural-independent circadian pacemaker (Hege et al 1997).

Overall, the DH_{44} neurons appear to be involved in a number of behaviours that could conceivably be related to feeding. Nutrient detection could coordinate excretory responses and signal to the reproductive system regarding the availability of nutrients for egg laying. Circadian rhythm could affect feeding behaviour via DH_{44} neurons. This could poise DH_{44} as a particularly useful neuropeptide for coordination of stress responses relating to the availability of food or water. In the absence of nutritive substances, the DH_{44} neurons may release less peptide, causing a decrease in reproductive activity and likely affecting secretion by the Malpighian tubules and gut movement.

1.3.2 Leucokinin

Although up to eight LK peptides have been discovered in insects, only one has been identified in *D. melanogaster* (Terhzaz et al 1999). When applied to

isolated Malpighian tubules, *D. melanogaster* LK acts on stellate cells, increasing fluid secretion by elevating intracellular Ca^{2+} levels and altering chloride shunt conductance (Cabrero et al 2014, Radford et al 2002, Terhzaz et al 1999).

LK has been localised to both the brain and the ventral nerve cord (Cantera & Nassel 1992). In adult *Drosophila*, the brain LK neurons are found in the lateral horn of the procerebrum and in the subesophageal ganglia (de Haro et al 2010, Liu et al 2015). In the ventral nerve cord, LK neurons are found that project to the heart and abdominal body wall (Cantera et al 1992). These are called abdominal neurons and can be split into two groups based on their appearance during development; the posterior abdominal LK neurons are found in both larvae and adults, while the anterior abdominal LK neurons appear only in adult flies (Liu et al 2015).

The LK receptor (LKR) of *Drosophila melanogaster* is a GPCR that is expressed in stellate cells of the Malpighian tubules, two pairs of three cells in the pars intercerebralis of the brain, and in the adult gonads (Radford et al 2002). The LKR-expressing pars intercerebralis neurons also express DH_{44} peptide (Cabrero et al 2002).

1.3.2.1 Functional studies of leucokinin signalling in *Drosophila melanogaster*

The role of LK signalling in fluid homeostasis is supported by the finding that the concentration of waste deposits is affected by manipulation of the LK neurons (Cognigni et al 2011). More specifically, activating the LK neurons using a heat activated ion channel resulted in less concentrated and more abundant deposits, which was interpreted to indicate that a higher ratio of fluid to solid waste was being excreted by the flies. Conversely, inactivation of LK neurons resulted in smaller and more concentrated waste deposits. Persistent inactivation of the LK neurons or ubiquitous knockdown of *LKR* results in bloating with fluid being retained outside of the gut, a phenotype that is not recapitulated by neuronal knockdown of *LKR* (Cognigni et al 2011, Liu et al 2015). Thus, it appears that LK influences fluid homeostasis specifically through action on LKR in non-neuronal tissues, which is consistent with a significant role for LK as a diuretic hormone acting on the Malpighian tubules.

LK signalling in the *D. melanogaster* brain has been shown to play a role in feeding behaviour, appearing to be particularly important for the termination of a meal (Al-Anzi et al 2010). Disruption of expression of the LK neuropeptide or receptor genes, via mutation or RNAi knockdown, results in increased meal size accompanied by reduced meal frequency. This phenotype can be rescued by pan-neuronal expression of either LK or LKR in its respective mutant background. Other feeding-related phenotypes have been observed following manipulation of LK signalling. For example, silencing of the LK neurons was found to influence olfaction and gustatory responses, although no clear pattern has emerged (Lopez-Arias et al 2011). Food intake is affected by the LK neurons, as persistent inactivation or conditional activation of the LK neurons both result in decreased overall food intake (Liu et al 2015).

Based on the existing research, it appears that LKR in the brain and in the tubule may specialise in the regulation of feeding and fluid homeostasis, respectively. These two roles may be complementary and contribute to coordination of feeding and excretion (Cognigni et al 2011).

As a neuropeptide involved in regulation of fluid homeostasis, it is not surprising that LK signalling has been implicated in desiccation stress tolerance. More specifically, conditional or persistent inactivation of the LK neurons was found to improve survival during desiccation stress, while conditional activation of the LK neurons impaired desiccation survival (Liu et al 2015). Conversely, in another report, silencing of the LK neurons via expression of an inward rectifier K+ channel, driven by a LK-GAL4 driver resulted in decreased survival during desiccation stress (Lopez-Arias et al 2011). This phenotype, however, was accompanied by necrosis and reduced lifespan, which calls into question the validity of the assay. Changes in levels of LK peptide have also been observed following desiccation, with decreases in the abdominal LK neurons being reversed by rehydration (Liu et al 2015).

1.3.3 Neuropeptide neuronal circuits and interplay

The colocalisation of LKR to the DH_{44} neurons presents a possibility for interaction between the two signalling pathways (Cabrero et al 2002). Both LK and DH_{44} are known to act as diuretic peptides on the Malpighian tubules in *D.*

melanogaster, although each targets a different cell type. In theory, interaction in the brain between these two signalling pathways could enable coordination of signals to the tubules that could affect both principal cells, through the presence of DH44-R2, and stellate cells, via LKR. This could therefore represent a coordinated neuronal circuit managing fluid homeostasis.

Interplay and regulation is not unprecedented in terms of insect neuropeptides as synergistic effects on Malpighian tubule fluid secretion have been previously noted among diuretic hormones, for example between LK and calcitonin-like diuretic hormone, and multiple neuronal circuits have been identified as key moderators of tubule function (Carlsson et al 2010, Coast et al 2001). Colocalisation is also observed between a number of other neuropeptides, including the presence of corozonin expression in DH44-R1 expressing neurons in both adult and larval brains (Johnson et al 2005).

1.4 Stress tolerance in insects

Insects have been found to have adaptive mechanisms underlying tolerance to a wide range of environmental stressors, including cold, heat, desiccation, and starvation (Davies et al 2014, Neven 2000, Overgaard & Sørensen 2008, Rion & Kawecki 2007, Teets & Denlinger 2013). Adaptation to stress can occur both within and across generations of insects, with the former being illustrated particularly well by studies of stress hardening and the latter by stress selection studies (Bubliy et al 2012, Rion & Kawecki 2007). The relevance of stress tolerance to survival of insects outside of the lab is supported by the variability in stress resistance observed in naturally occurring populations (Gibbs & Reynolds 2012).

Starvation and desiccation stress, although imposing differing burdens on an insect, share the common feature that both arise due to a shortage or lack of a critically important resource (Gibbs & Gefan 2009). Thus, the theory underlying survival of these stressors is broadly similar. It is thought that survival duration during resource scarcity can be extended via three different mechanisms: by storing a greater amount of the resource prior to the onset of scarcity, by using up resources more slowly, or by lowering the bottom threshold of the resource required to remain alive (Gibbs & Reynolds 2012, Rion & Kawecki 2007). A fourth

possibility has been considered, in which stressed insects that are housed in groups could cannibalise dead members under stressful conditions. This, however, has not been observed, at least in wild-type *D. melanogaster* (Huey et al 2004). Physiological changes could theoretically affect any of the three survival mechanisms both between generations of stress-selected insects and within the lifespan of individual insects that have been exposed to stress.

Stress hardening studies support the existence of mechanisms enabling stress adaptation by individual insects. In *Drosophila,* the suite of changes that follow exposure to resource restriction is sometimes thought of as a 'survival mode' that could enable the fly to survive longer during periods of environmental stress (Rion & Kawecki 2007). As changes in survival occur following an acute period of resource scarcity, it is evident that individual flies are able to use phenotypic plasticity to adapt within their lifetime to changing environmental conditions (Bubliy et al 2012).

1.4.1 Starvation tolerance

Energy is critically important for survival. The ability of an individual insect to adapt to a nutrient-poor environment can mean the difference between dying or surviving until the necessary resources are found. For a population of insects, genetic variation in starvation tolerance can enable some individuals to reproduce in spite of food scarcity, thus preventing the entire population from being wiped out by changes in the environment or habitat conditions.

Both across and within *Drosophila* species, there is a large variety in starvation tolerance (Gibbs & Reynolds 2012, Herrewege & David 1997, Schmidt et al 2005, Sisodia & Singh 2010). This variability in starvation resistance has been extensively studied in *Drosophila* by assessing differences in starvation resistance and associated characteristics in different species of *Drosophila* or by measuring phenotypic or genetic changes following laboratory selection for starvation resistance (Gibbs & Reynolds 2012, Hoffmann & Harshman 1999, Rion & Kawecki 2007).

One of the most consistent results emerging from studies of variation in natural *Drosophila* populations and from laboratory selection studies is that greater

energy storage is associated with greater starvation resistance (Rion & Kawecki 2007). Although both carbohydrates and lipids have been found to increase as a consequence of laboratory selection (Djawdan et al 1997, Schwasinger-Schmidt et al 2012), most studies have focused on lipid storage changes (Gibbs & Reynolds 2012). A positive association between starvation tolerance and lipid energy stores has also been observed both across (Herrewege & David 1997, Sharmila Bharathi et al 2003) and within *Drosophila* species (Ballard et al 2008, Goenaga et al 2013, Sisodia & Singh 2010).

Resource consumption during starvation corresponds with the selection and population studies, in that lipids have been found to be consumed by *Drosophila* during starvation (Aggarwal 2014, Marron et al 2003). Female *Drosophila* have been additionally found to consume glycogen stores during starvation stress (Aggarwal 2014). Lipid metabolism during starvation may be particularly important in certain tissues; mutation of nuclear receptor *Drosophila* HNF4, which is expressed highly in the midgut, gastric caeca, fat body, Malpighian tubules, and the oenocytes and which supports lipid catabolism, resulted in significantly impaired starvation survival (Palanker et al 2009). Some of the energy metabolites consumed during starvation stress may be depleted due to an acute increase in activity that occurs in wild-type *Drosophila* in the absence of food (Connolly 1966, Farhadian et al 2012), a behaviour that can be absent in laboratory starvation-selected fly strains (Williams et al 2004).

When experimental evidence is considered in light of the model of resource scarcity survival discussed in section 1.2, there is support for the idea that *Drosophila* might enhance starvation survival by storing up greater energy resources prior to the onset of stress. In contrast, a reduced rate of consumption of energy metabolites could contribute to greater starvation tolerance, but there is not a clear association between metabolic rate and differences in population starvation survival duration (Gibbs & Reynolds 2012). Likewise, no difference in energy threshold requirements has been observed across several *Drosophila leontia* populations with differing starvation stress tolerance levels (Aggarwal 2014).

Although it might seem theoretically advantageous for a *Drosophila* species to maximise its starvation tolerance and thereby be continually prepared to

tolerate this stress, these adaptations may require a trade-off and are unlikely to be generally adaptive. Indeed, female *Drosophila* that were subjected to periods of acute starvation exposure were found to have a reduced lifespan when compared to unstressed controls (Bubliy et al 2012). Thus, the most adaptive option may be for individual flies to have inducible mechanisms of starvation resistance that are triggered when environmental cues indicate that a period of nutrition shortage is underway or soon to begin (Rion & Kawecki 2007).

Individual flies are able to induce changes that enhance starvation survival in response to dietary restriction (Rion & Kawecki 2007). Starvation hardening, where insects are exposed to acute dietary restriction prior to a period of long-term starvation, is associated with improved starvation resistance (Bubliy et al 2012, Burger et al 2007, Rion & Kawecki 2007) and has been associated with reductions in metabolic rate in *Drosophila leontia* females (Aggarwal 2014). This indicates that *Drosophila* are both able to detect dietary stress and have resistance mechanisms for starvation that can be initiated when metabolic stress is detected.

Evidence from gene transcription studies suggests that the mechanisms induced by acute starvation stress differ from those that appear following generational adaptation to starvation exposure (Gibbs & Reynolds 2012). Specifically, gene expression changes observed during starvation exposure (Harbison et al 2005) differ from those induced by generational selection for starvation resistance (Sorensen et al 2007).

1.4.1.1 Endocrine response to starvation exposure

Given that feeding behaviour is known to be linked to neuropeptide signalling, it is not surprising that starvation exposure has also been associated with an endocrine response (Gibbs & Reynolds 2012). In *Drosophila,* the changes that take place during starvation appear to suppress biosynthesis and support catabolism, particularly of lipids (Gibbs & Reynolds 2012).

The metabolic changes observed during starvation stress in insects are thought to be mediated, at least in part, by changes in adipokinetic hormone and insulin signalling pathways. Adipokinetic hormone acts to initiate lipolysis, a

particularly important source of energy during starvation (Lee & Park 2004, Marron et al 2003). Insulin-like peptides are likewise important for metabolism and are involved in regulation of nutrient uptake, storage, and catabolism (Gibbs & Reynolds 2012). Release of insulin-like peptides depends on amino acid levels in the fat body and is decreased during starvation (Geminard et al 2009). Interestingly, abdominal neurons containing LK, a peptide which has previously been linked to both fluid homeostasis and feeding (section 1.3.2.1), also express receptors for insulin-like peptides, providing a possible site of interaction between these signalling pathways (Liu et al 2015). Manipulations of tachykinin signalling to the Malpighian tubules have also shown an effect on starvation survival in *Drosophila* (Soderberg et al 2011).

1.4.2 Desiccation tolerance

As a small insect, *Drosophila* has a high surface to volume ratio and is therefore particularly sensitive to desiccation stress (Schooley et al 2011). Larger flies, which have a reduced surface to volume ratio, show greater resistance to desiccation (Hoffmann & Harshman 1999). *Drosophila* species vary greatly in desiccation resistance (Matzkin et al 2009), and variation is found also within species and may be related to local climate differences, indicating that *Drosophila* likely experience desiccation stress intense enough to create a selective pressure (Hoffmann & Harshman 1999). The key adaptations thought to enhance desiccation tolerance in *Drosophila* depend on reducing the rate of water loss. These are the impermeable cuticle, behavioural modifications such as moving toward more humid areas when available, and a highly developed excretory system that is able to release concentrated metabolic waste (Bazinet et al 2010, Klowden 2008, Maddrell 1981, Prince & Parsons 1977, Stinziano et al 2015). Genetic analyses of *Drosophila melanogaster* native to desert regions and of *Drosophila* selected for desiccation resistance show that fluid homeostasis, and in particular, fluid transport regulation in the tubule, is a key factor in determining resistance to desiccation (Folk & Bradley 2003, Gibbs & Matzkin 2001, Telonis-Scott et al 2012).

Studies of laboratory selection for desiccation tolerance also provide support for the importance of reducing the rate of water loss during desiccation exposure and have additionally indicated that changes in metabolite rate may affect

desiccation survival (Gibbs et al 1997, Hoffmann & Harshman 1999). Reduced rate of water loss in desiccation resistant *Drosophila* strains may be due to changes in the cuticle or the spiracles, with the latter being potentially associated with changes in metabolic rate (Hoffmann & Harshman 1999). However, the evidence for metabolic rate alterations affecting desiccation tolerance is mixed (Hoffmann & Harshman 1999) despite an association between motor activity and desiccation resistance (Hoffmann & Parsons 1989, Hoffmann & Parsons 1993).

Other mechanisms of desiccation tolerance have been explored in desiccation selection studies, such as greater storage of water prior to desiccation onset in more resistant strains, or tolerance of a higher percentage loss of body water. There is some experimental support for the idea that desiccation tolerant species of *Drosophila* are able to tolerate a lower percentage of body water (Ramniwas & Kajla 2013). Conversely, higher water content is only sometimes associated with laboratory selection for desiccation tolerance (Hoffmann & Harshman 1999).

Higher glycogen levels are sometimes associated with improved desiccation tolerance (Hoffmann & Harshman 1999), a finding that may be due to greater water resources in the form of bulk water bound to glycogen (Marron et al 2003). Glycogen deposited in the liver and muscle has been found to bind up to five times its weight in water (Olsson & Saltin 1970, Schmidt-Nielsen 1997). The release of metabolic water when glycogen is consumed could thereby contribute to desiccation survival duration (Marron et al 2003).

1.4.2.1 Endocrine signalling during desiccation stress

As fluid homeostasis is modulated by the neuroendocrine system in *D. melanogaster* (section 1.3), it is not surprising that there is interaction between desiccation tolerance and endocrine signalling (Schooley et al 2011, Terhzaz et al 2015b, Treherne & Willmer 1975). In particular, modulation of the signalling pathways of the diuretic hormone capa, which acts to increase secretion by the Malpighian tubules via its principal-cell specific GPCR receptor capaR, has been shown to affect resistance to desiccation stress (Terhzaz et al 2012, Terhzaz et al 2015b). LK signalling has likewise been associated with survival during

desiccation exposure, and experimental manipulations of the neuropeptide tachykinin, which has been found to have a weakly diuretic effect on some insects, alters survival time of *Drosophila melanogaster* exposed to desiccation stress (Kahsai et al 2010, Liu et al 2015, Soderberg et al 2011). These findings support the hypothesis that utilizing neuropeptide signalling cascades to modify fluid transportation represents a distinct and effective method for desiccation resistance in insects.

1.5 Metabolomics

Metabolomics is a versatile technique enabling rapid identification of a large number of small molecules. The term itself was defined in 1998, although related methods were used for at least a couple of decades before the definition was in place (Oliver et al 1998, Pauling et al 1971). Metabolomic profiling has been used quite extensively in the study of plants, but has more recently been applied to examine model organisms such as *D. melanogaster* as well as humans (Kamleh et al 2009, Ryan & Robards 2006, Seger & Sturm 2007, Snart et al 2015). Although united in the goal of identifying as many metabolites as possible, there is a wide range of techniques used in metabolomics almost at every level, including sample preparation, separation of metabolites, detection of metabolites, processing of data, and statistical analysis of output (Kamleh et al 2009, Snart et al 2015).

Perhaps the most distinguishing difference between metabolomics methods is the diversity in detection methods. The majority of studies depend on the use of nuclear magnetic resonance (NMR) spectroscopy or mass spectroscopy (MS) (Dieterle et al 2011, Lei et al 2011). NMR is non-destructive and can provide information about metabolite structure, but is less suited for acquiring a wide coverage of the metabolome as it is less sensitive than the other techniques (Kim et al 2010, Lei et al 2011). MS methods have been found to be able to identify a large number of metabolites from samples with relatively low biomass when paired with chromatography methods (Snart et al 2015). The ability to detect metabolites reliably using small samples is particularly important for insect studies, where the metabolic starting material tends to be either a limiting factor, or labour-intensive to acquire.

1.5.1 Mass spectrometry

MS is performed by ionizing a sample, thereby producing charged molecules, and then distinguishing ions based on their mass to charge ratio, often by accelerating the molecules and separating them using either an electric or magnetic field. A detector will record the relative abundance of the charged particles and their mass-to-charge ratio, which is determined by the degree of deflection. This method enables highly accurate measurement of the mass of a molecule, which can then be used for metabolite identification.

1.5.1.1 Chromatography

Although samples can be directly analysed via MS, most metabolomics approaches will involve separating the sample using a chromatography column as there are substantial advantages to doing so (Lei et al 2011). In particular, chromatography can improve the accuracy of measurements by reducing matrix effects, that is the influence of the compounds that are present in a sample on the measurement of the metabolite of interest. Among these effects is ion suppression, which involves matrix compounds interfering with ionisation (section 1.5.1.2) and thereby altering the abundance of charged ions for particular compounds (Annesley 2003). This then results in inaccuracy or lack of detection of the components that have not been properly ionized (Muller et al 2002). As chromatography reduces the number of compounds in the solution by spreading out the analysis over another dimension, the possibility for interactions between compounds is reduced. Chromatography can also separate isomers and provides information (e.g. hydrophobicity) that can contribute toward identification of isomers.

There are a number of different chromatography approaches that can be paired with MS, although all aim to reduce the complexity of the sample prior to the point of injection into the mass spectrometer (Want et al 2007). The two main categories of chromatographic methods that are paired with MS are liquid chromatography (LC) and gas chromatography (GC) (Kamleh et al 2009). These are distinguished by the phase in which the sample travels along the column (i.e. as a liquid or as a gas). GC is most suitable for volatile substances, although compounds can be derivatised in order to use this method (Xue et al 2008).

LC can be performed using a variety of columns, although the main distinguishing feature is whether the stationary phase of the column is hydrophilic or hydrophobic. The former is called normal phase LC and is most suitable for separating polar metabolites, while the latter is termed reversed phase LC and enables separation of lipophilic metabolites (Lei et al 2011). Innovations include application of ultra-high pressure to the column, which enables more efficient metabolite separation (Cielecka-Piontek et al 2013). Hydrophilic interaction chromatography (HILIC) is particularly well suited for separation of polar metabolites as compounds are separated both via polarity interactions and solvation, that is by the association of a solvent with the metabolites (Idborg et al 2005, Jandera 2008). When a sample is applied to a HILIC column, the stationary aqueous phase interacts more strongly with more polar compounds, resulting in elution of increasingly polar metabolites (Cubbon et al 2010).

1.5.1.2 Ionisation

Following chromatography, the first step in the actual process of MS is to ionise the metabolites in the sample to impart a positive or negative charge (Ho et al 2003). The technique used can greatly influence the metabolite profile obtained. When using LC-MS, electrospray ionisation (ESI) is often used and is particularly well suited for use with polar compounds, while atmospheric pressure chemical ionization is typically used for neutral compounds (Dieterle et al 2011, Lei et al 2011). ESI involves applying a high voltage using electricity to a liquid sample, resulting in the production of charged liquid droplets (Ho et al 2003). These are then forced through the electrospray tip, an ultra-fine needle (Careri & Mangia 2011). The droplet solvent is evaporated upon exiting the needle by a combination of heat and/or drying gas, resulting in an increase of charge density that causes electrostatic repulsion and dispersal of aerosolized ions (Ho et al 2003).

ESI can be operated in both positive and negative ion mode, with each polarity resulting in detection of a different array of metabolites (Kamleh et al 2009). This is due to the variability of metabolite stability in their protonated or deprotonated forms. Thus, the comprehensiveness of a metabolic profile can be improved by obtaining and integrating data from both polarities. Many MS

instruments can alternate between polarities, enabling relatively facile acquisition of data from both modes (Lei et al 2011).

1.5.1.3 Mass analysers and detectors

The mass-to-charge ratio of the ions cause distinctive patterns of motion that can be identified by a mass analyser (Parker et al 2010). There are numerous approaches to separating molecules by this ratio, including by the time required to reach the detector when accelerating through an electric field (time-of-flight spectrometry) or the rotation of electrically excited molecules in a magnetic field (Fourier transform ion cyclotron mass spectrometry). Orbitrap mass analysers function by trapping ions in orbit around a central electrode (Zubarev & Makarov 2013). Each approach has a distinctive resolving power that underlies the degree to which components with a highly similar ratio of mass number to charge number (m/z) can be distinguished, typically measured in parts-per-million of the dimensionless m/z (ppm). The accuracy of the Orbitrap mass spectrometer is very good, with maximum variability being measured as low as 2 ppm (Olsen et al 2005). This provides substantial support to metabolite identification, as even ions with the same number of nucleons (protons and neutrons) can be distinguished based on differences in the exact mass (Chintapalli et al 2013a, Watson 2013). Thus, only isomers must be distinguished when using the exact mass, and these can often be separated by chromatography and information about isomer identity derived from column retention times (RT).

The final stage of MS is detection of the charged ions. The detection method is typically linked to the kind of mass analyser that is being used (Kamleh et al 2009). As the charged molecule comes close to or hits the detector, a charge or current is produced. This results in a mass spectrum, or information that can be transformed into a mass spectrum and used to determine the m/z of the detected species. In order to detect as many compounds as possible, amplification may be used to enhance the signal.

1.5.2 Untargeted metabolomics

Metabolomics approaches can be broadly divided into two categories: targeted and untargeted (Patti et al 2012). In a targeted experiment, the metabolites identified by the metabolomics technique are determined in advance, typically with the goal of testing a specific hypothesis (Roberts et al 2012). Untargeted metabolomics aims to identify as many metabolites as possible and thereby to attain an overall view of the metabolic profile of a sample (Alonso et al 2015). Targeted metabolomics can be used to follow up hypotheses generated by an untargeted experiment and can offer advantages such as more accurate metabolite quantification and greater confidence in metabolite identifications by inclusion of standards for all metabolites of interest.

Targeted and untargeted metabolomics differ in the extent to which they can be used for quantitative measurements. When using MS, an external standard calibration curve is required for absolute quantification of metabolite levels (Patti et al 2012). This can easily be paired with targeted metabolomics, where the identity of metabolites of interest is known and standards can be acquired ahead of time for calibration. Conversely, in untargeted metabolomics, the key metabolites are unknown, making the calibration curve approach untenable. Consequently, abundance values obtained from untargeted metabolomics are relative in nature (Dane et al 2014). Untargeted experiments will therefore often involve comparing a condition of interest to one or more control samples.

1.5.3 Computational data analysis

The data generated by metabolomic approaches are extensive and complex. Computational approaches have been developed to partly automate the analysis process. For example, the freeware MzMatch software package is a customizable tool for processing, filtering, and annotating mass spectrum data, enabling related peaks to be identified and combined (Scheltema et al 2011). The IDEOM interface, which runs in Microsoft Excel, helps guide the user through LC-MS data processing, making use of MzMatch (Creek et al 2012). It further facilitates analysis by enabling visualisation of relative abundance data.

1.5.4 Sample preparation for *Drosophila*

One of the main challenges that can arise when using metabolomics methods to study insects is a lack of biomass (Snart et al 2015). As *D. melanogaster* can be easily reared under laboratory conditions, sufficient starting material can be obtained by pooling samples. The number of flies or tissues required for a particular sample will depend in part on the sensitivity of the instrument being used to detect the metabolites.

An issue that can arise particularly when using whole organism samples for metabolomics is the possibility of culture media or excreted materials adhering to the surface of the insect and therefore being included in the set of metabolites extracted from the animal (Snart et al 2015). This can, in part, be controlled for by acquiring the metabolic profile of culture media, which can be used to judge whether a metabolite might be due to sample contamination. Although it would also be possible to rinse the insect off with high-purity water prior to metabolite extraction, including insect media as a control may serve an additional purpose as highly sensitive metabolomic detection techniques may be able to detect differences in gut content. As culture media would be the primary contents of the gut, this control would then provide a comparison point to determine whether the presence of a metabolite might be due to the presence of food in the gut (Snart et al 2015).

As numerous studies have already used *Drosophila* in both NMR and mass spectrometry based metabolomics, appropriate sample preparation and metabolite extraction methods can easily be adapted from these sources (Al Bratty et al 2011, Sarup et al 2012). Methodological variations have also been published in which *Drosophila* larvae are studied or where specific tissues are dissected and pooled for analysis (Al Bratty et al 2012, Chintapalli et al 2013a).

1.5.5 Applications of metabolomics to insects

Metabolomics methods have been applied to insects in at least 40 studies over the past decade, with a wide variety of aims (Snart et al 2015). For example, the effect of specific mutations on the whole fly metabolome can be used to probe the function of unknown proteins (Al Bratty et al 2012). Metabolic profiling of

flies with mutations in genes coding for specific metabolic enzymes can provide information about unexpected metabolic ramifications and unpredicted effects (Kamleh et al 2008). Changes in metabolic profile due to drug exposure have also been assessed in flies and can be used to test whether a drug has an expected effect on a relatively simple metabolic system before attempting to use it in more complex organisms (Al Bratty et al 2011). Male and female flies have been compared via metabolomics, and differences potentially relating to histone metabolism and egg production were identified (Zhang et al 2014).

1.5.5.1 Stress studies

A handful of studies has focused on the effect of environment stress exposure on the metabolic profile of *D. melanogaster*. Extreme temperature exposure is one of the main topics that has been explored in this species. Metabolic profiling has revealed that moderate and severe heat stress affect metabolism in whole adult flies (Malmendal et al 2006, Pedersen et al 2008). Periods of moderate heat have been shown to enable the metabolic profile to return to normal more quickly during subsequent periods of heat treatment, thus providing support for the idea of stress hardening (Malmendal et al 2006). Likewise, cold stress was found to significantly alter the metabolic profile of whole flies using a variety of metabolomic techniques, including untargeted NMR and targeted GC/MS approaches (Colinet et al 2012, Overgaard et al 2007, Pedersen et al 2008, Williams et al 2014). Metabolic changes following cold acclimation are associated with improved survival and ability to return to metabolic homeostasis following subsequent cold exposure. Chronic cold exposure of larvae was found to alter metabolite balance and induce restructuring of the glycerophospholipid composition of biological membranes (Kostal et al 2011). Warm or cool temperatures during development may be more reflective of temperatures that *D. melanogaster* is likely to encounter in the environment; however, only high temperatures have consistently been found to affect the metabolomic profile of whole flies (Hariharan et al 2014, Kristensen et al 2012).

Metabolomic studies of stress in *D. melanogaster* have typically used whole organism samples, with a few notable exceptions. *D. melanogaster* has occasionally been divided into subsections for examination, as was done in a study of the effect of hypoxia on the metabolic profile of the thorax using ^{1}H

NMR spectroscopy (Feala et al 2007). Lack of oxygen availability to the tissue was found to result in the accumulation of multiple metabolites. Similarly, adult flies raised with dietary restriction were analysed via mass spectroscopy after dissection into head, thorax, and abdomen (Laye et al 2015). Although the sample types used in these studies are more specific than in whole organism studies, each of the sections used requires the blending of multiple distinct tissues, which could obscure important metabolomic effects and which prevents attribution of metabolic changes to particular tissues (Chintapalli et al 2013a). In contrast, the metabolic profile of larval fat body, gut, hemolymph, and body wall were examined after cold acclimation, and analysis via GC/LC-MS (Koštál et al 2012). This approach of tissue-specific exploration presents the possibility of localising the changes in metabolic level and can offer a greater power for hypothesis generation and mechanism ideas.

As with *D. melanogaster,* most metabolomic studies exploring the effects of stress on the metabolic profile of insects have focused primarily or exclusively on extreme temperature, and involved using the entire organism. Metabolomic studies of extreme temperature have been conducted using larvae of the Antarctic midge (*Belgica antarctica),* flesh flies (*Sarcophaga crassipalpis*), parasitoid wasp (*Venturia canescens*), and pea aphid (Burke et al 2010, Foray et al 2013, Michaud et al 2008, Michaud & Denlinger 2007).

Only a handful of studies have examined the effects of desiccation on the metabolic profile of insects. Desiccation exposure was found to affect metabolite abundance in *B. antarctica* larvae, particularly in pathways relating to carbohydrate metabolism, and caused an overall decrease in amino acid abundance (Michaud et al 2008). As midge larvae were also exposed to heat and freezing stress in the same study, it was found that changes in sugar and polyol pools were similar in both freezing and desiccation, while no shared changes were observed between heat and desiccation. When mosquito *Anopheles gambiae* larvae were raised under dry season conditions, the female adults were found to have reduced levels of tricarboxylic acid cycle intermediates and isoleucine, and showed a decrease or no change in polyol and sugar levels (Mamai et al 2014). These results suggested that rearing under dry conditions results in overall lower metabolic activity than rearing under wet conditions. The differences between the results obtained from these two studies may reflect

the diversity of species and stress exposure applied. Survival strategies for tolerance of chronically dry conditions and acute desiccation are likely to diverge, and strategies may differ between insect species.

The finding that metabolite levels change due to desiccation is consistent with research using other more established methods. Changes in the levels of metabolites following desiccation have been found to correlate strongly with gene expression of metabolic enzymes when examined via next-generation RNA sequencing or microarrays in insects (Matzkin & Markow 2009, Teets et al 2012). More traditional enzyme or chemical assays have also revealed changes in the overall levels of lipids, carbohydrates or protein in response to both desiccation and starvation (Marron et al 2003).

Starvation exposure itself does not appear to have been metabolically characterised via metabolomics in an insect. However, the effect of larval crowding, and thereby nutrient deprivation, has been explored in adult *Aedes aegypti* (Price et al 2015). Lack of nutrition during development was found to result in a higher abundance of free amino acids in the adult fat body and changes in expression of genes relating to amino acid degradation and metabolism.

Overall, the variety of results obtained from metabolomic analysis of desiccated or starved insects does not give an entirely clear picture of the metabolic changes occurring during these stressors. This is mainly due to the scarcity of studies exploring this topic and the diversity of stressors applied. As both desiccation and starvation can be examined from a chronic or acute standpoint, with or without prior hardening exposure, a wide variety of experimental approaches can be applied.

1.5.5.2 Selection studies

Although stress tolerance selection studies have a long history in *D. melanogaster* (Hoffmann & Harshman 1999, Rion & Kawecki 2007), metabolomic analysis of lab-selected tolerant lines has only been applied recently (Malmendal et al 2013). *Drosophila* lines that were selected for survival of heat, cold, starvation, or desiccation were found to have a relatively subtle and generally

similar effect on the whole fly metabolome (Malmendal et al 2013). Changes identified in the stress-selected lines included increases in the abundance of maltose and histidine and decreases in levels of nicotinamide adenine dinucleotide and choline, as well as overall decreases in many of the lines in levels of free amino acids. The results of this study additionally suggested that stress tolerance is not dependent on the concentration of specific metabolites prior to stress onset, but that accumulation or depletion of metabolites rather reflects consequences of adaptations that increase stress tolerance.

1.5.5.3 Tissue-specific studies

The majority of metabolomic insect studies have used whole organism samples as the source material (Al Bratty et al 2012, Malmendal et al 2006, Williams et al 2014). However, recent work has indicated that, much like the tissue-specific nature of gene expression (Chintapalli et al 2007), individual tissues differ significantly from one another in their metabolic profile (Chintapalli et al 2013a). Some studies have either used a division of an insect, such as the thorax, or divided the insect into several parts for analysis (Feala et al 2007, Laye et al 2015). A few studies have even focused on very specific tissues, primarily the fat body (Koštál et al 2012, Price et al 2015). As individual tissues differ so greatly in their metabolic profile, studies which aim to investigate mechanisms of stress tolerance at a tissue-specific level may greatly benefit from the use of tissue-specific samples.

1.5.6 Identification of changes

When a large number of observations are made using a single set of samples, the risk of incorrectly rejecting the null hypothesis and accepting false positives becomes a pressing issue (Broadhurst & Kell 2006). Untargeted metabolomics can result in hundreds of putative metabolite identifications, each with relative abundance values. Depending on the nature of the study, the consequences of a type I statistical error, in which the null hypothesis is incorrectly rejected, can vary greatly. Thus, the statistical approach used will likely depend on the goals of the experiment.

In the study presented in this thesis, untargeted tissue-specific metabolomics is used as an exploratory tool for hypothesis generation. A false positive could lead to a follow-up experiment with negative results, but when contrasted with a targeted metabolomics study with the aim of disease diagnosis, it is clear that a false positive in this study holds relatively little risk. The consequences of falsely excluding true differences should also be taken into account when planning a statistical approach for a large dataset. When an exploratory approach is being used, it may be preferential to accept a few false positives if a much greater number of true positives will then be retained for analysis, rather than setting highly stringent criteria in order to make it unlikely that even a single false positive will be deemed significant. Thus, a balance between exclusion of true differences and inclusion of false differences must be found that is appropriate for the aims of each study.

One approach that can be used to control the false discovery rate, and which has been applied in this study is the Benjamini–Hochberg procedure (Benjamini & Hochberg 1995). This method controls the proportion of the statistically significant differences observed that are due to a type I error. For example, it is possible to determine that 1% or 5% of the differences found should be due to chance rather than a true difference in the population means. An alternative approach which is more suited for experiments where the probability of at least one false positive must be controlled are the familywise error rate procedures, such as the Bonferroni correction (Broadhurst & Kell 2006).

1.6 Aims of the thesis

Although DH_{44} has been characterised as a diuretic hormone acting on the Malpighian tubules in *D. melanogaster*, and other diuretic hormones have been linked to modulation of fluid homeostasis during desiccation stress, the role of DH_{44} neuropeptide during stress exposure has not been investigated. Consequently, this study tested the hypothesis that the DH_{44} signalling system is modified by desiccation stress. Evidence is presented supporting suppression of the DH_{44} signalling pathway following desiccation in wild-type flies. These data are supported by the finding that knocking down *DH_{44}* via RNAi specifically in the DH_{44} neurons improves desiccation tolerance. The study further explores the role of the DH_{44} neurons in stress tolerance by addressing an untouched attribute of

these neurons: the colocalised expression of LKR. Given the involvement of LKR in the brain in feeding behaviour, this provides a potential interaction point between nutritional and fluid homeostasis. A role for the DH_{44} neurons in starvation tolerance is explored, with an emphasis on the possible contributions of LK signalling via the DH_{44} neurons. Finally, changes in Malpighian tubule function during desiccation and starvation stress are described using tissue-specific metabolomic profiling of the Malpighian tubules. This analysis supports the neuropeptide work in suggesting that the tubules reduce their rate of secretion at the expense of accumulating metabolic end products during both desiccation and starvation stress. The specificity of the metabolic changes observed in Malpighian tubules following stress exposure is contrasted with the relatively unclear picture produced by examining whole flies. Overall, it is clear that studies of stress tolerance must move toward tissue-specific analyses in order to clarify the mechanisms underlying stress resistance. The results of the study are summarised and areas of future investigation are discussed in the final section.

2 Materials and Methods

The aim of this chapter is to provide sufficient detail and references so that the methods used during the study can be fully understood by the reader and replicated by other researchers. Statistical methods used to analyse the different types of data produced during the study are described at the end of each relevant subsection. Either Microsoft Excel for Mac 2011 or Graphpad Prism 6 was used to plot, analyse and statistically examine results, unless otherwise noted.

2.1 Drosophila melanogaster

Drosophila melanogaster was used extensively during this study and the methods used to maintain and rear these insects are described in this section. Additionally, microdissection of *Drosophila* tissues is also described here.

2.1.1 *Drosophila* Stocks

All experiments described in this thesis were conducted using *Drosophila melanogaster*. Several of the strains used were available in-house and are maintained by the Dow/Davies lab. Those strains that were not available in-house were ordered either from Bloomington Stock Center or from the Vienna Drosophila RNAi Centre, as detailed in Table 2.1. References are given where further information about the generation of particular strains has been published.

Table 2.1 *Drosophila* stocks used

Fly ID	Strain/Genotype (Source)	Description	Reference
CS	Canton-S (In-house)	Isogenic wild-type	Flybase
w^h	*white*^{honey} (In-house)	*w* mutant allele isogenised to CS	Flybase
DH_{44}-GAL4	w^{1118}; *P{*$y^{+t7.7}$ w^{+mC}*=GMR65C11GAL4}*attP2 (Bloomington Stock Center)	GAL4 element under the control of a 2871 residue DNA sequence in *DH_{44}*, with coordinates 3R: 5463840-5466711; drives expression in DH_{44} neurons	(Jenett et al 2012, Pfeiffer et al 2008)
DH44-R2-GAL4	w^{1118}; *P{*$y^{+t7.7}$ w^{+mC}*=GMR18A04-GAL4}*attP2 (Bloomington Stock Center)	GAL4 element under the control of a 1269 residue DNA sequence in *DH44-R2* with coordinates 2R: 8367428-8368697; drives expression in subset of neurons in brain and principal cells of Malpighian tubules	(Jenett et al 2012, Pfeiffer et al 2008)
c724-GAL4	*w; c724-GAL4* (Generated in-house)	Drives expression in stellate cells of Malpighian tubules; GAL4 enhancer trap	(Sozen et al 1997)

capaR-GAL4	*w; ; capaR-GAL4* (Generated in-house)	Drives expression in principal cells of Malpighian tubules	(Terhzaz et al 2012)
Actin-GAL4	*w; Act5c-GAL4/cyo::GFP* (In-house)	Drives expression ubiquitously	(Stergiopoulos et al 2009)
UAS- DH_{44} RNAi	y^1v^1; *P{*$y^{+t7.7}$ $v^{+t1.8}$*=TRiP.JF01822}*attP2 (Bloomington Stock Center)	Expresses double-stranded RNA for RNAi of DH_{44} under the control of UAS promoter	(Ni et al 2009)
UAS-*LKR* RNAi	*y,*w^{1118}*;P{attP,*y^+*,*w^3*`=KK102546 }*VIE-260B (Vienna Drosophila RNAi Centre)	Expresses double-stranded RNA for RNAi of *LKR* under the control of UAS promoter	(Dietzl et al 2007)
UAS-*LKR* RNAi	y^1 v^1; *P{*$y^{+t7.7}$ $v^{+t1.8}$*=TRiP.JF01956}*attP2 (Bloomington Stock Center)	Expresses double-stranded RNA for RNAi of *LKR* under the control of UAS promoter	(Ni et al 2009)
UAS-*DH44-R2* RNAi	*y,*w^{1118}*;P{attP,*y^+*,*w^3*`=KK*111461 *}*VIE-260B (Vienna Drosophila RNAi Centre)	Expresses double-stranded RNA for RNAi of *DH44-R2* under the control of UAS promoter	(Dietzl et al 2007)
UAS-*DH44-R2* RNAi	y^1 v^1; *P{*$y^{+t7.7}$ $v^{+t1.8}$*=TRiP.JF03289}*attP2 (Bloomington Stock Center)	Expresses double-stranded RNA for RNAi of *DH44-R2* under the control of UAS promoter	(Ni et al 2009)

UAS-*DH44-R1* RNAi	*y^1 v^1; P{$y^{+t7.7}$ $v^{+t1.8}$=TRiP.JF03208}*attP2 (Bloomington Stock Center)	Expresses double-stranded RNA for RNAi of *DH44-R1* under the control of UAS promoter	(Ni et al 2009)
UAS-*LK* RNAi	*y^1 v^1; P{$y^{+t7.7}$ $v^{+t1.8}$=TRiP.JF01816}*attP2 (Bloomington Stock Center)	Expresses double-stranded RNA for RNAi of *LK* under the control of UAS promoter	(Ni et al 2009)
UAS-*reaper*	w^{1118} P{w^{+mC}=UAS-rpr.C}27 (In-house; Bloomington Stock Center)	Expresses *reaper* under the control of UAS promoter, inducing cell death	(Aplin & Kaufman 1997)
UAS-*NaChBac*	*y^1 w^*; P{w^{+mC}=UAS-NaChBac-EGFP}1/TM3, Sb^1* (Bloomington Stock Center)	Expresses bacterial sodium channel that increases membrane excitability under the control of UAS promoter	(Nitabach et al 2006)
UAS-*GFP*	*w*; ; *UAS-GFP* (Bloomington Stock Center)	Expresses GFP under the control of UAS promoter	
VDRC control	*y,w^{1118};P{attP,y^+,w^3 = }*VIE-260B (In-house; Dr. Edward Green)	Control for VDRC RNAi lines; Contains an empty vector	

The following RNAi lines were tested for lethality when ubiquitously expressed by crossing to driver line Actin-GAL4: UAS-*DH44-R1* RNAi, UAS-*DH44-R2* RNAi (VDRC), UAS-*DH_{44}* RNAi, UAS-*LK* RNAi, and UAS-*LKR* RNAi (VDRC). Each RNAi line was also crossed to *w^h* and the progeny collected as a control. All crosses were

viable, with the only noted difference being that UAS-*LKR* RNAi/Actin-GAL4 flies that had inherited both constructs (indicated by straight wings) were lighter in colour than those which had inherited the balancer chromosome (indicated by curly wings) rather than Actin-GAL4.

2.1.2 *Drosophila* Rearing

Drosophila were reared in vials on standard *Drosophila* diet at 22°C, 45% relative humidity with a 12:12 hour light:dark photoperiod. *Drosophila* diet contains, per litre of water, 10 g agar, 15 g sugar, 30 g glucose, 35 g dried yeast, 15 g maize meal, 10 g wheat germ, 30 g treacle, and 10 g soya flour.

2.1.3 Crossing and Rearing Crosses

Crosses were established by placing female virgins of one genotype and male flies of another together into a vial. Crosses were tipped every 2-3 days. Progeny were collected every 2-3 days and separated into groups of either males or females. Progeny were tipped every 2-3 days to prevent the food from becoming sticky and compromising the health of the flies.

Female virgins were selected for crosses based on signs of recent emergence, including a visible meconium (dark spot on abdomen containing pupation waste products), folded wings, and lack of pigment (Ashburner 1989). Females that showed only some of these signs or where they were only weakly present were kept separately for 3-4 days. Females that laid viable eggs were discarded. Crosses were reared and maintained at 26°C, 55% relative humidity with a 12:12 hour light:dark photoperiod, as the GAL4/UAS system is more efficient at higher temperatures (Duffy 2002).

2.1.4 Dissection of *Drosophila*

Prior to dissection, 5-10 day old flies were anaesthetised on ice. Where dissections were performed on desiccated or starved flies and some flies in the vial were dead, only living flies were used. These were selected by briefly removing the flies from the ice and monitoring them for signs of life. Flies that moved were transferred quickly back onto the ice, while flies that were unable to move were considered to be dead and discarded. Dissections were performed

in Schneider's medium (Invitrogen; see Table 2.7 for composition), as described previously (Ashburner 1989, Dow et al 1994) and tissues were transferred from the dissection dish every 30 minutes, at minimum, into a bathing solution or buffer appropriate for their intended purpose.

Drosophila brains were dissected for immunocytochemistry using No. 5 Biology Grade dissection forceps (Dumont) by first removing the head and the proboscis, and then exposing the brain by gripping the eyes and gently pulling apart the head capsule. Brains were tidied by carefully removing trachea and any remaining eye pigment before being transferred using forceps to a dish for fixation, washing, and incubations.

Malpighian tubules were dissected for RNA extraction by gripping the genitalia of the fly and pulling until the abdomen tore open and the gut and tubules were exposed. Tubules were removed from the midgut by severing the ureter with the forceps. When tubules were used for live imaging or secretion assay, a gentler method was used to remove the tubules from the abdominal cavity so as to avoid damaging the tubules – in this case, the tubules were extracted from the abdomen by using the forceps to tear open the abdomen lengthwise before carefully scooping out the tubules and guts. Tubules were not stretched or gripped at any point, as this tended to cause them to become 'leaky'.

2.2 Nucleic Acid Isolation and Quantification

Messenger RNA (mRNA) was used to synthesise complementary DNA (cDNA) and provide a template for polymerase chain reaction (PCR). Two different methods were used to extract RNA, depending on the type of tissue being processed. These are described below, as is the method used to quantify mRNA.

2.2.1 Messenger RNA Extraction and DNase Treatment

RNA was extracted from 5-10 day old flies, using an equal number of males and females using ribonuclease-free (RNAse-free) materials. Samples consisted of 8 whole flies, 10 bodies, 20 heads, or the Malpighian tubules from 40 flies (80 pairs of tubules). RNA was extracted from whole flies, heads, and the bodies of *Drosophila* using acid guanidinium thiocyanate-phenol-chloroform extraction

(Chomczynski & Sacchi 1987), while Malpighian tubule samples were processed using the solid-phase nucleic acid method (Boom et al 1990, Gauch et al 1998, Marko et al 1982).

Whole fly and body samples were collected in 1.5 ml Eppendorf tubes on ice and suspended in 200 µl of TRIzol Reagent (Invitrogen). Samples were typically then stored at -80°C until the RNA was extracted. Following thawing on ice, samples were homogenized using a hand-held micropestle, then sonicated using an ultrasonic cell disruptor (Microson Inc., USA) 3 times for 1 second per application. 800 µl of TRIzol Reagent was then added to each sample, and the mixture was incubated for 5 minutes at room temperature. 200 µl of chloroform was added to each sample, followed by 15 seconds of vortexing, then a 3 minute incubation at room temperature. Samples were then centrifuged at 12,000 *g* for 15 minutes at 4°C, causing insoluble materials to pellet and separating the sample into two phases. 400 µl of the upper aqueous phase was transferred to a new 1.5 ml Eppendorf tube. A small volume of the RNA-containing supernatant was typically left behind so as to avoid transferring any of the lipid interphase. 200 µl (0.5x volume of transferred supernatant) of isopropyl alcohol was added to the samples, which were then vortexed. RNA was precipitated by incubating samples for 10 minutes at room temperature. Samples were centrifuged at 12,000 *g* for 10 minutes at 4°C, causing the precipitated RNA to pellet. The supernatant was then removed, being careful not to disturb the pellet. The pellet was dislodged and washed by adding 600 µl (1.5x volume of transferred supernatant) of ice-cold 70% ethanol and vortexing the sample briefly. Samples were then centrifuged at 8,000 *g* for 5 minutes at 4°C. The ethanol was carefully removed as completely as possible without disturbing the pellet, samples were briefly centrifuged and any remaining ethanol was again removed. The pellet was allowed to air-dry, typically for 1 minute, although for up to 3 minutes, if required to allow the ethanol to evaporate. RNA was resuspended in 20 µl of RNAse-free water by incubating the RNA and pellet at room temperature for 3 minutes and then flicking the tube gently to mix. Rarely, the RNA did not resuspend following this treatment. In these cases, the sample was heated to 55°C for 1 minute and the sample was again flicked to mix.

After RNA extraction using the acid guanidinium thiocyanate-phenol-chloroform extraction method, RNA concentration was quantified as described in section

2.2.2. Samples were then diluted to a concentration of 200 µg/mL, if necessary, using RNase-free water, and then DNase treated using the TURBO-DNA-*free* kit (Invitrogen). Typically, 200 µg of RNA was processed per sample, which usually equated to a 100 µl sample size. Samples were processed according to the manufacturer's instructions, re-quantified, and then stored at -80°C.

Malpighian tubule samples were collected in 100 µl RLT buffer (QIAGEN, UK) containing 10 µl/ml ß-Mercaptoethanol (Sigma-Aldrich, UK). During dissection, the buffer was kept on ice and samples were transferred into it every 20 minutes. Typically, samples were then stored at -80°C until the RNA was extracted. Following thawing on ice, samples were homogenised using an ultrasonic cell disruptor (Microson Inc., USA), by sonicating 3 times for 1 second per application. RNA extraction was then carried out using a QIAGEN RNeasy Mini kit and QIAGEN RNAse-free DNase set. The protocol was modified to include reloading the RLT buffer into the spin cartridge twice to enhance RNA yield by ensuring maximum binding of the RNA to the column. Samples were eluted by applying 30 µl of RNA-free water to the column and incubating at room temperature for 5 minutes prior to centrifugation. RNA was then quantified by spectrophotometry and stored at -80°C.

2.2.2 Purification of DNA from Agarose Gels

DNA was purified from agarose gels to produce RT-PCR standards for assessment of primer efficiency. After resolution on a 1% agarose gel as described in section 2.3.3, DNA bands were excised from the gel using a clean scalpel blade. DNA was purified using a QIAquick Gel Extraction Kit (QIAGEN, UK) following the manufacturer's instructions. DNA was eluted in nuclease-free water, quantified via spectrophotometry and stored at -20°C.

2.2.3 Nucleic Acid Quantification

The concentration of mRNA and DNA was estimated by using a NanoDrop spectrophotometer (ND-1000 V3.7.1; Thermo Scientific) according to the manufacturer's instructions. The optical density of 1 µl of RNA or DNA sample at 260 nm was measured after calibration with RNAse-free water. An optical density of 1 at 260 nm was taken to indicate a concentration of 40 µg/ml of

single-stranded RNA or a concentration of 50 µg/ml of DNA. Ratios of optical density at 230 nm, 260 nm, and 280 nm were used to estimate RNA purity as described in the T042-Technical Bulletin (Thermo Scientific) associated with the NanoDrop Spectrophotometer.

2.3 Polymerase Chain Reaction

RNA samples were used to estimate transcript abundance via real-time reverse transcription PCR (RT-PCR) based on the use of the TaqMan primer and probe system. Gel electrophoresis was used to resolve the RT-PCR products to verify that the primers were amplifying only one correctly sized product, and, where primers were designed to span an intron, to ensure that genomic contamination was absent. The size of expected products that would arise from genomic amplicons was calculated by adding the size of the corresponding intron, based on sequencing data from Ensembl release 81 (Cunningham et al 2015).

2.3.1 Synthesis of Complementary DNA

RNA sample were used to synthesise cDNA using Superscript II Reverse Transcriptase (Invitrogen) following the manufacturer's protocol "First-Strand cDNA Synthesis Using SuperScript II RT". Individual reaction volumes were 200 µl. Typically 500 ng of RNA was used to prepare each sample of cDNA, but as little as 30 ng was used when either the RNA concentration was too low to enable a greater quantity of RNA to be added to the reaction or when one sample was used for several RT-PCR assays. The same amount of RNA was always used to produce cDNA for samples that would be used in the same RT-PCR experiment. After synthesis, cDNA was either stored at 4°C for use the same day for RT-PCR or stored at -20°C.

2.3.2 Real Time TaqMan RT-PCR

Relative abundance of transcripts in cDNA samples was used to identify variations in gene expression via RT-PCR. The experiment was carried out using TaqMan reagents and according to the TaqMan Gene Expression Assays Protocol published by Life Technologies. Briefly, a 10 µl PCR reaction mix was prepared on ice containing 5 µl of TaqMan gene expression master mix (Life Technologies), 0.5 µl of TaqMan primer (reverse 250nM/forward 250 nM) and probe (250 nM)

mix, 2.5 µl water, and 2 µl cDNA (usually equating to 50 ng of RNA). Samples were pipetted into MicroAmp 0.2 ml Optical 8-Tube Strips, sealed with 8-Cap Strips, and amplified in an Applied Biosystems StepOnePlus Real-Time PCR system using a standard ramp rate and the thermal cycling conditions detailed in Table 2.2 (Gangisetty & Reddy 2009). Four technical replicates were used per gene in each assay alongside two 'blank' samples containing only TaqMan gene expression master mix, TaqMan primer (reverse/forward) and probe mix, and water. At least three biological replicates were performed for each RT-PCR experiment.

Table 2.2 Conditions used for RT-PCR with TaqMan primers and probe sets

Purpose of stage	Temperature	Duration	
AMPerase activation	50ºC	2 minutes	
Taq activation	95ºC	10 minutes	
Denaturation	95ºC	15 seconds	40 cycles
Annealing Extension Data collection	60ºC	1 minute	

The RT-PCR primers used generated products of less than 150 base pairs and all but one assay spanned an intron/exon boundary within the gene of interest (see Table 2.3). Using RT-PCR assays that span such a boundary reduces the risk of genomic contaminants influencing the measurements of RNA transcript abundance. For genes with more than one known transcript, including DH_{44} and *DH44-R2*, primers were selected that would detect all known transcripts. For all of the primer and probe sets used, the reporter dye FAM was linked to the 5' end of the probe and a nonfluorescent quencher was linked to the 3' end of the probe. Each experiment was set up to include an endogenous control, *alpha-tubulin 84b* and at least one gene of interest. Additionally, at least one biological control was used and at least one condition of interest. The biological variables typically included either a difference in genotype of the flies from which the starting material had been extracted for RT-PCR amplification, or a difference in experience of flies with the same genotype (i.e. presence or lack of a stress exposure).

Table 2.3 Primers used for TaqMan RT-PCR

Gene	Amplicon size	Spans exon	Primer sequence or product code	Source
DH_{44}	63	2-3	Dm02138400_m1	Life Technologies
DH44-R1	59	9-10	Dm01824019_g1	Life Technologies
DH44-R2	85	8-9	Dm01793188_g1	Life Technologies
DH44-R2	68	3-4	Dm01793183_g1	Life Technologies
LK	128	N/A	Dm01843317_s1	Life Technologies
LKR	73	3-4	Dm01840198_m1	Life Technologies
alpha-tubulin 84b	114	1-2	Forward: ***CCTCGAAATCGTAGCTCTACAC*** reverse: ***ACCAGCCTGACCAACATG*** probe: ***TCACACGCGACAAGGAAAATTCACAGA***	Integrated DNA Technologies (Thomas et al 2012)

2.3.2.1 Quantitative PCR Data Analysis

The main kind of data produced by RT-PCR is a series of amplification curves, with one curve being created per sample. A threshold cycle C_T value is produced for each sample, which is the number of PCR cycles required for the signal from the reporter dye to exceed an arbitrary threshold. The thresholds used during this study were set at approximately the midpoint of the exponential phase of amplification. This was used to calculate a fold change for target genes under experimental conditions relative to an endogenous control sample under control and experimental conditions, and relative to the target gene under control conditions (Pfaffl 2001, Schmittgen & Livak 2008). This comparative method of data analysis is called the comparative C_T method or $2^{-\Delta\Delta CT}$ method (Livak & Schmittgen 2001). This method requires a minimum of four input values, as outlined in Table 2.4.

Table 2.4 Input values for $\Delta\Delta C_T$ method of fold change calculation

Name	Gene	Conditions
$C_{T\,T,E}$	Target	Experimental
$C_{T\,T,C}$	Target	Control
$C_{T\,E,E}$	Endogenous control	Experimental
$C_{T\,E,C}$	Endogenous control	Control

The first step towards calculating the fold change is to calculate a ΔC_T individually for the experimental and control conditions:

$$\Delta C_{T\,E} = C_{T\,T\,E} - C_{T\,E\,E}$$

$$\Delta C_{T\,C} = C_{T\,T\,C} - C_{T\,E\,C}$$

These are then used to calculate a $\Delta\Delta C_T$ which captures the differences in amplification values between both the two conditions and the two genes tested:

$$\Delta\Delta C_T = \Delta C_{T\,E} - \Delta C_{T\,C}$$

Finally, these values are transformed into a fold change of the target gene in the experimental condition as compared to its expression in the control condition using the following formula:

$$\text{Fold change} = 2^{-\Delta\Delta CT}$$

Use of this method depends mathematically on the amplification efficiency of the endogenous control and the target gene being about the same and being close to 100% (Livak & Schmittgen 2001). As the TaqMan Gene Expression Assays produced by Life Technologies have been shown to have an amplification efficiency of 100% ± 10% (Life Technologies 2012) and the *alpha-tubulin 84b* primers were found to have an efficiency close to 100%, this method is suitable for use with these reagents.

Statistical analysis of the fold change of gene expression under experimental conditions relative to a control is complicated by the lack of any variability in the values of the control. When using the comparative C_T method of qPCR data analysis, the value of the control is normalized to 1. Thus, despite performing

multiple biological replicates, the value of the control for each set will be mathematically transformed to a value of 1. This results in a dataset with absolutely no variability. Given this situation, a one-sample *t*-test can be used to statistically evaluate the data (Levenson et al 2006, Roth et al 2009). When using a one-sample *t*-test, a particular value is selected as the hypothesis and a set of values is compared to this number to assess the probability that the current dataset was observed by chance if the hypothetical value were the true value. In this case, the purpose of the statistical test was to assess whether the fold change of the gene expression under experimental conditions is significantly different from no change. Thus, for this analysis a one-sample *t*-test with a null hypothesis (i.e. a fold change of 1) was compared to the set of fold changes values obtained for the experimental condition. In every case a two-tailed test was used as no assumptions were made as to whether the fold change would be greater or smaller than 1.

Where fold change of gene expression has been normalised for two sets of samples to a control condition, these are compared using a two-tailed two-sample Student's *t*-test. This test was selected in this case as both sets of data retain their variance.

2.3.2.2 Evaluation of primer efficiency

In order to use the comparative C_T method of RT-PCR data analysis, it is important to satisfy the underlying assumption of the mathematics that all primers used have similar amplification efficiency and that these efficiencies are all close to 100% (Livak & Schmittgen 2001). As the *alpha-tubulin* 84b primers were not a predesigned assay, but rather were generated based on a published sequence, it was necessary to test the amplification efficiency of the primer pair. The amplification efficiencies of DH_{44}, *DH44-R1*, and both *DH44-R2* TaqMan Gene Expression Assays (Life Technologies) are guaranteed by the manufacturer to be close to 100% efficient.

PCR product using the *alpha-tubulin 84b* primers was resolved on an agarose gel and purified as described in section 2.2.2. A series of five 100-fold dilutions were prepared from the purified DNA product, which were then amplified using the *alpha-tubulin 84b* primers TaqMan under standard RT-PCR conditions (Gangisetty

& Reddy 2009). The C_T values were plotted against the dilution factor (Figure 2.1A). A slope of the line of best fit and R^2 value for the best-fit line was generated in Microsoft Excel using the mean C_T values plotted against the power of the dilution factor. The slope of this line was used to calculate the amplification efficiency of the primers using the equation detailed in Figure 2.1B (Rutledge & Cote 2003). Applying this equation to the slope of 3.2763 determined from the *alpha-tubulin 84b* primer pair C_T plot results in a value of 1.02, or 102%. This value is within the required margin of error of 100% ± 10% and indicates that the primers can be used for comparative C_T RT-PCR data analysis.

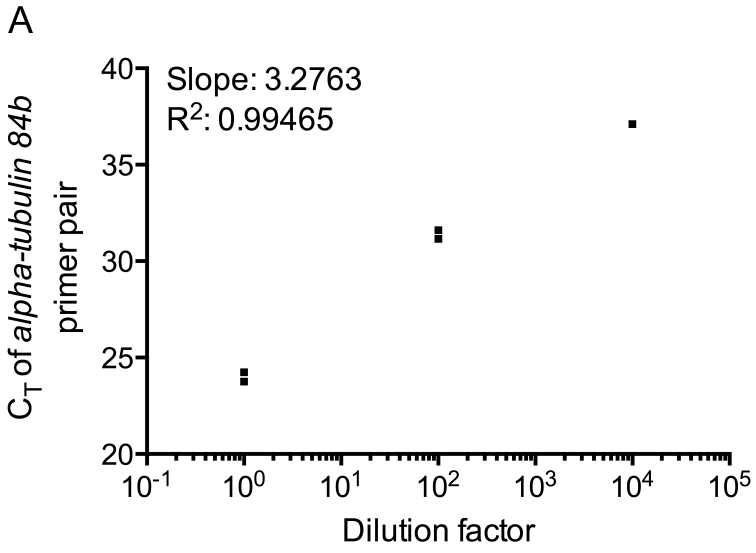

Figure 2.1 Verification of *alpha-tubulin 84b* primer pair amplification efficiency
A) C_T values obtained via TaqMan RT-PCR with the *alpha-tubulin 84b* primer pair are plotted on the y-axis in a linear scale against the dilution factor of amplified *alpha-tubulin 84b* primer product in a log scale. The slope of the line of best fit for the data points and the R^2 of this fit are displayed on the graph. **B)** Amplification efficiency is calculated from the slope of the line of best fit from the graph in part A using this equation (Rutledge & Cote 2003).

2.3.2.3 TaqMan primer resuspension

PrimeTime TaqMan Assay primers and probes ordered from Integrated DNA Technologies were resuspended according to the manufacturer's instructions. Assays were resuspended as 20X stocks for use in RT-PCR reactions.

2.3.3 Agarose Gel Electrophoresis of PCR product

When analysing products from RT-PCR reactions by gel electrophoresis, a 2% agarose gel in 0.5X TBE (90 mM Tris, 90 mM boric acid (pH 8.3), 2 mM EDTA) with 0.1 µg/ml ethidium bromide was used, as the primer products were within the range of 50-2000 base pairs (Sambrook & Russell 2001) and higher concentrations of gel provide better resolution for shorter DNA fragments. Prior to loading, gels were submerged in 0.5X TBE, which was used as an electrophoresis buffer, and loading dye was added to the samples.

Approximately 15 µl per sample was loaded into each well, and 500 ng of 1 kb+ DNA ladder (Invitrogen) was loaded into one lane on either side of the set of samples. Gels were run at 90 V and electrophoresis was ended based on the distance travelled by the dye front. The DNA in the gels was visualised using a high performance ultraviolet transilluminator (UVP, UK). The 1 kb+ ladder was used to estimate DNA fragment sizes.

2.3.4 Validation of primer sizes

In order to provide evidence that the TaqMan primers used to detect gene expression changes were amplifying the appropriate product, PCR product produced using each primer pair of interest was resolved on a 2% agarose gel. As shown in Figure 2.2, the products resolved on the gel were of the expected size for each primer set. No bands larger or smaller than those shown in the figure were observed when the gel was viewed under UV light. This suggests that non-specific amplification is unlikely to influence the fluorescent signal released during TaqMan qPCR amplification; signal validity is further supported by the additional specificity offered by the sequence-specific nature of the TaqMan probes themselves.

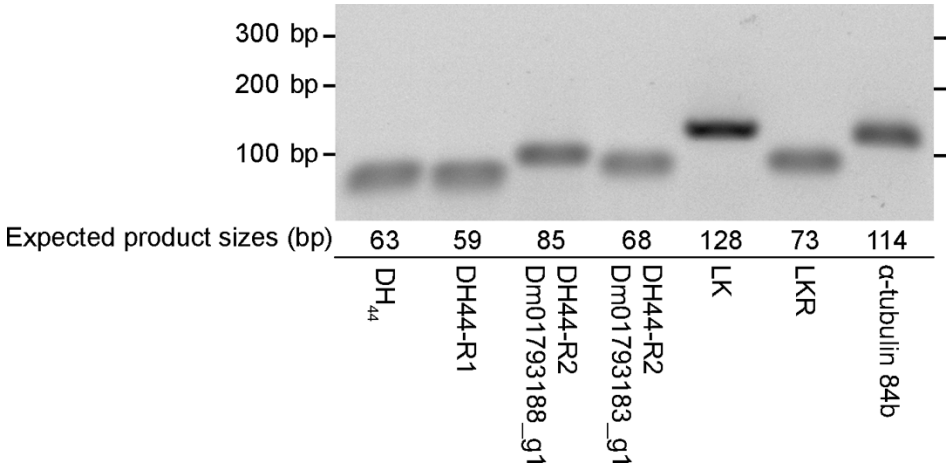

Figure 2.2 Validation of *DH$_{44}$*, *DH44-R1*, *alpha-tubulin 84b, LK, LKR,* and both *DH44-R2* primer pair product sizes

Agarose gel electrophoresis was used to resolve RT-PCR product samples using several different sets of primer pairs. These are listed alongside the size of product that is amplified when cDNA is used as a template. Ladder sizes are indicated on either side of the blot.

As all of the primer pairs shown in Figure 2.2 span an intron apart from *LKR*, the presence of genomic contamination would cause two bands to be shown in one lane if the product resulting from genomic material was small enough to be amplified under the TaqMan qPCR conditions. Using the known location of the primer pairs within each gene, the size of products that would be amplified in the presence of genomic contamination was calculated and can be found in Table 2.5. The products produced by the two pairs of *DH44-R2* primers are small enough to be within the ideal size range for a qPCR amplicon (50-150 bp), and the product produced by the *DH44-R1* primer pair is below the maximum recommended amplicon size (400 bp). Consequently, it would be expected that amplification of these products should be highly efficient. The lack of any double band in Figure 2.2 suggests that DNase treatment of the starting RNA material has been effective at reducing genomic contamination to a non-detectable level. The product that would be amplified from genomic contamination by the *LKR* primer pair is 1506 bp and may be too large to be amplified under the TaqMan qPCR conditions. As the *LK* gene does not have any introns, it is not possible to exclude genomic contaminants in this way. However, the lack of genomic contamination when using *alpha-tubulin* primers on cDNA

synthesised from the same RNA sample suggests that DNase treatment used in the study has been effective at minimising the presence of genomic material in the RNA samples produced.

Table 2.5 Size of PCR products produced by primer pairs when using either RNA or DNA as amplification material

Gene	Amplicon size (RNA)	Product size (DNA)
DH_{44}	63	2685
DH44-R1	59	307
DH44-R2 (spans exons 8-9)	85	151
DH44-R2 (spans exons 3-4)	68	120
LK	63	63
LKR	59	1506
alpha-tubulin 84b	114	603

2.4 Immunocytochemistry

Immunocytochemistry was performed on brains of *Drosophila* after dissection as described in section 2.1.4. Following dissection, brains were fixed in 4% paraformaldehyde in phosphate-buffered saline (PBS; 137 mM NaCl, 2.7 mM KCl, 10 mM Na_2HPO_4, 2 mM KH_2PO_4) for 20 minutes. Samples were washed 5-10 times in PBTA (0.5% Triton X-100, 0.1% azide in PBS) for at least 15 minutes per wash. Tissues were blocked by incubating with a blocking solution of 10% normal goat serum (Sigma) in PBTA for 2 hours, after which the tissues were transferred to a solution of primary antibody diluted in blocking solution for incubation overnight at 4°C. All primary antibodies used during the study were raised in rabbits; details of the antibodies used, their application, source, dilution, and duration of incubation can be found in Table 2.6. After incubation with the primary antibody, brains were washed with PBTA (changing the solution 5-10 times every 15 minutes), blocked with blocking solution for 2 hours, and incubated overnight in blocking solution with an anti-rabbit fluor-conjugated secondary antibody. If more than one primary antibody was to be used on the same tissue, this protocol was repeated by again washing and blocking the tissues, then incubating overnight with the other primary antibody, washing and blocking, and incubating overnight with a fluor-conjugated secondary antibody which responds to a

different wavelength than the first one used. Once all antibody incubations were complete, tissues were washed four times in PBTA for 15 minutes and twice in PBS for 15 minutes. Brains were then mounted on glass microscope slides in VectaShield (Vector Lab) and sealed below a 22 mm square glass coverslip using glycerol/gelatine (Sigma-Aldrich, UK).

Although anti-DH_{44} antibody, which was acquired from Professor Veenstra at the Université de Bordeaux, France, has been previously published with use at a dilution of 1:2000 (Cabrero et al 2002), it was found that the staining conditions detailed above gave clear results at a dilution of 1:4000.

Table 2.6 Antibodies used for immunocytochemistry

Antibody	Application	Source (Publication)	Dilution	Duration
Anti-DH_{44} (rabbit)	Primary antibody	Jan A. Veenstra (Cabrero et al 2002)	1:4000	Overnight
Anti-LKR (polyclonal rabbit)	Primary antibody	In-house (Radford et al 2002)	1:1000	Overnight
Anti-rabbit IgG-Alexa Fluor 546 (polyclonal goat)	Secondary antibody	Life Technologies	1:1000	Overnight
Anti-rabbit IgG-Alexa Fluor 488 (polyclonal goat)	Secondary antibody	Life Technologies	1:1000	Overnight

2.4.1 Immunocytochemistry data analysis

Semi-quantitative analysis of immunocytochemistry assays were carried out first by imaging tissues using confocal microscopy, as described in section 2.7. Z-stack images were then converted to grayscale and collapsed into a single image. Image J software was used to determine the mean pixel intensity of individual cell bodies (Schneider et al 2012). These values were compared statistically using a two-tailed two-sample *t*-test.

2.5 Preparation of Poly-L-lysine Dishes

Poly-L-lysine (0.1% w/v in H_2O, Sigma-Aldrich, MO, US) 35 mm glass-bottom dishes (MatTek Corporation, MA, USA) were prepared by pipetting 100 µl poly-L-lysine solution into the glass-bottom dish and incubating for 30 minutes at room temperature. After removing the solution, 100 µl of distilled water was pipetted into the dish and immediately removed by flicking. The dishes were then allowed to air-dry at room temperature until the water had evaporated, about 30-60 minutes.

2.6 Fluorescent-Tagged DH_{44} Peptide Labelling

Live Malpighian tubules from 7-10 day old male CS flies were labelled with a *Drosophila* DH_{44} analogue conjugated at an N-terminal cysteine to fluorophore tetramethylrhodamine (TMR)-C5-maleimide 543 BODIPY dye (DH_{44}-F). This is a stable fluorophore with high quantum efficiency. The reagent was acquired from Dr. Halberg and methods were shaped in collaboration with Dr. Halberg in line with recently published methods using fluorophore-labelled LK, capa-1, and DH_{31} (Halberg et al 2015). Validation of DH_{44}-F via secretion assay and ligand competition assay (see section 2.6.1) was carried out prior to experimental use.

A concentration of 10^{-7} M was used for the concentration of DH_{44}-F as it has been shown that this concentration is the threshold for DH_{44} peptide to provoke a physiological response in *Drosophila* Malpighian tubules, in terms of stimulation of fluid secretion and stimulation of cAMP signalling (Cabrero et al 2002). This suggests that it is a concentration at which a significant proportion of DH_{44} receptors are occupied, but it is unlikely that all receptors are occupied as higher concentrations of the peptide can provoke a greater increase in fluid secretion. However, in order to reduce background fluorescence, it is ideal to use as little DH_{44}-F in the bathing solution as possible while still achieving detectable receptor occupancy. The appropriateness of this concentration for use with DH_{44}-F was verified by a secretion assay confirming that a 10^{-7} M concentration of DH_{44}-F was able to induce a similar increase in fluid secretion by isolated Malpighian tubules as a 10^{-7} M concentration of DH_{44} peptide (see 2.9 for details of the secretion assay methodology).

For all live tissue experiments, including validation assays, Malpighian tubules were dissected as described in section 2.1.4 in Schneider's medium and transferred every 20 minutes into a freshly prepared mixture of Schneider's medium and *Drosophila* saline (1:1, v/v; see Table 2.7 for composition). Male CS flies aged 7-10 days old were used for all experiments and 15 pairs of tubules were dissected per condition. After dissections were complete, tissues were transferred to incubation solutions, all of which were made up in a 50:50 mixture of Schneider's medium and *Drosophila* saline and contained 500 ng/ml 4',6-diamidino-2-phenylindole (DAPI, Sigma-Aldrich, UK). The composition of each of the incubation solutions used for the different types of DH_{44}-F experiments performed can be found in Table 2.8. The incubation conditions used in all experiments were 15 minutes of gentle agitation at room temperature. Tissues were then mounted on poly-L-lysine-covered 35 mm glass-bottom dishes in PBS, which were prepared as described in section 2.5. The PBS was subsequently removed using a pipette and a fresh aliquot of the corresponding incubation solution was added to each dish. The tissues were then immediately imaged using a Zeiss LSM 510 Meta inverted confocal microscope (Zeiss, Oberkochen, Germany).

Table 2.7 Composition of Schneider's medium and *Drosophila* saline

Components	Schneider's medium (mM)	*Drosophila* saline (mM)
NaCl	35.9	117.5
$Na_2HPO_4 \cdot 2H_2O$	2.8	4.3
KH_2PO_4	5.0	
$CaCl_2$	4.1	2
KCl	21.5	20
$MgSO_4$	37	
$MgCl_2$		8.5
$NaHCO_3$		10.2
HEPES		15
α-ketoglutaric	1.4	
Succinic acid	0.8	
Fumaric acid	0.9	
Malic acid	0.7	
Glucose	11.1	20
Trehalose	5.3	
Yeastolate	2 g	
B-alanine	5.6	
L-arginine	2.3	
L-asparagine	0.3	
L-aspartic acid	4.0	
L-cysteine	0.5	
L-glutamic acid	5.4	
L-glutamine	12.3	
Glutathione	0.1	
Glycine	3.3	
L-histidine	2.6	
L-isoleucine	1.5	
L-leucine	1.1	
L-lysine	11.3	
L-methionine	5.4	
L-phenylalanine	1.5	
L-proline	14.8	
L-serine	2.5	
L-threonine	3.5	
L-tryptophan	1.0	
L-valine	2.6	
Fetal calf serum	18%	

Table 2.8 Incubation solutions used for DH_{44}-F validation and experiments.

All solutions were made up in a 1:1 (v/v) mixture of Schneider's medium and *Drosophila* saline

Experiment	Bathing solutions	Purpose
Optimisation of microscopy settings	500 ng/ml DAPI	Minimise baseline detection of autofluorescence
	500 ng/ml DAPI 10^{-7} M DH_{44}-F	Assess effectiveness of settings
Ligand competition assay	500 ng/ml DAPI 10^{-7} M DH_{44}-F	Control condition
	500 ng/ml DAPI 10^{-7} M DH_{44}-F 10^{-5} M DH_{44}	Determine whether DH_{44} can compete with DH_{44}-F for receptor binding sites; assess binding specificity
Hypothesis testing	500 ng/ml DAPI	Negative control
	500 ng/ml DAPI 10^{-7} M DH_{44}-F	Use on multiple biological groups to assess differences in peptide binding to receptor

2.6.1 Optimisation of Microscopy Settings

One group of Malpighian tubules was incubated in 500 ng/ml DAPI (negative condition), while the other was incubated in 500 ng/ml DAPI plus 10^{-7} M DH_{44}-F (positive condition). After incubation, tissues were mounted on poly-L-lysine-coated glass-bottom dishes. The negative condition sample was then used to adjust the baseline filter and exposure settings used for imaging in order to reduce the amount of autofluorescence signal detected. The positive condition sample was included to assess the effectiveness of the settings in detecting the receptor-ligand complex signal while excluding as much autofluorescence as possible. Details regarding the microscopy methods can be found in section 2.7.

2.6.2 Ligand Competition Assay

In order to verify the binding specificity of DH_{44}-F, a ligand competition assay was performed (Halberg et al 2015). Assuming that DH_{44} binds to DH44-R2 reversibly, then the labelled and unlabelled peptide should compete for available receptor binding sites. As described mathematically elsewhere (Halberg et al 2015, Lepre et al 2004), 10^{-5} M unlabelled peptide should be able to competitively displace 10^{-7} M labelled peptide, thereby causing an inhibition of the receptor-localised fluorescent signal. This was indeed the case and was

taken to indicate binding specificity of DH_{44}-F as well as reversibility of DH_{44} binding to DH44-R2.

Two incubation solutions were used for this experiment, one containing both 500 ng/ml DAPI and 10^{-7} M of DH_{44}-F (see Table 2.8), with the other containing both of these plus 10^{-5} M DH_{44}. After incubation, samples were mounted on poly-L-lysine-covered 35 mm glass-bottom dishes and immediately imaged using inverted confocal microscopy.

2.6.3 Live Tissue Labelling with DH_{44}-F

After validation of the DH_{44}-F labelling and imaging techniques, it was possible to use the method to test biological hypotheses. For this kind of experiment, at least three groups are required: a negative control, a positive control, and the condition of interest.

In this study, DH_{44}-F labelling was applied to Malpighian tubules dissected from 7-10 day old male CS *Drosophila* that had either been desiccated for 24 hours (condition of interest; see section 2.8.1 for details regarding desiccation methods) or normally fed on *Drosophila* standard diet (positive control) at 22°C, 45-55% relative humidity. 15 pairs of Malpighian tubules were dissected from desiccated *Drosophila*, ensuring that they were still alive as described in section 2.1.4, and 30 pairs of tubules were dissected from the normally fed *Drosophila*. Three incubation baths were prepared as detailed in Table 2.8. The Malpighian tubules from the desiccated flies and half of the tubules from the control flies were incubated in 10^{-7}M DH_{44}-F and 500 ng/ml DAPI, while the rest of the tubules from the control flies were incubated in 500 ng/ml DAPI only (negative control). After incubation, samples were mounted on poly-L-lysine-covered 35 mm glass-bottom dishes and immediately imaged using inverted confocal microscopy as detailed in section 2.7.

2.6.4 Fluorescent Signal Analysis

As identical slice sizes and microscope settings were used to capture images across different biological conditions, it was possible to compare the intensity of the fluorescent signal across conditions. Differences in signal intensity were

interpreted to be positively correlated with differences in the amounts of receptor-ligand complex present (Houchmandzadeh et al 2002).

As described elsewhere (Halberg et al 2015), intensity profiles were generated for individual principal cells of the Malpighian tubule using the Zeiss LSM 510 Meta confocal software. This involved first measuring the intensity of the fluorescent signal across an optical section of the Malpighian tubules by measuring this intensity at frequent intervals. More specifically, intensity was measured along a straight line that was perpendicular to the length of the Malpighian tubules. At least 750 measurements were used to gain a clear picture of the intensity profile of the Malpighian tubule staining. This was performed for at least 14 pairs of tubules in each biological group. As Malpighian tubules vary marginally in their width, data were normalised to the average width of measured tubules and average intensity trace ± standard error of the mean (SEM) was calculated for each biological set. Average intensity trace was then plotted in relation to its position along the plane of the width of the Malpighian tubule. Dr. Kenneth Halberg performed this analysis on the data generated from the DH_{44}-F labelling of tubules from desiccated and normally fed flies for the purposes of this study.

2.7 Confocal Microscopy

A Zeiss LSM 510 Meta inverted confocal microscope system (Zeiss, Oberkochen, Germany) was used to view and image both fixed and live tissue samples. Depending on the desired magnification, a x10, x20, x40 (oil immersion) or x63 (oil immersion) objective was used. An Argon laser was used to excite fluorophores with a 488 nm wavelength and a 505-530 band pass filter was used to receive emitted wavelengths. This laser was used to image GAL4/UAS driven expression of GFP and the Alexa Fluor-488-conjugated secondary antibody (Life Technologies), which emit wavelengths of approximately 520 nm. A He/Ne laser was used to excite fluorophores with a 543 nm wavelength and a 561-625 band pass filter was used to receive emitted wavelengths. Fluorophores imaged with this laser included the TMR-C5-maleimide 543 BODIPY dye conjugated to DH_{44} and the Alexa Fluor-546-conjugated secondary antibody (Life Technologies), which emit respective wavelengths of approximately 570 nm and 573 nm when

excited. DAPI was imaged by exciting it with the standard UV source (mercury lamp) and capturing the emitted signal using the confocal photomultipliers.

Where multiple fluorophore labels were detected in one sample, wavelengths were scanned sequentially for each optical section. This eliminates bleed-through of the fluorescent signal into non-corresponding channels. Images that were generated for comparisons of fluorophore signal intensity were captured using identical settings, including gain, exposure, and slice thickness.

2.7.1 Image Processing

Images were processed using the Zeiss LSM 510 Meta confocal software. In some cases the software was used to integrate the signals from multiple image slices at different depths (i.e. a Z-stack) in order to generate a single image. Scale bars were added to images using the Zeiss LSM 510 Meta software function.

2.8 Stress Tolerance Assays and Stress Exposure

Exposure to desiccation and starvation stress was used both to assess the effect of genotype on phenotypic ability to tolerate environmental stress and to generate samples that were used to assess the effect of these stressors on gene expression and metabolite composition of wild-type CS *Drosophila*. In all cases, 5-10 day old male flies were used, and the assays were conducted at 22°C with 45-55% relative humidity.

If samples were being generated for gene expression or metabolite composition, then groups of 30 male flies were either desiccated or starved for 24 hours alongside a designated control group using the desiccation or starvation vials described in sections 2.8.1 and 2.8.2 below. In these cases, stress exposure was usually initiated in the morning to allow time for the required experimental protocols to be completed the following day.

2.8.1 Desiccation Assay

Desiccation survival assays were performed by placing groups of approximately 30 flies into empty vials and counting the number of dead flies hourly until mortality reached 50%, and then approximately every 2 hours until mortality

reached 100% (Kahsai et al 2010, Terhzaz et al 2012, Terhzaz et al 2015b). Flies were counted as dead if they did not move upon agitation of the vial. *Drosophila* were typically transferred into empty vials between 4 pm and 6 pm and observation of mortality commenced at 9 am the following morning.

2.8.2 Starvation Assay

Starvation assay vials were prepared for the starvation assay at least 12 hours in advance by preparing a solution of 1% low melting point agar (Roche) and pipetting 2 ml into each tube. These were allowed to solidify at room temperature. After most of the condensation had evaporated from the interior of the tube, the end was blocked using a dense weave cellulose acetate plug.

Starvation assays were conducted by placing groups of approximately 30 flies into the starvation assay vials and counting dead flies every 2 hours until mortality reached 50%, and then approximately every 4 hours until mortality reached 100% (Iijima et al 2009, Terhzaz et al 2015b). This method differs from desiccation stress exposure as the flies are able to access the water content in the agar, but do not receive any metabolic sustenance from it nor from the flies housed with them (Huey et al 2004). As before, flies were counted as dead if they did not move upon agitation of the vial. *Drosophila* were typically transferred into starvation assay vials between 6 pm and 8 pm, and observation of mortality commenced around 35 and 39 hours later, between 7 am and 9 am.

2.8.2.1 The Starvation Assay as a Control for the Desiccation Assay

As the desiccation stress protocol described in section 2.8.1 involves placing *Drosophila* in empty vials, the flies are not only desiccated, but starved as well. To control for the potential contribution of starvation to survival in a desiccation stress assay, flies were additionally exposed to a starvation assay. Impaired starvation survival within the timeframe of the desiccation assay would indicate that poor survival was due rather to a lack of food than to a lack of water.

Gene expression assays of desiccated flies included samples of flies starved for the same period of time to assess the relative contribution of starvation to the gene expression changes. Due to the cost associated with metabolomics experiments, a starved control was only included in one of the two studies.

Consequently, the results of the experiment comparing only unstressed flies to desiccated flies should be interpreted in the light of the unknown nature of any metabolic effects that the starvation component of the desiccation exposure had during this experiment.

2.8.3 Stress Tolerance Assay Data Analysis

Survival data were plotted as Kaplan-Meier curves (Kaplan & Meier 1958). These graphs plot percentage surviving flies over a period of time. As the percentage flies surviving at a given point is taken to be an estimator of the true survival pattern of the whole population, it is useful to approximate the variance or confidence interval of the survival function. Variance can be estimated mathematically and was done so in this study using the Greenwood formula (Cox & Oakes 1984). Statistical comparisons of two survival curves were made using the Logrank test. This is a nonparametric test that uses comparisons between observed and expected number of deaths at each timepoint to test the null hypothesis of no difference in survival function between two groups.

Hazard ratios were calculated to provide an estimate of the effect size in each experiment using the Mantel Haenszel approach as this test has been found to perform more accurately than the log-rank calculation of hazard when using large sample sizes (Bernstein et al 1981). Hazard ratios compare the rate of death in the experimental group to the rate of death in the control group. This value is representative of the risk over the entire experiment. When interpreting the hazard ratio, a number lower than 1 indicates that the experimental group has a lower rate of death than the control, a number greater than 1 indicates that the experimental group has a higher rate of death than the control, and 1 indicates that the death rates are the same. A hazard ratio of 2 would indicate that, at any given timepoint, the chance of a surviving individual in the experimental group dying before the next measurement is twice that of a surviving individual in the control group.

Data are interpreted such that experimental cross progeny must survive differently than progeny of both control crosses, and in the same direction when compared to each (i.e. experimental cross progeny must survive longer than progeny from both control crosses or progeny from both control crosses must live

longer than experimental cross progeny) in order for an assay to be considered to conclusively reject the null hypothesis.

2.9 Fluid Secretion Assay

Measurements of the volume of fluid secreted from excised *Drosophila* Malpighian tubules over time enables calculation of the secretion rate of these epithelial tissues. Testing the secretion rate under different biological conditions, such as stress exposure or variation in genotype, allows calculation of a basal secretion rate, which can provide information about the basic functioning of the tubules. Application of diuretic peptides, such as DH_{44} or LK can be used to stimulate secretion above the basal rate and provides a measure of the stimulated secretion rate. Exposing excised Malpighian tubules to diuretic peptides across different biological conditions can reveal the effect of genetic manipulation or stress exposure on the responsiveness of the tissue to particular peptides.

Fluid secretion assays using *Drosophila* Malpighian tubules were performed using the modified Ramsay assay (Ramsay 1954), as described previously (Dow et al 1994). *Drosophila* aged 5-10 days old were anaesthetised on ice and dissected as detailed in section 2.1.4, with additional care to ensure that approximately half of the ureter was retained with each tubule pair. Equal numbers of males and females were used and at least 14 pairs of tubules were prepared for each of two conditions per assay. Individual tubule pairs were transferred to 9 µl drops of 1:1 (v/v) Schneider's medium: *Drosophila* saline (Cabrero et al 2002) every 20 minutes under x25 magnification (see Figure 2.3). These drops contained a small quantity of red Amaranth dye to facilitate viewing of emerging secretions and were submerged under white, heavy mineral oil (Sigma, UK). Adjacent to each drop was a small metal pin, around which was wrapped one end of each tubule pair using a fine glass rod after all pairs of tubules had been transferred to the assay dish. The other end remained in the 1:1 (v/v) Schneider's medium: *Drosophila* saline mixture. The ureter was positioned approximately halfway between the aqueous drop and the metal pin.

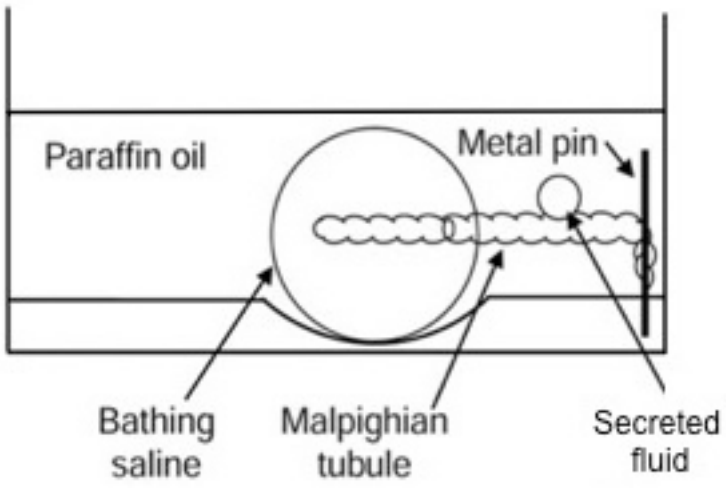

Figure 2.3 Modified Ramsay assay for the measurement of secretion by Malpighian tubules
Apparatus and set-up of the modified Ramsay assay shown. Figure adapted from (O'Donnell 2009) with permission from The Company of Biologists Ltd.

Secretion droplets that had accumulated at the common ureter of tubule pairs during the assay preparation were removed using a very fine glass rod and the Malpighian tubules were left to secrete for 10 minutes. Secreting and non-secreting tubules were noted at this point and the assay was conducted using only the functional tubule pairs. Tubule secretions were then removed and measured over the span of 10 minutes, timing it so as to enable secretions to be removed and measured from all pairs of tubules every 10 minutes. Secretion measurements were made by bringing secretion drops to the surface of the mineral oil and measuring the diameter with the eyepiece graticule at x50 magnification. The diameter was converted into a volume using the equation $V = (4/3)\pi r^3$, where r is the radius of the droplet and V is volume.

Baseline secretion was measured every 10 minutes for 30 minutes. Starting around 20 minutes after the assay had begun, 1 µl of diuretic peptide (10^{-6} M) was pipetted to rest near to the 9 µl drops of 1:1 Schneider's medium: *Drosophila* saline. This made it possible to add the drop of peptide to the larger drop containing the end of one tubule while making the final basal fluid secretion measurement for each tubule pair. Stimulated secretion rate was then measured every 10 minutes for 30 minutes. Increases in secretion rate following application of peptide were taken as an indication of diuretic effect. DH_{44} peptide was synthesised by Genosphere Biotechnologies (Paris, France) while LK

peptide that was produced by Cambridge Peptides (Birmingham, UK) was acquired from Dr. Kenneth Halberg (University of Glasgow, UK). Peptides were first diluted to 10^{-5} M in distilled water, then diluted 10x in 1:1 Schneider's medium: *Drosophila* saline, and finally diluted 10x again by adding 1 µl of this solution to the 9 µl drops of 1:1 Schneider's medium: *Drosophila* saline used in the secretion assay, resulting in a final concentration of 10^{-7} M LK or DH_{44} peptide.

2.9.1 Fluid secretion assay data analysis

Secretion droplet volumes (as determined in section 2.9) were used to calculate secretion rate in nl/min by dividing the volume by the 10 minute time interval that elapsed between measurements for individual tubule pairs. To determine whether the secretion rates of two biological groups differed significantly, independent two-tailed two-sample *t*-tests were applied for each of the measurements of secretion rate. For a typical secretion assay, six comparisons were made in this way, three for basal secretion results and three following stimulation with a peptide. These data were also used to determine whether a set of Malpighian tubules responded significantly to the peptide applied (i.e. a within-group comparison). After calculating an average basal secretion rate and an average stimulated secretion rate for each pair of tubules, these were compared using a paired-samples two-tailed *t*-test. A paired-samples *t*-test should be used when an individual tissue has been tested twice and is being compared to itself, as is the case in this instance.

Percentage change in secretion rate following application of peptide was calculated by dividing the maximum secretion rate measured after stimulation with the peptide divided by the mean of basal secretion rate across 30 minutes for each pair of tubules (MacPherson et al 2004). This value was calculated for each sample type used in the secretion assay and compared via independent two-sample two-tailed *t*-testing.

2.10 Wet and dry weight measurements

Measurements of wet and dry fly weight were made to identify a potential bloating phenotype (Cabrero et al 2014). *Drosophila* were prepared for

measurement of wet weight by briefly anesthetizing flies using CO_2 and transferring groups of 10 male or female flies to Eppendorf tubes on ice. Group weights were then measured using a GR-202 precision balance (A&D, Japan), which is accurate to 0.0001 grams. Flies were subsequently killed by being placed at -80ºC for 20 minutes. They were then dried at 60ºC for 24 hours with the Eppendorf tube lids open to allow air to circulate around the flies. Dried flies were then allowed to reach room temperature before being weighed in groups on the precision balance. At least five groups were weighed for each biological condition tested.

Total body water weight was determined by subtracting the dry weight of a group of flies from the corresponding wet weight measurement for the group. Water content was additionally expressed as a percentage of the wet weight (Folk et al 2001). Statistical comparisons were made using two-sample two-tailed Student's *t*-tests.

2.11 Metabolomics

Untargeted metabolomics was used to assess the effect of desiccation stress on metabolite composition of *Drosophila melanogaster*. This was assessed both at the level of the whole organism and at the level of the tissue of particular interest for this study, the Malpighian tubules.

2.11.1 Sample Preparation

Male CS flies aged 5-10 days old were desiccated, starved, or fed normally for 24 hours. They were then anesthetised on ice. Where dead flies were present in the desiccation and starvation conditions, only living flies were used. Either whole flies were used for samples, or Malpighian tubules were dissected as described in section 2.1.4. Whole fly samples were composed of six male flies. Adult fly tubule samples were composed of 20 pairs of tubules.

Samples were prepared by placing the whole organism or tissue into 250 µl of extraction buffer composed of methanol, chloroform and water (3:1:1 v/v/v) in a 1.5 ml microcentrifuge tube chilled on dry ice, as described elsewhere (Al Bratty et al 2011, Chintapalli et al 2013a). Where whole flies were used, samples

were homogenized in an Eppendorf tube using a plastic mortar. All samples were sonicated using an ultrasonic cell disruptor (Microson Inc., USA) for 10 one-second blasts and then centrifuged for 5 minutes at 13,000 *g* at 4ºC. The supernatant was transferred to a new Eppendorf tube, snap-frozen in liquid nitrogen, and stored at -80ºC.

2.11.2 Hydrophilic Interaction Liquid Chromatography-Mass Spectrometry

Samples were subjected to hydrophilic interaction liquid chromatography-mass spectrometry analysis by the Glasgow University Polyomics Group. Liquid chromatography was conducted using an UltiMate 3000 RSLC (Thermo Fisher Scientific) with a 150 x 4.6 mm ZIC-HILIC (Hydrophilic Interaction Chromatography) column running at 300 µl/min, while mass spectrometry was completed using an Orbitrap Exactive (Thermo Fisher Scientific) set at 50 000 resolution. Sample analysis was carried out using switching polarity. The capillary temperature was 275ºC, sheath gas flow rate was 40 arbitrary units and auxiliary gas flow rate was 20 arbitrary units. Solvent A was 0.1% formic acid in water and solvent B was 0.08% formic acid in acetonitrile. Injection volume was 10 µl. Gradient details are as follows: 80% B at 0 min, 20% B at 30 min, 5% B at 32 min, 5% B at 40 min, 80% B at 42 min, 80% B at 47 min.

2.11.3 Data Processing

Peaks were selected from the raw metabolomics data using XCMS (Smith et al 2006), MzMatch/PeakML was used for filtering and grouping (Scheltema et al 2011), and IDEOM was used to further filter and process the data and identify metabolites (Creek et al 2012). Peaks were searched against a list of compound masses compiled from KEGG, Metlin, Human Metabolome, and Lipid Maps databases (Fahy et al 2007, Kanehisa et al 2016, Tautenhahn et al 2012, Wishart et al 2013). A set of standard samples analysed in terms of mass and retention times (RT) were used to establish a set of core metabolite identifications. Mass and predicted RT (Creek et al 2011) enabled additional putative identifications. Where RT was measured directly, as for the standard samples, peaks were identified with 5% RT error, while those with calculated RT were identified with 45% RT error. Positive and negative mode data were combined in the final

analyses. Pathway analysis was facilitated using the online tool Pathos (Leader et al 2011).

2.11.4 Confidence ranking of putative metabolite identifications

The level of confidence in the metabolite identification is split into two categories. In the first category (level 1 accuracy), a standard was run for that particular compound, and the exact mass and retention time was matched to sample peaks within 1.5 ppm and 5% retention time. In the second category (level 2 accuracy), identification is based on the mass of the compound, with isomer predictions based on retention time. Thus, although the most likely isomer for each metabolite is listed and discussed, it is possible that the true identity of the compound could be a different isomer. Consequently, number of alternative isomers is listed in tables. Also included in the second category are compounds that were run alongside a standard, but the stringent 5% variability in retention time cut off was exceeded.

2.11.5 Metabolomics data analysis

Where a metabolite was detected in at least three samples in two conditions, statistical comparisons were made using two-tailed two-sample Student's *t*-test. Although statistical power can be gained when analysing large sets of data by assuming that standard deviation is consistent across samples, this is not appropriate for untargeted metabolomics as the units of detection are arbitrary units and the power of the units recorded can vary widely. Consequently, each *t*-test was performed individually without reference to the standard deviation of the rest of the dataset. The frequency of false positives was controlled by setting a False Discovery Rate using the Benjamini and Hochberg Method (Benjamini & Hochberg 1995, Morrow et al 2013, Nkuipou-Kenfack et al 2014). This was adjusted to 5% or 1% depending on the stringency desired for the analysis, as discussed in section 1.5.6. Values deemed to be different enough to warrant further consideration using this method are termed 'discoveries' rather than 'statistically significant'.

The Benjamini-Hochberg method is applied by first ordering the *P* values obtained during a series of *t*-tests from smallest to greatest and then calculating

a Benjamini-Hochberg critical value using the formula $(i/m)Q$, where i is the rank of the P value (the smallest P value has rank 1, and the next rank 2, and so on), m is the number of t-tests that was performed, and Q is the false discovery rate (in this study, 1 or 5). The Benjamini-Hochberg critical value for each metabolite is then compared to the P value. The largest P value for which the P value is less than the Benjamini-Hochberg critical value is deemed a discovery, as are all P values smaller than this one.

3 DH_{44} peptide signalling and stress tolerance

When exploring whether a neuroendocrine pathway is involved in stress tolerance in *Drosophila melanogaster*, there are two main ways of approaching the question. The first is to expose a wild-type *Drosophila* strain, like CS, to the stress conditions of interest and then to determine whether any components of the pathway have changed. This can be measured by assessing changes in gene expression, tissue function or response to upstream signals, or protein expression. The second is to manipulate components of the pathway and then to determine whether these changes have any effect on stress tolerance phenotypes.

3.1 Desiccation affects the DH_{44} signalling pathway in wild-type *Drosophila melanogaster*

A role for DH_{44} peptide in desiccation tolerance was proposed based on the findings that signalling by other diuretic neuropeptides modulates desiccation tolerance in *Drosophila* (Kahsai et al 2010, Soderberg et al 2011, Terhzaz et al 2012, Terhzaz et al 2015b), and evidence indicating that fluid homeostasis is a crucial aspect of survival during desiccation (Gibbs & Matzkin 2001, Telonis-Scott et al 2012). It was hypothesised that wild-type *Drosophila* would down-regulate the DH_{44} signalling pathway as a consequence of desiccation stress exposure. This was explored in several ways and at several biological levels. At the mRNA level, changes in gene expression of the three key components of DH_{44} signalling, *DH_{44}, DH44-R1*, and *DH44-R2* were explored following either desiccation or starvation stress (section 3.1.1). At the protein expression level, DH44-R2 presence on the basolateral membrane of the Malpighian tubule principal cells was assessed using fluorophore-tagged peptide labelling of live tissue following desiccation exposure (Halberg et al 2015) (section 3.2). Finally, at the phenotypic level, fluid secretion rates of Malpighian tubules from desiccated flies in response to DH_{44} were measured (section 3.1.2).

3.1.1 Desiccation, but not starvation, affects expression of genes in DH_{44} signalling pathway

As desiccation exposure has been found to modify the expression of genes involved in the signalling pathways of diuretic neuropeptides, including the *capa*

gene (Terhzaz et al 2015b) and *LKR* gene (Terhzaz, Cabrero unpublished data), it was hypothesised that expression of *DH$_{44}$* or DH$_{44}$ receptor genes *DH44-R1* and *DH44-R2* might also be affected by desiccation stress. Consequently, RNA samples were prepared from all-male groups of normally fed *Drosophila* and compared to RNA prepared from *Drosophila* that were exposed to desiccation stress for 24 hours. As the conditions used for desiccation require the insects to be without both food and water, a 24-hour starvation condition was included in the assay as an additional control (see section 2.8.2.1). If the effects seen after 24 hours under these conditions were due to the lack of food rather than to the lack of water, the starvation control would be expected to reveal this.

Gene expression data from the FlyAtlas microarray (Chintapalli et al 2007), which is available online at http://flyatlas.org were used to select the tissues used for RNA extraction and amplification of particular genes. Specifically, where a receptor gene was expressed in both gut and neural tissues, sample sets were designed to exclude neural expression.

The FlyAtlas resource details the tissue-specific expression of approximately 13,500 genes in *Drosophila* adults and larvae and can be used both for data mining (Chintapalli et al 2013b) and to hone experimental design. As FlyAtlas data indicate that *DH$_{44}$* and *DH44-R1* expression are enriched primarily in the brain and thoracicoabdominal ganglion (see Table 3.1), expression changes in these genes were explored using samples extracted from whole flies. Conversely, as shown in Table 3.1, *DH44-R2* expression is enriched not only in the brain of *Drosophila*, but also in the Malpighian tubules, crop, midgut and hindgut. So as to explore potential changes in DH44-R2 in non-neural tissues only, expression was analysed by using RNA samples extracted from the bodies of *Drosophila* by removing the heads during sample collection.

Table 3.1 Expression of genes in the DH_{44} signalling pathway in *Drosophila* tissues.
Table shows mRNA abundance of *DH_{44}*, *DH44-R1*, and *DH44-R2* in relevant fly tissues. Data displayed are from FlyAtlas (Chintapalli et al 2007) and show the mRNA signal in each sample ± SEM as well as the mRNA enrichment in each tissue relative to the signal detected in the whole fly. Not detected (ND) indicates that the Affymetrix present call indicated 0 detections out of 4 biological repeats. Enrichment values of 5 and above are highlighted in yellow, with values over 30 being indicated in red. Values in between these extremes are highlighted in various shades of orange.

	DH_{44}		***DH44-R1***		***DH44-R2***	
Tissue	mRNA Signal	Enrich-ment	mRNA Signal	Enrich-ment	mRNA Signal	Enrich-ment
Brain	654 ± 23	31.3	154 ± 6	20.6	136 ± 4	6.1
Thoracicoabdominal ganglion	124 ± 4	5.9	127 ± 7	17	100 ± 5	4.5
Crop	ND	ND	ND	ND	209 ± 11	9.4
Midgut	ND	ND	ND	ND	110 ± 3	5
Tubule	15 ± 8	0.7	ND	ND	410 ± 14	18.5
Hindgut	ND	ND	ND	ND	121 ± 4	5.5
Testis	77 ± 4	3.7	ND	ND	ND	ND
Whole fly	20 ± 1		7 ± 0		22 ± 1	

RNA extracted from either sets of 10 CS bodies (N = 3) or sets of 8 whole CS flies (N = 5) was used to synthesize cDNA and perform RT-PCR using TaqMan probe and primer sets for *DH_{44}*, *DH44-R1*, and *DH44-R2* (spanning exons 8-9), with *alpha-tubulin 84b* as the endogenous control. Comparative C_T analysis was used to calculate a fold change for each of the genes of interest in the two experimental conditions (starvation and desiccation) relative to the control condition (normally fed) as shown in Figure 3.1. This method is described in section 2.3.2.1, as is the rationale for selection of statistical tests used to analyse the data. A two-tailed one-sample Student's t-test was performed for each set of fold changes acquired for each gene under each of the two experimental conditions against a null hypothesis of a fold change of 1 (i.e. no change in expression). There was a significant difference between the null hypothesis and the fold changes obtained for *DH44-R2* expression after 24 hours of desiccation (M = 0.4167, SD = 0.00577, N = 3), $t(2) = 175$, $p < 0.0001$, indicating a 58% (95% CI: 57-60%) decrease in expression of *DH44-R2* relative to normally fed controls. Additionally, there was a significant difference identified in *DH_{44}* expression following 24 hours of starvation (M = 1.216, SD = 0.158, N = 3), $t(4) = 3.063$, $p = 0.0376$, indicating a 22% (95% CI: 2-41%) increase in

expression of DH_{44} relative to normally fed controls. All other *p* values obtained from this analysis were greater than 0.05; these results are shown in Table 3.2.

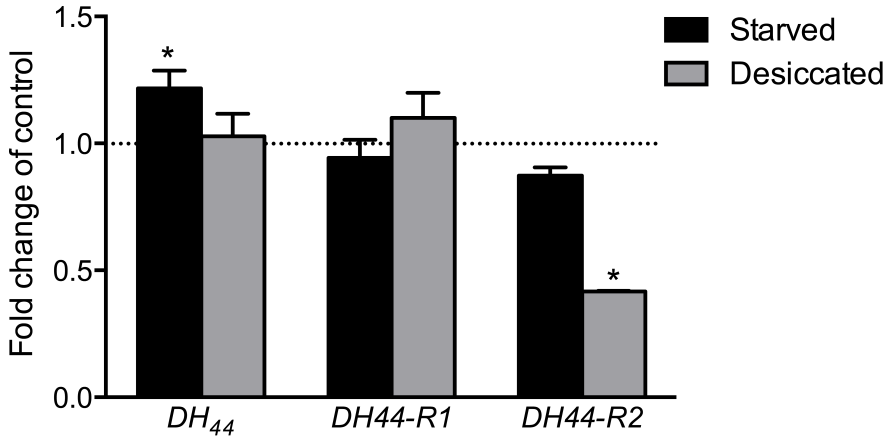

Figure 3.1 Gene expression of *DH44* is significantly increased by starvation stress and expression of *DH44-R2* is significantly reduced by desiccation stress.

Fold change in RNA transcript levels of *DH44* (*N*=5), *DH44-R1* (*N*=5), and *DH44-R2* (*N*=3) following 24 hours of starvation or desiccation in male CS flies relative to untreated controls (mean ± SEM). Exposure to desiccation stress for 24 hours decreased *DH44-R2* expression in *Drosophila* bodies by 58%. Starvation exposure increased *DH44* expression by 22% in whole *Drosophila*. Statistical significance is based on one-sample Student's *t*-test with null hypothesis of 1.0, **p*<0.05

Table 3.2 Two-tailed one-sample Student's t-test analysis of fold change of expression of genes in *DH44* signalling pathway

Statistically significant *p* values are highlighted in boldface red text.

	DH44		***DH44-R1***		***DH44-R2***	
	Desiccated	Starved	Desiccated	Starved	Desiccated	Starved
t	0.3108	3.063	1.757	0.5807	175	3.983
df	4	4	4	4	2	2
p	0.7715	**0.0376**	0.3602	0.4699	**<0.0001**	0.0576

The statistically significant decrease in *DH44-R2* expression following desiccation exposure represents a 2.4 fold decrease in the expression of this gene relative to a normally fed control condition. This result is not due to the starvation stress also endured during desiccation stress, as *DH44-R2* expression did not decrease significantly following a starvation stress exposure of the same duration. Consequently, it appears that this change in gene expression is due specifically to the lack of water during this experimental manipulation. These results indicate that desiccation stress is detected by the tubules and causes CS *Drosophila* to down-regulate expression of the receptor for DH_{44} peptide,

thereby implicating DH_{44} peptide signalling pathways not only in the stimulation of secretion, but also in the regulation of fluid homeostasis during desiccation stress.

Changes in gene expression in response to environmental stress are likely mediated by transcription factors. *D. melanogaster* selected for desiccation resistance show enrichment of multiple transcription regulators in whole fly (Telonis-Scott et al 2012). As the Malpighian tubules form one of the barriers between the internal and external environment and are known to be a stress sensing tissue, it is likely that some of these factors are involved in altering gene expression in response to desiccation stress in the tubules (Davies et al 2014). Indeed, transcriptional changes in the Malpighian tubules in response to desiccation stress or following capa-1 stimulation have been found to occur via the NF- κB signalling pathway (Terhzaz et al 2014).

The statistically significant result of an increase in *DH_{44}* expression following starvation exposure represents a potentially fairly small difference in expression. The 95% confidence interval of the increase gives a range of 2-42%. If the true mean lies close to the low end of this range, then it would appear that while the result may be significant, it is unlikely to be biologically relevant. If the true mean lies close to the high end of this range, it could be a potentially interesting result to pursue, particularly in light of the recent findings that DH_{44} signalling is required in order to select nutritive sugars (Dus et al 2015). As 24 hours is a relatively short starvation stress exposure (almost no male *Drosophila* were dead in the starvation vials after this period of time, in contrast with approximately 50% mortality among flies in the desiccation stress vials), it is possible that changes in *DH_{44}* expression following starvation stress might be more pronounced after longer periods of stress exposure than those used in this assay. However, it is also possible that this finding is a false positive. As several statistical comparisons were made, it could be argued that a correction for multiple testing should be applied to the data. In this case, it is evident that only the decrease in *DH44-R2* expression would remain statistically significant. A formal mathematical correction for multiple testing has not been applied in this case, but the possibility of a false positive is considered in the interpretation of the data, as discussed elsewhere (Rothman 1990, Saville 1990).

Based on the finding that *DH44-R2* expression decreases significantly (both statistically and numerically) following desiccation exposure, it was hypothesised that the Malpighian tubules of desiccated flies would be less responsive to the DH_{44} peptide than those of normally fed controls.

3.1.2 Effect of desiccation on diuretic response of Malpighian tubules to DH_{44} peptide stimulation

The effect of desiccation stress on the response of the Malpighian tubules to DH_{44} peptide was evaluated using the modified Ramsay assay (Ramsay 1954), which measures fluid secretion by *Drosophila* tubules (Dow et al 1994). Malpighian tubules were dissected from male CS *Drosophila* that were desiccated for 24 hours and from normally fed controls. As detailed in section 2.9, the volume of secretion by individual tubule pairs was measured every 10 minutes for 30 minutes to determine a baseline secretion rate, after which 10^{-7} M DH_{44} peptide was applied. Stimulated secretion volumes were then measured every 10 minutes for an additional 30 minutes to determine the secretion rate in response to peptide stimulation. Four biological repeats of the assay were performed and the data were analysed as described in section 2.9.1. One repeat that is representative of the overall data is presented in Figure 3.2A. Details of the statistical testing approach used, including the rationale for test selection can be found in section 2.9.1. Two-sample two-tailed Student's *t*-tests were performed on the measurements of secretion rate for each 10 minute time interval to compare the values acquired from desiccated flies to those from unstressed controls. The secretion rates of Malpighian tubules from desiccated flies were significantly lower than those from normally fed flies at all time points during baseline measurement and at all time points after stimulation with DH_{44} peptide ($p < 0.05$, see Table 3.3 for details).

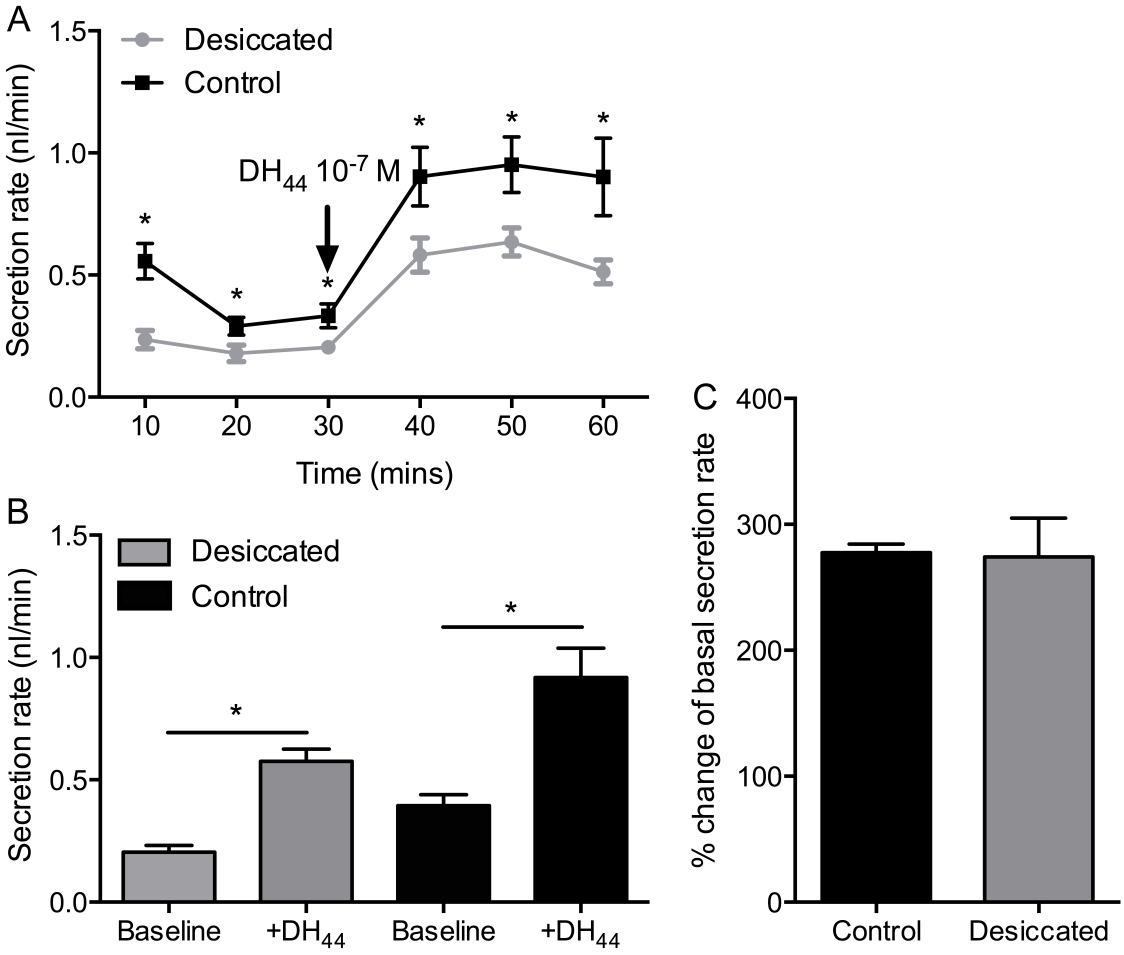

Figure 3.2 Fluid secretion rate of excised Malpighian tubules from male CS *Drosophila* following 24 hours of desiccation stress exposure or 24 hours of normal feeding.

A) Secretion rate of Malpighian tubules from desiccated flies (*N*=10) is consistently lower than that of normally fed controls (*N*=8) both during 30 minutes of continuous baseline secretion and in response to application of 10^{-7} M DH_{44} peptide. The graph is representative of four biological replicates. **B)** Malpighian tubules from both desiccated and normally fed flies increase secretion rate significantly in response to application of 10^{-7} M DH_{44} peptide. **C)** Secretion rate of excised Malpighian tubules increases by approximately 175% following stimulation with 10^{-7} M DH_{44} peptide in both desiccated and control conditions. Mean percentage change from each of four biological replicates of the assay is shown and was calculated as described in 2.9.1. * indicates a statistically significant difference (p<0.05). All graphs show mean ± SEM.

Table 3.3 Two-sample two-tailed Student's *t*-test analysis of secretion rate by Malpighian tubules following 24 hours of desiccation (*N*=10) or exposure to control conditions (*N*=8). Statistically significant *p* values are highlighted in boldface red text. D*f* = 16 for all comparisons

	Baseline secretion			Stimulated secretion		
Time (mins)	0-10	10-20	20-30	30-40	40-50	50-60
Desiccated *M*	0.236	0.180	0.204	0.582	0.635	0.513
Desiccated *SD*	0.036	0.035	0.027	0.067	0.054	0.047
Control *M*	0.568	0.291	0.334	0.903	0.952	0.902
Control *SD*	0.068	0.035	0.046	0.113	0.106	0.148
t	4.413	2.316	2.555	2.561	2.819	2.741
p	**0.0004**	**0.034**	**0.021**	**0.021**	**0.012**	**0.015**

Tubule response to peptide application in each of the two conditions was assessed as described in section 2.9.1 (Figure 3.2B). A paired-samples two-tailed Student's *t*-test was performed to compare baseline secretion rate and stimulated secretion rate in each of the two conditions (desiccated vs. control). There was a significant difference between the baseline secretion rate (M = 0.21, SD = 0.085) and stimulated secretion rate (M = 0.58, SD = 0.159) in the desiccated condition, $t(9) = 11.83$, $p < 0.0001$, indicating a 2.8 fold (95% CI: 2.4-3.1) increase in secretion rate following peptide stimulation. Similarly, there was a significant difference between the baseline secretion rate (M = 0.40, SD = 0.126) and stimulated secretion rate (M = 0.92, SD = 0.336) in the control condition, $t(7) = 6.173$, $p = 0.0005$, indicating a 2.3 fold (95% CI: 1.8-2.8) increase in secretion rate following peptide stimulation.

In order to compare the response of Malpighian tubules from desiccated *Drosophila* to that of normally fed *Drosophila* when exposed to DH_{44} peptide, a percentage change for each pair of tubules was calculated as described in section 2.9.1. These values were then used to determine a mean percentage change for each of the four biological replicates, which are plotted in Figure 3.2C. As the percentage change in response to peptide stimulation was very similar across both conditions, no statistical tests were performed.

The significantly lower basal secretion rate indicates that desiccation stress in general affects the Malpighian tubules by reducing the rate at which fluid is excreted. Reduced rate of water loss is associated with improved desiccation tolerance; changes in tubule secretion could contribute to this effect (Davies et

al 2014, Folk & Bradley 2003, Hoffmann & Harshman 1999, Terhzaz et al 2012, Terhzaz et al 2015b).

The significant increase in secretion rate after DH_{44} peptide application indicates that, in spite of the reduced transcription of *DH44-R2* following desiccation (as detailed in Figure 3.1), there is sufficient receptor present on the surface of the Malpighian tubules after 24 hours of desiccation stress to enable the peptide to have an effect on secretion rate. As changes in transcription level do not necessarily result in changes in actual protein levels (Taylor et al 2013, Vogel & Marcotte 2012), *DH44-R2* presence on the surface of the Malpighian tubules was investigated using the recently published method of live-tissue fluorophore-tagged peptide labelling (Halberg et al 2015).

3.2 Effect of desiccation on DH_{44} binding to Malpighian tubule receptor

Although immunocytochemistry or western blotting might be the standard methods for assessing protein level changes, both depend on the acquisition of a reliable antibody against the protein of interest. Moreover, the former requires an antibody that is additionally able to penetrate into tissue and the latter results in the loss of information about protein localisation. An alternative method has recently been used in *Drosophila* and other insects to probe the patterns of expression of peptide receptors (Halberg et al 2015) which uses a fluorophore-labelled peptide and live tissue to enable imaging of binding to peptide receptors. Here, using fluorophore-labelled DH_{44} (DH_{44}-F), this method is used to provide a semi-quantitative analysis of DH_{44} peptide-receptor complex levels in Malpighian tubules following desiccation (Figure 3.7). As ligand-receptor binding dynamics and fluorophore signalling each influence the intensity of signal captured during imaging, the method was not used to make any estimates of percentage change or relative amount. However, analysis of the fluorescent signal intensity can give an idea of whether there is less or more ligand-receptor complex present under different conditions (Waters 2009).

These experiments were carried out in collaboration with Dr. Kenneth Halberg (KH). All *Drosophila* husbandry, dissections, secretion assays, and fluorophore

incubations were performed by the author (EC), while the inverted confocal microscopy imaging and intensity trace analysis was carried out by KH.

3.2.1 Validation of tagged DH_{44}

Prior to labelling and imaging live-tissue with the fluorophore-labelled DH_{44} (for details see section 2.6), it was necessary to first validate the compound itself. The first step was to verify that the conjugation of the TMR-C_5-maleimide Bodipy dye to the peptide near the N-terminal region did not interfere with its ability to bind to DH44-R2. This was particularly important as studies of CRF-related diuretic hormones in *Manduca sexta* and *Achaeta domesticus* have indicated that in both species a region near the N-terminus of the peptide is required for receptor activation (Coast & Kay 1994, Reagan 1995, Schooley et al 2011). The integrity of the binding relationship was assessed by comparing changes in the secretion rate of Malpighian tubules in response to DH_{44}-F to changes in the secretion rate after stimulation by the unlabelled DH_{44} peptide. Similar responses by the Malpighian tubules (Figure 3.3) were taken to indicate that DH_{44}-F was able to bind to DH44-R2 without significant impairment by the conjugated fluorophore (Halberg et al 2015). The second step in the compound validation process was to determine whether DH_{44}-F binding to DH44-R2 was specific. This was assessed by verifying that DH_{44}-F binding was specific to Malpighian tubule principal cells, where DH_{44} binds to affect intracellular signalling (Cabrero et al 2002), and by using a ligand competition assay in which DH_{44}-F was outcompeted by unlabelled DH_{44} peptide (Figure 3.5) (Halberg et al 2015). If DH_{44}-F signal was observed even in the presence of a higher concentration of unlabelled DH_{44} peptide, this would indicate that DH_{44}-F was bound to the Malpighian tubule in a different pattern than the unlabelled peptide and was therefore not specifically binding in the same way as the native peptide.

3.2.1.1 Malpighian tubule response to labelled and unlabelled DH_{44} peptide

The ability of DH_{44}-F to bind to and induce signalling cascades by DH44-R2 in the Malpighian tubule was assessed by fluid secretion assay (see section 2.9). Malpighian tubules were dissected from male and female CS *Drosophila*. The volume of secretion by individual tubule pairs was measured every 10 minutes

for 30 minutes to determine a baseline secretion rate, after which either 10^{-7} M DH_{44} peptide or 10^{-7} M DH_{44}-F was applied. Stimulated secretion volumes were then measured every 10 minutes for an additional 30 minutes to determine the secretion rate in response to stimulation by the two compounds. Basal secretion rate was similar across the two groups, as expected given that the tissues were dissected from the same group of flies (Figure 3.3A). Moreover, following stimulation with either DH_{44}-F or DH_{44}, the fluid secretion rate increased to a similar extent. Data were analysed statistically as described in section 2.9.1, where the rationale for test selection is also detailed. Two-sample two-tailed Student's *t*-tests were performed on the measurements of secretion rate for each 10-minute time interval. There were no significant differences between the two groups at any point ($p > 0.05$, see Table 3.4 for details). Fluid secretion rates of Malpighian tubules stimulated by either labelled or unlabelled DH_{44} were also compared by calculating a percentage change in secretion rate (see section 2.9.1), as shown in Figure 3.3B. A two-sample two-tailed Student's *t*-test did not indicate any significant difference between the groups, $t(15) = 0.712$, $p = 0.49$.

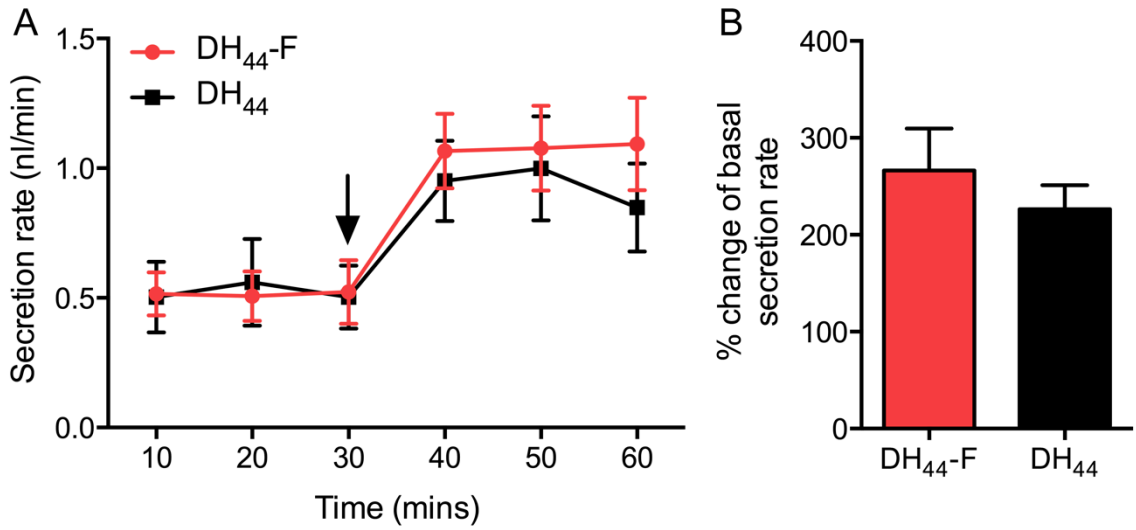

Figure 3.3 Fluid secretion rate of excised Malpighian tubules from male CS *Drosophila* before and after exposure to either DH_{44}-F or DH_{44} applied at 10^{-7} M.

A) Stimulated secretion rate of Malpighian tubules is similar after application of DH_{44} (N=7) or DH_{44}-F (*N*=10) at 30 minutes, indicated by the arrow. **B)** Secretion rate of excised Malpighian tubules increases by approximately 127% following stimulation with 10^{-7} M DH_{44} peptide and by approximately 166% following stimulation with 10^{-7} M DH_{44}-F. Graphs show mean ± SEM.

Table 3.4 Two-sample two-tailed Student's *t*-test analysis of secretion rate by Malpighian tubules of CS flies at baseline and following exposure to either DH_{44} (*N*=7) or exposure to DH_{44}-F (*N*=10).

	Baseline secretion			Stimulated secretion		
Time (mins)	0-10	10-20	20-30	30-40	40-50	50-60
t	0.091	0.315	0.123	0.559	0.322	1.009
df	15	15	15	15	15	15
p	0.41	0.33	0.61	0.78	0.75	0.33

These results show that DH_{44}-F is able to affect the secretion rate of *Drosophila* Malpighian tubules to a similar extent as unlabelled DH_{44}. This suggests that the addition of the fluorophore does not significantly affect the function of the peptide and that DH_{44}-F is likely binding to DH44-R2 to an extent that is biologically relevant.

3.2.1.2 DH_{44}-F labels principal cells, but not stellate cells

After determining that DH_{44}-F was capable of stimulating *Drosophila* Malpighian tubules similarly to unlabelled DH_{44}, it was necessary to verify that DH_{44}-F binds to the Malpighian tubule principal cells, as this is where the unlabelled neuropeptide binds to DH44-R2 (Cabrero et al 2002). In a prior study, DH_{44} stimulation induced signalling via cAMP in principal cells, but did not affect either cAMP or Ca^{2+} levels in stellate cells (Cabrero et al 2002). Additional evidence for the localisation of DH44-R2 to tubule principal cells was generated by assessing the expression of a DH44-R2-GAL4 driver line and by knocking down *DH44-R2* levels by expression of dsRNAi against *DH44-R2* in principal cells only (section 3.4.1).

Malpighian tubules from wild-type flies were labelled using 10^{-7} M DH_{44}-F and DAPI, then viewed and imaged using confocal microscopy. It was found that principal cells and not stellate cells were specifically labelled by DH_{44}-F (see Figure 3.4). This supports existing evidence that DH_{44} binds DH44-R2 that is present in the principal cells and not the stellate cells of the tubules (Cabrero et al 2002).

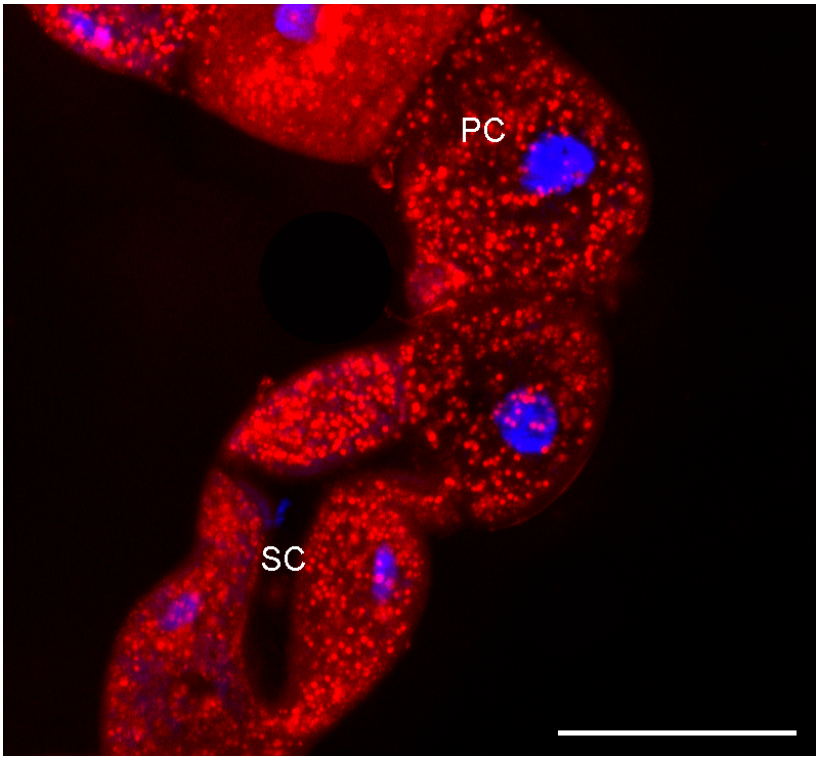

Figure 3.4 DH_{44}-F labels principal cells (PC), but not stellate cells (SC) of Malpighian tubules. Malpighian tubule labelled with 10^{-7} M DH_{44}-F (red) and DAPI (blue). Scale bar indicates 25 µm. This figure is the result of a collaborative experiment with Dr. Kenneth Halberg: Dissections and tissue incubations were performed by EC. Image acquisition and figure preparation were by KH.

3.2.1.3 Unlabelled DH_{44} peptide competes with labelled DH_{44} peptide

The binding specificity of DH_{44}-F was assessed using a ligand competition assay, as described in section 2.6.2. This experiment was conducted using an Zeiss LSM 510 Meta inverted confocal microscope. Microscopy settings were optimised for imaging of live Malpighian tubules using a pair of samples in which one sample was incubated only with DAPI and the other was labelled with DH_{44}-F and DAPI (see section 2.6.1). The main goal of the optimisation process was to minimise baseline detection of autofluorescence in the tubules. All images captured during this experiment used the same settings in order to make it possible to compare the signal intensities.

The ligand competition assay itself involved incubating freshly dissected Malpighian tubules from CS *Drosophila* with DAPI and either 10^{-7} M DH_{44}-F, or a mixture of 10^{-7} M DH_{44}-F and 10^{-5} M DH_{44}. As shown in Figure 3.5, the signal from DH_{44}-F was strongly reduced by the addition of a higher concentration of DH_{44}.

Also, as in section 3.2.1.2, Malpighian tubule principal cells, but not stellate cells, were labelled by DH_{44}-F.

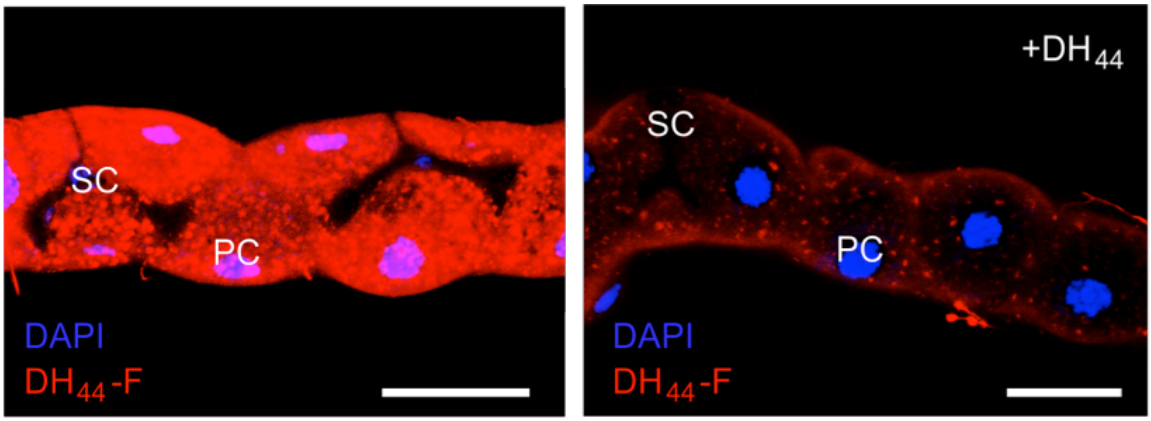

Figure 3.5 Binding specificity of fluorophore-labelled DH_{44} validated by sharp reduction in fluorescent signal during competitive inhibition with unlabelled DH_{44} peptide
DH_{44}-F labels principal cells (PC), but not stellate cells (SC) of Malpighian tubules and is displaced by incubation with higher concentrations of unlabelled peptide. Scale bars indicate 25 µm. Images are representative of *N*=10 pairs of tubules in each group which were observed by inverted confocal microscopy. Both images were taken using identical microscopy settings. This figure is the result of a collaborative experiment with Dr. Kenneth Halberg: Dissections and tissue incubations performed by EC. Image acquisition and figure preparation by KH.

As DH_{44} peptide was able to almost entirely abolish the DH_{44}-F signal and did not leave any notable areas of fluorescence, the results suggest that DH_{44}-F binds to receptors on the Malpighian tubules in the same pattern as DH_{44} peptide.

3.2.2 Labelling of Malpighian tubule principal cells by fluorescent tagged DH_{44} is decreased following desiccation

Live tissue labelling was performed as described in section 2.6.3. Male CS *Drosophila* were either exposed to 24 hours of desiccation stress or fed normally. Malpighian tubules were dissected from the flies, incubated in 10^{-7} M DH_{44}-F and immediately imaged using inverted confocal microscopy, resulting in images like those shown in Figure 3.6. The average intensity trace ± SEM for at least 14 pairs of tubules in each biological group was plotted as a function of distance, as detailed in section 2.6.4. As shown in Figure 3.7, the signal intensity from the DH_{44}-F labelling was overall lower following desiccation exposure, when compared to normally fed controls. The point of maximum intensity in the

control sample was selected for statistical comparison. A two-sample two-tailed Student's *t*-test did not indicate a statistically significant difference between the mean intensities of the labelling between the two groups, $t(27) = 0.792$, $p = 0.44$.

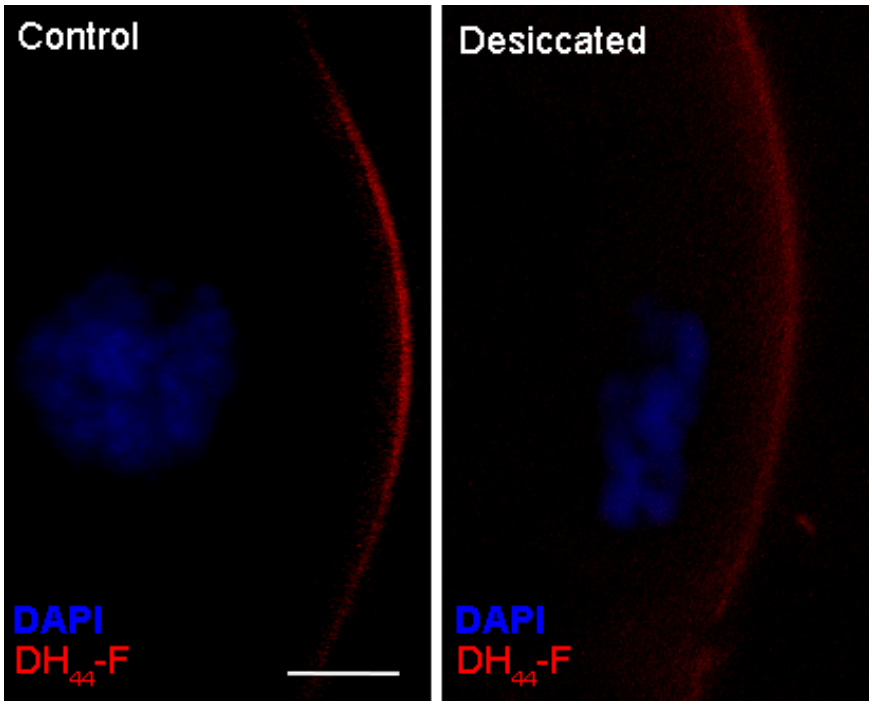

Figure 3.6 Labelling of basolateral membrane of Malpighian tubule principal cells by DH_{44}-F is affected by desiccation stress exposure.

Scale bar indicates 5 µm. Images are representative and were obtained by inverted confocal microscopy. Both images were taken using identical microscopy settings. This figure is the result of a collaborative experiment with Dr. Kenneth Halberg: Dissections, tissue incubations, and figure preparation were performed by EC. Images acquired by KH.

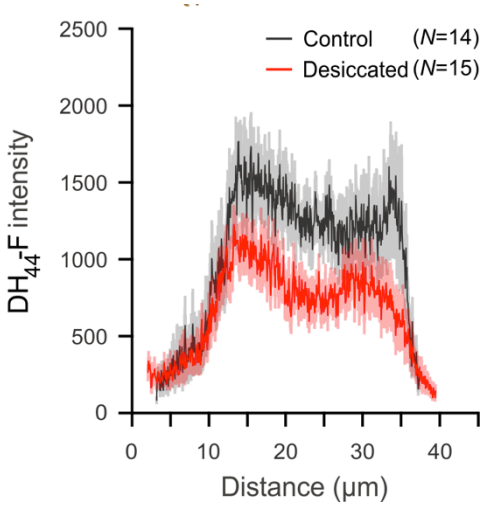

Figure 3.7 Desiccation exposure affects fluorescent signal intensity when *Drosophila* Malpighian tubules are labelled with DH_{44}-F.
Malpighian tubules were extracted from control and desiccated male CS flies and labelled with DH_{44}-F . Confocal microscopy was used to image the tubules, producing optical sections. Intensity of the fluorescent signal labelling principal cells was semi-quantitatively measured across the cells in a line perpendicular to the surface of the tubules. Signal intensity is plotted relative to distance from the basolateral membrane of the tubules, showing mean signal intensity ± SEM. DH_{44}-F signal shows a trend toward decreased labelling following desiccation exposure, as compared to normally fed controls. Further details about intensity trace analysis can be found in section 2.6.4. This figure is the result of a collaborative experiment with Dr. Kenneth Halberg: Desiccation stress exposure, dissections and tissue incubations were performed by EC. Image acquisition, intensity trace analysis, and figure preparation were by KH.

Although analysis of the data presented in Figure 3.7 did not result in rejection of the null hypothesis of no difference in labelling between the groups, it seems likely that this could be due to the use of a small sample size. Further repetition of the experiment to increase the number of samples analysed would serve to increase the statistical power of the experiment and would provide a clearer picture of the true difference between the groups. However, in the absence of such additional data, the current data do appear to indicate a trend toward decreased signal intensity after desiccation stress exposure relative to unstressed control samples.

Given the validation data indicating that DH_{44}-F and DH_{44} bind in similar patterns to the Malpighian tubules and have the same physiological affect on the tissue, a decrease in DH_{44}-F labelling following desiccation exposure suggests that less DH_{44} is bound to the tubules. This could be due to a decreased availability of

DH44-R2 at the cell surface, which complements the prior finding that *DH44-R2* gene expression is down-regulated following desiccation exposure. Overall, these two pieces of evidence suggest a decrease in DH44-R2 production and availability as a consequence of 24 hours of desiccation exposure in male wild-type (CS) *Drosophila*.

3.3 Manipulation of DH_{44}-producing neurons affects stress tolerance

One way to explore how a gene or its product is involved in a process is to impede expression of that gene and then to assess whether a phenotype related to the process of interest emerges, a method called reverse genetics (Dow & Davies 2003). In this study, the role of DH_{44} peptide signalling in desiccation tolerance was probed by assessing the affect on stress tolerance both after manipulating the neurons that produce DH_{44} peptide and after knocking down the expression of its receptor in the target tissue of interest, DH44-R2 in the Malpighian tubules. The results of the former set of experiments are related here, while the latter results are described in section 3.4.2.

DH_{44} peptide is expressed in two sets of three neurons in the pars intercerebralis in the *Drosophila* brain (section 1.3.1) (Cabrero et al 2002). To modify DH_{44} signalling, expression of the *DH_{44}* gene was specifically manipulated in these neurons using the GAL4/UAS system (Brand & Perrimon 1993, Fischer et al 1988). So as to make the manipulations as specific as possible, a highly specific driver line with expression limited to the DH_{44}-producing neurons was used to knock down *DH_{44}* expression or to ablate these neurons.

3.3.1 DH_{44} peptide expression

Immunocytochemical labelling of DH_{44} peptide with anti- DH_{44} antibody (details in Table 2.6) was used in adult *Drosophila* brain to reconfirm peptide localisation, as shown in Figure 3.8 and using methods described in section 2.4. It was additionally found that this pattern of labelling could be achieved using a 1:4000 dilution of the antibody, while publications have reported using a 1:2000 dilution.

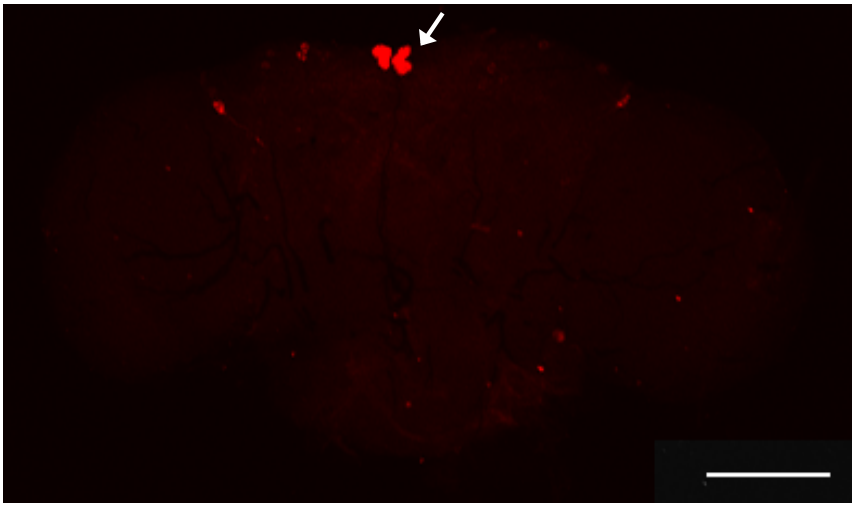

Figure 3.8 DH_{44} peptide is localised to the pars intercerebralis of the *D. melanogaster* brain. Staining the adult *Drosophila* brain with anti-DH_{44} antibody reproduced the previously identified pattern of labelling in the pars intercerebralis (Cabrero et al 2002, Cavanaugh et al 2014, Park et al 2008). Location of pars intercerebralis is indicated by a white arrow. The secondary antibody used was anti-rabbit IgG-Alexa Fluor 546 (polyclonal goat). Scale bar indicates 100 µm. The image was acquired using inverted confocal microscopy.

3.3.2 DH_{44}-GAL4 driver line selection

In order to probe the function of the six neurons shown to contain DH_{44} peptide, a highly specific driver line with an expression pattern restricted to these particular neurons was required. The collection of GAL4 lines produced by the Janelia Farm FlyLight Project Team proved to contain a candidate line in which GAL4 is expressed under the control of a known short fragment of genomic DNA from the *DH_{44}* gene (Jenett et al 2012). The team produced four different GAL4 driver lines under the control of defined cis-regulatory fragments of the *DH_{44}* gene between 1903 and 3723 residues in length. The location of these fragments relative to the *DH_{44}* gene is shown in Figure 3.9. Expression data available online at the Janelia Farm website indicate that only driver line R65C11 cleanly drives expression in only the six neurons known to contain DH_{44} peptide. Interestingly, this driver line is the only one created by the team in which the cis-regulatory DNA sequence used contains elements upstream of both the Dh44-RA and Dh44-RB protein coding sequences. In contrast, expression was less specific, almost non-existent, or unrelated to DH_{44} peptide localization when the enhancer fragments used were from different regions of the *DH_{44}* gene. Overall, this suggests that there are particular regulatory genetic sequences located in the

3R:5463840-5466711 region of the *D. melanogaster* genome which are crucial to the spatial specificity of *DH$_{44}$* gene expression (Arnone et al 2004, O'Kane & Gehring 1987).

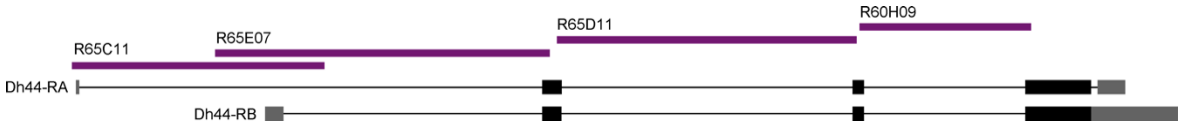

Figure 3.9 Location of cis-regulatory sequences relative to DH$_{44}$ transcripts used to construct GAL4 driver lines.
Four GAL4 lines were generated by the Janelia Farm FlyLight Project using different sections of the *DH$_{44}$* gene to drive expression. The location of these cis-regulatory fragments are shown relative to their position along the two *DH$_{44}$* protein coding sequences, Dh44-RA and Dh44-RB. Sequence location information obtained from the Janelia Farm FlyLight Project website (Jenett et al 2012).

The driver line denoted by Janelia Farm as R65C11 was selected for manipulation of the DH$_{44}$-containing neurons. As indicated in Table 2.1, this line will be referred to as DH$_{44}$-GAL4.

3.3.3 DH$_{44}$-GAL4 driver line characterisation

The specificity of the DH$_{44}$-GAL4 driver line was evaluated by crossing males from this line with virgin females of the UASmCD8::GFP genotype (see Table 2.1). These flies express cytosolic GFP when Gal4 protein binds to the upstream activation sequence (UAS), activating gene transcription (Duffy 2002). Progeny from the DH$_{44}$-GAL4 cross with UAS-*mCD8::GFP* were aged to 5-7 days old, after which brains were removed by careful dissection (*N*=10) as described in section 2.1.4. Immunocytochemical labelling with the anti-DH$_{44}$ antibody was performed using methods detailed in section 2.4 and brains were imaged using inverted confocal microscopy (section 2.7).

As shown in Figure 3.10, DH$_{44}$ immunostaining confirmed that the DH$_{44}$-GAL4 line drives expression in DH$_{44}$-producing neurons. Additional dissections revealed that the DH$_{44}$-GAL4 line does not drive expression in the Malpighian tubules.

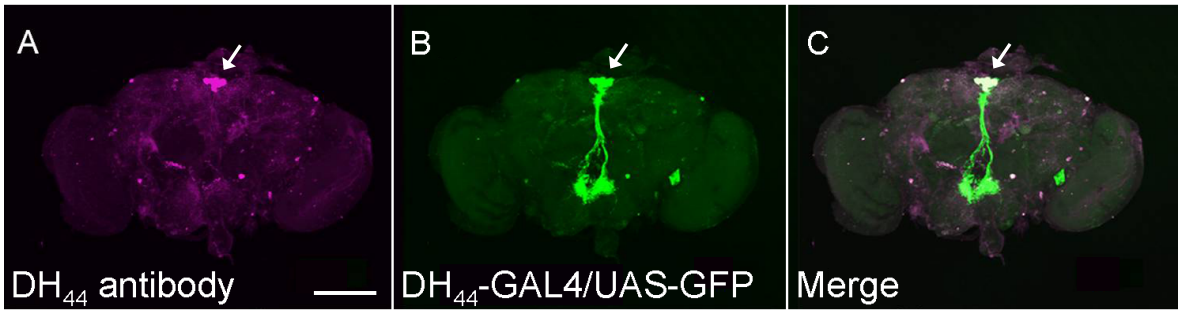

Figure 3.10 Expression pattern of DH_{44}-GAL4 line colocalises with the staining pattern of DH_{44} peptide in DH_{44}-producing neurons of the pars intercerebralis.
A) Staining pattern of DH_{44} peptide in brains of *Drosophila* expressing GFP under the control of DH_{44}-GAL4 promoter labels pars intercerebralis, as indicated by the white arrow. Scale bar indicates 100 µm. **B)** Cytosolic GFP expression pattern in *Drosophila* brains when driven by DH_{44}-GAL4 construct. **C)** Merge of images A and B show that DH_{44}-GAL4 driver line drives expression of UAS-GFP construct in the same neurons that contain DH_{44} peptide. DH_{44} immunostaining indicates that the DH_{44}-GAL4 line drives expression in DH_{44}-producing neurons. Image is representative of *N* = 10, with the same pattern observed in all samples.

As the DH_{44}-GAL4 driver was found to be a highly specific GAL4 driver with an expression pattern coinciding with that of the DH_{44} peptide, it was used for manipulation of the DH_{44}-producing neurons.

3.3.4 Ablation of DH_{44}-producing neurons and RNAi knockdown of DH_{44} via UAS/GAL4 system

The high specificity of the DH_{44}-GAL4 driver line made it possible to manipulate the DH_{44}-producing neurons in a very selective manner. Two different methods of altering these neurons were selected: expression of an RNAi construct against *DH_{44}* mRNA and ablation of the neurons by inducing expression of *reaper*. Probing neuron function through genetically induced ablation, as performed in this study, necessarily requires a highly selective driver line so that the results can be attributed to the effect on the neurons of interest, and not to ablation of any other cells or neurons. Although RNAi targeted against *DH_{44}* mRNA might have achieved fairly high selectivity due to the limited nature of DH_{44} expression, selective expression of the construct in the target tissue of interest reduces the possibility of unintended or off-target effects and serves to increase confidence that any effects observed are due specifically to the planned manipulation (Ma et al 2006, Seinen et al 2011).

The DH_{44}-GAL4 driver line was crossed with flies that express double-stranded RNA for RNAi of *DH_{44}* under the control of a UAS promoter, UAS-*DH_{44}* RNAi line (see Table 2.1). As a control, the DH_{44}-GAL4 driver line was additionally crossed to w^h flies. This line was used rather than the homozygous DH_{44}-GAL4 parental line to control for genetic background (i.e. single copy of DH_{44}-GAL4) in all assays using these lines. The progeny from both crosses were aged to 3-7 days, after which brains were removed by gentle dissection and subjected to immunocytochemistry using antibody against DH_{44} and anti-rabbit IgG-Alexa Fluor 546 ($N \geq 8$). Examination via confocal microscopy revealed that DH_{44} peptide expression in the pars intercerebralis was clearly visible in the progeny from the control cross (Figure 3.11A), but abolished in the pars intercerebralis of the progeny from the DH_{44}-GAL4/UAS-*DH_{44}* RNAi cross (Figure 3.11B).

The DH_{44}-GAL4 driver line was also crossed with flies that express the gene *reaper* under UAS control, resulting in DH_{44}-GAL4/UAS-*reaper* progeny. Expression of *reaper* induces cell death (Al-Anzi et al 2010, Aplin & Kaufman 1997). The progeny from this cross were aged to 3-7 days, after which brains were extracted and subjected to immunocytochemistry using DH_{44} antibody and anti-rabbit IgG-Alexa Fluor 546 ($N \geq 5$). Examination via confocal microscopy revealed that DH_{44} peptide expression in the pars intercerebralis was ablated through this experimental manipulation, as shown in Figure 3.11C.

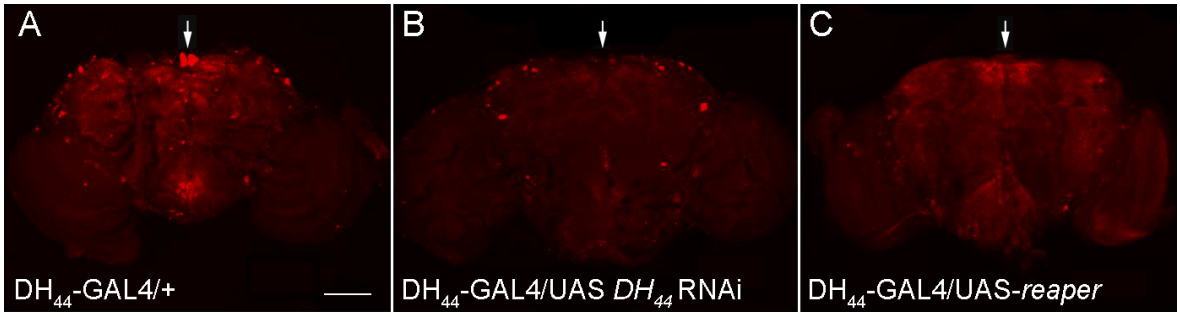

Figure 3.11 Elimination of characteristic DH_{44} peptide staining pattern in pars intercerebralis achieved via RNAi knockdown and neuronal ablation.

A) Adult *Drosophila* brains from DH_{44}-GAL4/w^h flies stained for DH_{44} show labelling in the pars intercerebralis when imaged via inverted confocal microscopy. Scale bar indicates 100 μm, arrow indicates location of the pars intercerebralis. **B)** DH_{44}-GAL4/UAS-*DH_{44}* RNAi brains do not show any staining of DH_{44} peptide in the pars intercerebralis. **C)** Ablation of DH_{44} neurons eliminates the distinctive DH_{44} staining pattern. Images are representative of $N \geq 5$, with patterns observed being consistent for all samples within each biological group.

The effect of the DH_{44}-producing neuron manipulations on *DH_{44}* gene expression was tested via RT-PCR. *DH_{44}* gene expression in the heads of each of the experimental crosses (DH_{44}-GAL4/UAS-*DH_{44}* RNAi and DH_{44}-GAL4/UAS-*reaper*) was compared to crosses of each parental control to w^h. See Table 3.5 for a list of the crosses used in this experiment and their purposes.

Table 3.5 Crossing scheme for assessing the effect of DH_{44}-producing neuron manipulation on *DH_{44}* gene expression

Cross	Purpose	Details
DH_{44}-GAL4/w^h	Control	One copy of driver construct
DH_{44}-GAL4/UAS-*DH_{44}* RNAi	Experimental	RNAi knockdown of *DH_{44}*
w^h/UAS-*DH_{44}* RNAi	Control	One copy of RNAi construct
DH_{44}-GAL4/UAS-*reaper*	Experimental	Ablation of DH_{44}-producing neurons
w^h/UAS-*reaper*	Control	One copy of ablation construct

RNA was extracted from the heads of adult progeny from the crosses listed in Table 3.5 and used to synthesize cDNA as described in sections 2.2.1 and 2.3.1. RT-PCR was performed using TaqMan probe and primer sets for *DH_{44}* with *alpha-tubulin 84b* as the endogenous control. Head RNA was used rather than whole fly RNA as extracting RNA from the tissue of interest was found to result in the amplification signal being identified earlier during the PCR process, suggesting a greater enrichment of the target sequences in these tissues as compared to in the whole organism. Comparative C_T analysis was used to calculate a fold change for *DH_{44}* expression relative to the control cross DH_{44}-GAL4/w^h, the only control in common across the two groups, as shown in Figure 3.12. The comparative C_T method is described in section 2.3.2.1, as is the rationale for selection of statistical tests used to analyse qPCR data.

Four statistical comparisons were planned as the progeny of the experimental crosses were to be compared to each of their two related controls. As the expression level of *DH_{44}* in the DH_{44}-GAL4/w^h samples was set at a value of 1 in order to calculate relative expression, the relative expression values obtained for each experimental cross were compared to this control using a two-tailed one-sample Student's t-test against a null hypothesis of a fold change of 1 (i.e. same expression level as the DH_{44}-GAL4/w^h control). There was a significant difference between the null hypothesis and the relative expression obtained for *DH_{44}* expression from the heads of cross DH_{44}-GAL4/UAS-*DH_{44}* RNAi (*M* = 0.48, *SD*

= 0.202, N = 4), $t(3)$ = 5.131, p = 0.0143, indicating a 52% decrease in expression relative to the control progeny. There was also a significant difference between the null hypothesis and the relative expression obtained for *DH44* expression from the heads of cross DH44-GAL4/UAS-*reaper* (M = 0.61, SD = 0.188, N = 4), $t(3)$ = 4.125, p = 0.0258, indicating a 39% decrease in expression relative to the control progeny. The final two comparisons were made using a two-tailed two-sample Student's t-test as the values for the other two controls were normalized to the DH44-GAL4/w^h control and so retained a distribution of error, which is required for two-sample t-testing. Testing in this way revealed a statistically significant difference between *DH44* expression from the heads of cross DH44-GAL4/UAS-*DH44* RNAi and those of cross w^h/UAS-*DH44* RNAi (M = 1.34, SD = 0.402, N = 4), $t(6)$ = 3.788, p = 0.0091, indicating a 64% decrease in expression in the experimental cross progeny relative to the control cross progeny. There was also a statistically significant difference between *DH44* expression from the heads of cross DH44-GAL4/UAS-*reaper* and those of cross w^h/UAS-*reaper* (M = 1.66, SD = 0.450, N = 3), $t(5)$ = 4.287, p = 0.0078, indicating a 63% decrease in expression in the experimental cross progeny relative to the control cross progeny.

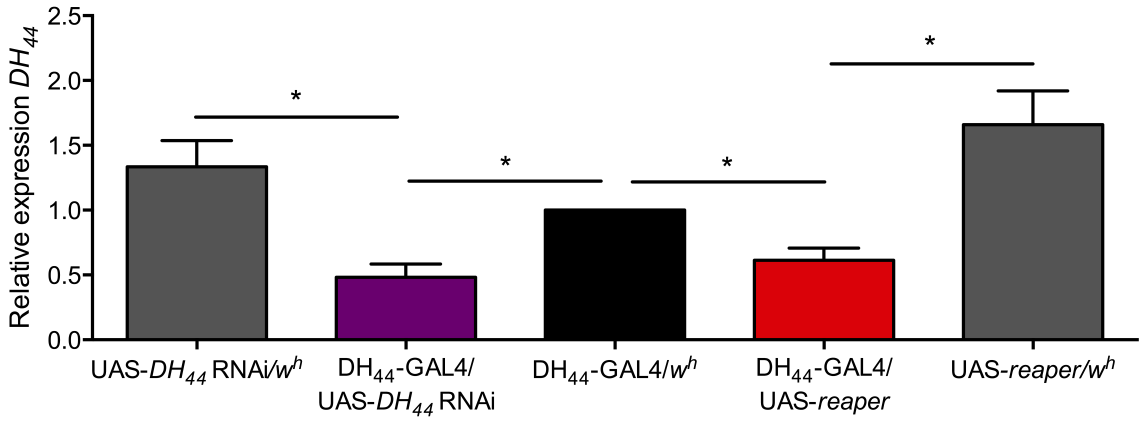

Figure 3.12 RNAi knockdown of *DH44* in DH44 neurons and ablation of DH44 neurons affects mRNA levels of *DH44* in the heads of cross progeny.

DH44 expression is significantly reduced in head following expression of RNAi against *DH44* in DH44 neurons (N=4) and following ablation of DH44 neurons (N≥3), mean ± SEM shown. Statistical significance is based on two-tailed one-sample Student's t-testing with null hypothesis of 1.0 when compared to *DH44*-GAL4/w^h, or based on two-tailed two-sample Student's t-testing when comparing experimental crosses to UAS-*DH44* RNAi/w^h or UAS-*reaper*/w^h, *p<0.05.

As all of the statistical tests indicate that *DH44* transcript level is significantly lower in the experimental crosses than in the control crosses, the manipulations

of the DH_{44} neurons outlined in Table 3.5 have been effective. The data also suggest that the majority of *DH_{44}* expression in the head of *Drosophila* is in the DH_{44} neurons as manipulation of this small subset of cells was able to significantly influence the *DH_{44}* transcript levels in the whole sample.

When considered together, the results of the RT-PCR and immunocytochemistry experiments indicate that the crosses outlined in Table 3.5 have been effective at manipulating DH_{44} transcript and protein levels. Furthermore, due to the highly specific nature of the driver line, this was achieved while expressing the RNAi/*reaper* constructs in the DH_{44} neurons. As these manipulations were deemed to be successful and significant, the next step taken was to determine whether manipulation of the DH_{44} signalling pathway has an effect on desiccation tolerance.

3.3.5 Manipulation of DH_{44}-producing neurons affects survival phenotype

In order to test the hypothesis that the DH_{44} peptide is involved in modulating desiccation resistance, progeny from all five crosses listed in Table 3.5 were exposed to a desiccation stress assay. This provided a dataset with two different methods of decreasing DH_{44} levels in the brain, thus decreasing DH_{44} availability. Flies with the DH_{44}-GAL4 driver construct were also crossed to those with a low threshold voltage-gated bacterial sodium channel expressed under UAS control, called UAS-*NaChBac*. This bacterial sodium channel has been shown to increase membrane excitability (Nitabach et al 2006) and was introduced with the aim of increasing DH_{44} availability.

The desiccation tolerance assay is conducted by placing groups of male flies aged 5-10 days old in an empty vial and scoring survival until all flies have died (section 2.8.1) (Kahsai et al 2010, Terhzaz et al 2012). As the desiccation stress protocol used requires *Drosophila* to be placed in empty vials, this necessitates that they be not only desiccated, but starved as well (section 2.8.2.1). So as to rule out any possibility that the phenotype shown during desiccation stress was due to starvation rather than to lack of water, flies were exposed to a starvation assay (section 2.8.2).

It was hypothesised that the flies with manipulated DH_{44} neurons would survive differently than the control crosses when exposed to desiccation stress across all three manipulations. In the neuronal ablation condition, results of this kind would indicate an involvement of the DH_{44} neurons in desiccation tolerance, while the *DH_{44}* RNAi knockdown condition would more specifically indicate reduction of DH_{44} peptide in these neurons as affecting desiccation tolerance. Overexcitation of the DH_{44} neurons by expression of UAS-*NaChBac* was anticipated to have an opposite effect to DH_{44} neuron ablation and *DH_{44}* RNAi knockdown.

In terms of starvation tolerance, it was expected that starvation would not play an important role in survival within the timeframe of the desiccation stress assays. This would indicate that the results observed during the desiccation exposure assay were due to the effect of the absence of water rather than due to the lack of food. However, as the starvation assays were conducted past the threshold of where a potential influence on desiccation would be detected, the assay also detects effects of these manipulations on starvation tolerance. There is a precedent for a potential effect of DH_{44} neuron manipulation on starvation survival both as recent evidence has implicated the DH_{44} neurons in nutrient sensing (Dus et al 2015) and as the DH_{44} neurons also express LKR, which has been shown to be involved in the regulation of feeding and meal size (Al-Anzi et al 2010). The statistical significance of changes in survival was tested as described in section 2.8.3.

3.3.5.1 *DH_{44}* RNAi knockdown results in increased desiccation tolerance, but does not affect starvation tolerance

The effect of targeted *DH_{44}* knockdown via RNAi (genotype details in Table 3.5) on desiccation and starvation tolerance was assessed using experimental methods described in sections 2.8.1 and 2.8.2. The rationale for the use of the statistical methods applied to the survival data is detailed in section 2.8.3 along with further information about the individual tests and interpretation of their results, where applicable. The reasons for inclusion of a starvation assay alongside a desiccation assay are described in section 2.8.2.1.

As shown in Figure 3.13A, knockdown of *DH44* expression in the DH_{44} neurons was found to significantly extend survival time during desiccation exposure. Specifically, Logrank testing indicated that DH_{44}-GAL4/UAS-*DH44* RNAi flies (Median survival = 24 hours) survived significantly longer than both DH_{44}-GAL4/w^h (Median survival = 19 hours), $X^2(1) = 58.78$, $p < 0.0001$, and w^h/UAS-*DH44* RNAi (Median survival = 21 hours), $X^2(1) = 25.25$, $p < 0.0001$. The ratio of the rate of death of DH_{44}-GAL4/UAS-*DH44* RNAi flies relative to the rate of death of DH_{44}-GAL4/w^h was 0.12 (95% CI: 0.07-0.21), representing an 8.2 fold decrease in death rate and a 26% increase in median survival time. The ratio of the rate of death of DH_{44}-GAL4/UAS-*DH44* RNAi flies relative to the rate of death of w^h/UAS-*DH44* RNAi was 0.37 (95% CI: 0.25-0.54), representing a 2.7 fold decrease in death rate and a 14% increase in median survival time.

Knockdown of *DH44* expression in the DH_{44} neurons was found to significantly affect survival time during starvation exposure relative to only one of the two controls, as shown in Figure 3.13B. Specifically, Logrank testing indicated that the DH_{44}-GAL4/UAS-*DH44* RNAi flies (Median survival = 42 hours) survived for a significantly shorter period than DH_{44}-GAL4/w^h (Median survival = 44 hours), $X^2(1) = 32.48$, $p < 0.0001$, but for a period no different than w^h/UAS-*DH44* RNAi, $X^2(1) = 0.80$, $p = 0.37$. The ratio of the rate of death of DH_{44}-GAL4/UAS-*DH44* RNAi flies relative to the rate of death of DH_{44}-GAL4/w^h was 1.84 (95% CI: 1.49-2.28), indicating a 1.8 fold increase in death rate with a 5% decrease in median survival time.

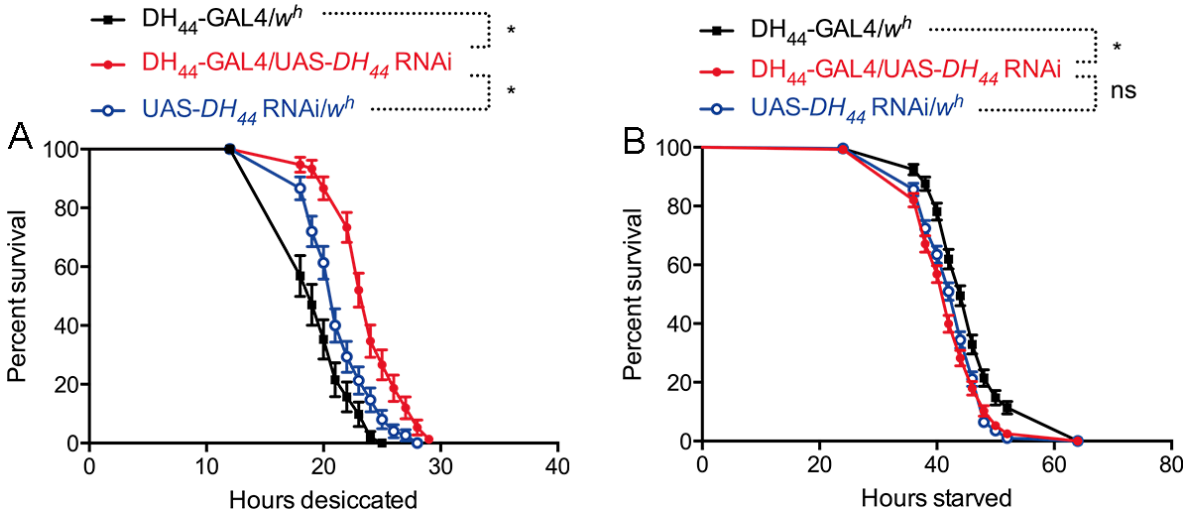

Figure 3.13 Knockdown of *DH44* in the DH44 neurons affects survival during desiccation and starvation stress exposure.

A) Survival of male DH44-GAL4/UAS-*DH44* RNAi cross progeny (*N*=74) exceeds that of progeny from control crosses DH44-GAL4/w^h (*N*=51) and w^h/UAS-*DH44* RNAi (*N*=75) during desiccation stress. The graph is representative of three biological repeats. **B)** Survival of male DH44-GAL4/UAS-*DH44* RNAi cross progeny (*N*=283) does not differ significantly from that of progeny from control cross w^h/UAS-*DH44* RNAi (*N*=279), but is significantly lower than that of progeny from control cross DH44-GAL4/w^h (*N*=210) during starvation stress. Data are pooled across four biological repeats. Statistical comparisons were made using the Logrank test, *p<0.05.

The increase in desiccation tolerance by DH44-GAL4/UAS-*DH44* RNAi flies compared to both controls indicates that reducing DH44 peptide levels in these neurons provides an organismal advantage under these circumstances. The overall longer survival for all crosses under starvation stress as compared to desiccation stress indicates that the latter is a more severe stress.

Although a statistically significant reduction in survival for DH44-GAL4/UAS-*DH44* RNAi flies was observed relative to one of the two control crosses, the biological significance of this difference is less obvious. The DH44-GAL4/UAS-*DH44* RNAi progeny differed from the one control to approximately the same extent that the control crosses differ from each other, making it unlikely that the data should be taken as an indication of *DH44* knockdown being disadvantageous to starvation survival. Rather, as DH44-GAL4/UAS-*DH44* RNAi survival fell within the range of the control crosses, it seems more likely that the manipulation does not affect starvation survival to a great extent.

Overall, the data indicate that knockdown of *DH$_{44}$* mRNA in the DH$_{44}$ neurons affects desiccation tolerance in adult male *Drosophila* in a way that cannot be explained by a lack of food availability during the desiccation stress assay. Moreover, the direction of this influence is such that a decrease in DH$_{44}$ peptide levels in the brain causes increased desiccation tolerance.

3.3.5.2 DH$_{44}$-producing neuron ablation results in increased desiccation tolerance and increased starvation tolerance

The effects of DH$_{44}$ neuron ablation via *reaper* expression (genotype details in Table 3.5) on desiccation and starvation tolerance was assessed using experimental methods described in sections 2.8.1 and 2.8.2. The rationale for the use of the statistical methods applied to the survival data is detailed in section 2.8.3 along with further information about the individual tests and interpretation of their results, where applicable. The reasons for inclusion of a starvation assay alongside a desiccation assay are described in section 2.8.2.1.

As shown in Figure 3.14A, DH$_{44}$ neuron ablation was found to significantly extend survival time during desiccation exposure. Specifically, Logrank testing indicated that DH$_{44}$-GAL4/UAS-*reaper* flies (Median survival = 23 hours) survived significantly longer than both DH$_{44}$-GAL4/w^h (Median survival = 19 hours), $X^2(1) = 48.62$, $p < 0.0001$, and w^h/UAS-*reaper* (Median survival = 21 hours), $X^2(1) = 20.71$, $p < 0.0001$. The ratio of the rate of death of DH$_{44}$-GAL4/UAS-*reaper* flies relative to the rate of death of DH$_{44}$-GAL4/w^h was 0.16 (95% CI: 0.09-0.26), representing a 6.4 fold decrease in death rate and a 21% increase in median survival time. The ratio of the rate of death of DH$_{44}$-GAL4/UAS-*reaper* flies relative to the rate of death of w^h/UAS-*reaper* was 0.38 (95% CI: 0.25-0.58), representing a 2.6 fold decrease in death rate and a 10% increase in median survival time.

DH$_{44}$ neuron ablation was found to significantly increase survival time during starvation exposure, as shown in Figure 3.14B. Specifically, Logrank testing indicated DH$_{44}$-GAL4/UAS-*reaper* flies (Median survival = 55 hours) survived significantly longer during starvation exposure than both DH$_{44}$-GAL4/w^h (Median survival = 46 hours), $X^2(1) = 70.64$, $p < 0.0001$ and w^h/UAS-*reaper* (Median survival = 48 hours), $X^2(1) = 52.52$, $p < 0.0001$. The ratio of the rate of death of

DH_{44}-GAL4/UAS-*reaper* flies relative to the rate of death of DH_{44}-GAL4/w^h was 0.37 (95% CI: 0.29-0.47), indicating a 2.7 fold decrease in death rate with a 20% increase in median survival time. The ratio of the rate of death of DH_{44}-GAL4/UAS-*reaper* flies relative to the rate of death of w^h/UAS-*reaper* was 0.48 (95% CI: 0.39-0.58), indicating a 2.1 fold decrease in death rate with a 15% increase in median survival time.

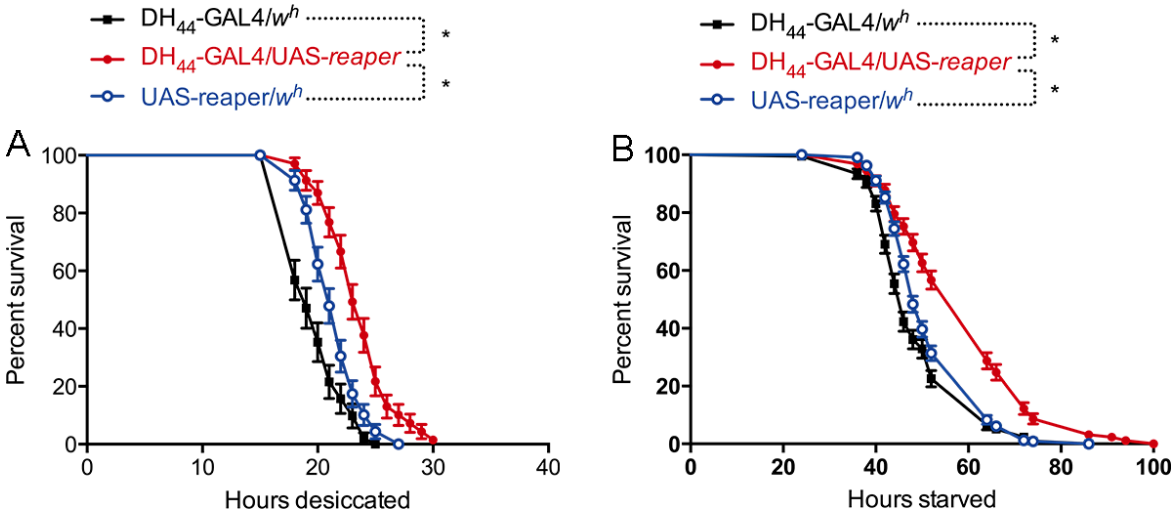

Figure 3.14 DH_{44} neuron ablation affects survival during desiccation and starvation stress exposure.

A) Survival of male DH_{44}-GAL4/UAS-*reaper* cross progeny (*N*=68) exceeds that of progeny from control crosses DH_{44}-GAL4/w^h (*N*=51) and w^h/UAS-*reaper* (*N*=69) during desiccation stress. The graph is representative of 3 biological repeats. **B)** Survival of male DH_{44}-GAL4/UAS-*reaper* cross progeny (*N*=254) exceeds that of progeny from control crosses DH_{44}-GAL4/w^h (*N*=213) and w^h/UAS-*reaper* (*N*=325) during starvation stress. Data are pooled across four biological repeats. Statistical comparisons are made using the Logrank test, *p<0.05

The increase in survival duration during both desiccation and starvation stress in the flies with the DH_{44} neuron ablation relative to controls indicates that absence of these neurons provides an advantage under both stress conditions. However, the nature of ablation as a technique means that it does not clarify what aspect of the neurons is involved in generating the effect.

Ablation of the DH_{44} neurons increases desiccation tolerance to a similar extent as RNAi knockdown of *DH44* in the DH_{44} neurons (Figure 3.13A). Thus, it seems likely that the phenotype observed is primarily due to interference with DH_{44} signalling. Conversely, while DH_{44} neuron ablation enhances starvation

tolerance, reduction of *DH$_{44}$* expression via RNAi does not affect starvation survival (Figure 3.13B). This indicates that DH$_{44}$ neuron ablation does not affect starvation through manipulation of DH$_{44}$ signalling alone. DH$_{44}$ neuron ablation also affects LKR, which is colocalised with DH$_{44}$ in the DH$_{44}$ neurons (Cabrero et al 2002), and additionally disrupts neuronal signalling connections as the DH$_{44}$ neurons were not only manipulated, but eliminated altogether. The possibility that abolition of LKR in the DH$_{44}$ neurons underlies this phenotype was tested via RNAi knockdown of *LKR* (see section 4.3.3).

3.3.5.3 Overexcitation of DH$_{44}$-producing neurons results in increased desiccation tolerance

Male *Drosophila* in which a low threshold voltage-gated bacterial sodium channel was expressed in the DH$_{44}$ neurons and the progeny of two control crosses (DH$_{44}$-GAL4/w^h and w^h/UAS-*NaChBac*) were exposed to both a desiccation stress assay and a starvation stress assay. Expression of this transgene results in hyperpolarisation of neurons, which can result in neurotransmitter or peptide release occurring more readily. In this case, it was expected that increased release of DH$_{44}$ would impair desiccation survival. Experimental methods used are described in sections 2.8.1 and 2.8.2. The rationale for the use of the statistical methods applied to the survival data is detailed in section 2.8.3 along with further information about the individual tests and interpretation of their results, where applicable.

As shown in Figure 3.15, increasing the excitability of the DH$_{44}$ neurons was found to significantly extend survival time during desiccation exposure. Specifically, Logrank testing indicated that DH$_{44}$-GAL4/UAS-*NaChBac* flies (Median survival = 22 hours) survived significantly longer than both DH$_{44}$-GAL4/w^h (Median survival = 21 hours), $X^2(1) = 21.37$, $p < 0.0001$, and w^h/UAS-*NaChBac* (Median survival = 20 hours), $X^2(1) = 13.90$, $p = 0.0002$. The ratio of the rate of death of DH$_{44}$-GAL4/UAS-*NaChBac* flies relative to the rate of death of DH$_{44}$-GAL4/w^h was 0.62 (95% CI: 0.51-0.76), representing a 1.6 fold decrease in death rate and a 5% increase in median survival time. The ratio of the rate of death of DH$_{44}$-GAL4/UAS-*NaChBac* flies relative to the rate of death of w^h/UAS-*reaper* was 0.55 (95% CI: 0.40-0.75), representing a 1.88 fold decrease in death rate and a 10% increase in median survival time.

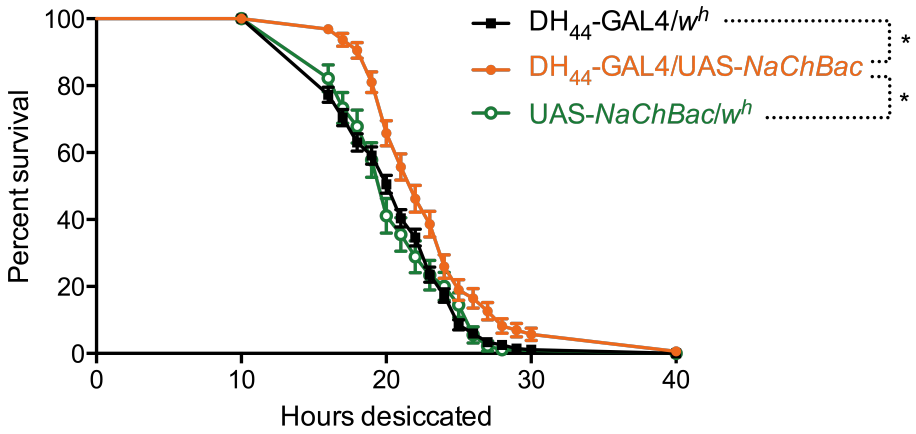

Figure 3.15 Expression of a low threshold voltage-gated sodium channel in DH_{44} neurons results in improved survival during desiccation exposure.

Survival of male DH_{44}-GAL4/UAS-*NaChBac* cross progeny (*N*=158) exceeds that of progeny from control crosses DH_{44}-GAL4/w^h (*N*=352) and w^h/UAS-*NaChBac* (*N*=90) during desiccation stress. Data are pooled across six biological repeats. Statistical comparisons were made using the Logrank test, **p*<0.05

Although the increase in survival duration during desiccation stress in the flies with hyperpolarised DH_{44} neurons relative to both controls is statistically significant, the increase in median survival time is small (approximately 8%). An effect size twice as large (approximately 16%) was observed when DH_{44} peptide was knocked down in the DH_{44} neurons (Figure 3.13A) and an approximately 20% increase in median survival was found when ablating DH_{44} neurons (Figure 3.14A). Thus, it is not evident that increasing excitability of the DH_{44} neurons has a significant effect on desiccation tolerance.

If the subtle increase in desiccation tolerance represents a true effect, then the result is unexpected given the prior findings that decreasing DH_{44} peptide in the brain results in increased desiccation tolerance (sections 3.3.5.1 and 3.3.5.2). This might potentially be explained by a secondary effect of having the DH_{44} neurons in a constantly over-excited state. Indeed this would not be unprecedented as constitutive hyperpolarisation of LK neurons did not affect desiccation tolerance, while conditional hyperpolarisation did have an effect (Liu et al 2015), suggesting that compensatory mechanisms affected the phenotype observed when using a constitutive manipulation. Perhaps conditional rather than constitutive expression of a hyperpolarising construct would yield different results when applied to the DH_{44} neurons as well by preventing the development of compensatory mechanisms prior to the onset of desiccation.

3.3.6 *DH$_{44}$* RNAi knockdown does not affect percentage of body water

As the DH_{44} peptide acts on the Malpighian tubules to stimulate fluid secretion, it is possible that reducing the availability of DH_{44} peptide could result in the build-up of fluid or bloating phenotype due to reduced fluid secretion by the Malpighian tubules. This can be measured by weighing flies to obtain a 'wet weight' measurement, and then drying them and re-weighing the sample groups to obtain a 'dry weight' measurement, as described in section 2.10 (Cabrero et al 2014). If manipulation of the DH_{44} neurons causes excess fluid to build up, the wet weight of the experimental cross progeny outlined in Table 3.5 would exceed those of the control cross progeny, while dry weights of all groups would be similar. A reduced wet weight in the experimental group would suggest that these flies have reduced hemolymph content relative to controls, if the dry weights of all groups are similar. Differences in dry weight would suggest that the flies themselves are differently sized. Flies are weighed in groups of 10 flies due to the small weights that must be measured. The percentage of the weight of the fly that is due to water content can be calculated from the wet and dry weights, assuming that all of the weight that is lost during the drying phase is due to loss of water (Folk et al 2001).

Wet and dry weight measurements were acquired for DH_{44}-GAL4/UAS-*DH$_{44}$* RNAi flies and controls (genotype details in Table 3.5). The results from the experimental group were compared to each of the control groups using two-tailed two-sample Student's *t*-tests for all measurements (wet weight/dry weight/percentage water), and treating the data separately for males and females. As shown in Figure 3.16A and statistically detailed in Table 3.6, female DH_{44}-GAL4/UAS-*DH$_{44}$* RNAi flies had significantly lower wet and dry weights than DH_{44}-GAL4/w^h flies. Male DH_{44}-GAL4/UAS-*DH$_{44}$* RNAi flies had a significantly lower wet weight than DH_{44}-GAL4/w^h flies, but dry weights did not differ. Neither male nor female DH_{44}-GAL4/UAS-*DH$_{44}$* RNAi flies differed significantly from w^h/UAS-*DH$_{44}$* RNAi flies in either wet weight or dry weight. As shown in Figure 3.16B and statistically detailed in Table 3.7, neither male nor female DH_{44}-GAL4/UAS-*DH$_{44}$* RNAi flies had significantly different percentage of body water than either control.

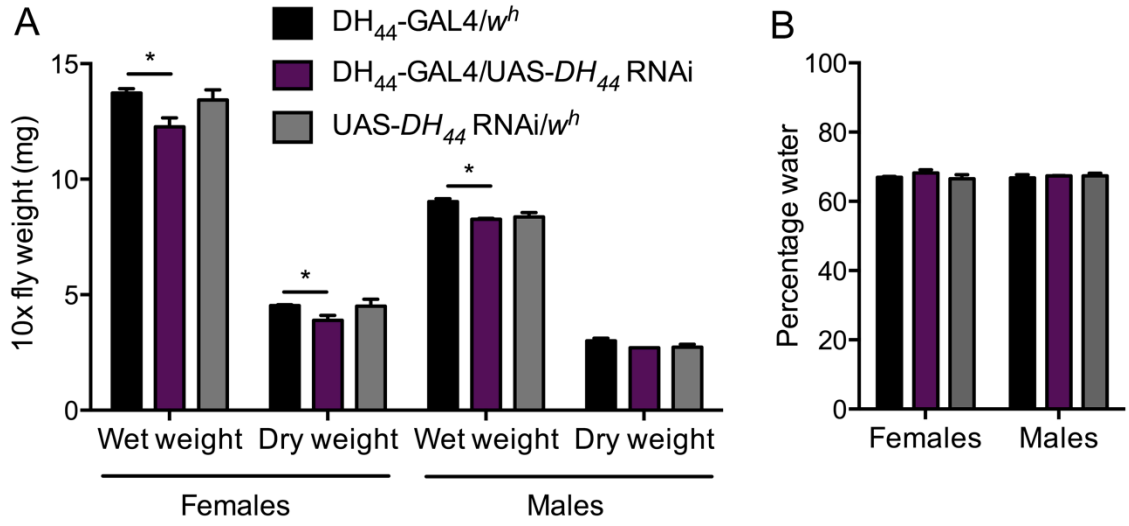

Figure 3.16 Flies with *DH44* RNAi knockdown in DH_{44} neurons weigh significantly less than control, but have similar percentage of body water.

A) Flies with genotype DH_{44}-GAL4/w^h have a significantly higher wet weight than those with genotype DH_{44}-GAL4/UAS-*DH44* RNAi, regardless of sex. Female flies with genotype DH_{44}-GAL4/w^h have a significantly higher dry weight than females with genotype DH_{44}-GAL4/UAS-*DH44* RNAi. *N*=3 for all genotypes. **B)** Male and female flies with DH_{44} knockdown in the DH_{44} neurons have a percentage body water that is similar to progeny of control crosses. All statistical comparisons were made using two-sample two-tailed Student's *t*-testing, **p*<0.05. Graphs show mean ± SEM.

Table 3.6 Two-sample two-tailed Student's *t*-test analysis of wet weight and dry weight in *Drosophila* with *DH44* expression knocked down in the DH_{44} neurons (*N*=3) compared to progeny of control crosses (*N*=3). Data are presented for each sex separately.
Statistically significant *p* values are highlighted in boldface red text.

Females

Group	Weight	*M* (mg)	*SD*	*t*	df	*p*
DH_{44}-GAL4/w^h	Wet	13.73	0.1856	3.436	4	**0.0264**
DH_{44}-GAL4/ UAS-*DH44* RNAi	Wet	12.27	0.3844	2.004	4	0.1156
w^h/UAS-*DH44* RNAi	Wet	13.43	0.4372			
DH_{44}-GAL4/w^h	Dry	4.533	0.0333	3.004	4	**0.0398**
DH_{44}-GAL4/ UAS-*DH44* RNAi	Dry	3.900	0.2082	1.643	4	0.1757
w^h/UAS-*DH44* RNAi	Dry	4.500	0.300			

Males

Group	Weight	*M* (mg)	*SD*	*t*	df	*p*
DH_{44}-GAL4/w^h	Wet	9.033	0.120	6.147	4	**0.0036**
DH_{44}-GAL4/ UAS-*DH_{44}* RNAi	Wet	8.267	0.033			
w^h/UAS-*DH_{44}* RNAi	Wet	8.367	0.186	0.530	4	0.6240
DH_{44}-GAL4/w^h	Dry	3.000	0.1155	2.598	4	0.0602
DH_{44}-GAL4/ UAS-*DH_{44}* RNAi	Dry	2.700	0.0			
w^h/UAS-*DH_{44}* RNAi	Dry	2.733	0.1202	0.2773	4	0.7953

Table 3.7 Two-sample two-tailed Student's *t*-test analysis of percentage body water in male and female *Drosophila* with *DH_{44}* expression knocked down in the DH_{44} neurons (*N*=3) compared to male and female progeny of control crosses (*N*=3).

Genotype	**DH_{44}-GAL4/w^h**		**w^h/UAS-*DH_{44}* RNAi**	
Sex	Females	Males	Females	Males
t	1.446	0.6036	1.187	0.03371
df	4	4	4	4
p	0.2218	0.5787	0.3010	0.9747

The statistically lower weight observed in DH_{44}-GAL4/UAS-*DH_{44}* RNAi flies relative to control DH_{44}-GAL4/w^h is observed across both males and females for the wet weight measurements and in females in the dry weight measurements. This same trend is seen in the values observed for males in the dry weight measurements, with the control group having a mean weight of 3.0 and the experimental group having a mean weight of 2.7, although the result falls slightly short of statistical significance (p = 0.06). Nevertheless, these data together indicate that it is likely that the DH_{44}-GAL4/UAS-*DH_{44}* RNAi flies are smaller than DH_{44}-GAL4/w^h flies. The mean weights observed for the w^h/UAS-*DH_{44}* RNAi control cross are also generally higher than those of the experimental group for female flies, although the greater standard deviation in these measurements has prevented the differences from being identified as significantly different. This trend was not present for male flies, however. Overall, the data do not indicate a bloating phenotype, but the approximately 11% lower weight (mean of the weight change in experimental group relative to DH_{44}-GAL4/w^h control for both sexes and both wet and dry measurements) in the experimental group relative to the DH_{44}-GAL4/w^h control will be considered in the analysis of the stress tolerance assays.

The lack of effect of *DH_{44}* RNAi knockdown on body water content indicates that this manipulation of the DH_{44} neurons does not cause a bloating phenotype.

3.4 Role of tubule receptor DH44-R2 in stress tolerance

DH_{44} peptide binds to and activates DH44-R2 (Hector et al 2009), which shows enriched expression in the Malpighian tubules (Table 3.1). In order to assess whether DH44-R2 in the Malpighian tubules is involved in desiccation tolerance, a highly specific method of downregulating DH44-R2 presence in the tubules was sought. The first step toward achieving this aim was to verify the previously reported localisation of DH44-R2 to the principal cells of the tubules (Cabrero et al 2002). This was assessed by crossing a DH44-R2-GAL4 driver line to a UAS-*GFP* line (see Table 2.1 for fly line details) and evaluating the expression pattern of the driver in the tubules via confocal microscopy (see section 2.7). These data indicated a specific expression pattern localised to the principal cells of the tubules and excluding the stellate cells (Figure 3.17), a finding that agrees with DH_{44}-F labelling results (Figure 3.4).

A Malpighian tubule principal-cell specific driver line, capaR-GAL4 (Terhzaz et al 2012), was then used to drive expression of double-stranded RNAi against *DH44-R2* in order to specifically knock down the expression of this receptor (Figure 3.18; see Table 2.1 for fly line details). The effect of the knockdown on fluid secretion was used to assess the role of DH44-R2 in fluid homeostasis (Figure 3.19), while the effect of tubule DH44-R2 on desiccation and starvation tolerance was examined via survival assay (Figure 3.20).

3.4.1 Evidence for localisation of DH44-R2 to Malpighian tubule principal cells

DH_{44} affects fluid homeostasis by binding to DH44-R2 in the principal cells of the Malpighian tubule (Cabrero et al 2002). This localisation was reconfirmed by crossing a DH44-R2-GAL4 driver line to a UAS-*GFP* line and imaging the Malpighian tubules using confocal microscopy. GFP signal was observed in the main segment, but not in the initial and transitional segments of the tubules. Additionally, expression was not present in all tubule cells and lack of staining in the typical shape of stellate cells was observed (see Figure 3.17). The specificity

of this expression pattern indicates that expression of this gene occurs only in the principal cells and not in the stellate cells of the Malpighian tubules.

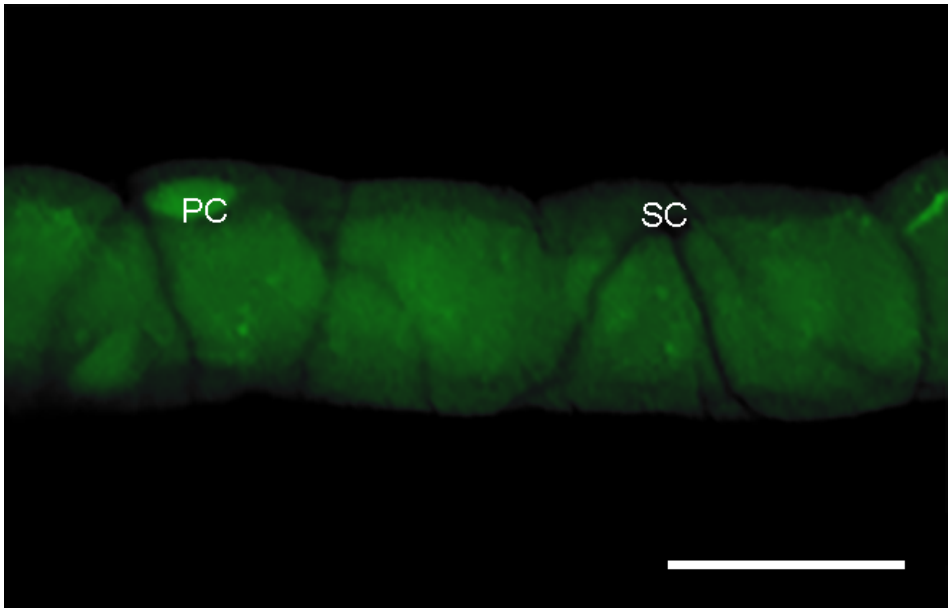

Figure 3.17 Expression pattern of DH44-R2-GAL4 in the Malpighian tubule revealed by crossing to UAS-GFP.
GFP labels principal cells (PC), but not stellate cells (SC). Scale bar indicates 25 μm.

These data support published research in indicating that DH44-R2 is likely expressed and present only in the principal cells of the Malpighian tubules (Cabrero et al 2002).

3.4.2 Knockdown of DH44-R2 in the principal cells of the Malpighian tubules

DH44-R2 expression in the Malpighian tubules was knocked down via RNAi in a highly specific way using driver line capaR-GAL4 (Terhzaz et al 2012). CapaR is the receptor of the diuretic hormone capa. This line was selected as it drives expression in principal cells of the Malpighian tubules. As a control, capaR-GAL4 was crossed to the 'VDRC control line' (see Table 2.1 for details). A RNAi line expressing double-stranded RNAi against *DH44-R2* purchased from Bloomington Stock Center (Table 2.1) was crossed with the capaR-GAL4 driver and was not found to significantly affect *DH44-R2* expression when compared to progeny of crosses in which each parental line was crossed to w^h. This line was therefore not used for any further assays in this study.

Malpighian tubules were dissected from capaR-GAL4/UAS-*DH44-R2* RNAi and capaR-GAL4/VDRC control flies that were 5-10 days old. RNA was extracted and used to synthesise cDNA. RT-PCR was performed using *DH44-R2* TaqMan primer and probe set (spanning exons 8-9) and *alpha-tubulin 84b* as the endogenous control. Comparative C_T analysis was used to calculate a fold change for *DH44-R2* expression relative to the control cross, as shown in Figure 3.18. The comparative C_T method is described in section 2.3.2.1, as is the rationale for selection of statistical tests used to analyse qPCR data.

As the expression level of *DH44-R2* in the control samples was set at a value of 1 to calculate relative expression, the relative expression values obtained for the experimental cross were compared to this control using a two-tailed one-sample Student's t-test against a null hypothesis of 1 (i.e. no difference in expression levels). There was a significant difference between the null hypothesis and the relative expression obtained for *DH44-R2* expression from the Malpighian tubules of cross capaR-GAL4/UAS-*DH44-R2* RNAi (M = 0.395, SD = 0.104, N = 3), $t(2)$ = 10.11, p = 0.0097, indicating a 60% (95% CI: 35-86%) decrease in expression in the experimental cross progeny relative to the control cross progeny.

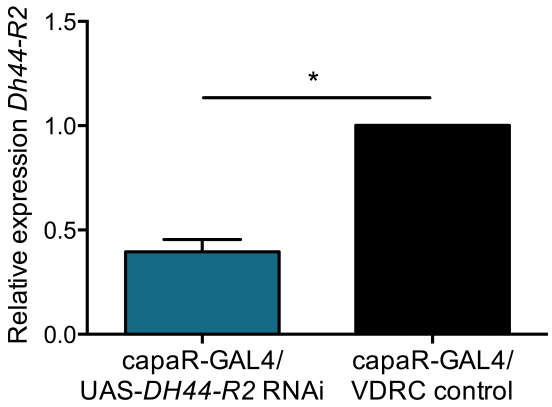

Figure 3.18 RNAi knockdown of *DH44-R2* in the principal cells of the Malpighian tubules. Expression of dsRNAi against *DH44-R2* in the principal cells of the Malpighian tubules results in a 60% decrease in *DH44-R2* expression in the Malpighian tubules when compared to control cross progeny. Mean ± SEM shown, with N=3 for both genotypes. Statistical comparison was made using a one-sample two-tailed Student's *t*-test against a null hypothesis of 1, *p<0.05.

The significantly lower *DH44-R2* expression in capaR-GAL4/UAS-*DH44-R2* RNAi flies relative to the control provides evidence that the *DH44-R2* RNAi

successfully targeted the *DH44-R2* mRNA. However, as the *DH44-R2* mRNA level was only reduced by 60% by this manipulation, it appears that the RNAi line used is not able to fully eliminate the *DH44-R2* mRNA. Nonetheless, as an effective knockdown was achieved, flies with reduced *DH44-R2* mRNA levels were exposed to assays probing the phenotypic effect of this manipulation, including secretion assay and survival assays. In future experiments, this knockdown could potentially be enhanced by driving overexpression of Dicer alongside the *DH44-R2* dsRNAi (Dietzl et al 2007).

3.4.2.1 Knockdown of DH44-R2 in the Malpighian tubules does not affect secretion phenotype

The effect of *DH44-R2* knockdown in the Malpighian tubule principal cells via *DH44-R2* RNAi on basal and DH_{44}-stimulated fluid secretion rates was assessed. Malpighian tubules were dissected from capaR-GAL4/UAS-*DH44-R2* RNAi and capaR-GAL4/VDRC control flies (see section 2.1.4). The modified Ramsay assay was carried out as described in section 2.9. Data were analysed statistically as described in section 2.9.1, where the rationale for test selection is also detailed.

As shown in Figure 3.19A, the basal secretion rate was similar across the two groups and the fluid secretion rate increased to a similar extent following stimulation with DH_{44} peptide. Two-sample two-tailed Student's *t*-tests were performed on the measurements of secretion rate for each 10-minute time interval. There were no significant differences between the two groups at any point ($p > 0.05$, see Table 3.8 for details). Malpighian tubule response to the two compounds was also compared by calculating a percentage change in secretion rate, as shown in Figure 3.19B. A two-sample two-tailed Student's *t*-test did not indicate any significant difference between the groups, $t(21) = 0.7053$, $p = 0.4884$.

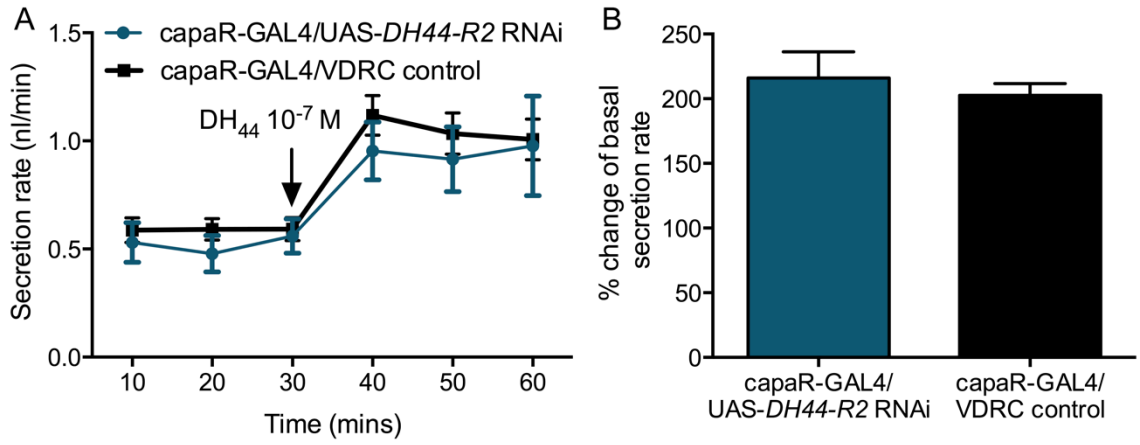

Figure 3.19 Basal and DH_{44}-stimulated secretion rate are similar in Malpighian tubules of flies with *DH44-R2* knockdown.

A) DH_{44}-stimulated secretion rates by excised Malpighian tubules are similar in control progeny (*N*=15) and in flies expressing dsRNAi against *DH44-R2* (*N*=8) in the main segment principal cells. 10^{-7} M DH_{44} application timepoint indicated by the arrow. Mean ± SEM shown for data pooled across three biological repeats. **B)** Secretion rates of excised Malpighian tubules increases to a similar extent following stimulation with 10^{-7} M DH_{44} peptide in both the control group and in flies with RNAi knockdown of *DH44-R2* in the Malpighian tubules.

Table 3.8 Two-sample two-tailed Student's *t*-test analysis comparing basal and DH_{44}-stimulated secretion rates by Malpighian tubules of flies with *DH44-R2* knockdown in the principal cells of the Malpighian tubules (*N*=8) to secretion rates by Malpighian tubules of control flies (*N*=15).

	Baseline secretion			Stimulated secretion		
Time (mins)	0-10	10-20	20-30	30-40	40-50	50-60
t	0.5821	1.285	0.3577	1.075	0.7369	0.1462
df	21	21	21	21	21	21
p	0.5667	0.2127	0.7241	0.2944	0.4693	0.8852

As the basal secretion rate was similar across both the control group and the Malpighian tubules with a *DH44-R2* knockdown, it appears that *DH44-R2* knockdown did not affect fluid homeostasis under non-stimulated conditions for this tissue. Furthermore, the similarity in DH_{44}-stimulated secretion rates between *DH44-R2* knockdown and control tubules support the idea that this manipulation has only partially affected DH44-R2 levels (60% mRNA reduction, Figure 3.18) resulting in sufficient receptor expression to enable a response to DH_{44}. Thus, either 40% expression level of *DH44-R2* can still initiate the signalling cascades required to affect fluid homeostasis in response to DH_{44}, or the knockdown in mRNA levels may not necessarily correspond to a significant effect

on DH44-R2 protein levels (Taylor et al 2013, Vogel & Marcotte 2012). DH44-R2 protein levels following *DH44-R2* knockdown could be semi-quantitatively assessed by labelling with DH_{44}-F. It is possible that a more complete knockdown of *DH44-R2* would have an effect on the ability of the Malpighian tubules to respond to the DH_{44} peptide.

3.4.2.2 Knockdown of DH44-R2 results in increased desiccation tolerance and decreased starvation tolerance

The effect of knocking down *DH44-R2* in the Malpighian tubules principal cells on desiccation and starvation tolerance was assessed using experimental methods described in sections 2.8.1 and 2.8.2. The rationale for the use of the statistical methods applied to the survival data is detailed in section 2.8.3 along with further information about the individual tests and interpretation of their results, where applicable. The reasons for inclusion of a starvation assay alongside a desiccation assay are described in section 2.8.2.1.

As shown in Figure 3.20A, knockdown of *DH44-R2* expression in the main segment principal cells of the Malpighian tubules was found to significantly increase survival time during desiccation exposure. Specifically, Logrank testing indicated that capaR-GAL4/UAS-*DH44-R2* RNAi flies (Median survival = 21 hours) survived significantly longer than capaR-GAL4/VDRC control (Median survival = 20 hours) during desiccation stress, $X^2(1) = 12.18$, $p = 0.0005$. The ratio of the rate of death of capaR-GAL4/UAS-*DH44-R2* RNAi flies relative to the rate of death of capaR-GAL4/VDRC control was 0.63 (95% CI: 0.48-0.82), representing a 1.6 fold decrease in death rate and a 5% increase in median survival time.

Knockdown of *DH44-R2* expression in the Malpighian tubules was found to significantly decrease survival time during starvation exposure, as shown in Figure 3.20B. Specifically, Logrank testing indicated that capaR-GAL4/UAS-*DH44-R2* RNAi flies (Median survival = 44 hours) survived significantly worse than capaR-GAL4/VDRC control (Median survival = 48 hours) during starvation stress, $X^2(1) = 10.90$, $p = 0.001$. The ratio of the rate of death of capaR-GAL4/UAS-*DH44-R2* RNAi flies relative to the rate of death of capaR-GAL4/VDRC control was 1.6 (95% CI: 1.2-2.1), with a 9% lower median survival time.

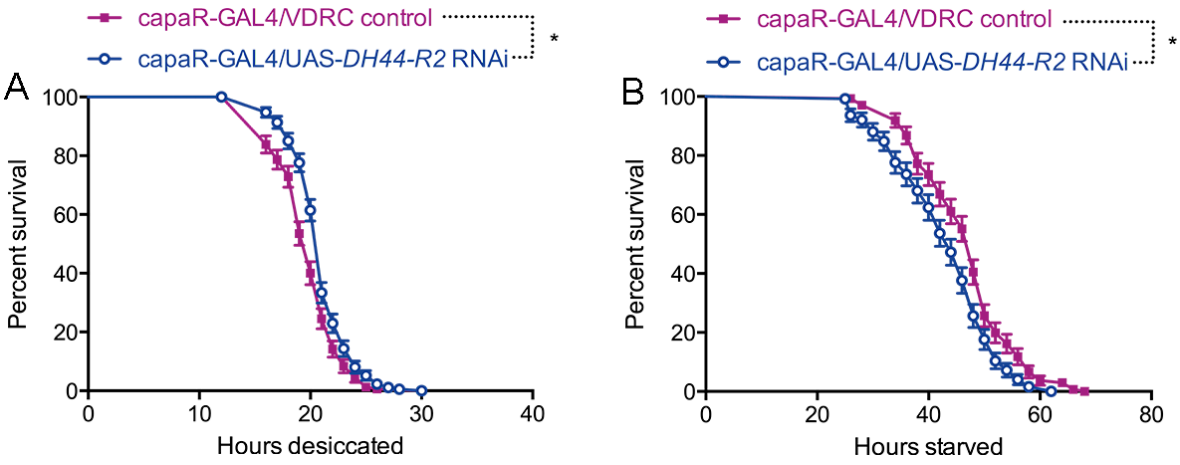

Figure 3.20 Knockdown of *DH44-R2* in Malpighian tubule principal cells affects survival during desiccation and starvation stress exposure.

A) Survival of male capaR-GAL4/UAS-*DH44-R2* RNAi cross progeny (*N*=174) exceeds that of progeny from control cross capaR-GAL4/VDRC control (*N*=155) during desiccation stress. Data are pooled across 5 biological repeats. **B)** Survival of male capaR-GAL4/UAS-*DH44-R2* RNAi cross progeny (*N*=125) is worse than that of progeny from control cross capaR-GAL4/VDRC control (*N*=136) during starvation stress. Data are pooled across five biological repeats. Statistical comparisons were made using the Logrank test, **p*<0.05.

The increase in median survival during desiccation stress in *DH44-R2* knockdown flies indicates that reduced expression, and therefore potentially reduced receptor protein levels, provide an advantage under these circumstances. The effect of the DH44-R2 knockdown on survival duration was quite modest (5%), which is not entirely surprising given the lack of effect that the knockdown had on the secretion rate of excised Malpighian tubules (Figure 3.19). The subtle nature of the desiccation survival phenotype may be due to insufficiency of the DH44-R2 knockdown (Figure 3.18). Overall, the data suggest that DH44-R2 in the Malpighian tubules is involved in desiccation tolerance and agree with the findings that knockdown or ablation of DH_{44} in the DH_{44} neurons improves desiccation tolerance (Figure 3.13A and Figure 3.14A).

The shapes of the curves show a slightly larger difference between survival percentage in the control and *DH44-R2* knockdown groups in the first approximately 20 hours of the assay (Figure 3.18). This might suggest that lack of DH44-R2 could be most advantageous prior to this timepoint. If this is a true effect, this could be due to *DH44-R2* levels being endogenously reduced to a similar extent after 24 hours of desiccation exposure (58%, Figure 3.1). However,

replication of the assay with a more complete *DH44-R2* knockdown would likely be better able to tease apart such subtle effects.

Decreased survival duration during starvation stress in the flies with the *DH44-R2* knockdown in Malpighian tubules relative to control cross progeny indicates that reduction of expression of this receptor impairs starvation tolerance. Ablation of the DH_{44} neurons was found to improve starvation survival (Figure 3.14B), similarly implicating DH_{44} signalling in starvation tolerance. However, it is possible that a reduction of DH44-R2 in the tubules could cause a general survival disadvantage in spite of the lack of an effect on secretion rate phenotype in the Malpighian tubules (section 3.4.2.1). Exposure to an acute period of desiccation stress can impair starvation tolerance (Bubliy et al 2012); reduction of DH44-R2 may be one of the mechanisms used by flies to improve desiccation tolerance (sections 3.1 and 3.2) and this adaptation could require a trade off in fitness in survival of starvation stress.

3.5 Apparent genetic variation in *DH44-R2* coding of *Drosophila* laboratory strains

RT-PCR results using primers and probes against *DH44-R2* spanning exons 8-9 yielded some unexpected results that initially appeared to suggest that the *DH44-R2* mRNA was completely absent from certain samples. Via biological testing of receptor response and re-analysis of the RNA samples using *DH44-R2* primers and probes spanning exons 3-4, it became evident that DH44-R2 was present in the Malpighian tubules of these flies. However, no PCR product is observed in these samples if they are resolved on an agarose gel. Consequently, it seems likely that the there is genetic variability among *Drosophila* laboratory strains near to *DH44-R2* exons 8-9 that interferes with the ability of the primers to amplify the relevant cDNA sequences. Re-analysis of mRNA samples by RT-PCR that indicated absence of *DH44-R2* when using the exon 8-9 spanning primers revealed similar levels of DH44-R2 to controls when using exon 3-4 spanning primers for *DH44-R2*.

RT-PCR analysis of Malpighian tubules capaR-GAL4/UAS-*DH44-R2* RNAi flies and controls indicated an almost total absence of *DH44-R2* transcript in the capaR-GAL4/w^h flies when using *DH44-R2* primers and probes which spanned the exon

8-9 junction (see Figure 3.21A). Specifically, the results suggested that *DH44-R2* levels in the Malpighian tubules of capaR-GAL4/w^h flies were 0.08% that of the control UAS-*DH44-R2* RNAi/w^h. The validity of this result was assessed by determining whether the Malpighian tubules of capaR-GAL4/w^h flies were able to respond to DH_{44} peptide, which would suggest that there was indeed DH44-R2 present in the tubules. This was tested via secretion assay. As shown in Figure 3.21B, the tubules from capaR-GAL4/w^h flies were able to respond at least as well as those of UAS-*DH44-R2* RNAi/w^h flies when challenged with DH_{44} peptide.

One possible explanation for these results is that one of the DH44-R2 primers is not able to anneal to the appropriate template in samples from certain *Drosophila*. Another possibility is that the probe is unable to bind. However, as resolving the RT-PCR product on gel shows no band when the starting cDNA is synthesised from capaR-GAL4/w^h mRNA, this suggests that the issue likely lies with the primer binding (Figure 3.21C).

A similar lack of signal was observed when amplifying *DH44-R2* in UAS-*DH_{44}* RNAi/w^h Malpighian tubule samples using RT-PCR primers that spanned the exon 8-9 junction and comparing these results to those obtained from DH_{44}-GAL4/w^h samples (Figure 3.21D). In this case, the data suggested that the Malpighian tubules of UAS-*DH_{44}* RNAi/w^h flies contained 0.1% of the level of *DH44-R2* transcript of tubules from DH_{44}-GAL4/w^h flies. However, re-analysis of the samples using a *DH44-R2* primer and probe set that spans exons 3-4 revealed similar levels of *DH44-R2* expression in the two groups (Figure 3.21E).

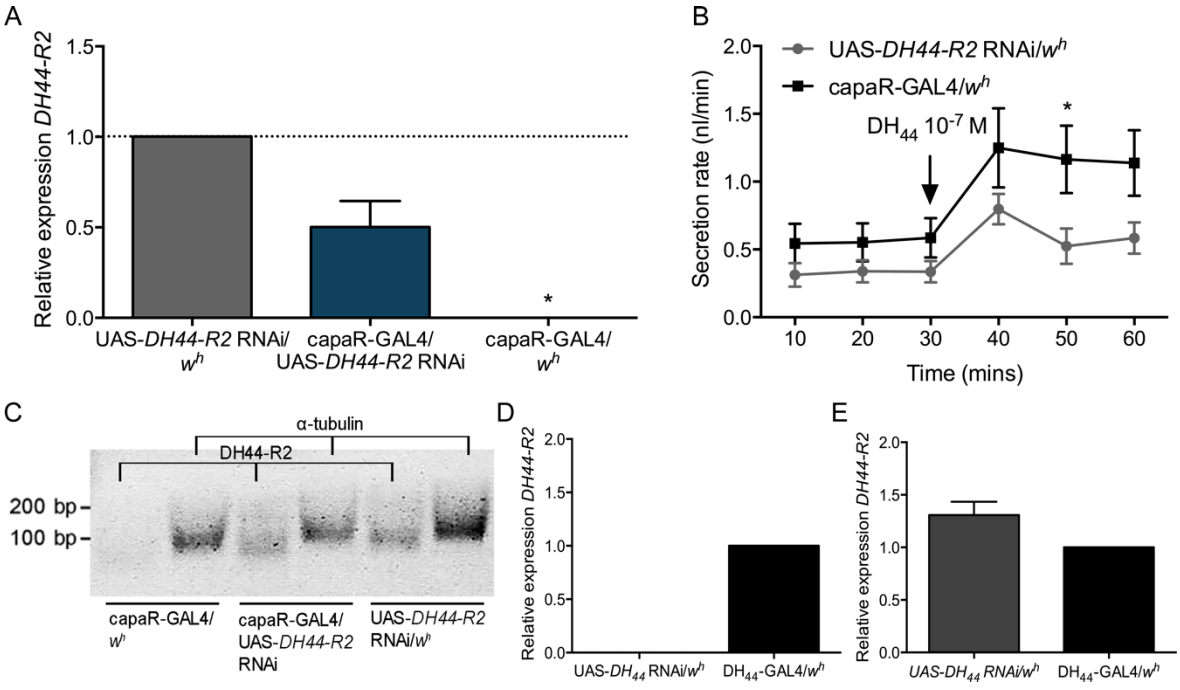

Figure 3.21 Putative genetic variability around the exon 8-9 junction in *DH44-R2* mRNA interferes with RT-PCR amplification in some *Drosophila* cross progeny.

A) RT-PCR amplification of mRNA from Malpighian tubules in flies with *DH44-R2* RNAi expressed in the principal cells and control cross progeny indicates a *DH44-R2* transcript level of 0.0008 (mean) in capaR-GAL4/w^h flies relative to control UAS-*DH44-R2* RNAi/w^h when the *DH44-R2* primers used span exons 8-9. **B)** Secretion assay indicates that capaR-GAL4/w^h tubules and UAS-*DH44-R2* RNAi/w^h tubules respond similarly to DH_{44} peptide. **C)** Agarose gel electrophoresis of PCR product amplified by RT-PCR of mRNA from Malpighian tubules in flies with *DH44-R2* RNAi expressed in the principal cells and from control cross progeny. The genetic background of the flies from which tubules were extracted is indicated below the gel, while the primer pairs used for amplification is indicated above. Specifically, *DH44-R2* primers were used to amplify the products resolved in the 1st, 3rd, and 5th lanes, while *alpha-tubulin 84b* primers were used to amplify the products resolved in lanes 2, 4, and 6. No product is amplified by *DH44-R2* primers spanning the exon 8-9 junction in tubules of capaR-GAL4/w^h flies, while product is amplified in these samples by endogenous control *alpha-tubulin 84b*, indicating that the samples contain mRNA. **D)** RT-PCR amplification of mRNA from Malpighian tubules in flies with *DH_{44}* RNAi expressed in the DH_{44} neurons and control cross progeny indicates a *DH44-R2* transcript level of 0.001 (mean) in UAS-*DH_{44}* RNAi/w^h flies relative to control DH_{44}-GAL4/w^h when the *DH44-R2* primers used span exons 8-9. **E)** RT-PCR amplification of mRNA from Malpighian tubules in flies with *DH_{44}* RNAi expressed in the DH_{44} neurons and control cross progeny indicates similar level of *DH44-R2* transcript in UAS-*DH_{44}* RNAi/w^h and DH_{44}-GAL4/w^h flies when the *DH44-R2* primers used span exons 3-4. The samples used in this panel are the same as those used in part D. All graphs show mean ± SEM. Statistical significance is based on two-tailed one or two-sample Student's *t*-test, *p<0.05.

Overall, these data indicate that the set of primers used in this study that span exons 8-9 of the *DH44-R2* gene are not able to amplify product in *Drosophila* of some genotypes. It is interesting that the mRNA can be detected when using a primer set spanning a different set of exons. Gene expression patterns as assessed by microarray have been found to vary due to different genetic backgrounds in *D. melanogaster*; perhaps some of these variations may be due to the sequences used in the probe set (Sarup et al 2011).

3.6 Discussion

The primary aim of the experiments described in this chapter was to gather evidence regarding the role of DH_{44} signalling pathways in desiccation tolerance. This question was explored from a variety of angles, with the two main approaches used being to expose wild-type flies to desiccation stress and assess changes in components of the DH_{44} pathway after this event, and to manipulate the DH_{44} pathway and assess the effect that this has on survival during desiccation stress. Although primarily addressing this main question, the results also raise other new questions.

With regards to the main question of DH_{44} involvement in desiccation, the results overall appear to implicate changes in DH44-R2 expression as a potential endogenous mechanism of desiccation survival. Wild-type flies were found to have reduced transcript levels of *DH44-R2* in bodies only after 24 hours of desiccation and less fluorescent-labelled DH_{44} was bound to the principal cells of the Malpighian tubules after 24 hours of desiccation relative to unstressed controls, implying reduced receptor presence at least at the surface of these cells. Similarly, partially knocking down *DH44-R2* in the Malpighian tubules alone resulted in improved survival during desiccation. Prior experiments in which *DH44-R2* was knocked down in the entire fly, thereby including DH44-R2 in the brain, found an increase in sensitivity to osmotic challenge when feeding the flies a high-salt diet (Hector et al 2009). These results could be explained by the involvement of DH44-R2 in the Malpighian tubule on fluid transport as this tissue is involved in osmotic stress tolerance (Stergiopoulos et al 2009). The methods used, however, do not exclude the possibility that DH44-R2 in the brain is responsible for the phenotype observed as a central circuit component contributing to the coordination of physiological responses to osmotic stress. The

experiments presented here more specifically implicate DH44-R2 in the Malpighian tubules in desiccation stress tolerance, and therefore in the management of fluid homeostasis in *Drosophila*, by excluding brain DH44-R2 from mRNA extractions and by driving RNAi constructs specifically in the tubules.

Further support for this hypothesis was garnered by manipulating the neurons that produce DH_{44} in *Drosophila* brain. In these experiments it was found that either ablation or RNAi knockdown of *DH_{44}* in these neurons has the effect of improving survival of flies during desiccation stress. Thus, as in the DH44-R2 experiments, it was found that decreasing the functioning of the DH_{44} signalling pathways is advantageous for desiccation survival. This further supports the hypothesis that downregulation of this signalling pathway could be an endogenous mechanism used by *Drosophila* to improve survival during desiccation stress after desiccation conditions have been detected. This is likely to be achieved via a decrease in fluid excretion, and therefore better fluid retention as a result of DH_{44} signalling suppression. This idea is supported by the finding that DH_{44} mutants and mutants for DH_{44} receptors excrete less than normal controls when measured in terms of numbers of waste deposits (Dus et al 2015).

A 58% decrease in *DH44-R2* expression was observed after 24 hours of desiccation stress, and a trend toward reduced DH_{44}-F binding to the Malpighian tubules was found after a similar period of time. This time point was chosen as it is the time after which typically 50% of male wild-type *Drosophila* have died when exposed to desiccation. Although this change has been found to take place by 24 hours, a time course assay would clarify the timescale over which these changes take place. The pattern of desiccation survival in flies with a 60% *DH44-R2* knockdown in the Malpighian tubules indicates that *DH44-R2* knockdown may be most beneficial in the first 20 hours of the assay, as survival after 20 hours is similar in *DH44-R2* knockdown and control flies (Figure 3.20A). This suggests that reduced *DH44-R2* is no longer advantageous after this time point. This could potentially be because the extent of knockdown of *DH44-R2* via RNAi (60%) is very similar to that which was observed to occur in wild-type flies after 24 hours (58%).

Experimental results also imply a role for the DH_{44} signalling pathway in starvation tolerance. This was not entirely unprecedented as the DH_{44} neurons also have receptors for LK, which have been shown to be involved in the regulation of feeding (Kahsai et al 2010). Indeed, ablation of the DH_{44} neurons resulted in increased survival during starvation exposure, while knockdown of *DH_{44}* expression in the DH_{44} neurons via RNAi did not clearly affect starvation tolerance. However, in spite of the apparent lack of involvement of *DH_{44}* in the DH_{44} neurons in starvation tolerance, a decrease in survival during starvation exposure was observed following knockdown of *DH44-R2* in the Malpighian tubules. Consistent with these data was the finding that *DH_{44}* expression level is slightly increased after mild starvation exposure. These two pieces of data seem to imply that decreased receipt of DH_{44} signal to the tubules is disadvantageous during starvation exposure and that flies increase *DH_{44}* levels during starvation exposure, potentially to increase this signal strength. However, the increase in *DH_{44}* expression requires investigation of DH_{44} protein levels and peptide release to determine whether changes in mRNA levels result in changes in signal strength. If increased DH_{44} release contributes to starvation survival, it would be expected that knockdown of *DH_{44}* in the DH_{44} neurons would impair starvation survival, an effect that was not observed in this study.

Impairment of starvation survival by DH44-R2 knockdown could potentially be underpinned by a reduction in food consumption due to bloating, but secretion assay showed the tubules of *DH44-R2* knockdown flies to be similar in function to control flies and no evident bloating was observed. The involvement of the DH_{44} neurons in starvation, however, is clearly indicated by the finding that ablation of these neurons greatly improves starvation survival. These neurons may be involved in circuitry that coordinates the physiological response to starvation, a finding that is perhaps consistent with the involvement of these neurons in nutrient sensing and the colocalisation of LKR in these neurons, a receptor that has been found to affect feeding behaviour (Al-Anzi et al 2010, Dus et al 2015).

Interpretation of stress survival data for DH_{44}-GAL4/UAS-*DH_{44}* RNAi flies and controls must be considered in light of the finding that male DH_{44}-GAL4/UAS-*DH_{44}* RNAi flies were shown to weigh less than DH_{44}-GAL4/w^h flies when wet weight was measured. Several studies have found a positive correlation between wet weight of *Drosophila* and survival of both desiccation and starvation stress,

as reviewed elsewhere (Hoffmann & Harshman 1999, Rion & Kawecki 2007, Telonis-Scott et al 2006). As the smaller size of the DH_{44}-GAL4/UAS-*DH44* RNAi flies would then confer a disadvantage during stress survival compared to DH_{44}-GAL4/w^h flies, it would be anticipated that they would not live as long during stress exposure and that this would not be the case when compared to control cross UAS-*DH44* RNAi/ w^h, which was not found to differ in size from the experimental cross. This was indeed the case during the starvation stress assay, and it is possible that this small difference in weight can account for the improved survival of DH_{44}-GAL4/w^h compared to the two other groups. However, wet weight differences would not predict the greater survival of the DH_{44}-GAL4/UAS-*DH44* RNAi flies in spite of the smaller size. Consequently, it appears that other factors, potentially related to DH_{44} peptide signalling, are involved in producing this phenotype.

The finding that a 58% decrease in *DH44-R2* expression in the bodies of male *Drosophila* following 24 hours of desiccation exposure does not interfere with the stimulation of secretion by DH_{44} peptide mirrors the results found when measuring secretion rate of Malpighian tubules from flies with a 60% knockdown of *DH44-R2* expression in the tubules. These data collectively indicate that decreasing mRNA levels of *DH44-R2* to this extent is not enough to interfere with the ability of the receptor to respond to the peptide and initiate signalling pathways required to induce increased secretion. Although reducing mRNA levels doesn't necessarily equate to a reduction in protein levels, DH_{44}-F labelling of Malpighian tubules from desiccated flies did indicate that receptor density at the surface of the principal cells was reduced following desiccation exposure. However, it seems that receptor density was still high enough in the presence of a saturating concentration of DH_{44} to trigger the cAMP signalling cascades in the principal cells that result in increased secretion via altered membrane potential.

In conclusion, the results presented in this chapter provide evidence that suppressing the DH_{44} signalling pathways, either by manipulating the DH_{44} neurons or by affecting the DH44-R2 in the tubules, improves desiccation survival. Moreover, wild-type flies show a reduction both in *DH44-R2* expression in the body and DH44-R2 levels in the Malpighian tubules following desiccation exposure. These results together indicate the DH_{44} signalling pathway as a potentially important mechanism that can be used by *Drosophila* to respond to

desiccation stress in order to extend survival duration. Additionally, this study has provided new evidence that confirms prior findings that DH44-R2 is present in principal cells only (Cabrero et al 2002). The results presented here have also indicated that the DH_{44} neurons and DH44-R2 in the tubules have an effect on starvation. Future studies investigating these pathways could further probe the nature of the effect using conditional manipulations.

4 The role of the leucokinin receptor in desiccation and starvation stress tolerance

As with the DH_{44} peptide, a role for the diuretic hormone leucokinin (LK) in desiccation tolerance can be hypothesised based on the finding that other diuretic hormones affect desiccation survival in *Drosophila* (Kahsai et al 2010, Soderberg et al 2011, Terhzaz et al 2012, Terhzaz et al 2015b). Furthermore, a role in starvation tolerance is also plausible as LK signalling is involved in the regulation of feeding behaviour (Al-Anzi et al 2010, Liu et al 2015). Data presented in section 3.3.5.2 also provide some support for this idea as ablation of DH_{44} neurons, and therefore the elimination of LKR in these neurons, had an effect on survival during starvation exposure, while RNAi knockdown of *DH_{44}* only did not have a similar effect (section 3.3.5.1).

In order to assess whether LK signalling is involved in desiccation or starvation stress tolerance, a number of approaches were applied. Changes in gene expression of pathway component genes *LK* and *LKR* were measured after exposure to either desiccation or starvation stress. The involvement of LKR in desiccation or starvation tolerance was explored by knocking down expression of the receptor in a tissue-specific manner. Specifically, *LKR* was knocked down in the DH_{44} neurons and in the stellate cells of the Malpighian tubules, enabling the role of this receptor in desiccation and starvation tolerance to be separately assessed for each of these tissues.

It was expected that knockdown of *LKR* in the DH_{44} neurons would replicate the effect of ablating these neurons by extending starvation survival. Conversely, it was hypothesised that knockdown of this receptor in the tubules would affect desiccation stress tolerance owing to a potential decrease in fluid secretion and that this would additionally result in a bloating phenotype.

4.1 Starvation affects gene expression in wild-type *Drosophila melanogaster*

Stress exposure has been found to affect the expression of the genes of neuropeptides and their receptors (Terhzaz et al 2015b, Zhao et al 2010). Consequently, it was hypothesised that *LK* or *LKR* gene expression might be

affected by either desiccation or starvation stress exposure. As this study focuses mainly on the role of Malpighian tubule receptors for *Drosophila* neuropeptides, FlyAtlas expression data was considered to determine which tissues to use when assessing gene expression changes (Chintapalli et al 2007, Chintapalli et al 2013b). As shown in Table 4.1, *LK* is expressed mainly in the brain and thoracicoabdominal ganglion. Whole fly samples were used to probe these changes. As *LKR* is expressed in both neural (brain and thoracicoabdominal ganglion) and gut tissues (Malpighian tubules and hindgut), gene expression was assessed in bodies only.

Table 4.1 Gene expression of LK signalling pathway in *Drosophila* tissues

Table shows mRNA abundance of *LK*, and *LKR* in relevant fly tissues. Data displayed are from FlyAtlas (Chintapalli et al 2007) and show the mRNA signal in each sample ± SEM as well as the mRNA enrichment in each tissue relative to the signal detected in the whole fly. Not detected (ND) indicates that the Affymetrix present call indicated 0 detections out of 4 biological repeats. Enrichment values above 5 are highlighted in yellow, with values over 40 being indicated in red. Values in between these extremes are highlighted in various shades of orange.

	Leucokinin		**Leucokinin receptor**	
Tissue	mRNA Signal	Enrichment	mRNA Signal	Enrichment
Brain	165 ± 6	5.2	78 ± 2	8.1
Thoracicoabdominal ganglion	1537 ± 33	47.9	108 ± 4	11.3
Crop	ND	ND	ND	ND
Midgut	ND	ND	ND	ND
Tubule	ND	ND	348 ± 44	36.2
Hindgut	ND	ND	57 ± 6	6
Testis	ND	ND	6 ± 2	0.7
Virgin spermatheca	ND	ND	22 ± 1	2.31
Mated spermatheca	ND	ND	26 ± 3	2.78
Whole fly	32 ± 1		9 ± 0	

Wild-type CS flies were exposed to either 24 hours of desiccation stress or 24 hours of starvation stress. RNA was then extracted from either bodies (N = 3) or whole flies (N = 5) and used to synthesize cDNA. RT-PCR was performed on the samples using TaqMan probe and primer sets for *LK* and *LKR*, with *alpha-tubulin 84b* as the endogenous control. Comparative C_T analysis was used to calculate a fold change for each of the genes of interest in the two experimental conditions (starvation and desiccation) relative to the control condition (normally fed) as

shown in Figure 4.1. The comparative C_T method is described in section 2.3.2.1, as is the rationale for selection of statistical tests used to analyse qPCR data.

A two-tailed one-sample Student's *t*-test was performed for each set of fold changes acquired for each gene under each of the two experimental conditions against a null hypothesis of a fold change of 1 (i.e. no change in expression). There was a significant difference between the null hypothesis and the fold changes obtained for *LKR* expression after 24 hours of starvation (M = 1.966, SD = 0.07917, N = 3), $t(2) = 21.12$, $p = 0.0022$, indicating a 97% (95% CI: 77-116%) increase in expression of *LKR* relative to normally fed controls. All other *p* values obtained from this analysis were greater than 0.05; these results can be found in Table 4.2.

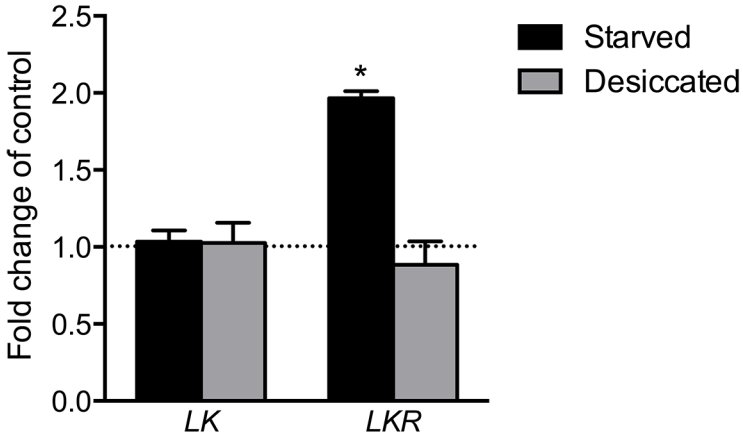

Figure 4.1 Fold change in RNA transcript levels of *LK* and *LKR* following 24 hours of starvation or desiccation in male CS flies relative to untreated controls.
Exposure to starvation stress for 24 hours increased *LKR* expression in *Drosophila* bodies (N=3) by 97%, but did not alter *LK* expression in whole flies (N=5) . Mean ± SEM shown, with statistical significance based on one-sample Student's *t*-test with null hypothesis of 1.0, *p<0.05

Table 4.2 Two-tailed one-sample Student's t-test analysis of fold change of expression of genes in DH_{44} signalling pathway
Statistically significant *p* values are highlighted in boldface red text.

	LK		***LKR***	
	Desiccated	Starved	Desiccated	Starved
t	0.2061	0.4783	0.7610	21.12
df	4	4	2	2
p	0.8467	0.6574	0.5261	**0.0022**

The statistically significant increase in *LKR* expression following starvation exposure for 24 hours represents a 2 fold change in expression relative to the unstressed controls. As the samples used to assess expression changes of this gene were derived from bodies only, this indicates that the changes observed in expression are not due to an increase of expression in the brain. This then suggests that LKR in the Malpighian tubules and hindgut may play a role in enabling *Drosophila* to survive starvation stress exposure. The effect of *LKR* knockdown in the Malpighian tubule on starvation tolerance further explores this possibility, as detailed in section 4.2.1.3.

Changes in gene transcription have been observed to occur as early as 6 hours after flies are transferred to starvation conditions (Hentze et al 2015). Moreover, starvation periods of 18 hours induce starvation acclimation that enhances survival during subsequent longer bouts of starvation exposure (Bubliy et al 2012). The increase in *LKR* expression after 24 hours of starvation exposure may therefore indicate that stress-induced gene expression is initiated significantly before the metabolic stress becomes fatal, which in the male *D. melanogaster* used in this study tended to begin around 35 hours after the onset of starvation.

4.2 Role of Malpighian tubule LKR in stress tolerance

The increase in *LKR* expression in wild-type *Drosophila* bodies following starvation stress exposure (section 4.1) could be due to changes in *LKR* expression in multiple tissues – Malpighian tubule and hindgut are both enriched for *LKR* transcript; the whole body samples could additionally contain some thoracicoabdominal ganglion where *LKR* transcript is also enriched, or tissues that normally have low levels of *LKR* expression could potentially increase expression levels under stress conditions. The role of LKR involvement in stress tolerance was further investigated using RNAi knockdown.

4.2.1 Knockdown of LKR in the stellate cells of the Malpighian tubules

In order to knock down *LKR* expression in the Malpighian tubules, a highly specific driver line was sought. As the receptor is localised on the basolateral membrane of Malpighian tubule stellate cells (Radford et al 2002), a stellate-cell specific driver was used, c724-GAL4 (Table 2.1) which drives expression in the

stellate cells and bar-shaped cells of the initial segment of the anterior tubules (Sozen et al 1997). The specificity of the driver was verified by crossing the line to UAS-*GFP*.

LKR transcript levels in the Malpighian tubules were manipulated by crossing c724-GAL4 flies to *Drosophila* with a UAS-*LKR* RNAi construct or to flies with an empty vector (VDRC control). The effectiveness of the knockdown was assessed by extracting RNA from dissected tubules, synthesising cDNA, and performing RT-PCR using TaqMan primers and probe sets for *LKR* and *alpha-tubulin 84b*. Comparative C_T analysis was used to calculate a fold change for *LKR* expression relative to the control cross. The comparative C_T method is described in section 2.3.2.1, as is the rationale for selection of statistical tests used to analyse qPCR data.

As the expression level of *LKR* in the control samples was set at a value of 1 to calculate relative expression, the relative expression values obtained for the experimental cross were compared to this control using a two-tailed one-sample Student's t-test against a null hypothesis of 1 (i.e. no difference in expression levels). As shown in Figure 4.2, there was a significant difference between the null hypothesis and the relative expression obtained for *LKR* expression from the Malpighian tubules of c724-GAL4/UAS-*LKR* RNAi flies (M = 0.085, SD = 0.019, N = 3), $t(2) = 82.64$, $p = 0.0001$, indicating a 91% (95% CI: 87-96%) decrease in expression relative to the control.

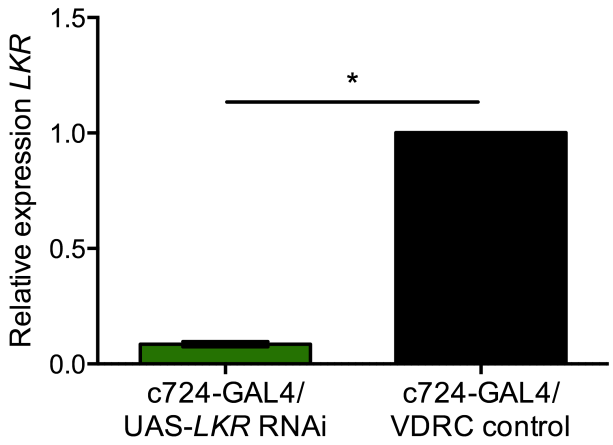

Figure 4.2 RNAi knockdown of *LKR* in the stellate cells of the Malpighian tubules results in a 91% decrease in *LKR* mRNA levels in the Malpighian tubules when compared to control cross progeny

Mean ± SEM shown for three biological replicates. Statistical comparison was made using a one-sample two-tailed Student's *t*-test against a null hypothesis of 1, *$p<0.05$.

The significant decrease in *LKR* transcript levels after RNAi knockdown in the stellate cells indicates that the approach has successfully targeted *LKR* mRNA. Moreover, as driving RNAi against *LKR* in only the tubule stellate cells was able to significantly affect overall *LKR* levels, it supports previous evidence that *LKR* expression in this tissue is indeed specific to the stellate cells as obtained by antibody binding and by labelled LK binding (Halberg et al 2015, Radford et al 2002).

The phenotypic effects of *LKR* knockdown in the stellate cells of the Malpighian tubules on fluid homeostasis and stress tolerance was explored by secretion assay (Figure 4.3), measurement of body water (Figure 4.4), and desiccation and starvation exposure (Figure 4.5).

4.2.1.1 Knockdown of *LKR* reduces the fluid secretion response to LK peptide

The effect of *LKR* knockdown in the Malpighian tubule stellate cells on fluid homeostasis was assessed using the modified Ramsay assay, as described in section 2.9. Data were analysed statistically as described in section 2.9.1, where the rationale for test selection is also detailed.

As shown in Figure 4.3A, the basal secretion rate was not affected by knockdown of *LKR* in the stellate cells of the Malpighian tubules, while the LK stimulated secretion rate was significantly impaired in c724-GAL4/UAS-*LKR* RNAi flies at all three measurement timepoints ($p < 0.05$; see Table 3.3 for statistical details). A percentage change following stimulation relative to basal secretion for each pair of tubules was calculated (see Figure 4.3B) and compared across groups using a two-sample two-tailed Student's *t*-test. The secretion rate of Malpighian tubules from control flies following stimulation with LK was found to be 177% (*SD* = 8.224) of the basal secretion rate, while the secretion rate of tubules from c724-GAL4/UAS-*LKR* RNAi flies was 131% (*SD* = 5.601) of basal secretion; these values were statistically significantly different $t(34) = 4.625$, $p < 0.0001$.

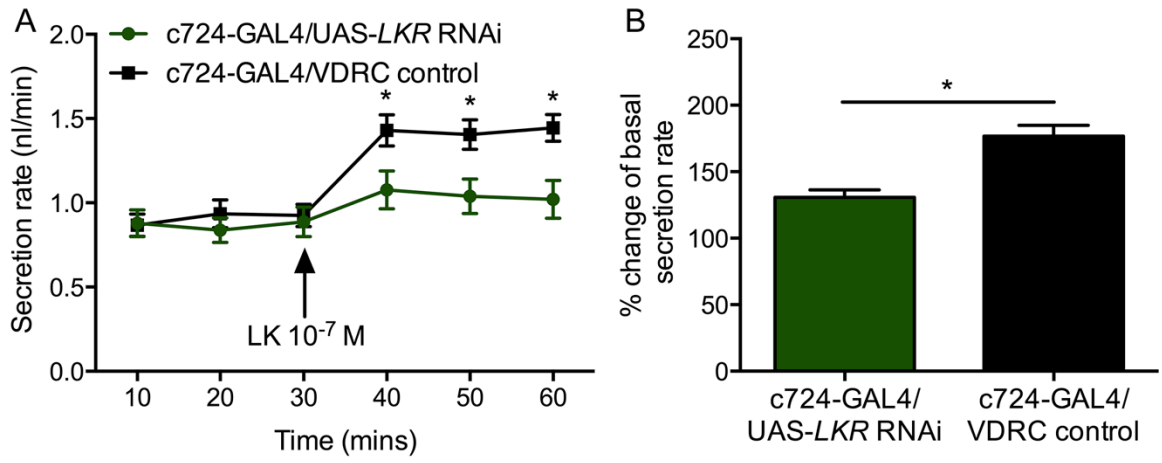

Figure 4.3 Malpighian tubules of flies with *LKR* knockdown in the tubules have a reduced response to LK relative to control cross progeny.

A) Basal secretion rates of live Malpighian tubules from control flies (*N*=18) and flies with *LKR* knockdown in tubule stellate cells (*N*=18) are similar. Secretion rate after stimulation with 10^{-7} M LK is significantly lower in *LKR* knockdown tubules than in control tubules. Peptide application timepoint indicated by the arrow. Mean ± SEM shown with data pooled across two biological repeats. **B)** Percentage change in secretion rates following LK stimulation for tubules from c724-GAL4/UAS-*LKR* RNAi flies differs from those of tubules from control line. Statistical significance tested using unpaired two-sample two-tailed Student's *t*-test, *$p<0.05$.

Table 4.3 Two-sample two-tailed Student's *t*-test analysis comparing basal and LK-stimulated secretion rates by Malpighian tubules of flies with LKR knockdown in stellate cells (*N*=18) to secretion rates by Malpighian tubules of control flies (*N*=18).
Statistically significant *p* values are highlighted in boldface red text.

	Baseline secretion			Stimulated secretion		
Time (mins)	0-10	10-20	20-30	30-40	40-50	50-60
LKR RNAi *M*	0.8793	0.8372	0.8865	1.077	1.039	1.021
LKR RNAi *SD*	0.0779	0.0714	0.0855	0.1089	0.0994	0.1085
Control *M*	0.8668	0.9356	0.9250	1.429	1.406	1.445
Control *SD*	0.0642	0.0811	0.0649	0.0895	0.0856	0.0770
t	0.1242	0.9105	0.3588	2.499	2.796	3.192
df	34	34	34	34	34	34
p	0.9019	0.3690	0.7220	**0.0175**	**0.0085**	**0.0030**

The similarity in basal secretion rate between c724-GAL4/UAS-*LKR* RNAi flies and the control indicates that this manipulation does not affect fluid homeostasis under non-stimulated conditions for this tissue. The significantly lower response to LK peptide in c724-GAL4/UAS-*LKR* RNAi flies relative to the control indicates that the manipulation interferes with the ability of the tubule to respond to the LK. Based on this finding, it appears that constitutively targeting dsRNA against *LKR* using the GAL4/UAS system was effective at reducing not only transcript levels, but also receptor protein level and availability in the tubules. Moreover, these results add to the substantial body of evidence indicating that LK is the ligand which activates LKR in the tubule stellate cell (Halberg et al 2015, Radford et al 2002, Rosay et al 1997, Terhzaz et al 1999).

4.2.1.2 *LKR* knockdown in the Malpighian tubules does not affect percentage of body water

Inhibition of LK signalling pathways has previously been shown to result in a bloating phenotype of the abdomen (Liu et al 2015) and an inflated crop in the gut (Al-Anzi et al 2010). The phenotype observed by Liu and colleagues is thought to be due to an increase in hemolymph volume. This could potentially be due to the loss of the diuretic action of LK on the Malpighian tubule, thereby disrupting one of the neuropeptide signalling pathways which increase fluid secretion. Based on this evidence of the importance of LK signalling for fluid homeostasis, it was expected that knockdown of *LKR* in the Malpighian tubules would cause a build-up of fluid that could be detected as a weight difference and a change in the percentage of the body weight that is due to water. It was

also expected that this weight difference would disappear after the flies were killed, dried, and re-weighed, as any extra hemolymph volume would have then evaporated.

Groups of 10 male or female c724-GAL4/UAS-*LKR* RNAi flies and c724-GAL4/VDRC control flies were weighed in groups both after being briefly anesthetised with CO_2 to obtain a 'wet weight' and then after being killed and dried for 24 hours to obtain a 'dry weight' (section 2.10). As shown in Figure 4.4A, neither wet nor dry weight in either males or females was found to be different between c724-GAL4/UAS-*LKR* RNAi flies and control when analysed using two-tailed two-sample Student's *t*-tests (see Table 4.4). A percentage water for each group of ten flies was calculated, as shown in Figure 4.4B and also showed no statistically significant differences between groups in either males or females (Table 4.5).

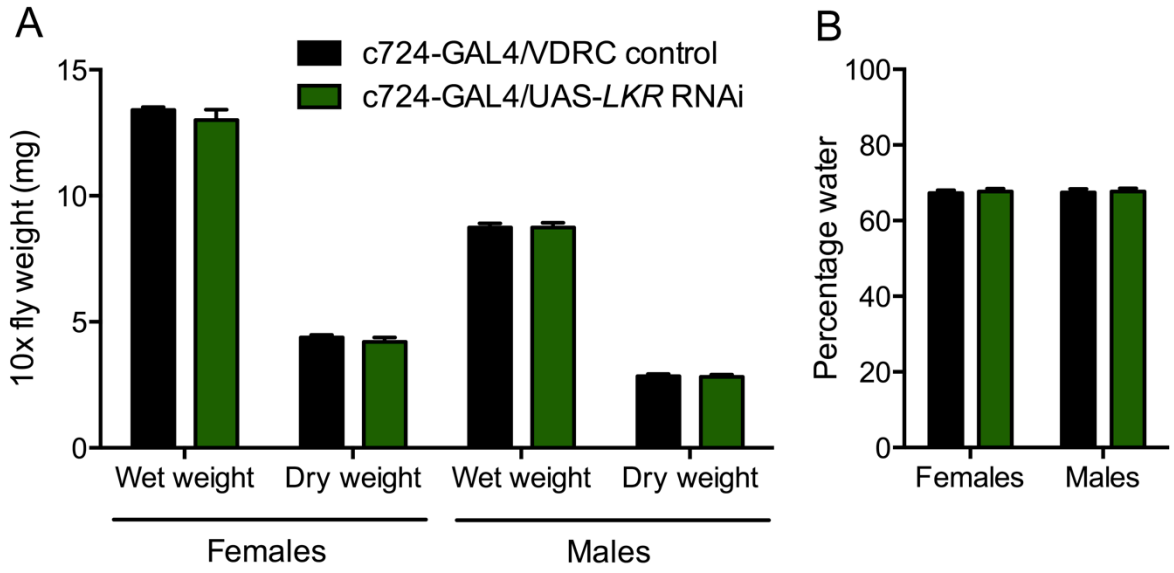

Figure 4.4 Weight measurements comparing *LKR* RNAi knockdown in the Malpighian tubules to control crosses does not indicate any differences in either females or males. **A)** Neither male (*N*=5) nor female (*N*=6) flies with genotype c724-GAL4/UAS-*LKR* RNAi differ in wet or dry weight from flies with genotype c724-GAL4/VDRC control. Mean ± SEM shown. **B)** Male and female c724-GAL4/UAS-*LKR* RNAI flies have a percentage body water that is similar to progeny of a control cross.

Table 4.4 Two-sample two-tailed Student's *t*-test analysis of wet weight and dry weight in *Drosophila* with *LKR* expression knocked down in the stellate cells of the Malpighian tubules (Females *N=6;* Males *N*=5) compared to progeny of control cross c724-GAL4/VDRC control.

Sex	Females		Males	
Measurement	Wet weight	Dry weight	Wet weight	Dry weight
t	0.9325	0.8987	7.6 x 10-7	0.1690
df	10	10	8	8
p	0.3730	0.3899	>0.9999	0.8700

Table 4.5 Two-sample two-tailed Student's *t*-test analysis of percentage body water in male (*N*=5) and female (*N*=6) *Drosophila* with *LKR* expression knocked down in the stellate cells of the Malpighian tubules compared to male and female progeny of control cross c724-GAL4/VDRC control.

Sex	Females	Males
t	0.4115	0.1785
df	10	8
p	0.6894	0.8628

The similarity of both wet weights and percentage water of c724-GAL4/UAS-*LKR* RNAi and control flies indicates that the reduction in *LKR* levels in the tubules, which was shown to impair stimulation of secretion rate by LK (Figure 4.3), does not cause a bloating phenotype. This suggests that the organism is able to maintain fluid homeostasis, at least in terms of hemolymph volume. Several diuretic neuropeptides are present in *Drosophila* (Coast et al 2002) and the biogenic amine tyramine activates the same signalling cascades as LK in the tubule stellate cells (Cabrero et al 2013); one or more of these signalling pathways may be able to maintain fluid homeostasis when *LKR* is constitutively knocked down. If compensation by other signalling pathways or possibly by an increase in LK production or release is enabling fluid homeostasis in c724-GAL4/UAS-*LKR* RNAi flies, then a conditional interference with tubule LKR could potentially result in fluid retention and an associated bloating phenotype.

The similarity in dry weights of c724-GAL4/UAS-*LKR* RNAi and c724-GAL4/VDRC control progeny indicates that knocking down *LKR* in the tubules does not interfere with growth or development.

4.2.1.3 Knockdown of *LKR* affects starvation tolerance, but not desiccation tolerance

The role of Malpighian tubule LKR in desiccation and starvation stress tolerance was investigated by exposing flies with *LKR* RNAi knockdown in the tubule stellate cells to stress survival assays using experimental methods described in sections 2.8.1 and 2.8.2. The rationale for the use of the statistical methods applied to the survival data is detailed in section 2.8.3 along with further information about the individual tests and interpretation of their results, where applicable. The role of the starvation assay as a control for desiccation exposure is described in section 2.8.2.1.

An effect on desiccation survival is not unprecedented as LK is a diuretic hormone which acts on the Malpighian tubules and other diuretic hormone signalling systems have been found to affect desiccation survival (Kahsai et al 2010, Terhzaz et al 2012, Terhzaz et al 2015b). Data presented in section 4.1 additionally indicate a potential role for non-neural LKR in starvation survival. A Logrank test was used to compare experimental and control group survival for statistical significance.

Knockdown of *LKR* mRNA levels in Malpighian tubule stellate cells did not significantly affect survival during desiccation exposure (Figure 4.5A), $X^2(1) = 0.1108$, $p = 0.7393$. Starvation survival differed significantly between groups, with c724-GAL4/UAS-*LKR* RNAi (Median survival = 54 hours) flies surviving for a significantly shorter period than c724-GAL4/VDRC control flies (Median survival = 68 hours), $X^2(1) = 59.40$, $p < 0.0001$ (Figure 4.5B). The ratio of the rate of death of c724-GAL4/UAS-*LKR* RNAi progeny relative to the rate of death of c724-GAL4/VDRC control progeny was 3.7 (95% CI: 2.6-5.2), with a 26% lower median survival time.

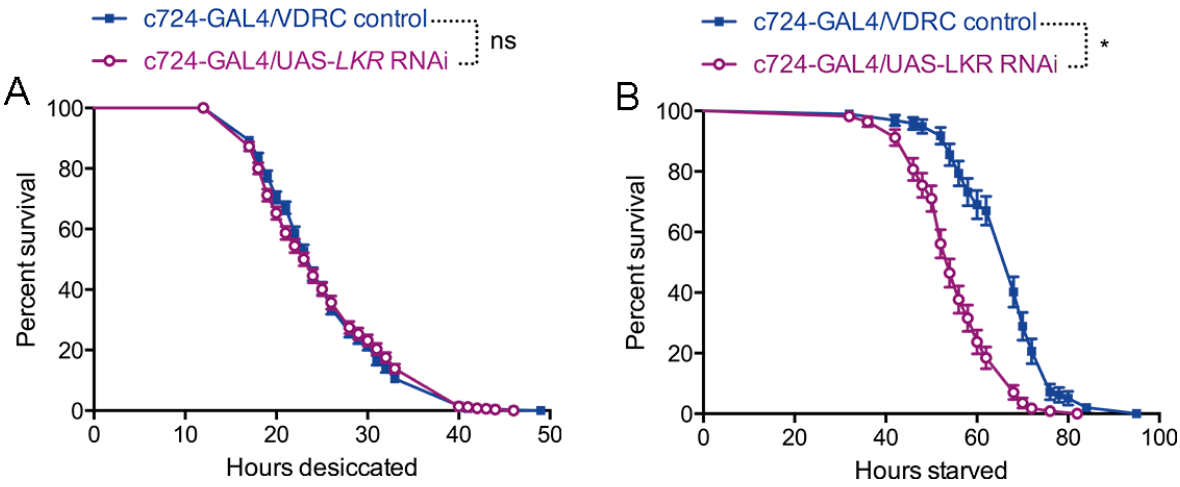

Figure 4.5 *LKR* RNAi knockdown in Malpighian tubule stellate cell impairs survival during starvation stress, but not during desiccation stress.

A) Survival of c724-GAL4/UAS-*LKR* RNAi flies (*N*=496) does not differ from that of c724-GAL4/VDRC control flies (*N*=552) during desiccation stress. Data are pooled across 9 biological repeats. **B)** Survival of c724-GAL4/UAS-*LKR* RNAi flies (*N*=114) is significantly shorter than that of c724-GAL4/VDRC control flies (*N*=114) during starvation stress. Data are pooled across five biological repeats. Statistical comparisons were made using the Logrank test, *$p<0.05$.

The similarity in survival between c724-GAL4/UAS-*LKR* RNAi flies and the control line does not support the hypothesis that LKR is involved in desiccation tolerance. This is consistent with the lack of a bloating phenotype in c724-GAL4/UAS-*LKR* RNAi flies (Figure 4.4). The results could indicate that constitutive knockdown of *LKR* has induced compensatory mechanisms as other studies have found an effect on hemolymph volume and desiccation survival when manipulating LK signalling (Liu et al 2015). This possibility could be tested using a conditional manipulation of LKR in the Malpighian tubules.

The significant reduction in survival during starvation stress in c724-GAL4/UAS-*LKR* RNAi flies suggests that LKR in the Malpighian tubule modulates starvation tolerance and that significant reduction of LKR levels interferes with the ability of the organism to respond in an adaptive manner when food is not available. As interference with LK signalling pathways was previously found to induce a bloating phenotype in *Drosophila* (Liu et al 2015), it is conceivable that the observed reduction in starvation tolerance after manipulating tubule LKR could be due to a bloating-related impairment of feeding. However, as knockdown

flies were found to have a similar percentage body water as control flies (section 4.2.1.2), this explanation seems unlikely.

LK signalling has been linked to feeding (Al-Anzi et al 2010, Liu et al 2015), although a role for LKR in the Malpighian tubules in starvation tolerance has not previously been identified. A distantly related neuropeptide, tachykinin, has been found to be important for starvation tolerance in *Drosophila* (Kahsai et al 2010). This peptide acts on the tachykinin receptor in Malpighian tubule principal cells, and principal-cell specific manipulation of the tachykinin receptor modifies survival during starvation stress (Soderberg et al 2011). Although the role of the Malpighian tubules in fluid homeostasis is well established (Dow 2013), evidence also indicates that the tubules are critically important for multiple processes including detoxification, immune signalling, and oxidative and osmotic stress (Chahine & O'Donnell 2011, Davies et al 2014, Davies et al 2012, Naikkhwah & O'Donnell 2011, Terhzaz et al 2010). The data presented here implicate the Malpighian tubule stellate cells in whole organism survival during dietary restriction. A possible mechanism which could underlie this effect is discussed in section 4.4.

4.3 Role of LKR in the DH_{44}-producing neurons in stress tolerance

In addition to its localisation in the Malpighian tubule principal cells, LKR has been shown to be present in the DH_{44} neurons in the pars intercerebralis of the *Drosophila* brain (Cabrero et al 2002). As a role for DH_{44} in the DH_{44} neurons in desiccation tolerance was identified (section 3.3) and a role for the DH_{44} neurons was observed in starvation tolerance (section 3.3.5.2), the contribution of the LKR in these neurons to tolerance of desiccation and starvation was assessed. Although a role for LKR in the Malpighian tubules in starvation survival was found in section 4.2, LKR in the brain may have a different role, or may not be involved in modulating stress survival.

4.3.1 Colocalisation of LKR to DH_{44}-producing neurons

Prior to manipulation of LKR in the DH_{44} neurons, the colocalisation of LKR and DH_{44} was reconfirmed by double-labelling adult *Drosophila* brains with DH_{44}

antibody overnight (Cabrero et al 2002), followed by an overnight incubation with anti-rabbit Alexafluor goat 546. Brains were then labelled with anti-LKR antibody (Radford et al 2002) overnight followed by incubation with anti-rabbit Alexafluor goat 488 overnight. After washing in PBS, brains were mounted on slides and analysed using confocal microscopy.

Colocalisation of DH_{44} peptide and LKR was clearly observed in the pars intercerebralis of the wild-type adult *Drosophila* brain, as shown in Figure 4.6. Staining using the LKR antibody alone also reveals additional staining in a medial dorsal area of the brain which is of much lower intensity than the six neurons in the pars intercerebralis (Figure 4.7).

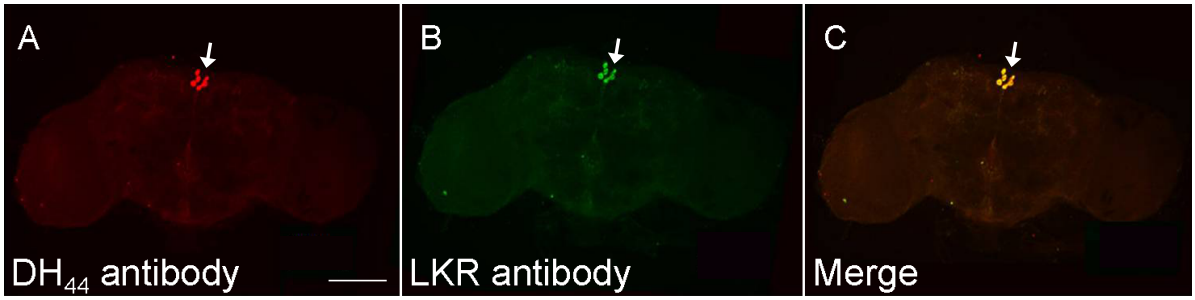

Figure 4.6 Double staining of a wild-type Drosophila brain shows that DH_{44} peptide and LKR colocalise in six neuronal cell bodies of the pars intercerebralis.
A) Staining pattern of anti-DH_{44} antibody in wild-type brains. Scale bar indicates 100 µm, arrow indicates location of the pars intercerebralis **B)** Staining pattern of anti-LKR antibody in wild-type brains. **C)** Merging the DH_{44} and LKR staining patterns shows colocalisation to six neurons in the par intercerebralis.

Colocalisation of DH_{44} and LKR indicates that the LKR is present in the DH_{44} neurons, as shown previously (Cabrero et al 2002). It is therefore possible that the role of the DH_{44} neurons in starvation tolerance identified in section 3.3.5.2 could be modulated by LKR in the DH_{44} neurons.

4.3.2 Manipulation of LKR in the DH_{44}-producing neurons via neuron ablation and RNAi knockdown of *LKR*

LKR in the DH_{44}-producing neurons was manipulated to assess its involvement in desiccation and starvation tolerance. In particular, as a significant increase in starvation survival duration was observed when the DH_{44} neurons were ablated, but not when *DH_{44}* was knocked down in these neurons, it was hypothesised that

the LKR present in these neurons could be responsible for the survival phenotype. The validity of the latter hypothesis was assessed first by confirming that LKR in the DH_{44} neurons was indeed eliminated by the ablation of the neurons. Then a LKR knockdown via RNAi expressed against *LKR* in the DH_{44} neurons was applied and the effectiveness of the knockdown assessed.

As *LKR* is expressed both in the nervous system of *Drosophila* and in the Malpighian tubules (Table 4.1), exploration of the role of this receptor in the DH_{44} neurons cannot be achieved using *LKR* mutants or an ubiquitous knockdown. Consequently, a tissue-specific RNAi approach was applied. Two UAS-*LKR* RNAi lines were crossed to the DH_{44}-GAL4 driver (for assessment of driver line specificity, see section 3.3.3). Each of the parental lines was additionally crossed to w^h to provide control cross progeny. The effectiveness of the knockdowns at reducing LKR in the DH_{44} neurons was assessed by staining adult brains with anti-LKR antibody and viewing via confocal microscopy (Radford et al 2002). Images were taken of controls and experimental crosses using identical settings. Where this method showed differences in staining intensity, signal intensity was quantified (Figure 4.8). RT-PCR was additionally used to attempt to quantify the changes in receptor expression (Figure 4.9).

Progeny of a cross between UAS-*LKR* RNAi line from Bloomington Stock Center (Table 2.1) and DH_{44}-GAL4 driver line did not show any effect on LKR staining intensity relative to the control cross progeny. Conversely, crossing a UAS-*LKR* RNAi line from the VDRC (Table 2.1), which was also used to effectively knockdown LKR in the Malpighian tubules (Figure 4.3), to DH_{44}-GAL4 was found to reduce the intensity of LKR staining, as shown in Figure 4.7A-B.

LKR in the DH_{44} neurons was additionally manipulated by ablating the DH_{44} neurons via a cross between DH_{44}-GAL4 and UAS-*reaper*. As LKR is colocalised with DH_{44} in the DH_{44} neurons (Figure 4.6), it was anticipated that ablation of these neurons would abolish the specific pattern of six labelled cell bodies in the pars intercerebralis. This was indeed found to be the case, as shown in Figure 4.7C.

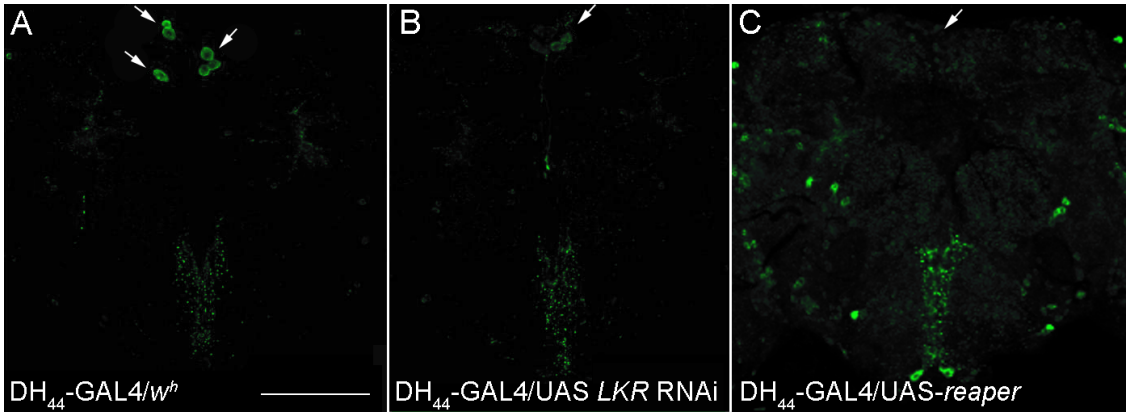

Figure 4.7 Manipulation of LKR in pars intercerebralis achieved via neuronal ablation and RNAi knockdown of *LKR*.

A) Adult *Drosophila* brains from DH_{44}-GAL4/w^h flies stained for LKR show clear labelling in the pars intercerebralis when imaged via inverted confocal microscopy. Scale bar indicates 100 µm. **B)** Progeny from the cross between DH_{44}-GAL4 and UAS-*LKR* RNAi show less intense staining of LKR in the pars intercerebralis when viewed using identical confocal settings to part A. **C)** Ablation of DH_{44}-producing neurons via a cross between DH_{44}-GAL4 and UAS-*reaper* eliminates the pars intercerebralis LKR staining pattern of six neurons, while not affecting staining in the medial dorsal regions of the brain.

The finding that DH_{44} neuron ablation eliminates labelling of these neurons by anti-LKR antibody confirms that LKR is present in the DH_{44} neurons. The reduction in anti-LKR labelling in the pars intercerebralis when RNAi was expressed in the DH_{44} neurons against *LKR* indicates that this method has been successful in partially reducing the presence of the receptor in this area of the brain. This is consistent with the finding that driving expression of the same UAS-*LKR* RNAi line in the stellate cells of the Malpighian tubules significantly reduced *LKR* mRNA levels in the tubules (Figure 4.2) and significantly reduced tubule response to LK peptide (Figure 4.3).

The reduction in anti-LKR labelling in the pars intercerebralis observed when visually inspecting brains from DH_{44}-GAL4/UAS-*LKR* RNAi cross progeny and DH_{44}-GAL4/w^h progeny was semi-quantitatively analysed by quantifying mean pixel intensity of stained cells (Liu et al 2015). The images used to generate these values were taken using identical confocal microscopy settings and the brains used were stained in parallel. All six neurons which are typical of the staining pattern of LKR in the pars intercerebralis were visible in both the control and knockdown samples.

As shown in Figure 4.8, the mean pixel intensity of the control samples (*M* = 81.8, *SD* = 10.1, *N* = 12) was significantly higher than that of DH_{44}-GAL4/UAS-*LKR* RNAi flies (*M* = 31.3, *SD* = 3.87, *N* = 12) when compared using an unpaired two-sample two-tailed Student's *t*-test, $t(22) = 4.688$, $p = 0.0001$.

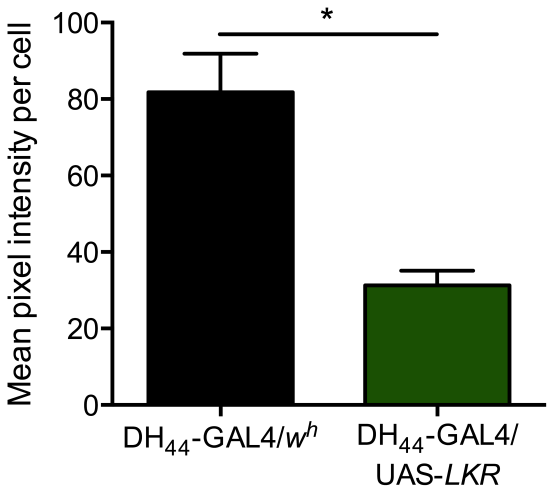

Figure 4.8 Knockdown of *LKR* in DH_{44} neurons results in reduced anti-LKR immunocytochemical staining

Mean pixel intensity of cells labelled with anti-LKR antibody using grayscale images in Image J is lower in flies with LKR knockdown (*N*=12) than in controls (*N*=12). Graph shows mean ± SEM. Statistical significance tested using an unpaired two-sample two-tailed Student's *t*-test, *$p<0.05$.

This data supports the results of the visual inspection, which appeared to indicate that there was a reduction of LKR staining intensity when the receptor was knocked down using RNAi. Thus, there is less LKR present in the DH_{44} neurons of DH_{44}-GAL4/UAS-*LKR* RNAi flies than in these neurons in DH_{44}-GAL4/w^h.

The possibility of additionally quantifying the manipulations of LKR in the DH_{44} neurons using RT-PCR was explored by first determining whether ablation of the DH_{44} neurons affected levels of *LKR* mRNA in head samples. As the RNAi knockdown was observed to be only a partial knockdown, while DH_{44} neuron ablation fully eliminated the LKR staining in the pars intercerebralis, it was expected that *LKR* mRNA levels would be more likely to be affected following ablation rather than following *LKR* RNAi knockdown. RNA from heads of DH_{44}-GAL4/UAS-*reaper* and two controls was extracted and *LKR* mRNA levels were assessed using RT-PCR. As a comparative C_T approach was applied, primer and

probe sets for *LKR* and endogenous control *alpha-tubulin 84b* were used. The comparative C_T method is described in section 2.3.2.1, as is the rationale for selection of statistical tests used to analyse qPCR data. Fold change of *LKR* expression relative to DH_{44}-GAL4/w^h heads was calculated; relative expression of *LKR* in DH_{44}-GAL4/UAS-*reaper* heads was compared to DH_{44}-GAL4/w^h using a one-sample two-tailed Student's *t*-test with a null hypothesis of 1 (i.e. equal level of expression) and compared to UAS-*reaper*/w^h using a two-tailed two-sample Student's *t*-test.

LKR levels in the heads of DH_{44}-GAL4/UAS-*reaper* flies was not significantly different from either control (Figure 4.9). Specifically, *LKR* expression did not differ significantly from DH_{44}-GAL4/w^h, $t(3) = 1.893$, $p = 0.15$, or UAS-*reaper*/w^h samples, $t(6) = 0.057$, $p = 0.96$.

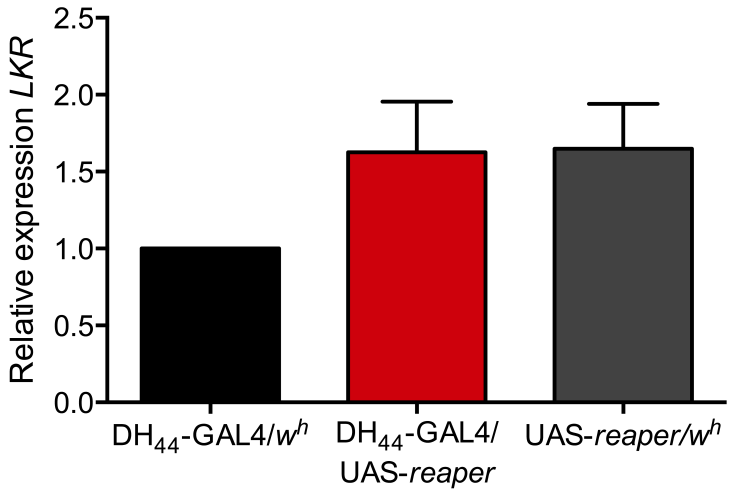

Figure 4.9 Ablation of DH_{44}-producing neurons does not significantly affect mRNA levels of *LKR* in the heads of cross progeny.
Graph shows mean ± SE of four biological replicates.

As this approach was not able to identify changes even after abolition of LKR staining in the pars intercerebralis, it was not used to attempt to quantify changes in *LKR* expression in flies with a *LKR* knockdown in the DH_{44} neurons, as this was expected to have a smaller effect on overall *LKR* levels in the head.

4.3.3 LKR RNAi knockdown in the DH_{44} neurons affects stress tolerance

As DH_{44} signalling via the DH_{44} neurons was shown in section 3.3 to be involved in desiccation stress, LKR that is colocalised to the DH_{44} neurons has a potential to affect fluid homeostasis by modifying DH_{44} neuron function. Moreover, as the DH_{44} neurons were found to affect starvation survival, it is possible that LKR in these neurons could have a role in starvation tolerance.

The specific contribution of LKR in the DH_{44} neurons to stress tolerance was explored by exposing flies in which *LKR* expression was partially knocked down in the DH_{44} neurons (Figure 4.8) to desiccation and starvation tolerance assays using experimental methods described in sections 2.8.1 and 2.8.2. The rationale for the use of the statistical methods applied to the survival data is detailed in section 2.8.3 along with further information about the individual tests and interpretation of their results, where applicable. The role of the starvation assay as a control for desiccation exposure is described in section 2.8.2.1.

As shown in Figure 4.10A, *LKR* knockdown in the DH_{44} neurons significantly impaired survival time during desiccation exposure. Specifically, Logrank testing indicated that DH_{44}-GAL4/UAS-*LKR* RNAi flies (Median survival = 24 hours) survived for a significantly shorter period than both DH_{44}-GAL4/w^h (Median survival = 26 hours), $X^2(1) = 59.58$, $p < 0.0001$, and w^h/UAS-*LKR* RNAi (Median survival = 26 hours), $X^2(1) = 24.59$, $p < 0.0001$. The ratio of the rate of death of DH_{44}-GAL4/UAS-*LKR* RNAi flies relative to the rate of death of DH_{44}-GAL4/w^h was 2.38 (95% CI: 1.91-2.97), with an 8% decrease in median survival time. The ratio of the rate of death of DH_{44}-GAL4/UAS-*DH44* RNAi flies relative to the rate of death of w^h/UAS-*LKR* RNAi was 1.75 (95% CI: 1.40-2.18), with an 8% decrease in median survival time.

Logrank testing also indicated statistically significant differences in survival during starvation stress between DH_{44}-GAL4/UAS-*LKR* RNAi flies and controls (Figure 4.10B). Specifically, Logrank testing indicated that DH_{44}-GAL4/UAS-*LKR* RNAi flies (Median survival = 48 hours) survived for a significantly shorter period than DH_{44}-GAL4/w^h (Median survival = 52 hours), $X^2(1) = 18.28$, $p < 0.0001$. Logrank testing also identified a difference in survival between DH_{44}-GAL4/UAS-

LKR RNAi flies and w^h/UAS-*LKR* RNAi (Median survival = 48 hours), $X^2(1) = 4.412$, $p = 0.0357$. The ratio of the rate of death of DH_{44}-GAL4/UAS-*LKR* RNAi flies relative to DH_{44}-GAL4/w^h was 1.42 (95% CI: 1.21-1.67), with an 8% decrease in median survival time. A hazard ratio for survival of DH_{44}-GAL4/UAS-*DH44* RNAi relative to w^h/UAS-*LKR* RNAi is not reported as the survival lines cross, indicating that hazard is not proportional across time in this dataset. Median survival time was the same in these two groups.

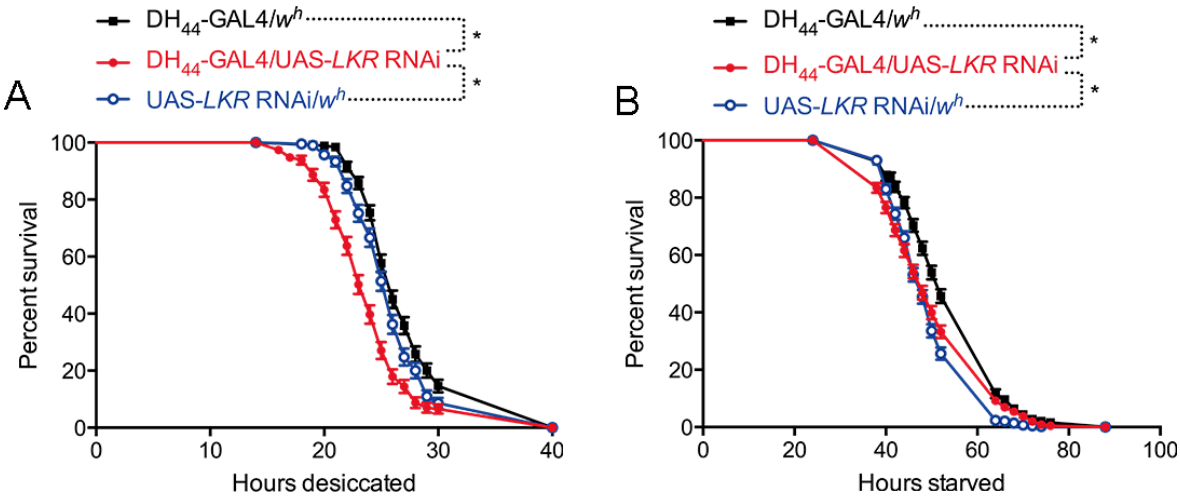

Figure 4.10 *LKR* RNAi knockdown in the DH_{44} neurons impairs survival during desiccation stress.

A) Survival of male DH_{44}-GAL4/UAS-*LKR* RNAi flies (*N*=229) is shorter than that of controls DH_{44}-GAL4/w^h (*N*=260) and w^h/UAS-*LKR* RNAi (*N*=210) during desiccation stress. Data is pooled across five biological repeats. **B)** Survival of male DH_{44}-GAL4/UAS-*LKR* RNAi flies (*N*=448) differs significantly from that of w^h/UAS-*LKR* RNAi (*N*=429), and is significantly lower than that of DH_{44}-GAL4/w^h (*N*=438) during starvation stress. Data are pooled across nine biological repeats. Statistical comparisons were made using the Logrank test, *$p<0.05$

The significant reduction in desiccation survival in *Drosophila* with *LKR* knockdown in the DH_{44} neurons implicates these neurons in desiccation tolerance. Interestingly, the direction of the effect is opposite to that observed when knocking down *DH44* in the DH_{44} neurons or when ablating the neurons altogether (section 3.3), and contrasts with the finding that knocking down DH44-R2 in the Malpighian tubules improves desiccation survival (section 3.4.2.2) This suggests that LKR in the DH_{44} neurons may oppose DH_{44} signalling pathways during desiccation stress.

A statistically significant reduction in starvation survival for DH_{44}-GAL4/UAS-*LKR* RNAi flies was observed relative to only one of the two control crosses. As the survival of *LKR* knockdown flies is not clearly different from both controls, the assay does not provide strong evidence that LKR in the DH_{44} neurons is involved in starvation tolerance. Moreover, the data clearly do not replicate the starvation survival phenotype observed when ablating DH_{44} neurons (section 3.3.5.2). This could potentially be due to insufficiency of the *LKR* knockdown (Figure 4.7).

4.4 Discussion

The goal of the experiments presented in this chapter were to investigate whether LK signalling is involved in desiccation and starvation stress tolerance. Specifically, the study was designed to assess whether LK signalling via LKR in the DH_{44} neurons affects survival during stress through RNAi manipulations of LKR in these neurons. Contrasting these phenotypic results with those obtained by knocking down *LKR* in the Malpighian tubules highlights the tissue-specific nature of receptor involvement in stress tolerance. These findings are further informed by gene expression analysis of stress-exposed wild-type flies. The results presented in the chapter and considered in this discussion are summarized in Table 4.6.

Table 4.6 Summary of results investigating role of LK signalling in survival of desiccation and starvation stress

HR = Hazard ratio

	Desiccation	**Starvation**
LK expression following stress exposure	No change	No change
LKR expression following stress exposure	No change	2 fold increase
LKR knockdown in Malpighian tubules: survival phenotype	No change	26% decrease median survival duration; 3.7 HR
LKR knockdown in DH_{44} neurons: survival phenotype	8% decrease median survival duration; approx. 2.1 HR	No change

Evidence for the involvement of LK signalling in desiccation tolerance was somewhat limited. No changes in either whole fly *LK* expression or non-neural

LKR expression (i.e. body samples) were found following 24 hours of desiccation exposure. Consistent with these results was the finding that knockdown of *LKR* in the stellate cells of the Malpighian tubules does not affect desiccation survival. These results together seem to suggest that LKR in the body of flies does not affect desiccation tolerance, at least under the conditions used in this study. This is consistent with functional studies of the Malpighian tubules, in which the principal cells have been identified as playing an important role in stress signalling and survival (Davies et al 2014). The evidence for principal cell involvement in desiccation tolerance includes modulation of desiccation survival by manipulation of the DH_{44} (Chapter 3) and capa family signalling pathways, which affect fluid homeostasis through the principal cells (Terhzaz et al 2012, Terhzaz et al 2015b). Perhaps neuropeptide modification of secretion rate during desiccation is specialised to the principal cells.

It is also possible that a role for LKR in the Malpighian tubules in desiccation stress tolerance could be found using other methods. In particular, constitutive knockdowns can yield different results from conditional manipulation, presumably due to the development of compensatory mechanisms (Liu et al 2015). Although the results of the secretion assay indicated that constitutive knockdown of *LKR* in the Malpighian tubules impairs stimulation of secretion rate by LK peptide (section 4.2.1.1), it is possible that compensatory mechanisms could occur elsewhere in the organism to maintain fluid homeostasis. For example, it is possible that flies with *LKR* knockdown in the tubules might produce and release higher levels of LK to compensate for reduced sensitivity of the target tissue. Alternatively, as there are several different diuretic neuropeptides in *Drosophila* (Coast 2006), the organism may shift dependency away from LK signalling toward other diuretic peptides when LKR in the Malpighian tubules is compromised. Signalling by the biogenic amine tyramine to tubule stellate cells has been shown to affect intracellular calcium to a similar extent and thereby to increase fluid production (Cabrero et al 2013). Tyramine signalling could therefore have the potential to compensate for a constitutive reduction in LK signalling. It would be interesting to explore these questions further by using a conditional knockdown approach to manipulate LKR in the stellate cells of the Malpighian tubules. Additionally, knockdown of multiple diuretic neuropeptide receptors in the Malpighian tubules could have the

potential to uncover a synergistic effect if there is redundancy between peptides in desiccation stress signalling.

LK signalling via the DH_{44} neurons was implicated in survival of desiccation stress. Specifically, knockdown of *LKR* in the DH_{44} neurons resulted in impaired desiccation tolerance. These results suggest that LKR modifies the signalling of the DH_{44} neurons during desiccation exposure, and may therefore indicate that LKR in these neurons is involved in regulating the release of DH_{44} peptide. Although *LKR* expression was not found to change in the bodies of *Drosophila* following desiccation, it is possible that changes in *LKR* expression in the brain could occur in response to a lack of fluid availability. Assessing changes in *Drosophila* brains following desiccation stress exposure could provide evidence as to whether changes in *LKR* levels in the brain are an endogenous mechanism of desiccation resistance.

The possibility that compensatory mechanisms may modify the phenotype of *Drosophila* with *LKR* expression knocked down in the Malpighian tubules is not unlikely when considered in the context of other experiments involving manipulation of LK signalling. It was previously found that activation of LK neurons (described in section 1.3.2) results in increased excretion and inactivation of these neurons results in reduced secretion (Cognigni et al 2011). Persistent inactivation, however, resulted in a twofold increase in defecation rate. This indicates that persistent changes in LK signalling pathways can induce compensatory changes in the regulation of fluid homeostasis. The absence of a bloating phenotype in flies with *LKR* knockdown in the tubules (section 4.2.1.2) is somewhat surprising given prior findings that even constitutive inactivation of the LK neurons in *Drosophila* cause the abdomen to become bloated (Cognigni et al 2011, Liu et al 2015). This contrast seems to suggest that LK neuron manipulation has farther reaching consequences than preventing LK from acting on the Malpighian tubules. Or perhaps the LK neurons are able to compensate for changes in the Malpighian tubule LKR levels, while the tubules do not modify sensitivity to LK when neuron functionality is impaired.

The findings of this study additionally indicate that a 91% knockdown of *LKR* in tubules is sufficient to interfere with tubule response to LK peptide. A 65% knockdown of *capaR* in the tubules was previously found to impair tubule

response to capa-1 diuretic peptide (Terhzaz et al 2012), although a 60% knockdown of *DH44-R2* did not impair stimulation of secretion rate by DH_{44} (section 3.4.2.1).

As LK signalling has previously been linked to feeding (Al-Anzi et al 2010, Liu et al 2015), a potential role for this neuropeptide in starvation tolerance is not unprecedented. Somewhat unexpected, however, was the finding that *LKR* knockdown in the DH_{44} neurons did not affect survival during starvation, while knockdown of *LKR* in the Malpighian tubules significantly impaired starvation survival. Likewise expression of *LKR* in the bodies of *Drosophila* that had been exposed to starvation survival for 24 hours was 2-fold that of unstressed controls. Overall, these results indicate that non-neural LKR, including that in the Malpighian tubules, may be important in *Drosophila* for supporting survival in the absence of food. This then raises questions regarding how fluid secretion might interact with metabolism and processing of food.

The Malpighian tubules are critical tissues not only for fluid homeostasis, but also for detoxification (Chung et al 2009, Davies et al 2014, Dow 2009, Terhzaz et al 2014). Evidence indicates that lipid metabolism in the fat body is a particularly crucial source of energy during starvation (Palanker et al 2009). Lipid mobilisation results in waste products being released into the hemolymph, which are then taken up by the Malpighian tubules for processing and excretion (Palanker et al 2009). Interference with this process by reducing the ability of the Malpighian tubules to increase fluid secretion, potentially in response to changes in hemolymph osmolarity, could affect the ability of the organism to mobilise energy resources. Thus, it could be interference with the role of the Malpighian tubule in detoxification, rather than in fluid homeostasis, that affects starvation tolerance when *LKR* is knocked down in the tubules. Moreover, the *LKR* gene has seven predicted binding sites for transcription factors (Radford et al 2002), thereby providing several possible sites that could be used to modify gene expression during stress exposure.

The data presented in this chapter support the previously reported findings that LKR is colocalised to the DH_{44} neurons (Cabrero et al 2002), by indicating that LKR is certainly present on the DH_{44} neurons, as ablation of the DH_{44} neurons abolished LKR signal in the pars intercerebralis (section 4.3.2). Likewise, the

RNAi manipulation of *LKR* in the Malpighian tubules has provided additional support for previous findings of LKR function in tubule stellate cells (Halberg et al 2015, Radford et al 2002) as knockdown of LKR in the stellate cells alone decreased *LKR* mRNA levels in the tubules by 91% and additionally affected the ability of the tissue to respond to synthetic LK peptide.

The opposing effects on desiccation tolerance observed when knocking down *LKR* or *DH_{44}* in the DH_{44} neurons suggests that the LKR acts in these neurons to affect the same signalling pathways as DH_{44} during desiccation. Moreover, the finding that ablating the neurons altogether has the same effect as knocking down *DH_{44}* suggests that LKR plays a role upstream of DH_{44} signalling. Because of the opposing nature of the effects observed, it also seems that LKR in the DH_{44} neurons acts in opposition to DH_{44} signalling. It seems possible that activating LKR in the DH_{44} neurons could potentially inhibit DH_{44} signalling, perhaps by suppressing DH_{44} synthesis, neuron firing or release of DH_{44} peptide.

If LKR does act to suppress DH_{44} signalling via the DH_{44} neurons, this could provide an interface where diuretic neuropeptides LK and DH_{44} could be co-regulated. As LK acts on stellate cells and DH_{44} on principal cells in the Malpighian tubules, these peptides could together regulate fluid secretion by both key secretory cell types in the Malpighian tubules. Interactions between neuropeptides and even classical neurotransmitters in the form of modulatory circuits have been proposed to occur elsewhere in the *Drosophila* brain (Carlsson et al 2010, Taghert & Nitabach 2012). DH_{44} and LK signalling interactions are explored in the following chapter.

5 Effect of manipulation of DH_{44}-producing neurons on Malpighian tubules

Manipulation of the DH_{44} neurons, which also express LKR (Cabrero et al 2002, Radford et al 2002) affects desiccation tolerance (section 3.3.5.1), and in the case of neuronal ablation, also modifies starvation tolerance (section 3.3.5.2). Knockdown of *DH44-R2* in the principal cells of the Malpighian tubules also affects both desiccation and starvation survival (section 3.4.2.2) and *LKR* knockdown in the stellate cells of the tubules impairs starvation survival (section 4.2.1.3). Thus, manipulation of the DH_{44} neurons could potentially influence desiccation or starvation tolerance by altering the abundance or functionality of DH44-R2 or LKR in the Malpighian tubules. Potential changes in receptor levels were explored by assessing gene expression of *DH44-R2* and *LKR* in the tubules, while potential effects of DH_{44} neuron manipulation on fluid homeostasis in the Malpighian tubules were explored via secretion assay.

5.1 Manipulation of DH_{44} neurons affects *DH44-R2* gene expression levels in Malpighian tubules

The effect of DH_{44} neuron manipulation on gene expression of *DH44-R2* in the Malpighian tubules was assessed. RNA was extracted from sets of 80 pairs of tubules from DH_{44}-GAL4/UAS-*DH_{44}* RNAi flies, DH_{44}-GAL4/UAS-*reaper* flies and controls aged 5-10 days old. Samples were used to synthesise cDNA and TaqMan RT-PCR was performed using primer and probe sets detecting *DH44-R2* (spanning exons 3-4) and *alpha-tubulin 84b*, the endogenous control. Comparative C_T analysis was used to calculate a fold change for *DH44-R2* relative to controls for each of three biological repeats. The comparative C_T method is described in section 2.3.2.1, as is the rationale for selection of statistical tests used to analyse qPCR data. Relative expression of *DH44-R2* in DH_{44}-GAL4/UAS-*DH_{44}* RNAi and DH_{44}-GAL4/UAS-*reaper* tubules was compared to DH_{44}-GAL4/w^h using a one-sample two-tailed Student's *t*-test with a null hypothesis of 1 (i.e. equal level of expression) and compared to either UAS-*reaper*/w^h or UAS-*DH_{44}* RNAi/w^h using a two-tailed two-sample Student's *t*-test.

DH44-R2 transcript level in DH_{44}-GAL4/UAS-*DH_{44}* RNAi tubules was significantly higher than in both controls (Figure 5.1). Specifically, there was a significant

difference between the null hypothesis (comparison to DH_{44}-GAL4/w^h) and the relative expression level of *DH44-R2* in DH_{44}-GAL4/UAS-*DH_{44}* RNAi tubules (*M*=3.215, *SD*=0.4672), $t(2) = 4.742$, $p = 0.0417$, indicating a 222% increase in expression relative to control flies. There was also a statistically significant difference between *DH44-R2* expression in DH_{44}-GAL4/UAS-*DH_{44}* RNAi tubules and UAS-*DH_{44}* RNAi/w^h (*M*=1.307, *SD*=0.1275), $t(4) = 3.941$, $p = 0.0169$, indicating a 146% increase in expression. *DH44-R2* transcript level in DH_{44}-GAL4/UAS-*reaper* tubules did not differ significantly either from UAS-*reaper*/w^h, $t(4) = 1.442$, $p = 0.2227$, or from the null hypothesis (comparison to DH_{44}-GAL4/w^h), $t(2) = 2.277$, $p = 0.1505$.

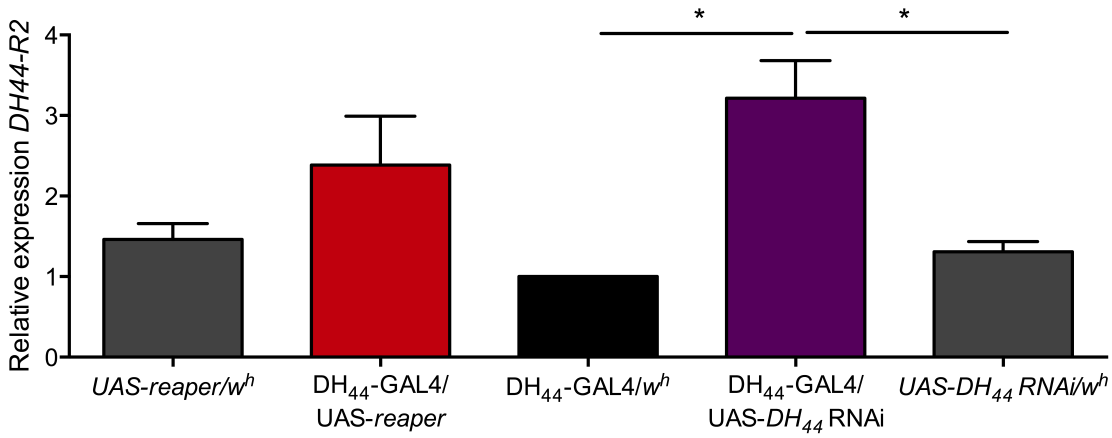

Figure 5.1 Manipulation of DH_{44} neurons affects mRNA levels of *DH44-R2* in the Malpighian tubules.

Mean ± SEM shown for three biological replicates for all genotypes. *DH44-R2* expression is significantly increased in the Malpighian tubules following expression of RNAi against *DH_{44}* in DH_{44}-producing neurons. DH_{44}-GAL4/UAS-*DH_{44}* RNAi compared to *DH_{44}*-GAL4/w^h via two-tailed one-sample Student's *t*-test with null hypothesis of 1.0 and to UAS-*DH_{44}* RNAi/w^h via two-tailed two-sample Student's *t*-test, *$p<0.05$

The increase in *DH44-R2* expression in the Malpighian tubules following *DH_{44}* knockdown in the DH_{44} neurons indicates that the tubules are affected by the neuronal manipulation. Given the finding that DH_{44} peptide staining is abolished in the pars intercerebralis of the *DH_{44}* knockdown flies, it is likely that the tubules receive lower levels of stimulation by DH_{44} than controls. The tubules may be increasing expression of *DH44-R2* to compensate for the reduced strength of the DH_{44} signal. There is a trend towards increased *DH44-R2*

expression in the DH_{44}-GAL4/UAS-*reaper* tubules as well, although this difference was not significantly different from controls. The effect of these expression changes on receptor availability could be evaluated by labelling with DH_{44}-F.

5.2 Manipulation of DH_{44} neurons affects *LKR* gene expression levels in Malpighian tubules

Gene expression changes in Malpighian tubule *LKR* were assessed following manipulation of the DH_{44} neurons. RNA was extracted from sets of 80 pairs of tubules from DH_{44}-GAL4/UAS-*DH_{44}* RNAi flies, DH_{44}-GAL4/UAS-*reaper* flies and controls aged 5-10 days old. Samples were used to synthesise cDNA and TaqMan RT-PCR was performed using primer and probe sets detecting *LKR* (spanning exons 3-4) and *alpha-tubulin 84b,* the endogenous control. Comparative C_T analysis was used to calculate a fold change for *LKR* relative to controls for each of three biological repeats, as described in section 2.3.2.1. Relative expression of *LKR* was compared across samples as described in section 5.1.

LKR transcript level in DH_{44}-GAL4/UAS-*reaper* tubules was significantly lower than in both controls (Figure 5.2). Specifically, there was a significant difference between the null hypothesis (comparison to DH_{44}-GAL4/w^h) and the relative expression of *LKR* in DH_{44}-GAL4/UAS-*reaper* tubules (M=0.4584, SD=0.0095), $t(2) = 56.89$, $p = 0.0003$, indicating a 54% decrease in expression relative to control flies. There was also a statistically significant difference between *LKR* expression in DH_{44}-GAL4/UAS-*DH_{44}* RNAi tubules and UAS-*reaper*/w^h (M=1.131, SD=0.1728), $t(4) = 3.885$, $p = 0.0178$, indicating a 59% decrease in expression. *LKR* transcript level in DH_{44}-GAL4/UAS- *DH_{44}* RNAi tubules (M=0.7914, SD=0.06727) was statistically significantly different than UAS-*DH_{44}* RNAi/ w^h (M=1.239, SD=0.1363), $t(4) = 2.943$, $p = 0.0422$, indicating a 36% decrease in expression relative to control. However, *LKR* transcript level in DH_{44}-GAL4/UAS- *DH_{44}* RNAi tubules did not differ significantly from the null hypothesis (comparison to DH_{44}-GAL4/w^h), $t(2) = 3.101$, $p = 0.0901$.

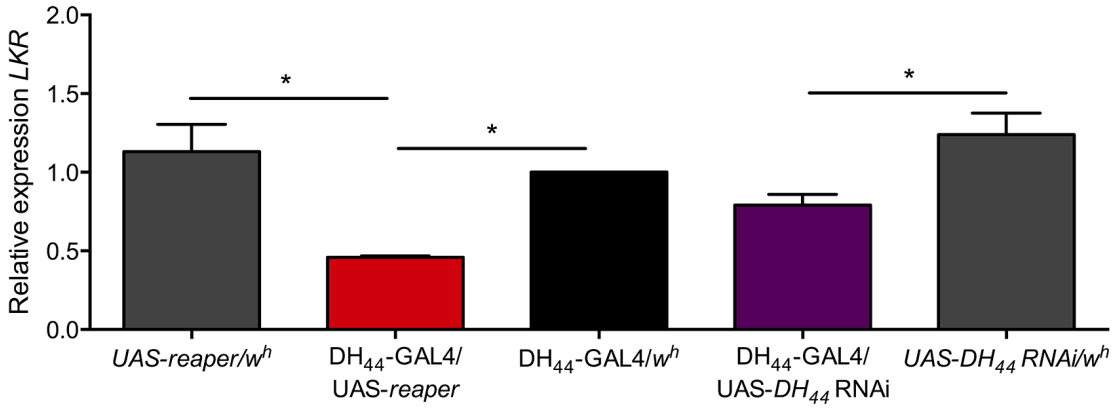

Figure 5.2 Manipulation of DH_{44} neurons affects mRNA levels of *LKR* in the Malpighian tubules.

Mean ± SEM shown for three biological replicates for all genotypes. *LKR* expression is significantly reduced in the Malpighian tubules following ablation of DH_{44} neurons or expression of RNAi against *DH_{44}* in DH_{44} neurons. DH_{44}-GAL4/UAS-*reaper* were compared to *DH_{44}*-GAL4/w^h via a two-tailed one-sample Student's *t*-test with null hypothesis of 1.0 and to UAS-*reaper*/w^h via a two-tailed two-sample Student's *t*-test. DH_{44}-GAL4/UAS-*DH_{44}* RNAi were compared to UAS-*DH_{44}* RNAi/w^h via a two-tailed two-sample Student's *t*-test, *p<0.05

The significant decreases in *LKR* expression in the Malpighian tubules following manipulation of the DH_{44} neurons indicates that the tubules are affected by the loss of these neurons. This effect is somewhat surprising as the DH_{44} neurons appear to release only DH_{44} peptide, begging the question of why *LKR* expression in the tubules might change in response to alterations in signalling by these neurons.

Increased expression of *LKR* in the tubules in response to *DH_{44}* knockdown could be consistent with a general compensatory mechanism in which diuretic peptide signalling pathways are more heavily depended upon to maintain fluid homeostasis in the absence of DH_{44} signalling. However, as DH_{44} acts on principal cells, compensatory mechanisms by stellate cells, in which *LKR* is expressed, might not be expected. In any case, compensation would be anticipated to result in increased expression of diuretic peptide receptors in the Malpighian tubules. The data presented here show the opposite effect occurring, at least in the case of LK: downregulation of LKR in the tubules. Therefore the data are not compatible with a compensation model, and suggest that another mechanism is responsible for the effect observed.

In theory, a decrease in expression of LKR by the tubules could indicate that the tubules are being exposed to a higher dose of LK peptide than controls and that the tubules are maintaining homeostasis by reducing expression of the receptor. If this is the case, then this indicates a role for the DH_{44} neurons in regulation of LK release. The more subtle decrease in *LKR* expression in the tubules after knockdown of *DH_{44}* in the DH_{44} neurons suggests that DH_{44} signalling itself may be involved in regulating LK neurons, although the observed decrease in expression was only statistically significant relative to one of the controls. The presence of LKR on the DH_{44} neurons could signify the presence of a regulatory feedback loop controlling LK levels.

Interestingly, this is not the only instance in which LK and DH_{44} signalling via the DH_{44} neurons were found to have opposite effects. In section 3.3.5.1, it was shown that knockdown of *DH_{44}* in the DH_{44} neurons improves desiccation tolerance, while knockdown of *LKR* in the DH_{44} neurons resulted in impaired desiccation survival (section 4.3.3). The first set of experiments suggests that LKR activation may act to inhibit signalling by the DH_{44} neurons, while these data could indicate that reduced DH_{44} release by the DH_{44} neurons is interpreted by the Malpighian tubules as an increase in LK signalling.

5.3 RNAi knockdown of *DH_{44}* in DH_{44}-producing neurons does not affect fluid homeostasis in Malpighian tubules

Malpighian tubules were excised from flies in which *DH_{44}* expression was knocked down via RNAi in the DH_{44} neurons and from UAS-*DH_{44}* RNAi/w^h flies. These were used to perform a fluid secretion assay, as described in section 2.9. Data were analysed statistically as described in section 2.9.1, where the rationale for test selection is also detailed.

Three biological repeats of the assay were performed. The data from these were pooled together and are shown in Figure 5.3A. Two-sample two-tailed Student's *t*-tests were performed on the measurements of secretion rate for each 10 minute time interval to compare the values acquired from DH_{44}-GAL4/UAS-*DH_{44}* RNAi flies to UAS-*DH_{44}* RNAi/w^h flies. No significant differences were noted at any time point between the groups ($p > 0.05$, see Table 5.1 for details).

Malpighian tubule response to 10^{-7} M DH_{44} stimulation was also compared by calculating a percentage change in secretion rate, as shown in Figure 5.3B. A two-sample two-tailed Student's *t*-test did not indicate any significant difference between the groups, $t(35) = 0.6967$, $p = 0.4906$.

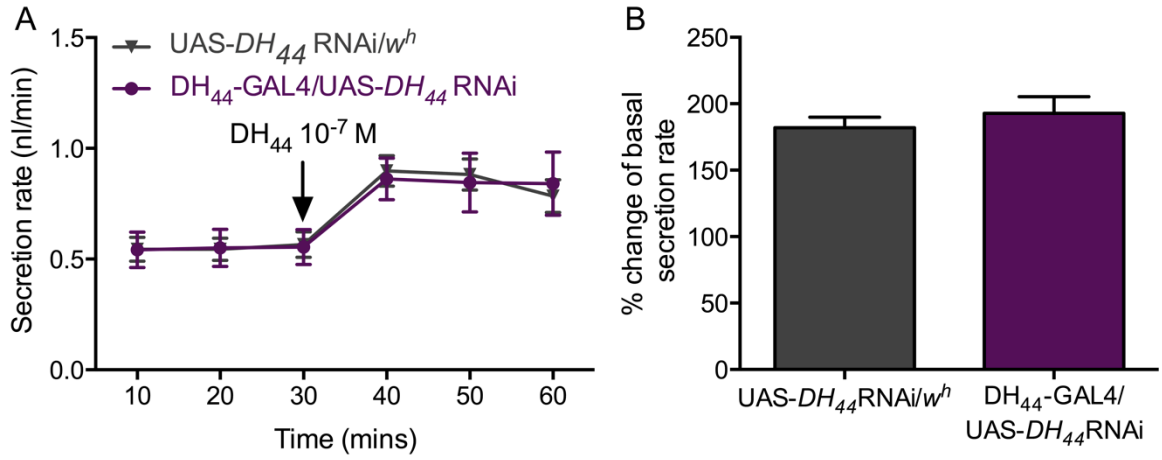

Figure 5.3 Malpighian tubules of flies with *DH44* knockdown in the DH_{44}-producing neurons show a similar secretion rate to control cross progeny, both at a basal level and after stimulation with 10^{-7} M DH_{44} peptide.

A) Basal secretion rate and secretion rate of excised Malpighian tubules after application of 10^{-7} M DH_{44} peptide is similar in DH_{44}-GAL4/UAS-*DH44* RNAi flies (*N*=20) and in control (*N*=17). Application timepoint of DH_{44} peptide is indicated by the arrow, mean ± SEM; data are pooled across 3 biological repeats. **B)** Secretion rate of excised Malpighian tubules increases to a similar extent following stimulation with 10^{-7} M DH_{44} in both the control group and in flies with RNAi knockdown of *DH44* in the DH_{44} neurons.

Table 5.1 Two-sample two-tailed Student's *t*-test analysis comparing basal and DH_{44}-stimulated secretion rates by Malpighian tubules of flies with DH_{44} knockdown in DH_{44} neurons (*N=20*) to secretion rates by Malpighian tubules of control flies (*N*=17).

	Baseline secretion			Stimulated secretion		
Time (mins)	0-10	10-20	20-30	30-40	40-50	50-60
t	0.0257	0.0631	0.1185	0.3068	0.2277	0.3404
df	35	35	35	35	35	35
p	0.9797	0.9501	0.9063	0.7608	0.8212	0.7356

Malpighian tubules of DH_{44}-GAL4/ UAS-*DH44* RNAi flies secrete similarly to controls in terms of basal secretion, and respond similarly to stimulation with DH_{44} peptide. The absence of a secretion phenotype might be considered surprising given the finding that *DH44-R2* expression in the tubules is more than doubled in DH_{44} knockdown flies when compared to controls. However,

consistent with these results, overexpression of *capaR,* the receptor for another diuretic neuropeptide, was not found to affect fluid secretion basal rates or response to peptide (Terhzaz et al 2012). This receptor is found in the same cell type as DH44-R2 in the tubules, although downstream signalling mechanisms differ (section 1.2.1.1). Specifically, while the capa peptide family alters fluid secretion in the tubules through cGMP and Ca^{2+} signalling, DH_{44} signals via cAMP (Cabrero et al 2002, Davies et al 2013, Davies et al 1995). Therefore, it may be that the presence and activation of more receptor does not affect downstream signalling in the principal cells to an extent that could alter the secretion response. Alternatively, the results presented might indicate that the increase in *DH44-R2* expression in DH_{44} knockdown flies does not correspond to an increase in DH44-R2 protein levels. This possibility could be investigated using DH_{44}-F labelling.

5.4 Ablation of DH_{44}-producing neurons does not affect fluid homeostasis in Malpighian tubules

Malpighian tubules were excised from flies in which the DH_{44} neurons were ablated using UAS-*reaper* and used to perform a fluid secretion assay with UAS-*reaper*/w^h used as a control. The assay was performed as in section 2.9. Data were analysed statistically as described in section 2.9.1, where the rationale for test selection is also detailed.

Three biological repeats of the assay were performed. The data from these were pooled together and are shown in Figure 5.4A. Two-sample two-tailed Student's *t*-tests were performed on the measurements of secretion rate for each 10 minute time interval to compare the values acquired from DH_{44}-GAL4/UAS-*DH_{44}* RNAi flies to control flies. No significant differences were noted at any time point between the groups ($p > 0.05$, see Table 5.2 for details). Malpighian tubule response to 10^{-7} M DH_{44} stimulation was also compared by calculating a percentage change in secretion rate, as shown in Figure 5.4B. A two-sample two-tailed Student's *t*-test did not indicate any significant difference between the groups, $t(25) = 0.1719$, $p = 0.8649$.

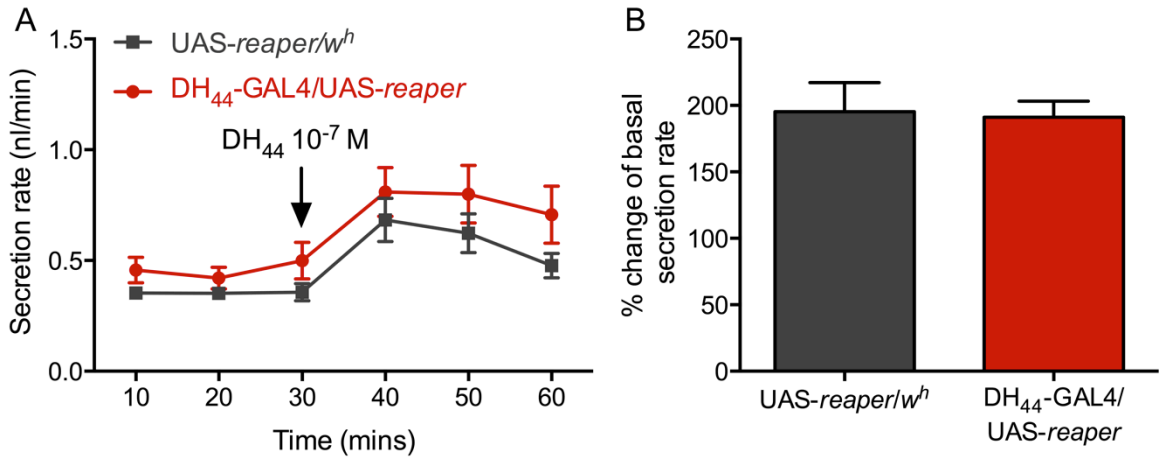

Figure 5.4 Ablation of DH_{44} neurons does not affect the basal secretion rate of Malpighian tubules or the ability of the tubules to respond to DH_{44} peptide.
A) Baseline secretion rate and secretion rate following stimulation with 10^{-7} M DH_{44} peptide are similar in flies with ablated DH_{44} neurons (*N*=15) and in UAS-*reaper*/w^h (*N*=12), mean ± SEM; data were pooled across 3 biological repeats. **B)** Ablation of DH_{44} neurons does not influence the percentage change in secretion rate following stimulation with DH_{44} peptide.

Table 5.2 Two-sample two-tailed Student's *t*-test analysis comparing basal and DH_{44} - stimulated secretion rates by Malpighian tubules of flies with DH_{44} neuron ablation (*N*=15) to secretion rates by Malpighian tubules of control flies (*N*=12).

	Baseline secretion			Stimulated secretion		
Time (mins)	0-10	10-20	20-30	30-40	40-50	50-60
t	1.557	1.218	1.478	0.8718	1.101	1.551
df	25	25	25	25	25	25
p	0.1320	0.2345	0.1520	0.3916	0.2813	0.1334

Malpighian tubules of DH_{44}-GAL4/UAS-*DH_{44}* RNAi flies secrete similarly to controls in terms of basal secretion and respond similarly to stimulation with DH_{44} peptide. These data are consistent with those discussed in section 5.3 and are not surprising given the finding that *DH44-R2* expression is only moderately increased in the tubules following ablation of DH_{44} neurons (section 5.1).

5.5 Discussion

The experiments detailed in this chapter were carried out to investigate the interactions between the DH_{44} neurons and the DH44-R2 and LKR in the Malpighian tubules. The purpose was to explore whether these interactions exist and to investigate whether they have any functional consequences. Overall, the

results support the idea that signalling by the DH_{44} neurons affects the Malpighian tubules, as expression levels of *DH44-R2* and *LKR* are altered by manipulation of the DH_{44} neurons. Specifically, knockdown of DH_{44} appears to have a direct effect on the tubules such that *DH44-R2* expression is increased. Conversely, *LKR* expression is decreased in the tubules following DH_{44} knockdown, an effect which is not clearly explainable at present, but which is likely related to the presence of LKR in the DH_{44} neurons and which suggests an indirect effect on LK signalling to the tubules via these neurons. The results could be taken to indicate that DH_{44} release normally has an inhibitory effect on LK signalling. Functionally, the changes in receptor levels were not found to alter basal fluid secretion rates by the tubules, and the increase in DH44-R2 expression did not translate into any changes in the tubule secretion response to DH_{44} peptide.

The evidence presented in this chapter complements previous experiments in which knockdowns of *LKR* and *DH_{44}* in the DH_{44} neurons were found to have opposite effects on desiccation tolerance (sections 3.3.5.1 and 4.3.3). From those results, it was suggested that activation of LKR in the DH_{44} neurons may inhibit DH_{44} release. Here, the results suggest that DH_{44} signalling may inhibit LK release. If this is indeed the case, then the interaction between the signalling pathways of these two diuretic neuropeptides could serve to enable coordinated regulation of peptide levels for both peptides. This kind of co-regulation might be particularly useful as LK and DH_{44} act to increase secretion rate via different cell types, thus potentially enabling coordination of a whole-tissue secretory response. Both LK and DH_{44} signalling are involved in feeding behaviour, with DH_{44} signalling being stimulated by nutrient detection and LK signalling in the brain being required for normal meal termination (Al-Anzi et al 2010, Dus et al 2015). Interaction between the two might underlie the timing of the tubule response to a meal.

The results presented in this chapter must also be considered in light of the desiccation phenotypes observed following manipulation of the DH_{44} neurons. Are these genuine results, or are the phenotypes observed due to compensatory changes in receptor level in the Malpighian tubules? In sections 3.3.5.1 and 4.3.3, it was found that manipulation of the DH_{44} neurons, either via knockdown of *DH_{44}* or ablation of the neurons, resulted in improved desiccation survival. The

trend toward increased expression of *DH44-R2* in the Malpighian tubules of these flies found in section 5.1 is unlikely to underlie this phenotype as lower levels of *DH44-R2* in the Malpighian tubules were found to improve desiccation tolerance (section 3.4.2.2). Similarly, the decreased expression of *LKR* observed in the flies with DH_{44} neuron manipulations detailed in section 5.2 does not explain the phenotype as knockdown of *LKR* in the tubules was not found to affect desiccation survival (section 4.2.1.3).

Ablation of DH_{44} neurons was found in section 3.3.5.2 to result in improved survival during starvation, a finding that contrasts with a significant impairment in starvation tolerance following knockdown of *LKR* in the Malpighian tubules (section 4.2.1.3). Based on the latter, the significant decrease in *LKR* expression in tubules following DH_{44} neuron ablation could be expected to result in impaired starvation survival. As the opposite effect was observed, it is evident that the starvation phenotype cannot be explained by compensatory changes in Malpighian tubule *LKR* levels. Conversely, it is possible that the compensatory trend toward increased *DH44-R2* levels might affect the starvation phenotype as *DH44-R2* knockdown in the tubules was found to impair starvation tolerance. This could be explored by assessing the effect of *DH44-R2* overexpression in the Malpighian tubules on starvation tolerance. However, if this were true, then it would be expected that flies with DH_{44} knockdown in the DH_{44} neurons would also have improved starvation survival, which was not the case (section 3.3.5.1).

Thus, overall, these results serve to improve confidence in the survival phenotypes reported elsewhere as in most cases, compensatory changes in the Malpighian tubule receptor expression are inconsistent with the direction of the phenotype observed. Moreover, the results support the existence of interaction between the LK and DH_{44} signalling pathways, although the details of this interaction remain to be explored.

6 Desiccation, starvation, and the metabolic pathways of *Drosophila*

Desiccation stress and starvation stress have both been found to affect the levels of carbohydrates, lipids, and proteins in multiple *Drosophila* species (Marron et al 2003). Changes in affected proteins are not limited only to protein levels, but also protein structure, as desiccation stress has been associated with aggregation and denaturation of proteins (Prestrelski et al 1993). This might be partly due to shortages of water for hydrogen-bonding, leading proteins to form hydrogen bonds with other molecules (Hayward et al 2004). Lipid changes include dehydration causing membrane phospholipids to lose association with water, triggering changes in membrane fluidity (Crowe et al 1992).

The metabolic effect of stress exposure on insects has recently been explored using metabolomics. This has revealed numerous changes in the metabolic content of insects in response to stress (Laye et al 2015, Mamai et al 2014, Michaud et al 2008, Price et al 2015). This approach offers two advantages over assays measuring either levels of individual compounds or overall levels of categories of metabolites: many metabolites can be measured using the same set of samples, and specific metabolites can be identified with a fair degree of confidence. Thus, it is possible to obtain a 'snapshot' of the metabolic status of an insect (Snart et al 2015).

Changes in the metabolite profile of insects following desiccation have been explored in the Antarctic midge, *Belgica antarctica*, where desiccation exposure was found to alter levels of numerous metabolites (Michaud et al 2008, Teets et al 2012). Metabolic changes were also observed in *Anopheles gambiae* after exposure to dry season conditions (Mamai et al 2014). The effect of starvation stress on the metabolome does not seem to have been specifically examined in insects, although long term dietary restriction of *D. melanogaster* and larval crowding resulting in nutritional deprivation in *Aedes aegypti* have both been found to affect metabolic profile (Laye et al 2015, Price et al 2015).

As desiccation stress was previously found to alter metabolism in *D. melanogaster*, an untargeted metabolomics approach was applied to whole organism samples to investigate the nature of some of these changes (section

6.1). As noted in section 2.8.2.1 and discussed in section 6.1.3, the desiccation exposure method used in this study inherently involves starvation exposure. Consequently, the effects on metabolite levels presented in section 6.1 could potentially be explained rather by lack of food than by lack of water. The metabolic profile of Malpighian tubules following desiccation was additionally explored (section 6.2) because individual *D. melanogaster* tissues differ significantly in their metabolic profiles (Chintapalli et al 2013a) and the tubules are a critical tissue for the maintenance of homeostasis and stress survival (Davies et al 2014, Davies et al 2012). This experiment included tubules of starved flies as a control and the results following desiccation and starvation are compared to draw out any effects potentially caused by lack of food rather than by lack of water. Both experiments should be considered exploratory in nature and were carried out with the intention of gaining an overall picture of the metabolic changes induced by desiccation. The metabolomics methods used for both experiments are detailed in section 2.11.

6.1 Metabolomics of desiccation stress in the whole fly

Sets of 30 male wild-type CS *Drosophila melanogaster* were placed either in empty vials for 24-26 hours to induce desiccation stress or in regular vials containing food for the same amount of time. Following stress exposure, metabolites were extracted from flies as described in section 2.11.1. This was repeated using food samples, as an additional control. As a starvation control was not included in this experiment, it is not possible to fully distinguish between metabolic changes due only to lack of water rather than due also to the starvation aspects inherent in the desiccation procedure (see section 2.8.2.1). The inclusion of food as a control, however, was useful in this initial experiment as a proof-of-principal for the technique and can be used to some extent to differentiate food-related metabolites, as discussed in section 6.1.3.

Five biological replicates for each sample type were resolved alongside standards and quality control samples using hydrophilic interaction liquid chromatography-mass spectrometry analysis, as detailed in section 2.11.2. The quality control samples which were run alongside the experimental samples yielded consistent results, indicating that the instruments were operating appropriately. The intensity values achieved from the samples were high in both

conditions and in the food samples and consistent across replicates; total ion current for each sample type during positive polarity detection is shown in Figure 6.1. Very little was detected in the blank sample, as expected.

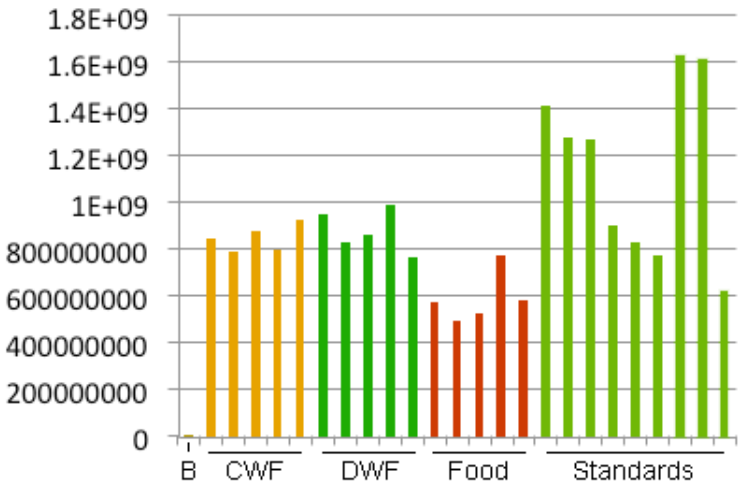

Figure 6.1 Positive ionisation total ion current for metabolomics of whole *D. melanogaster* and *Drosophila* standard diet

Five biological samples of desiccated flies, control (unstressed flies), and *Drosophila* food were resolved using hydrophilic interaction liquid chromatography-mass spectrometry analysis. Total ion current is consistent within sample types, and low in the blank. Units shown are arbitrary 'relative abundance' values. Abbreviations: B = blank, CWF = control whole flies, DWF = desiccated whole flies.

Over 750 features (peaks) were identified in the sample sets, as exemplified by selected peaks shown in Figure 6.2. After filtering, 153 polar metabolites were putatively identified. Exact mass was used as the primary identifier and a cut off of 1.5 ppm deviation from the predicted formula mass was set (Chintapalli et al 2013a). This stringent criteria for mass specificity excludes isobaric compounds from the possible metabolite identifications as isobaric compounds almost always differ in mass by at least 5 ppm (Watson 2013). Comparison of actual retention time relative to estimated retention time of compounds was used to predict the most likely metabolite, which is considered in this analysis as a 'putative identification'. Identification confidence was categorised into two ranks, as detailed in section 2.11.4.

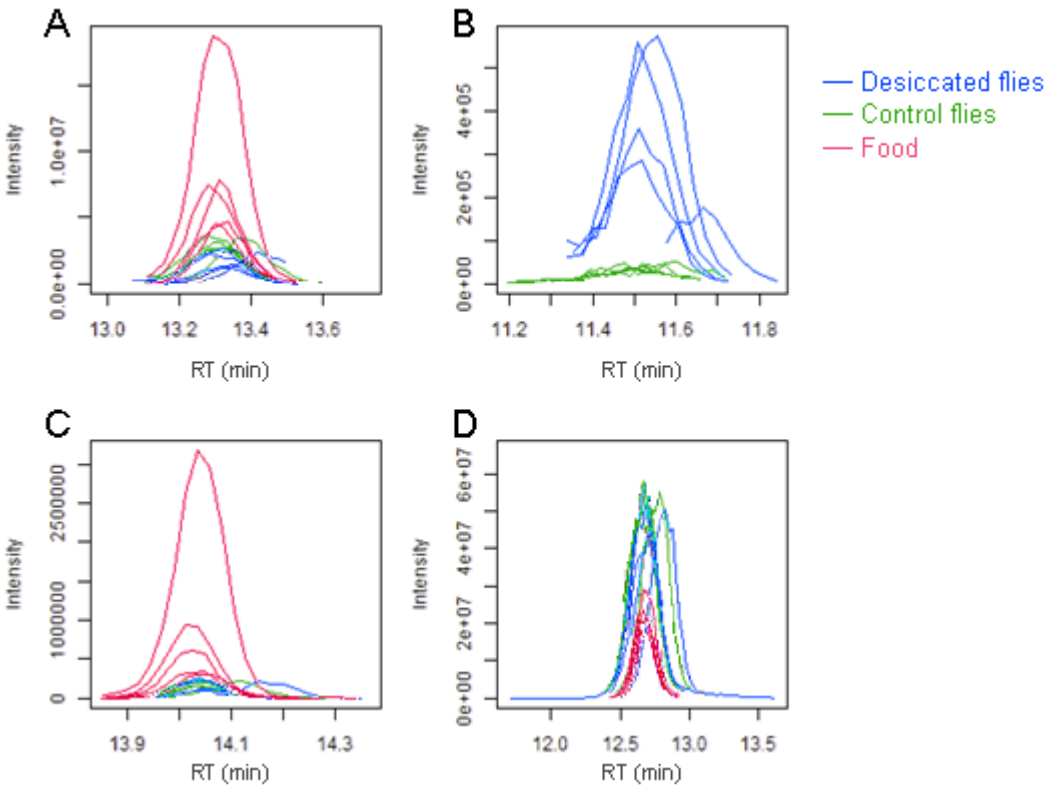

Figure 6.2 Relative abundance peaks for metabolites resolved using LC-MS
Chromatograms for individual metabolites showing relative signal intensity as detected by the Orbitrap Exactive for five replicates of three different sample types against retention time (RT) in minutes on the ZIC-HILIC column. **A)** L-Glutamate has a high relative abundance in food and is clearly detected in whole fly samples. **B)** 5,6-Dihydrouracil is detected primarily in desiccated flies, with some minimal abundance detected in control flies and no detection in food. **C)** L-Asparagine is relatively abundant in food and is also detected in flies. **D)** L-Proline is similarly abundant in desiccated and control flies, while relatively lower in abundance in food.

Among the putatively identified metabolites, only those that were detected in at least three out of five biological replicates in at least one of the sample sets (control whole fly, desiccated whole fly, or food) were retained for further analysis. Following the screening process, 153 metabolites remained. A principal component analysis was performed on these metabolites to determine whether samples clustered according to type (Laye et al 2015, Michaud et al 2008). Lack of clustering would suggest that sample types do not differ in a systematic or significant way, while clustering of fly metabolic samples by sample collection date, for example, could indicate that conditions on the day of sampling influence metabolism more significantly than the stressor applied. As shown in Figure 6.3, samples clearly clustered into three categories, indicating that there are distinct features of each category of sample. In particular, the main

principal component, which accounts for 54.2% of variability observed across the samples, serves to separate the two sets of fly samples from food samples. This indicates that the metabolic profiles of flies differ substantially from that of their food, which is not at all surprising. The second principal component accounts for a smaller proportion of the variability, 14.8%, and separates the control fly samples from the desiccated fly samples. As these samples cluster independently without any overlap, it is clear that they differ substantially in their metabolic profiles, although the small proportion of variance accounted for by this separation indicates that they do not differ as strongly from one another as flies differ from food. It is also interesting to note that the control fly samples cluster more tightly than the desiccated fly samples, showing that variability in the latter set of samples is greater.

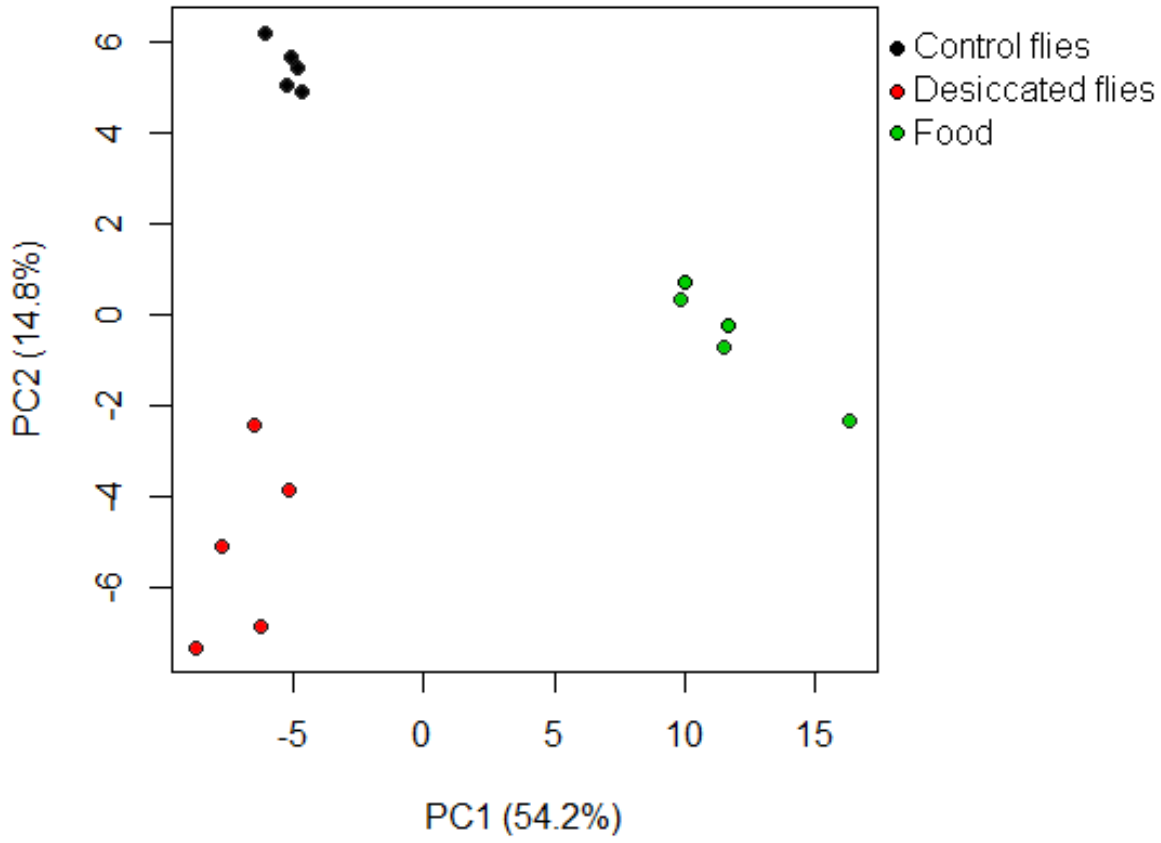

Figure 6.3 Principal component analysis of metabolite profile of control and desiccated *D. melanogaster* and *Drosophila* standard medium

Sample types cluster distinctly when plotted against the first and second principal components. Each point indicates an individual biological replicate. Abbreviations: PC1 = Principal component 1, PC2 = principal component 2

As the principal component analysis indicated that there are substantial differences between sample types which outweigh variability within sample sets, the metabolic dataset was further analysed to determine the identity of the metabolites that differ most significantly between sample groups. The specific nature of the systematic metabolite differences between desiccated and control flies is explored in the following section, 6.1.1, while metabolite features distinguishing control flies from *Drosophila* diet are described in 6.1.2. In both cases, a statistical method is applied based on two-tailed two-sample Student's *t*-tests and controlling for errors of multiple testing by applying a False Discovery Rate using the Benjamini and Hochberg method (Benjamini & Hochberg 1995, Morrow et al 2013, Nkuipou-Kenfack et al 2014). The statistical approach used is further detailed and explained in section 2.11.5, while the justification for using the applied approach is discussed in section 1.5.6.

6.1.1 Effect of desiccation on the whole fly metabolome

As indicated by the principal component analysis (Figure 6.3), desiccated flies differ substantially in their metabolic profile from unstressed control flies. However, it should be noted that some of these differences may be due to the starvation aspects inherent in the procedure used to desiccate the flies (see sections 2.8.2.1 and 6.1.3). A statistical approach was applied to identify the most robust metabolic changes incurred by desiccation exposure. The method used takes into account within-group variability and compares it to between-group variability, meaning that although it might exclude large differences if they are highly variable, it will select those that are most reliable. Metabolites selected by this method are then considered in terms of their fold change following desiccation. A further set of metabolites is considered in this section that cannot be compared statistically due to infrequent detection in either desiccated or control fly samples. These comparisons are not excluded from analysis as they can represent some of the greatest changes in metabolite abundance.

Relative abundance of metabolites in the whole fly following 24 hours of desiccation or in unstressed controls was compared using individual two-tailed two-sample Student's *t*-tests (i.e. without assumption of consistent standard deviation across metabolites). Only metabolites that were detected in at least

three out of five biological samples in both the stressed and unstressed conditions were evaluated in this way. After applying all selection criteria, 123 metabolite abundances were compared. Statistical results were filtered by setting the False Discovery Rate at 5% using the Benjamini and Hochberg method (Benjamini & Hochberg 1995, Morrow et al 2013, Nkuipou-Kenfack et al 2014). This could be considered a permissive level of false positives, but the goal of this experiment is to gain an idea of the overall fingerprint of metabolic changes during desiccation stress in *Drosophila*, so it is advantageous to include more true differences at the expense of a few false ones rather than to exclude a large proportion of potentially interesting changes in order to reduce the possibility of false positives to a very low level.

Using the statistical methods outlined above, 38 metabolites were found to differ in abundance between desiccated and unstressed whole fly metabolite samples, as detailed in Table 6.1. Raw *p* values are shown (i.e. without adjustment), with the cut-off determined by the Benjamini-Hochberg procedure. With a False Discovery Rate of 5%, it can be estimated that approximately 2 of these results are expected to be due to random scatter of data.

Table 6.1 Relative abundance of metabolites in desiccated and unstressed whole fly compared using two-tailed two-sample Student's *t*-tests, with False Discovery Rate set at 5% using the Benjamini and Hochberg method.

Degrees of freedom for statistical testing of all discoveries is 8.

Putative metabolite	Control WF mean	Desiccated WF mean	Difference	SE of difference	t ratio	P value
Betaine	48776120	9717035	39059080	1999840	19.5	<0.0001
2-Phenyl-acetamide	387494	1846859	1459365	170053	8.58	<0.0001
O-Acetylcarnitine	25950700	72434880	46484180	5739185	8.10	<0.0001
Adenosine	769012	2713816	1944804	255746	7.60	<0.0001
sn-glycero-3-Phosphocholine	5874373	10538310	4663933	621464	7.50	<0.0001
5-Hydroxy-indoleacetate	1305405	2431307	1125901	152368	7.39	<0.0001
Imidazole-4-acetate	85940	581949	496009	82291	6.03	0.0003
5-Oxoproline	148096	1118717	970621	161520	6.01	0.0003
Hydroxymethyl-phosphonate	5735	24858	19123	3201	5.97	0.0003

4-Guanidino-butanoate	181809	66122	115687	19678	5.88	0.0004
L-Pipecolate	324586	94123	230463	40033	5.76	0.0004
O-Acetyl-L-homoserine	28051	156818	128768	22484	5.73	0.0004
L-Carnitine	108982600	88388600	20593960	3865595	5.33	0.0007
Imidazole-4-acetaldehyde	15450	27421	11972	2302	5.20	0.0008
L-Tyrosine methyl ester	6935019	1597940	5337078	1042459	5.12	0.0009
L-Leucine	898288	2364706	1466418	290821	5.04	0.0010
L-Tyrosine	342523	147867	194656	39894	4.88	0.0012
N-Acetylglutamine	42063	185290	143228	32136	4.46	0.0021
5,6-Dihydrouracil	46392	391715	345323	77731	4.44	0.0022
4-Methylene-L-glutamine	71511	212071	140561	31810	4.42	0.0022
4-Trimethyl-ammoniobutanoate	228409	129616	98793	23079	4.28	0.0027
Glutathione	3238472	1383376	1855096	449981	4.12	0.0033
3-Butynoate	1702516	3428942	1726427	422882	4.08	0.0035
D-Alanine	16074	142373	126300	31652	3.99	0.0040
L-Aspartate	158876	97006	61870	15829	3.91	0.0045
Phenyl-acetaldehyde	14429	65249	50820	13024	3.90	0.0045
Dopamine	1429761	450068	979693	257572	3.80	0.0052
4-(beta-Acetylamino-ethyl)imidazole	55532450	47554770	7977679	2100442	3.80	0.0053
Homoarginine	12938	4906	8032	2158	3.72	0.0059
(S)-1-Pyrroline-5-carboxylate	269032	130730	138302	37734	3.67	0.0064
L-Glutamate	3153347	1999391	1153956	322355	3.58	0.0072
L-Threonine	354349	651861	297512	83216	3.58	0.0072
3-Butyn-1-ol	6256	3046	3210	905	3.55	0.0075
4-Hydroxyphenyl-acetaldehyde	141000	93353	47646	13458	3.54	0.0076
Acetylcholine	584684	21289	563394	161465	3.49	0.0082
N6-Acetyl-L-lysine	22707	60529	37822	10898	3.47	0.0084
Adenosine 2',5'-bisphosphate	249888	97337	152551	46348	3.29	0.0110
N6,N6,N6-Trimethyl-L-lysine	67618	31157	36461	11467	3.18	0.0130

A fold change was calculated for individual metabolites by dividing mean relative abundance in stressed flies by mean metabolite relative abundance in unstressed flies, to determine which were most depleted or most enriched following 24 hours of desiccation. Metabolites were evenly split into the two categories, with 19 metabolites being enriched following desiccation and 19 metabolites being depleted. These are displayed in Table 6.2 and Table 6.3, respectively. Pathway involvement information is listed in the tables and was acquired from Kyoto Encyclopedia of Genes and Genomes (Kanehisa et al 2014). The number of alternative isomers for individual masses is additionally indicated in metabolite tables, as identified by IDEOM software (Creek et al 2012). Confidence in the metabolite identification was ranked as described in section 2.11.4, and is indicated in the tables.

Table 6.2 Metabolites enriched in *D. melanogaster* following 24 hours of desiccation stress. Exact mass and retention time (RT) listed with the name of the most likely isomer. Fold change indicates abundance in desiccated flies relative to unstressed flies.

Mass	RT	Name	Rank	Isomers	Fold change	Pathway
89.0477	11.4	D-Alanine	2	8	8.86	Amino acid metabolism
114.0430	11.5	5,6-Dihydrouracil	2	7	8.44	Nucleotide metabolism
129.0427	10.3	5-Oxoproline	1	5	7.55	Amino acid metabolism
126.0429	11.3	Imidazole-4-acetate	1	1	6.77	Amino acid metabolism
161.0687	11.3	O-Acetyl-L-homoserine	1	9	5.59	Amino acid metabolism
135.0684	7.5	2-Phenylacetamide	2	3	4.77	Amino acid metabolism
120.0575	5.6	Phenylacetaldehyde	2	7	4.52	Amino acid metabolism
188.0797	10.6	N-Acetylglutamine	1	1	4.41	Unassigned
111.9925	10.8	Hydroxymethyl-phosphonate	2	1	4.33	Amino acid metabolism
267.0967	9.7	Adenosine	1	2	3.53	Nucleotide metabolism
158.0691	14.5	4-Methylene-L-glutamine	2	1	2.97	Carbohydrate metabolism
203.1158	11.4	O-Acetylcarnitine	1	0	2.79	Amino acid metabolism
188.1161	14.0	N6-Acetyl-L-lysine	2	6	2.67	Amino acid metabolism

131.0947	11.4	L-Leucine	1	11	2.63	Amino acid metabolism
84.0211	11.6	3-Butynoate	2	1	2.01	Carbohydrate metabolism
191.0582	11.2	5-Hydroxyindoleacetate	2	4	1.86	Amino acid metabolism
119.0583	13.6	L-Threonine	1	10	1.84	Amino acid metabolism
257.1028	13.6	sn-glycero-3-Phosphocholine	1	0	1.79	Lipid metabolism
110.0481	10.8	Imidazole-4-acetaldehyde	2	1	1.77	Amino acid metabolism

Table 6.3 Metabolites depleted in *D. melanogaster* following 24 hours of desiccation stress
Exact mass and retention time (RT) listed with the name of the most likely isomer. Fold change indicates abundance in desiccated flies relative to unstressed flies.

Mass	RT	Name	Rank	Isomers	Fold change	Pathway
145.1103	15.9	Acetylcholine	1	5	0.04	Lipid metabolism
117.0790	11.6	Betaine	1	15	0.20	Amino acid metabolism
195.0896	7.4	L-Tyrosine methyl ester	2	5	0.23	Amino acid metabolism
129.0790	12.4	L-Pipecolate	2	8	0.29	Amino acid metabolism
153.0790	7.5	Dopamine	1	4	0.31	Amino acid metabolism
145.0851	14.3	4-Guanidinobutanoate	2	2	0.36	Amino acid metabolism
188.1273	20.6	Homoarginine	2	4	0.38	Amino acid metabolism
427.0295	13.8	Adenosine 2',5'-bisphosphate	1	5	0.39	Nucleotide metabolism
307.0838	13.1	Glutathione	1	2	0.43	Amino acid metabolism
181.0740	12.8	L-Tyrosine	1	10	0.43	Amino acid metabolism
188.1525	19.1	N6,N6,N6-Trimethyl-L-lysine	2	1	0.46	Amino acid metabolism
113.0477	9.8	(S)-1-Pyrroline-5-carboxylate	2	5	0.49	Amino acid metabolism
70.0420	14.3	3-Butyn-1-ol	2	2	0.49	Carbohydrate metabolism
145.1103	13.0	4-Trimethylammonio-butanoate	1	5	0.57	Amino acid metabolism

133.0375	13.5	L-Aspartate	1	3	0.61	Amino acid metabolism
147.0531	13.4	L-Glutamate	2	13	0.63	Amino acid metabolism
136.0525	9.3	4-Hydroxyphenyl-acetaldehyde	2	15	0.66	Amino acid metabolism
161.1052	13.0	L-Carnitine	1	1	0.81	Amino acid metabolism
153.0902	7.8	4-(beta-Acetylamino-ethyl)imidazole	1	2	0.86	Amino acid metabolism

Twelve metabolites could not be included in the statistical analysis as they were not detected in at least three of the five biological replicates for both stressed and unstressed fly samples, as listed in Table 6.4. Including these samples would be unlikely to identify even large differences as the statistical power of the analysis would be very low. However, some of these differences, particularly where a metabolite is detected in all five biological replicates from one condition and in few or none of the replicates from the other, can represent some of the greatest changes in metabolite level and thusly, should not be excluded from consideration.

Table 6.4 Metabolites detected reliably only in desiccated or control *D. melanogaster*

Mean relative abundance of putative metabolites in control and desiccated samples. SEM was calculated where possible (i.e. at least two detection values). Number of detections out of sets of five biological replicates are indicated for both control and desiccated sample sets.

Putative metabolite	Control mean ± SEM	Desiccated mean ± SEM	Detections	
			Control	Desiccated
D-Alanyl-D-alanine	20257 ± 2167		3	0
D-Galactosamine	18417 ± 7955		3	0
L-Arginine phosphate	63551 ± 13260	4593 ± 2398	5	2
6-Amino-2-oxohexanoate	21445	9862	5	2
trans-Cinnamate	1232 ± 63	1339 ± 336	4	2
5-Aminopentanamide	2048 ± 243	2533 ± 21	4	2
L-Lysine 1,6-lactam	4864	16956 ± 6122	1	3
L-Lysine	123141 ± 30859	329227 ± 50569	2	3
8-Methoxykynurenate	4646	11661 ± 1519	1	5
D-Serine		8336 ± 581	0	5
5-Aminoimidazole	23350	1336239 ± 337216	1	5
6-Acetamido-2-oxohexanoate	8942	100792 ± 26883	1	5

For nine of the twelve metabolites, a fold change was calculated using the mean relative abundance from samples in which the metabolite was detected. However, two metabolites were not detected in desiccated flies despite being reliably detected in control samples. In these cases, it was assumed that the metabolite abundance was below the threshold of detection in the desiccated fly samples, and failure to detect the metabolite was taken as an indication that these samples contained lower levels of the metabolite than in the control samples. Due to the lack of information regarding relative abundance and the difficulty of estimating the threshold of detection for individual metabolites, these data cannot be used to calculate a fold change, but can only be used to give an indication of an increase or a decrease in metabolite levels.

Among the six metabolites detected reliably only in desiccated *D. melanogaster*, all were found to increase in abundance following desiccation (Table 6.5). Of the six metabolites detected reliably in unstressed flies, but not in desiccated flies, four were found to be depleted following desiccation and two were found to increase slightly in abundance (Table 6.6). Confidence in the identity of metabolites is indicated in the tables in the rank column; the ranking categories used are detailed in section 2.11.4.

Table 6.5 Relative abundance of metabolites detected reliably only following 24 hours of desiccation stress

Exact mass and retention time (RT) are listed with the name of the most likely isomer. Fold change indicates abundance in desiccated flies relative to unstressed flies. No fold change indicates that the metabolite was detected only in desiccated flies.

Mass	RT	Name	Rank	Isomers	Fold change	Pathway
105.0426	10.6	D-Serine	2	2		Amino acid metabolism
83.0484	11.4	5-Aminoimidazole	2	1	57.23	Nucleotide metabolism
145.0739	13.6	6-Acetamido-2-oxohexanoate	2	5	11.27	Amino acid metabolism
128.0950	14.1	L-Lysine 1,6-lactam	2	2	3.49	Amino acid metabolism
145.0739	13.6	L-Lysine	1	7	2.67	Amino acid metabolism
219.0533	10.6	8-Methoxykynurenate	2	1	2.51	Amino acid metabolism

Table 6.6 Relative abundance of metabolites detected reliably in unstressed flies, but not following 24 hours of desiccation stress

Exact mass and retention time (RT) are listed with the name of the most likely isomer. Fold change indicates abundance in desiccated flies relative to unstressed flies. No fold change indicates that the metabolite was detected only in unstressed flies.

Mass	RT	Name	Rank	Isomers	Fold change	Pathway
160.0848	12.7	D-Alanyl-D-alanine	2	3		Amino acid metabolism
179.0793	13.6	D-Galactosamine	2	9		Carbohydrate metabolism
254.0779	14.9	L-Arginine phosphate	2	0	0.07	Amino acid metabolism
187.0845	7.6	6-Amino-2-oxohexanoate	2	8	0.46	Amino acid metabolism
148.0525	5.0	trans-Cinnamate	2	6	1.09	Amino acid metabolism
116.0950	20.0	5-Aminopentanamide	2	1	1.24	Amino acid metabolism

6.1.1.1 Desiccation stress significantly affects multiple metabolic pathways

Multiple metabolic pathways were significantly affected by desiccation exposure, although some of the changes detailed in this section may be due to starvation exposure, as described in section 2.8.2.1 and discussed in section 6.1.3. Of the metabolites identified in desiccated or unstressed whole flies, the vast majority are components of amino acid metabolism pathways (Figure 6.4A). Metabolites were additionally identified that are components of other metabolic pathways, including nucleotide metabolism, lipid metabolism, metabolism of cofactors and vitamins, and carbohydrate metabolism. Three metabolites were identified that have not been associated with any metabolic pathways on the KEGG database, 6-methylaminopurine, N-acetylglutamine, and phenylhydrazine (Kanehisa et al 2014). Only N-acetylglutamine was found to change following desiccation. This metabolite increased in abundance; it is produced by adding an acetyl group to the amino acid glutamine. It has been found in human urine and is highly enriched in patients with the inborn error of metabolism involving aminoacylase I deficiency (Sugahara et al 1994, Van Coster et al 2005). Thus, although it has not been specifically placed in a metabolic pathway, it is likely related to amino acid metabolism.

Interestingly, 29% of the identified metabolites changed by at least 2-fold following desiccation. This suggests that overall the majority of the metabolites between fly samples is the same, even when faced with intensive stress exposure. When metabolite changes were examined in individual metabolism areas, the percentage of identified metabolites was found to increase or decrease in each metabolism area to a fairly similar extent, with the exception of nucleotide metabolism (Figure 6.4B). Three of the 16 identified components of nucleotide metabolism increased in abundance following desiccation, while only one was found to be decreased. The proportionally most changed metabolic area was carbohydrate metabolism, where 4 of the 6 identified metabolites changed. Amino acid metabolism was also strongly affected by desiccation stress, with changes in 35% of identified metabolites known to be involved in this metabolic pathway. These were fairly evenly split, although a higher number of metabolites was enriched than depleted following desiccation. There were no changes in any of the seven identified metabolites involved in the metabolism of cofactors and vitamins. Lipid metabolism was only moderately affected, with one metabolite of the eight identified increasing in abundance and one decreasing in abundance following desiccation stress.

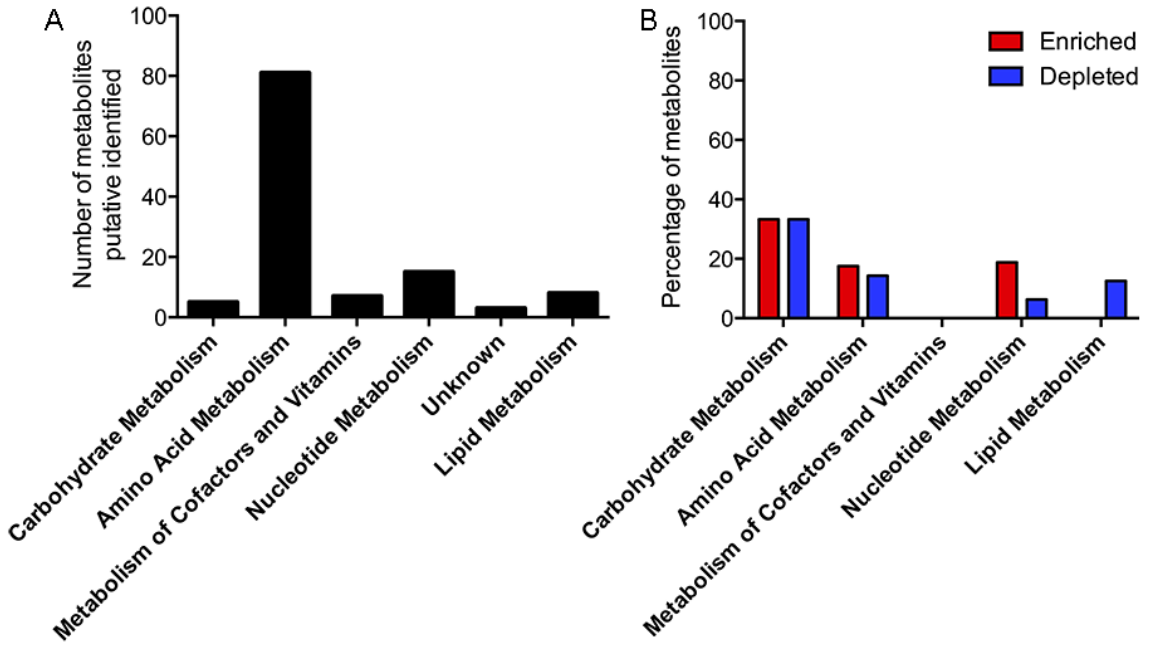

Figure 6.4 Desiccation stress affects metabolite levels in multiple metabolic pathways
A) The majority of metabolites identified in either desiccated or unstressed whole flies is involved in amino acid metabolism. **B)** Percentage of metabolites from each metabolism area enriched or depleted following desiccation, calculated by dividing the number of metabolites in each category that are either significantly higher or lower in abundance in desiccated flies by the number of metabolites in total identified in that category in the entire whole fly dataset.

This snapshot of metabolic change following desiccation supports previous work in indicating that changes in lipid, protein, and carbohydrate levels occur during desiccation exposure (Marron et al 2003). In work by Marron and colleagues, desiccation over the course of 9 hours was found to result in progressively decreasing lipid and carbohydrate levels, as well as an initial increase in protein levels during the first 6 hours, followed by a slight decrease at 9 hours. In the present study, a much longer period of desiccation was applied (24 hours) with a higher percentage of relative humidity. However, in both cases, the metabolic profile was assessed at the point at which approximately 50% of flies had died. Although changes in overall metabolite levels cannot be determined using this dataset, the substantial changes observed in abundance of metabolites involved in carbohydrate metabolism support the findings that carbohydrate metabolism is significantly affected by desiccation. Few lipids were identified in this study, but changes were observed in lipid metabolism components, as in the study by Marron and colleagues.

Enrichment in amino acid and nucleotide metabolism compounds suggests that this metabolic area increases in activity or results in product accumulation in the absence of water. However, this enrichment could also be due to the starvation component of desiccation exposure as these products may also accumulate as body proteins and nucleic acids are broken down. To distinguish the relative contribution of starvation to this metabolic change, it would be necessary to include a starvation control, as described in section 2.8.2.1. Regardless, it is likely that it would be difficult to eliminate some of the products of metabolism during dehydration as excretion is decreased to conserve liquid. This could also indicate that proteins are being degraded and potentially metabolised during desiccation, possibly due to protein instability during osmotic stress or due to the lack of dietary protein intake. Desiccation stress is linked to osmotic stress; as liquid levels decrease, the concentration of molecules in the remaining water increases (Levis et al 2012). The osmolality of the insect hemolymph has been found to increase during desiccation stress (Williams & Lee 2011) and results in water being pulled out of cells, which can result in cell damage (Levis et al 2012). Greatly reduced body water levels, which accompany severe desiccation, have also been connected with changes in cell membrane composition (Holmstrup et al 2002) and induce increased expression of heat shock proteins (Hayward et al 2004), presumably to handle denatured proteins. Thus, it is possible that amino acids may accumulate in whole *Drosophila* during desiccation as proteins become denatured. It is also likely that the lack of food has required breakdown of proteins, contributing to increased amino acid levels.

6.1.2 Metabolite profile of *Drosophila* is distinct from metabolite source

As unstressed *D. melanogaster* have unlimited access to standard *Drosophila* medium and as this substrate is their sole source of input metabolites, it could be possible that the metabolite profile of the flies would be highly influenced by the metabolites present in their food. To test for this possibility, the metabolic profile of *Drosophila* medium, the recipe for which is detailed in Materials and Methods, was acquired and compared to the metabolic profile of unstressed whole flies. This assay was run in parallel with that discussed in section 6.1.1 and the unstressed whole fly samples used in this analysis are the same samples which were contrasted with the metabolomic profile of desiccated flies.

After applying the filtering rubric described in section 6.1.1 to the metabolite profiles of whole unstressed *D. melanogaster* and *Drosophila* medium, 105 metabolites remained that were reliably detected (meaning that the metabolite was detected in at least three of the five biological replicates) across both sample types. There were a further 39 metabolites that were only detected reliably in one sample type.

The set of 105 reliably detected metabolites was statistically compared as detailed and explained in section 2.11.5. The justification for using the selected tests is discussed in section 1.5.6. Briefly, relative abundance of metabolites was compared using individual two-tailed two-sample multiple t-tests. The False Discovery Rate was set relatively conservatively at 1% using the Benjamini and Hochberg method, as the purpose of the analysis was to determine whether the metabolite content of the samples was broadly similar or broadly different, so it was desirable to limit the number of false positives permitted by the analysis. The result of this test was that 69 of the metabolites were deemed to differ in abundance between *Drosophila* and *Drosophila* medium, as detailed in Table 6.7.

Table 6.7 Relative abundance of metabolites in *Drosophila* standard diet and unstressed whole fly compared using two-tailed two-sample Student's *t*-tests, with False Discovery Rate set at 1% using the Benjamini and Hochberg method.

Putative metabolite	Control mean	Food mean	Difference	SE of difference	t ratio	df	P value
4-(beta-Acetylamino-ethyl)-imidazole	55532450	19550	55512900	1229366	45.16	8	<0.0001
Methyl-imidazole-acetic acid	1949	13773	11825	192	61.71	7	<0.0001
O-Acetyl-carnitine	25950700	38352	25912350	631932	41.01	8	<0.0001
L-Carnitine	108982600	1512028	107470500	3024548	35.53	8	<0.0001
Xanthurenic acid	6098079	4423	6093656	210994	28.88	8	<0.0001
N(pi)-Methyl-L-histidine	12899570	73279	12826300	578329	22.18	8	<0.0001
Choline phosphate	60522920	1011789	59511130	3063404	19.43	8	<0.0001
Nicotinamide	343909	3580728	3236819	187716	17.24	8	<0.0001

Hypoxanthine	1554895	49152	1505743	100996	14.91	8	<0.0001
(S)-1-Pyrroline-5-carboxylate	269032	31914	237118	16380	14.48	8	<0.0001
L-Histidine	25184650	781368	24403280	1711768	14.26	8	<0.0001
L-Proline	54969030	22120520	32848510	2614851	12.56	8	<0.0001
7-Methyladenine	1809414	7081	1802333	148334	12.15	8	<0.0001
Imidazole-4-acetaldehyde	15450	270298	254848	21377	11.92	8	<0.0001
2-Phenyl-acetamide	387494	61058	326436	27980	11.67	8	<0.0001
Cytosine	193665	48933	144732	12728	11.37	8	<0.0001
3-Amino-3-(4-hydroxy-phenyl)-propanoate	9876	142388	132513	11660	11.36	8	<0.0001
2,3-Dihydroxy-indole	144398	12418	131980	11873	11.12	8	<0.0001
4-Hydroxy-phenylacetaldehyde	141000	8306	132693	13148	10.09	8	<0.0001
Isopyridoxal	9950	53984	44035	4560	9.66	8	<0.0001
3,4-Dihydroxy-phenyl-acetaldehyde	1655	15308	13653	1438	9.50	8	<0.0001
L-Methionine	1242532	177482	1065050	112570	9.46	8	<0.0001
Betaine	48776120	88929010	40152900	4329275	9.27	8	<0.0001
Adenine	276495	1807865	1531370	167503	9.14	8	<0.0001
Indoxyl	2647	11172	8526	956	8.91	8	<0.0001
Glutathione	3238472	22436	3216036	321479	10.00	7	<0.0001
Choline	5992200	18688250	12696050	1466885	8.66	8	<0.0001
Piperideine	77007	2393870	2316863	278850	8.31	8	<0.0001
L-Pipecolate	324586	7764506	7439919	896443	8.30	8	<0.0001
2,3,4,5-Tetrahydro-pyridine-2-carboxylate	61871	15298	46574	5683	8.20	8	<0.0001
L-Glutamine	9375278	1111404	8263874	1075609	7.68	8	0.0001
sn-glycero-3-Phospho-choline	5874372	30762920	24888550	3332920	7.47	8	0.0001
AMP	2985102	423474	2561628	347413	7.37	8	0.0001
L-Tyrosine methyl ester	6935018	109434	6825584	952831	7.16	8	0.0001
Adenosine	769012	9323396	8554385	1196553	7.15	8	0.0001

Imidazole-4-acetate	85940	49731	36209	5233	6.92	8	0.0001
6-Methyl-aminopurine	1973	31658	29685	4351	6.82	8	0.0001
L-Alanine	4621750	597103	4024647	590622	6.81	8	0.0001
3-Butynoate	1702516	39593	1662923	244433	6.80	8	0.0001
5-Hydroxy-indoleacetate	1305405	6835	1298570	151674	8.56	6	0.0001
2-Oxobutanoate	10184	15036	4852	716	6.77	8	0.0001
6-Amino-2-oxohexanoate	21445	55659	34214	5255	6.51	8	0.0002
Benzoate	2809	6570	3761	597	6.30	8	0.0002
D-Alanine	16074	140276	124202	20613	6.03	8	0.0003
Riboflavin	44833	1810	43023	5955	7.22	6	0.0004
N-Acetyl-glutamine	42063	3939	38123	5559	6.86	6	0.0005
Homoarginine	12938	138490	125552	22171	5.66	8	0.0005
L-Methionine S-oxide	4627536	54981	4572555	810937	5.64	8	0.0005
Dopamine	1429761	86603	1343157	240006	5.60	8	0.0005
Phenylacetic acid	2233200	26303	2206898	396746	5.56	8	0.0005
Phosphono-acetaldehyde	268697	28717	239980	43448	5.52	8	0.0006
Butanoic acid	53755	23622	30133	5468	5.51	8	0.0006
4-Acetamido-butanoate	4602	32769	28167	5305	5.31	8	0.0007
Purine	6439	2829	3610	570	6.33	6	0.0007
4,8-Dihydroxy-quinoline	21874	3754	18120	3649	4.97	8	0.0011
4-Imidazolone-5-propanoate	6493	369637	363144	77136	4.71	8	0.0015
4,6-Dihydroxy-quinoline	80712	5352	75360	16039	4.70	8	0.0015
4-Guanidino-butanoate	181809	2061238	1879429	406007	4.63	8	0.0017
L-Lysine 1,6-lactam	18616	42370	23754	5154	4.61	8	0.0017
5,6-Dihydroxy-indole	58077	22292	35785	7800	4.59	8	0.0018
(Z)-4-Hydroxy-phenyl-acetaldehyde-oxime	48680	143505	94826	20921	4.53	8	0.0019
Guanine	306905	210965	95940	21511	4.46	8	0.0021
L-Nor-metanephrine	90077	16081	73996	16871	4.39	8	0.0023

5-Oxo-pentanoate	1926	844	1082	255	4.25	8	0.0028
L-Histidinal	2105	16298	14193	3220	4.41	7	0.0031
Phenyl-acetaldehyde	14429	25962	11533	2793	4.13	8	0.0033
N6,N6,N6-Trimethyl-L-lysine	67618	454777	387159	96235	4.02	8	0.0038
Indole	317478	162323	155155	40499	3.83	8	0.0050
D-Alanyl-D-alanine	20257	158826	138569	34058	4.07	6	0.0066

Of the metabolites which were found to differ, 29 of these were enriched in food (Table 6.8), while the remaining 40 metabolites had a lower relative abundance in food than in *D. melanogaster* whole fly samples (Table 6.9). An enrichment value for each metabolite was calculated by dividing mean relative abundance in *Drosophila* standard diet by mean abundance in unstressed flies. Confidence in the identity of metabolites is indicated in the tables in the rank column; the ranking categories used are detailed in section 2.11.4.

Table 6.8 Metabolites enriched in *Drosophila* medium relative to *D. melanogaster*

Exact mass and retention time (RT) are listed with the name of the most likely isomer. Enrichment indicates abundance in food relative to unstressed flies.

Mass	RT	Name	Rank	Iso-mers	Enrich ment	Pathway
156.0534897	10.98	4-Imidazolone-5-propanoate	2	3	56.93	Amino Acid Metabolism
83.07351307	12.68	Piperideine	2	3	31.09	Amino Acid Metabolism
129.0790116	12.40	L-Pipecolate	2	8	23.92	Amino Acid Metabolism
110.048071	10.81	Imidazole-4-acetaldehyde	2	1	17.50	Amino Acid Metabolism
149.0701189	8.05	6-Methylaminopurine	2	4	16.05	Unknown
181.0739999	7.34	3-Amino-3-(4-hydroxyphenyl)-propanoate	2	10	14.42	Amino Acid Metabolism
267.0967386	9.66	Adenosine	1	2	12.12	Nucleotide Metabolism
145.085105	14.27	4-Guanidino-butanoate	2	2	11.34	Amino Acid Metabolism
188.1272714	20.63	Homoarginine	2	4	10.70	Amino Acid Metabolism

122.0480414	7.43	Nicotinamide	2	3	10.41	Metabolism of Cofactors and Vitamins
152.0472903	4.88	3,4-Dihydroxy-phenyl-acetaldehyde	2	24	9.25	Amino Acid Metabolism
89.04770451	11.41	D-Alanine	2	8	8.73	Amino Acid Metabolism
160.0847796	12.73	D-Alanyl-D-alanine	2	3	7.84	Amino Acid Metabolism
139.0745703	8.27	L-Histidinal	2	2	7.74	Amino Acid Metabolism
145.0739106	9.53	4-Acetamido-butanoate	2	8	7.12	Amino Acid Metabolism
140.0585567	9.95	Methylimidazole-acetic acid	2	6	7.07	Amino Acid Metabolism
188.1524518	19.15	N6,N6,N6-Trimethyl-L-lysine	2	1	6.73	Amino Acid Metabolism
135.0545473	10.16	Adenine	1	0	6.54	Nucleotide Metabolism
167.0582933	12.20	Isopyridoxal	2	8	5.43	Metabolism of Cofactors and Vitamins
257.1028521	13.60	sn-glycero-3-Phosphocholine	1	0	5.24	Lipid Metabolism
133.0527497	12.34	Indoxyl	2	6	4.22	Amino Acid Metabolism
103.0997071	20.08	Choline	1	0	3.12	Amino Acid Metabolism
151.0633549	8.31	(Z)-4-Hydroxyphenyl-acetaldehyde-oxime	2	16	2.95	Amino Acid Metabolism
145.0739224	13.58	6-Amino-2-oxohexanoate	2	8	2.60	Amino Acid Metabolism
122.0367885	5.13	Benzoate	2	5	2.34	Amino Acid Metabolism
128.0949645	13.01	L-Lysine 1,6-lactam	2	2	2.28	Amino Acid Metabolism
117.0789853	11.64	Betaine	1	15	1.82	Amino Acid Metabolism
120.0575421	5.69	Phenyl-acetaldehyde	2	7	1.80	Amino Acid Metabolism
102.0316985	10.89	2-Oxobutanoate	2	7	1.48	Amino Acid Metabolism

Table 6.9 Metabolites low in abundance in *Drosophila* medium relative to *D. melanogaster*
Exact mass and retention time (RT) are listed with the name of the most likely isomer. Enrichment indicates abundance in food relative to unstressed flies.

Mass	RT	Name	Rank	Iso-mers	Enrich ment	Pathway
153.0902043	7.79	4-(beta-Acetyl-aminoethyl)-imidazole	1	2	0.0004	Amino Acid Metabolism
205.0375758	10.45	Xanthurenic acid	2	1	0.001	Amino Acid Metabolism
203.1158034	11.43	O-Acetylcarnitine	1	0	0.001	Amino Acid Metabolism
149.0701668	14.24	7-Methyladenine	2	4	0.004	Nucleotide Metabolism
191.0582397	11.27	5-Hydroxy-indoleacetate	2	4	0.01	Amino Acid Metabolism
169.0850918	12.44	N(pi)-Methyl-L-histidine	1	4	0.01	Amino Acid Metabolism
307.0838331	13.06	Glutathione	1	2	0.01	Amino Acid Metabolism
136.0524836	7.24	Phenylacetic acid	2	15	0.01	Amino Acid Metabolism
165.0459709	12.71	L-Methionine S-oxide	2	3	0.01	Amino Acid Metabolism
161.1051846	12.99	L-Carnitine	1	1	0.01	Amino Acid Metabolism
195.0896182	7.39	L-Tyrosine methyl ester	2	5	0.02	Amino Acid Metabolism
183.0661009	13.67	Choline phosphate	1	0	0.02	Lipid Metabolism
84.02113415	11.61	3-Butynoate	2	1	0.02	Carbohydrate Metabolism
155.0694982	13.91	L-Histidine	1	4	0.03	Amino Acid Metabolism
136.0385378	11.21	Hypoxanthine	1	2	0.03	Nucleotide Metabolism
376.1383014	9.22	Riboflavin	1	1	0.04	Metabolism of Cofactors and Vitamins
136.0524917	9.27	4-Hydroxy-phenylacetaldehyde	2	15	0.06	Amino Acid Metabolism
153.0789796	7.52	Dopamine	1	4	0.06	Amino Acid Metabolism
161.0476401	8.78	4,6-Dihydroxyquinoline	2	6	0.07	Amino Acid Metabolism
149.04768	11.22	2,3-Dihydroxyindole	2	7	0.09	Amino Acid Metabolism
188.0796961	10.56	N-Acetylglutamine	2	1	0.09	Unknown
123.9926044	13.63	Phosphono-acetaldehyde	2	0	0.11	Amino Acid Metabolism
146.0691284	13.98	L-Glutamine	2	5	0.12	Amino Acid Metabolism
113.0477368	9.66	(S)-1-Pyrroline-5-carboxylate	2	5	0.12	Amino Acid Metabolism

89.04769804	14.17	L-Alanine	1	8	0.13	Amino Acid Metabolism
347.0630677	12.57	AMP	1	6	0.14	Nucleotide Metabolism
149.0510923	11.73	L-Methionine	1	4	0.14	Amino Acid Metabolism
135.0684509	7.5	2-Phenylacetamide	2	3	0.16	Amino Acid Metabolism
161.0476045	6.65	4,8-Dihydroxyquinoline	2	6	0.17	Amino Acid Metabolism
183.0895607	6.15	L-Normetanephrine	2	2	0.18	Amino Acid Metabolism
127.063321	6.61	2,3,4,5-Tetrahydropyridine-2-carboxylate	2	6	0.25	Amino Acid Metabolism
111.0432725	12.04	Cytosine	1	0	0.25	Nucleotide Metabolism
149.0477148	6.69	5,6-Dihydroxyindole	2	7	0.38	Amino Acid Metabolism
115.0633622	12.77	L-Proline	1	3	0.4	Amino Acid Metabolism
116.0473142	15.85	5-Oxopentanoate	2	8	0.44	Amino Acid Metabolism
120.0436185	10.91	Purine	2	0	0.44	Nucleotide Metabolism
88.05242781	7.35	Butanoic acid	2	6	0.44	Carbohydrate Metabolism
117.0579005	11.84	Indole	2	1	0.51	Amino Acid Metabolism
126.0429456	11.36	Imidazole-4-acetate	1	1	0.58	Amino Acid Metabolism
151.0494064	12.62	Guanine	1	2	0.69	Nucleotide Metabolism

Metabolites that were not detected in at least three of the five replicates for both *Drosophila* diet and unstressed fly samples could not be included in the statistical analysis as the statistical power of such comparisons would be very low. There were 39 metabolites that were detected reliably only in either *Drosophila* medium or *D. melanogaster* whole organism samples, as listed in Table 6.10.

Table 6.10 Metabolites detected reliably only in *Drosophila* diet or control *D. melanogaster*
Mean relative abundance of putative metabolites in *Drosophila* medium or in *D. melanogaster*. SEM are calculated where possible (i.e. at least two detection values). Number of detections out of sets of five biological replicates is indicated for both control and desiccated sample sets.

Putative metabolite	Mean whole fly ± SEM	Mean *Drosophila* diet ± SEM	Detections	
			Flies	Diet
S-Adenosyl-L-homocysteine		57185 ± 15213	0	5
3-Oxalomalate		15802 ± 2377	0	5
(S)-2-Aceto-2-hydroxybutanoate		14670 ± 3071	0	5
6-Hydroxymelatonin		3373 ± 525	0	5
D-Serine		3334 ± 469	0	5
L-2-Aminoadipate	4148	121880 ± 33525	1	5
Deoxyadenosine	2171	33046 ± 9802	1	5
L-Ornithine	4303 ± 344	57236 ± 5452	2	5
Formylanthranilate	2449	15195 ± 4352	1	5
6-Acetamido-2-oxohexanoate	8942	23999 ± 3698	1	5
L-Lysine	123141 ± 30859	112841 ± 15103	2	5
D-Glucose	98400 ± 5522	11681339 ± 1361909	2	3
L-Asparagine	918473 ± 43125	13937882 ± 2467085	2	3
L-Threonine	473360 ± 146377	1516973 ± 53686	2	3
[FA hydroxy,oxo(7:0/2:0)] 4-hydroxy-2-oxo-Heptanedioic acid	6402 ± 791	20237 ± 4379	2	3
L-Serine	138972 ± 7097	408311 ± 73602	2	3
Sucrose	10869809 ± 349552	27435803 ± 3088555	2	3
(R)-2-Hydroxyglutarate	1574892 ± 67893	2876504 ± 154610	2	3
(S)-Malate	13550483 ± 30525	17976923 ± 4563536	2	3
Melatonin	1288	1392 ± 213	1	3
Taurine	4931560 ± 310946	168735 ± 8997	2	3
Adenosine 2',5'-bisphosphate	249888 ± 39851	15867 ± 4489	5	2
Kynurenate	12148 ± 1848	2686 ± 1258	5	2
Pyrrole-2-carboxylate	21489 ± 1775	4752 ± 503	5	2
5-Methylcytosine	27109 ± 12534	690	5	1
Ergothioneine	129434 ± 9992	9705	5	1
Indole-3-acetaldehyde	46162 ± 38516	90850	5	1
4-(2-Aminophenyl)-2,4-dioxobutanoate	1240359 ± 114173		5	0
sn-Glycerol 3-phosphate	338802 ± 29291		5	0
Ethanolamine phosphate	153996 ± 15992		5	0
4-Pyridoxolactone	102742 ± 18166		5	0
S-Adenosyl-L-methionine	87164 ± 22164		5	0
L-Arginine phosphate	63551 ± 13260		5	0
5,6-Dihydrouracil	46392 ± 1367		5	0

Inosine	44314 ± 6670		5	0
1,2-Dihydroxy-5-(methylthio)pent-1-en-3-one	19652 ± 2961		5	0
Hydroxymethyl-phosphonate	5735 ± 363		5	0
3-Hydroxy-N6,N6,N6-trimethyl-L-lysine	5376 ± 819		5	0
Cytidine	5280 ± 673		5	0

For 22 of the 39 metabolites reliably detected only in either food or *D. melanogaster*, a fold change was calculated using the mean relative abundance from samples in which the metabolite was detected. A fold change could not be calculated for 17 of the metabolites as they were detected only in one sample type. These values can therefore only be used to indicate whether a metabolite is higher or lower than in the detected sample group, presuming that a failure to detect a metabolite in all five replicates indicates that the abundance is below the detection threshold, and therefore lower than in a sample group where the metabolite is detected.

Of the 21 metabolites detected reliably in *Drosophila* standard medium, but not in whole flies, all but two were found to be higher in abundance in food (Table 6.11). There were 18 metabolites detected reliably in flies, but not in *Drosophila* medium. Of these, all but one were lower in abundance in food than in whole fly samples (Table 6.12). Confidence in the identity of metabolites is indicated in the tables in the rank column and is graded as detailed in section 2.11.4.

Table 6.11 Relative abundance of metabolites detected reliably in *Drosophila* diet, but not in whole *D. melanogaster*

Exact mass and retention time (RT) listed with the name of the most likely isomer. Enrichment indicates abundance in *Drosophila* standard medium relative to unstressed flies. No enrichment value indicates that the metabolite was detected only in food.

Mass	RT	Name	Rank	Iso-mers	Enrich-ment	Pathway
384.12147	12.92	S-Adenosyl-L-homocysteine	1	1		Amino Acid Metabolism
206.0060312	16.08	3-Oxalomalate	2	0		Carbohydrate Metabolism
146.0578536	12.61	(S)-2-Aceto-2-hydroxybutanoate	2	15		Amino Acid Metabolism
248.115974	5.23	6-Hydroxymelatonin	2	0		Amino Acid Metabolism
105.0426156	10.62	D-Serine	2	2		Amino Acid Metabolism
180.0632166	13.95	D-Glucose	2	56	118.71	Carbohydrate Metabolism
161.0687656	14.06	L-2-Aminoadipate	1	9	29.38	Amino Acid Metabolism
251.1017706	8.51	Deoxyadenosine	1	3	15.22	Nucleotide Metabolism
132.0534168	14.07	L-Asparagine	1	5	15.18	Amino Acid Metabolism
132.0897911	19.36	L-Ornithine	1	5	13.30	Amino Acid Metabolism
165.0426005	6.47	Formylanthranilate	2	7	6.20	Amino Acid Metabolism
119.0583286	13.66	L-Threonine	1	10	3.20	Amino Acid Metabolism
190.0476755	14.61	[FA hydroxy,oxo(7:0/2:0)] 4-hydroxy-2-oxo-Heptanedioic acid	2	3	3.16	Amino Acid Metabolism
105.042633	14.50	L-Serine	1	2	2.94	Amino Acid Metabolism
187.0844723	7.53	6-Acetamido-2-oxohexanoate	2	5	2.68	Amino Acid Metabolism
342.1163953	14.53	Sucrose	1	41	2.52	Carbohydrate Metabolism
148.0370399	13.47	(R)-2-Hydroxyglutarate	2	17	1.83	Amino Acid Metabolism
134.0214348	13.98	(S)-Malate	1	3	1.33	Carbohydrate Metabolism
232.1212102	4.98	Melatonin	1	1	1.08	Amino Acid Metabolism
146.1054016	20.74	L-Lysine	1	7	0.92	Amino Acid Metabolism
125.0145923	13.87	Taurine	2	0	0.03	Lipid Metabolism

Table 6.12 Relative abundance of metabolites detected reliably in *D. melanogaster*, but not in *Drosophila* diet

Exact mass and retention time (RT) listed with the name of the most likely isomer. Enrichment indicates abundance in *Drosophila* standard medium relative to unstressed flies. No enrichment value indicates that the metabolite was detected only in whole fly samples.

Mass	RT	Name	Rank	Iso-mers	Enrich ment	Pathway
207.0532466	12.80	4-(2-Aminophenyl)-2,4-dioxobutanoate	2	5		Amino Acid Metabolism
172.0137575	13.34	sn-Glycerol 3-phosphate	2	2		Lipid Metabolism
141.0191169	14.34	Ethanolamine phosphate	2	1		Amino Acid Metabolism
165.0426097	12.94	4-Pyridoxolactone	2	7		Metabolism of Cofactors and Vitamins
398.1372279	14.60	S-Adenosyl-L-methionine	2	0		Amino Acid Metabolism
254.0779323	14.86	L-Arginine phosphate	2	0		Amino Acid Metabolism
114.0429874	11.54	5,6-Dihydrouracil	2	5		Nucleotide Metabolism
268.0807277	11.27	Inosine	2	2		Nucleotide Metabolism
162.0349772	15.18	1,2-Dihydroxy-5-(methylthio)pent-1-en-3-one	2	2		Amino Acid Metabolism
111.9925495	10.76	Hydroxymethyl-phosphonate	2	1		Amino Acid Metabolism
204.1474057	17.20	3-Hydroxy-N6,N6,N6-trimethyl-L-lysine	2	0		Amino Acid Metabolism
243.085453	12.14	Cytidine	1	3		Nucleotide Metabolism
125.0589432	6.81	5-Methylcytosine	2	3	0.03	Nucleotide Metabolism
427.0295328	13.83	Adenosine 2',5'-bisphosphate	1	5	0.06	Nucleotide Metabolism
229.0884558	14.04	Ergothioneine	2	1	0.07	Amino Acid Metabolism
189.0426178	5.94	Kynurenate	2	5	0.22	Amino Acid Metabolism
111.0321016	13.10	Pyrrole-2-carboxylate	2	6	0.22	Amino Acid Metabolism
159.0683734	11.88	Indole-3-acetaldehyde	2	3	1.97	Amino Acid Metabolism

6.1.2.1 Metabolic profile of food diverges highly from that of whole *D. melanogaster*

Metabolites identified in either *D. melanogaster* flies or in *Drosophila* medium include 95 that are associated with amino acid metabolism (Figure 6.5A). The next most represented pathway was nucleotide metabolism, with 16 identifications. In decreasing order, the remaining metabolites are involved in lipid metabolism, carbohydrate metabolism, metabolism of cofactors, and metabolism of vitamins and cofactors. Three metabolites were additionally identified that have not been assigned to a metabolic area in the KEGG database; these are: N-acetylglutamine, phenylhydrazine, and 6-methylaminopurine. These are the same three unassigned metabolites identified in desiccated and unstressed whole fly samples and discussed in section 6.1.1.1.

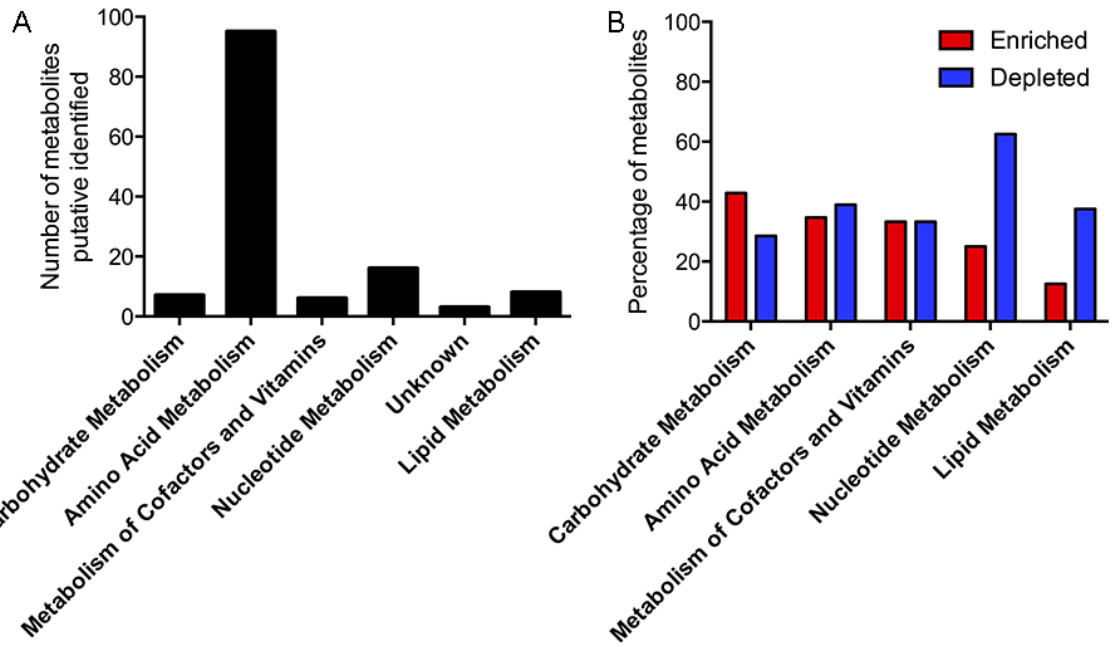

Figure 6.5 *Drosophila* standard diet differs greatly in metabolic content from *D. melanogaster* whole flies

A) The number of metabolites identified in the entire dataset involved in different metabolic processes is heavily weighted toward amino acid metabolism metabolites. **B)** Percentage of metabolites from each metabolism area enriched or depleted in food, calculated by dividing number of metabolites in each category that are either significantly higher or lower in abundance in food by the number of metabolites in total identified in that category in the entire whole fly dataset.

When metabolites were screened to include only those that are higher or lower in abundance by at least 2-fold in food relative to flies, then it is found that 73%

of metabolites are differently abundant. This is much higher than the differences found between desiccated and control whole fly (29%), clearly indicating that flies and food differ to a much greater extent. Although this is entirely expected, it provides a validation of the method used, even at this exploratory stage, by identifying a greater proportion of differences between sample sets that are clearly more divergent in nature.

Metabolite abundance differences between flies and food were further examined by plotting as a percentage change of the identified metabolites in the dataset (Figure 6.5B). There were slightly more metabolites related to carbohydrate metabolism enriched in food than depleted in food, while metabolites related to nucleotide metabolism and lipid metabolism were frequently enriched in flies.

6.1.3 Food-enriched metabolites decrease following desiccation

The desiccation method used in this study requires *D. melanogaster* to be placed into empty vials without water or food (see section 2.8.1). Consequently, flies are simultaneously starved and desiccated (see section 2.8.2.1). Thus, after 24 hours of desiccation exposure, metabolites that were present in the fly due to any recent meals should be decreased. However, by comparing only the metabolic profiles of stressed and unstressed flies, it is not possible to distinguish the origin of metabolites that have decreased in abundance following desiccation. Including the metabolic profile of food into this comparison can be used to narrow down the range of metabolites included in the analysis. Theoretically, metabolites which are present in the fly due to consumption of *Drosophila* medium should be enriched in food when compared to fly samples, and should additionally be enriched in recently fed flies (control) relative to flies that have not eaten in 24 hours (desiccated). This analysis therefore sheds light on the more specific reasons underlying the depletion of some metabolites following desiccation (Table 6.3 and Table 6.6). It also identifies some metabolites as potentially interesting which were excluded from comparisons of stressed and unstressed fly samples due to infrequent detection of relative abundance.

Metabolites were screened initially by including only those with at least three detections out of five biological replicates for food samples and at least one

detection in control *D. melanogaster* samples. As previous analyses found that detection frequency is associated with a higher relative abundance (e.g. Table 6.11), apart from a few exceptions, these values were selected to ensure that only potentially food-enriched metabolites were included in the analysis. A low number of detections for control samples was selected to avoid eliminating any potentially interesting metabolites from the analysis. No threshold was required for the desiccated flies as the metabolites of particular interest in this case would include those that were reduced below the detection threshold of the instruments. Metabolites were further screened to include only those with an enrichment of at least 1.5 in food relative to unstressed *D. melanogaster*, and to likewise require an enrichment of at least 1.5 in control flies relative to desiccated flies. Eighteen metabolites were identified by this approach as potentially being specifically meal-related metabolites, as shown in Table 6.13.

Table 6.13 Meal-specific metabolites are highly enriched in *Drosophila* medium and decrease in abundance following desiccation stress

An asterisk indicates that the comparison was deemed a discovery using the Benjamini and Hochberg method, while NS (not significant) indicates values that were included in the analysis but which were not discoveries. Where neither label is present, the values were not compared statistically. Abbreviations: CWF = control whole flies, DWF = desiccated whole flies

	Detections			Enrichment		
Putative metabolite	CWF	DWF	Food	Food/ DWF	Food/ CWF	CWF/ DWF
D-Glucose	2	3	3	188.40	118.71*	1.59 NS
L-2-Aminoadipate	1	0	5		29.38	
L-Pipecolate	5	5	5	82.49	23.92*	3.45*
Piperideine	5	5	5	50.30	31.09*	1.62 NS
4-Guanidinobutanoate	5	5	5	31.17	11.34*	2.75*
3-Amino-3-(4-hydroxyphenyl)propanoate	5	5	5	28.34	14.42*	1.97 NS
Homoarginine	5	5	5	28.23	10.70*	2.64*
D-Alanyl-D-alanine	3	0	5		7.84*	
Sucrose	2	2	3	28.11	2.52	11.14
6-Methylaminopurine	5	5	5	25.46	16.05*	1.59 NS
2-Oxobutanoate	3	3	3	18.43	10.61*	1.74 NS
3,4-Dihydroxyphenylacetaldehyde	5	4	5	15.21	9.25*	1.64 NS
N6,N6,N6-Trimethyl-L-lysine	5	5	5	14.60	6.73*	2.17*
4-Acetamidobutanoate	5	5	5	13.38	7.12*	1.88 NS
Betaine	5	5	5	9.15	1.82*	5.02*
Isopyridoxal	5	5	5	8.45	5.43*	1.56 NS
6-Amino-2-oxohexanoate	5	2	5	5.64	2.60*	2.17
L-Glutamate	5	5	5	4.33	2.74 NS	1.58*

6.1.3.1 Energy metabolites are depleted by desiccation exposure

One of the most expected results of 24 hours of desiccation exposure in a small organism like *D. melanogaster* is the consumption of metabolites that can be used to generate energy. This is especially the case as starvation exposure is inherent in the desiccation exposure assay applied (see section 2.8.2.1). As a starvation only control was not included in this experiment, metabolite increases and decreases following desiccation exposure could be due to the lack of food rather than due to lack of water. In the absence of metabolic input (i.e. food), those metabolites that should be the most depleted are those that cannot be synthesised by the fly. As carbohydrates are considered to be the main energy source for *Diptera,* two metabolites that were identified in the study and which might be particularly depleted by the desiccation exposure applied are glucose and sucrose (Sacktor 1965, Steele 1981).

Indeed, in this study, both glucose and sucrose were found to be decreased in abundance in flies following 24 hours of desiccation exposure (Table 6.13). Glucose levels were less depleted than sucrose in desiccated flies relative to unstressed flies, possibly because *D. melanogaster* can release glucose from stored glycogen or, perhaps more importantly in the fly, from trehalose (Reyes-DelaTorre et al 2012). Sucrose, conversely, is derived solely from the diet.

The enrichment of both glucose and sucrose in *Drosophila* diet relative to the flies themselves is consistent with the expectation that flies acquire these metabolites primarily or exclusively from food. Although glucose is required as a ready energy source, it is thought that excess glucose is quickly converted into trehalose for storage (Steele 1981). Thus, it is not surprising that the level of glucose in the fly was found to be lower than that of *Drosophila* medium.

Another metabolite that could conceivably be depleted in flies due to metabolism in the absence of food is aspartate, which can be used for cellular metabolism after aspartate transaminase catalyses its conversion into oxaloacetate (Wu 2009). Aspartate levels were found to significantly decrease in the Antarctic midge, *Belgica antarctica,* following desiccation stress (Michaud et al 2008). Likewise, in this dataset it was found that aspartate was significantly reduced in abundance in desiccated *D. melanogaster* (Table 6.3).

6.1.3.2 Lysine degradation pathway is affected by desiccation exposure

Lysine cannot be synthesised by *D. melanogaster* and is therefore an essential amino acid (Al Bratty et al 2012). It does, however, undergo catabolism. The primary source of lysine in insects is from the breakdown of proteins (Nation 2015b). Thus, is it not surprising that in the absence of dietary protein, decreases are observed in the levels of several metabolites relating to the breakdown of lysine from protein, as shown in Figure 6.6.

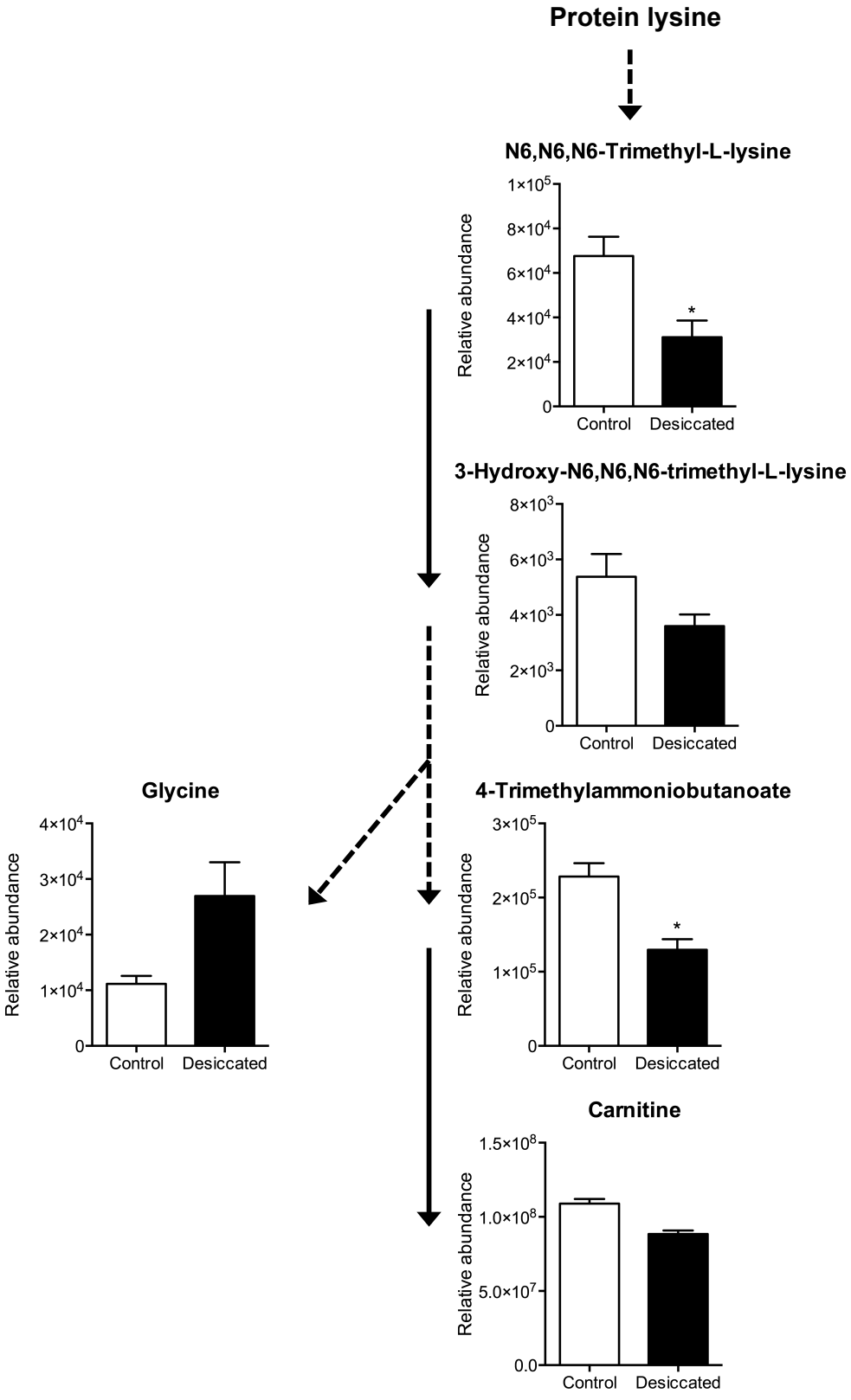

Figure 6.6 Catabolism of protein lysine in *D. melanogaster* is significantly affected by desiccation exposure

Relative abundance of metabolites in the protein lysine catabolism pathway is shown in desiccated or unstressed whole flies. Arrows indicate direction of metabolism. A solid arrow indicates a direct relation, while dashed arrows indicate that a metabolic intermediate step is thought to exist, but was not detected in this experiment.

Perhaps a surprising outlier in the overall generally depleted abundance of protein lysine degradation metabolites is the increased level of glycine. As proteins can be broken down to provide substrate for the tricarboxylic acid cycle, it is possible that glycine may accumulate in desiccated flies as a by-product of increased protein lysine catabolism. Although glycine itself can be broken down, the predominant pathway of glycine degradation, via the glycine cleavage enzyme, involves the production of ammonium. As it appears that ammonia may accumulate in flies during desiccation stress (see section 6.2.2.7), it is possible that glycine degradation may become unfavourable under these conditions.

Substantial changes are also found in the abundance of metabolites of the L-lysine degradation pathway, as shown in Figure 6.7. Indeed, in this dataset, the lysine catabolism pathway is the single metabolic pathway with the most identified changes in metabolite levels.

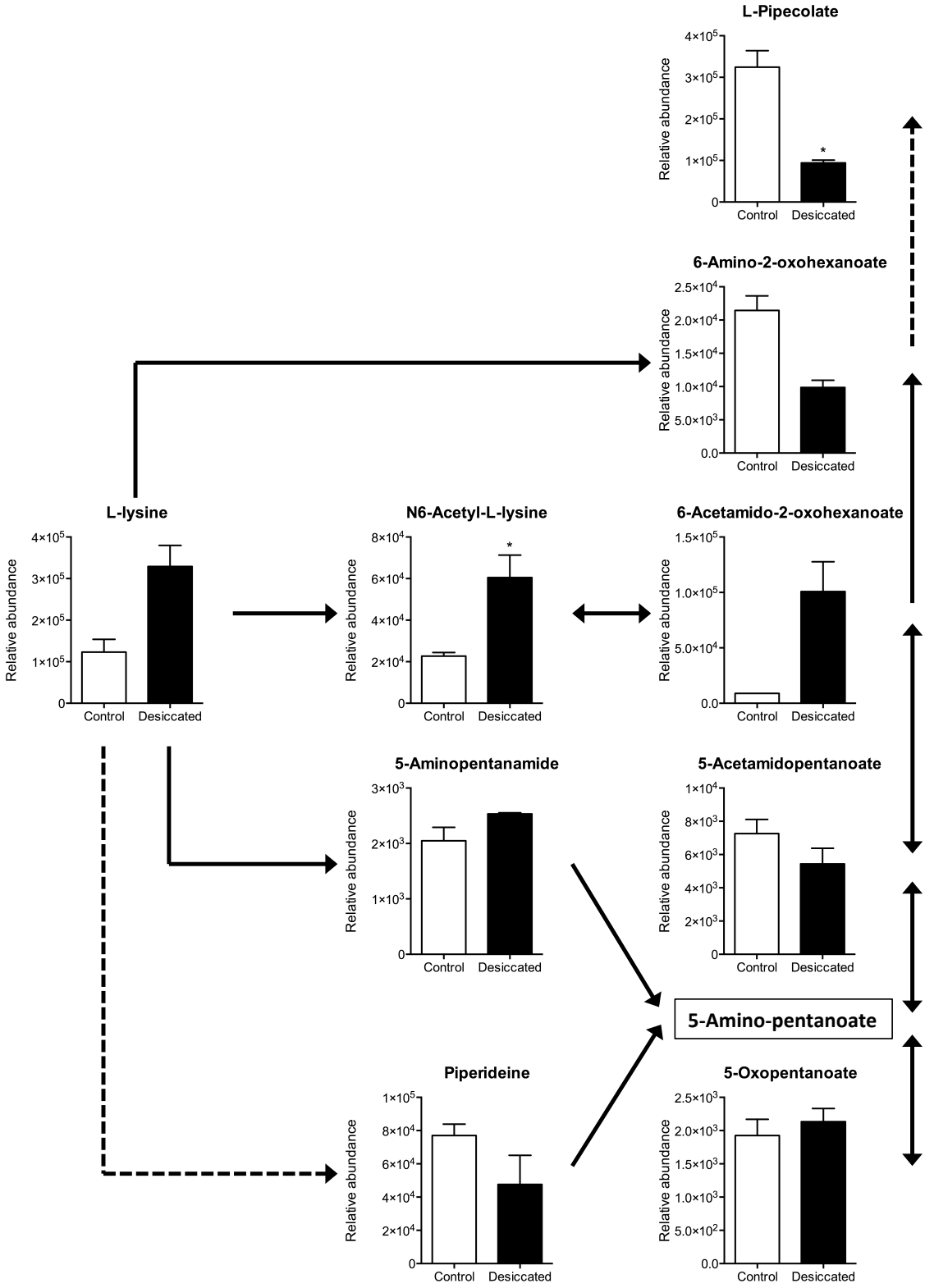

Figure 6.7 Lysine degradation is significantly affected by desiccation in *D. melanogaster*
Relative abundance of metabolites in the lysine degradation pathway is shown in desiccated or unstressed whole flies. Arrows indicate direction of metabolism. A solid arrow indicates a direct relation, while dashed arrows indicate that a metabolic intermediate step is thought to exist, but was not detected in this experiment.

Changes in abundance of metabolites in both lysine degradation pathways have previously been observed in *D. melanogaster* with the *y* mutation using metabolomics methods (Al Bratty et al 2012). These changes were linked to alterations in histone binding and consequent modifications of gene expression. Regulation of lysine catabolism has been linked to stress in plants (Galili et al 2001), although it is not entirely clear how this might play a role in desiccation survival in an insect. Moreover, further experimentation would be required to elucidate whether the observed changes are due to desiccation alone, or if they have been caused by the starvation component of desiccation exposure (see section 2.8.2.1).

6.1.3.3 Desiccation induces changes in cell signalling molecules

In theory, desiccation stress might induce changes in cell signalling molecules in order to coordinate adaptive alterations that could enhance survival. For example, reductions in metabolic rate could have a survival effect during desiccation by consuming less energy resources and thereby producing fewer metabolic end products requiring excretion. As starvation exposure occurs concomitant with desiccation, reducing the metabolic rate could equally be a mechanism for enhancing survival of a period of metabolic restriction of unknown duration. One way to reduce energy consumption is to reduce movement (Steele 1981). Therefore, it could be possible that neurotransmitters associated with movement and activity in *D. melanogaster* might be reduced in abundance following a period of intensive stress like desiccation or following mild starvation exposure. Two neurotransmitters which are associated with movement and which were identified in this dataset are dopamine and acetylcholine.

A number of studies have linked dopamine signalling in *D. melanogaster* to activity level and amount of sleep (Friggi-Grelin et al 2003, Lima & Miesenbock 2005, Yellman et al 1997). When production of dopamine is impaired in the nervous system, flies move less and sleep more (Riemensperger et al 2011), and changes in dopamine levels have been linked to changes in metabolic rate (Ueno et al 2012). Dopamine production has been found to be decreased in *D. melanogaster* following 24 hours of starvation stress (Neckameyer & Weinstein

2005). Desiccation stress, which also comprises a starvation component, may therefore result in an overall decrease in dopamine levels as well.

Acetylcholine has been associated with movement in insects. It is highly abundant and is the primary excitatory neurotransmitter in the central nervous system of *D. melanogaster* (Lee & O'Dowd 1999, Lewis & Smallman 1956, O'Kane 2011). Insect motor functions require acetylcholine signalling, and interference with the breakdown of acetylcholine results in consumption of energy resources via uncontrolled activity (Gauthier 2010, Nation 2015a), a result that is also produced by neonicotinoid insecticides (Gibbons et al 2015). Thus, it is possible that reductions in acetylcholine levels may have the opposite effect of overall reducing total movement in flies.

In this study, levels of both dopamine and tyrosine, which is used to produce dopamine via the intermediary L-3-4-dihydroxyl-phenylalanine (Hsouna et al 2007, Nagatsu et al 1964), were decreased by at least 130% following desiccation stress (Table 6.3). Similarly, acetylcholine levels were greatly reduced, with a staggering 25-fold lower level of acetylcholine in desiccated flies relative to control flies (Table 6.3). It is possible that these reductions in metabolite levels may correspond to a reduction in energy consumption through movement suppression.

This is not the first instance of neurotransmitter changes being observed in insects following desiccation stress via metabolomics analysis. Levels of the primary inhibitory neurotransmitter γ-aminobutyric acid were elevated twofold following desiccation of the midge *Belgica antarctica* (Michaud et al 2008).

In the present study, a 3.53 fold increase was observed in the abundance of adenosine following desiccation (Table 6.2). Extracellular adenosine acts as a neurotransmitter and has been found to be released following systemic or cellular stress (Hasko et al 2002, Sperlagh et al 2000). It is thought that it may be involved in coordinating stress-related responses and may be induced in this case in response to intense desiccation stress and/or mild starvation stress.

6.2 Metabolomics of desiccation and starvation stress in the Malpighian tubules

Many studies of insect metabolism and metabolites have relied on whole organism samples (Chintapalli et al 2013a). However, as it has become evident that individual tissues differ not only in their gene expression profiles (Chintapalli et al 2007), but also in their metabolite profiles (Chintapalli et al 2013a), the importance of examining not only whole-organism but also tissue-specific profiles has become clear. Although whole organism samples can provide an overall picture of metabolic changes, even dramatic tissue-specific changes may not be detected as individual tissues only contribute a small percentage to the overall metabolite levels of the whole organism (Chintapalli et al 2013a). Indeed, recent insect studies using metabolomics have involved more specific sample types than whole organism studies, such as profiling of mosquito fat body (Price et al 2015) and division of *D. melanogaster* into thorax, abdomen, and head (Laye et al 2015). However, even within the abdomen, the metabolic enrichment profiles of midgut and Malpighian tubules differ significantly and potentially interesting metabolite profiles may be lost by combining these two tissue types (Chintapalli et al 2013a).

As a key regulator of homeostasis and hemolymph osmolality (Luan et al 2015) and as a tissue critically involved in stress survival (Davies et al 2014), the Malpighian tubules can therefore be expected to be particularly involved in and affected by desiccation stress. Fluid secretion rate by the tubules following desiccation is depressed (section 3.1.2), and changes have also been observed in diuretic peptide receptor levels of stressed flies (Terhzaz et al 2015b). Consequently, it is likely that the metabolic profile of the tubules would be particularly affected by desiccation stress.

6.2.1 Metabolic profile of Malpighian tubules is distinct from fly and food

Five biological replicates of two additional sample types were run alongside the sample sets of desiccated flies, control flies, and food. Both were extracted from 20 pairs of *D. melanogaster* Malpighian tubules, one from desiccated flies and the other from unstressed (control) flies. However, the variability within

these groups resulted in there being no statistically significant differences between tubules from desiccated and control flies. Consequently, this experiment was repeated using a larger sample size, as detailed in section 6.2.2.

Although desiccated flies, control flies, and food separate into clear clusters when plotted via principal component analysis (Figure 6.3), including the desiccated and control Malpighian tubule samples resulted in a clear clustering by sample type (Figure 6.8). Specifically, both Malpighian tubule sample sets clustered closely together, as did the desiccated and control whole fly samples; food clustered independently. This analysis therefore shows that the differences due to sample type are much greater than the differences incurred by desiccation stress. This is not surprising and indicates that, in general, differences in metabolite abundance within sample types are more subtle and/or less numerous than the differences between food and flies. The more subtle these effects, the larger the sample size required to identify them, as was found in this study when five replicates did not give sufficient statistical power for identifying changes in metabolite levels.

Further examination of the two principal components shown in Figure 6.8 can provide information about the extent of the differences between the sample groups. The main principal component, which accounts for 35.8% of the variability, clearly separates the food from the whole fly samples. Malpighian tubules, however, do not share all of these differences as they lie rather on the midline between the food and whole fly samples in terms of the first principal component. The substantial difference between the Malpighian tubules and the other two sample types is indicated by the second principal component, which accounts for 28.3% of the variability. Overall, these data support previous work in showing that individual insect tissues have metabolic profiles which diverge greatly from the whole organism profile (Chintapalli et al 2013a).

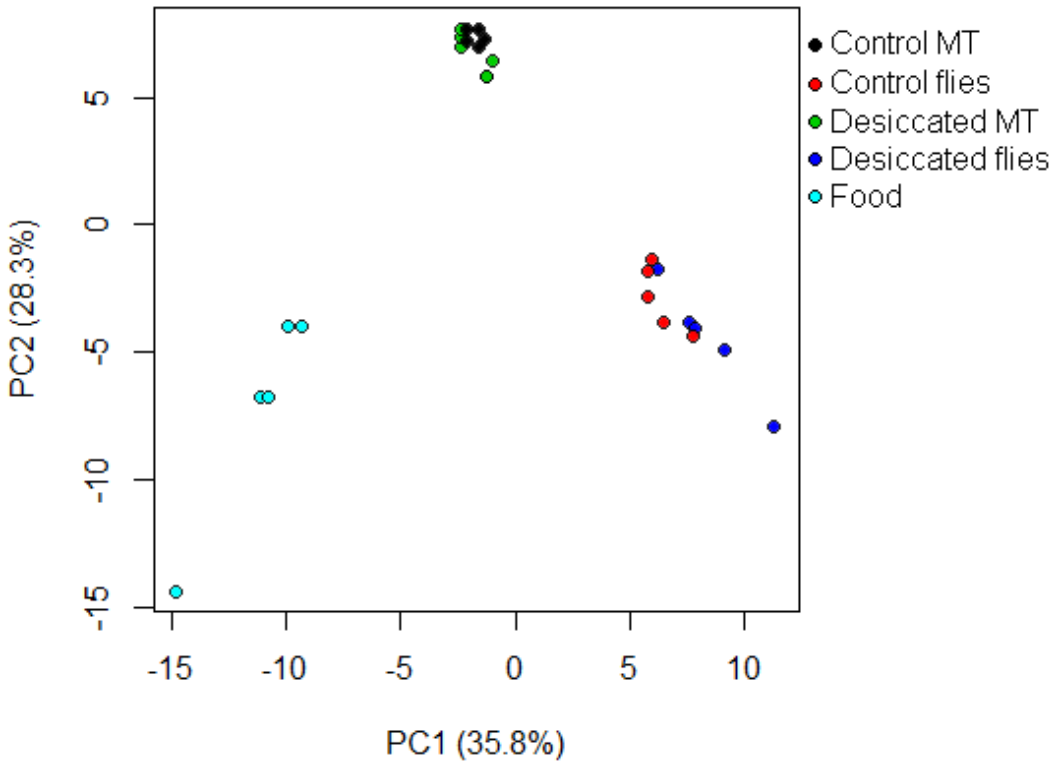

Figure 6.8 Principal component analysis of metabolite profile of whole fly and Malpighian tubules of control and desiccated *D. melanogaster* and *Drosophila* standard medium
Samples cluster into type, with food, Malpighian tubules, and whole fly showing distinct clusters when plotted against the first and second principal components. Each point indicates one of five individual biological replicates per sample type. Abbreviations: PC1 = Principal component 1, PC2 = principal component 2, MT = Malpighian tubules

As evidence indicates that the Malpighian tubules differ substantially in their metabolic profile and as this tissue is particularly important for stress and desiccation survival, the metabolic profile of Malpighian tubules following desiccation stress was again probed, as described and discussed in section 6.2.2.

6.2.2 Malpighian tubule metabolite profile following severe desiccation or mild starvation

Sets of 30 male wild-type CS *Drosophila melanogaster* were desiccated or starved for 24-26 hours, as described in section 0. Malpighian tubules were dissected from living flies only (section 2.1.4) and metabolites were extracted from sets of tubules as detailed in section 2.11.1. Including starvation as a specific sample set in the experiment enabled the effects of the starvation component of desiccation exposure to be clarified (section 2.8.2.1) and

therefore making it possible to elucidate desiccation-specific metabolic effects (section 6.2.2.4). Eight biological replicates were performed for desiccated and starved flies, and seven biological replicates were used for control samples.

As in section 6.1, exact mass was used to identify metabolites with a maximum deviation of 1.5 ppm. Retention time was used to predict the most likely isomeric identity of metabolites. Of over 420 features (peaks) across the three sets of Malpighian tubule samples, 72 metabolites were identified with high confidence, including 29 that were run alongside compound standards. Identification confidence is split into two categories as described in section 2.11.4. Detection frequency was very consistent across sample types, with all metabolites identified being detected at least three times in control, desiccated, and starved Malpighian tubules.

Principal component analysis of relative metabolite abundance in Malpighian tubules of desiccated, starved, and control flies revealed distinct clustering of each group, as shown in Figure 6.9. Together, the first and second principal components account for 52.1% of the variability. Neither component clearly distinguished sample types, with clusters rather being separated partly by each component. The most tightly clustered group was the control tubules, indicating that this group had the lowest variability between biological replicates. Starvation and desiccation exposure resulted in increasing inter-replicate variability, which corresponds with the intensity of the stress: 24 hours of desiccation stress is severe as approximately 50% of the flies are dead at this point (only living flies were included in the samples as detailed in section 2.1.4), while 24 hours of starvation stress is rather mild, with almost 100% of flies surviving this degree of starvation exposure. Thus it appears that the greater the severity of the stress, the greater the variability in the metabolic profile of the Malpighian tubules. Interestingly, the metabolite profile of starved Malpighian tubules clustered between those of control tubules and desiccated tubules, indicating that desiccated and starved samples share many similarities, but the extent of the changes in the desiccated tubules is greater than in starved tubules.

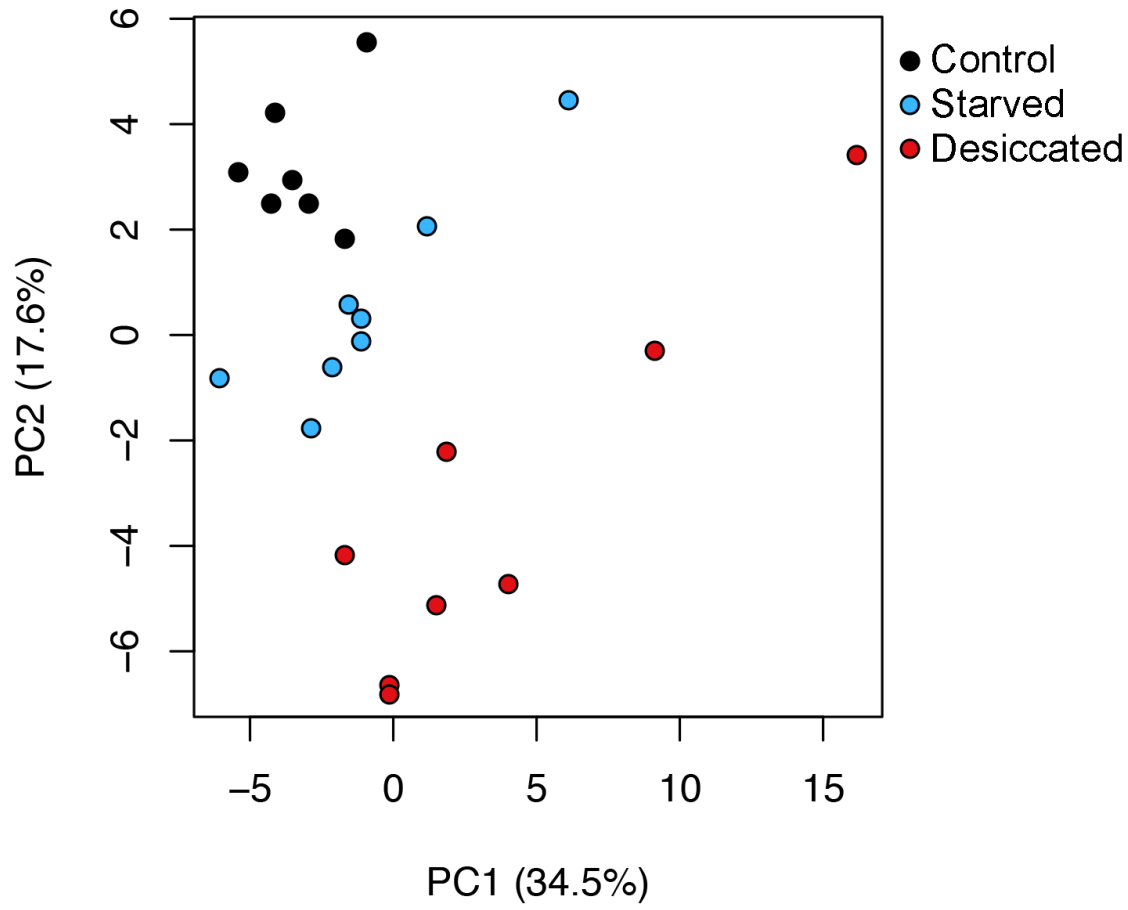

Figure 6.9 Principal component analysis of metabolite profile of Malpighian tubules of control, starved, and desiccated *D. melanogaster*

Samples cluster into type when plotted against the first and second principal components. Each point indicates one of eight individual biological replicates for starved and desiccated samples and one of seven biological replicates for control samples. Abbreviations: PC1 = Principal component 1, PC2 = principal component 2.

Metabolic changes were assessed using a statistical approach to identify robust changes, as detailed and described in section 2.11.5. The rationale for the selection of the applied tests can be found in section 1.5.6. A cross-comparison analysis reveals desiccation and starvation-specific changes and can be found in section 6.2.2.5.

6.2.2.1 Effect of desiccation on metabolic profile of Malpighian tubules

To determine statistically which metabolites differed to an interesting extent following desiccation, relative abundance of all 72 reliably detected metabolites in Malpighian tubules from desiccation flies and from control flies were statistically compared using individual two-tailed two-sample multiple t-tests

(see section 2.11.5 for details of statistical approach used and section 1.5.6 for a discussion of the rationale used in test selection). The results of this comparison should be considered together with the statistical comparison of differences between the metabolic profile of tubules from desiccated and starved flies (section 6.2.2.4). As starvation exposure is inherent in the desiccation protocol applied (section 2.8.2.1), desiccation-unique changes in metabolite profile are revealed not by comparing control samples to desiccated samples, but rather starved samples to desiccated samples.

The False Discovery Rate was set at 5% using the Benjamini and Hochberg method, as the experiment is exploratory and the goal of the analysis was to identify as many potentially interesting changes in metabolite level as possible. The result of the test was that 22 metabolites were found to differ in abundance in the Malpighian tubules following desiccation exposure (Table 6.14).

Table 6.14 Relative abundance of metabolites in Malpighian tubules (MT) of desiccated and unstressed flies compared using two-tailed two-sample Student's *t*-tests, with False Discovery Rate set at 5% using the Benjamini and Hochberg method.

Putative metabolite	Control MT mean	Desiccated MT mean	Difference	SE of difference	t ratio	df	P value
Urate	488794	3652733	3163940	171665	18.4	13	<0.0001
L-Arginine phosphate	2910.71	1174.88	1735.84	124.724	13.9	13	<0.0001
L-Tryptophan	2187179	5628447	3441268	248171	13.9	13	<0.0001
Choline phosphate	1114944	293724	821220	77720.6	10.6	13	<0.0001
Orotate	418	2069.12	1651.12	164.711	10.0	13	<0.0001
Kynurenate	11849.4	83178.5	71329.1	7935.46	9.0	13	<0.0001
myo-Inositol	45182.9	5315.12	39867.7	5280.56	7.5	13	<0.0001
Quinate	3563.14	955.286	2607.86	389.865	6.7	12	<0.0001
L-Arabinonate	7562.86	2217.62	5345.23	865.022	6.2	13	<0.0001
Xanthine	8703	22336.5	13633.5	2226.2	6.1	13	<0.0001
Pyridoxine	7010.43	11296.5	4286.07	749.558	5.7	13	0.0001
Adenine	62898.9	108505	45605.8	9584.75	4.8	13	0.0004
Choline	180737	121668	59068.3	12626.6	4.7	13	0.0004
L-Formyl-kynurenine	19139.6	31456.4	12316.8	2785.38	4.4	13	0.0007
4-(beta-Acetylamino-ethyl)-imidazole	6235	19072	12837	2949.7	4.4	12	0.0009

sn-glycero-3-Phospho-ethanolamine	2107.29	7558.5	5451.21	1346.38	4.0	13	0.0014
L-Methionine	3386285	5690111	2303826	601356	3.8	13	0.0021
L-Kynurenine	2554834	3690158	1135325	299021	3.8	13	0.0022
4-Guanidino-butanoate	14106.9	10179.5	3927.36	1043.1	3.8	13	0.0024
Taurine	3378.57	2083.62	1294.95	377.138	3.4	13	0.0044
Allantoin	2636.29	5877.38	3241.09	1002.82	3.2	13	0.0066
sn-glycero-3-Phospho-choline	38502.3	113588	75085.8	26602	2.8	13	0.0144

Relative abundance of the metabolites identified as discoveries was used to calculate a fold change following desiccation for individual metabolites. This was accomplished by dividing mean relative abundance in tubules from desiccated flies by mean metabolite relative abundance in tubules of unstressed flies. The majority of significantly changed metabolites (14/22) were found to be enriched following desiccation, as shown in Table 6.15. The remaining 8 metabolites were depleted in tubules following desiccation stress (Table 6.16). Confidence in the identification of the metabolites is indicated in the rank column of the tables, and the categories used described in section 2.11.4.

Table 6.15 Metabolites enriched in Malpighian tubules following 24 hours of desiccation stress

Exact mass and retention time (RT) are listed with the name of the most likely isomer. Fold change indicates abundance in Malpighian tubules of desiccated flies relative to abundance in tubules of control flies.

Mass	RT	Putative metabolite	Rank	Isomers	Fold change	Pathway
168.028253	11.0	Urate	2	0	7.47	Nucleotide metabolism
189.0424562	7.2	Kynurenate	2	5	7.02	Amino Acid Metabolism
156.01703	9.3	Orotate	1	1	4.95	Nucleotide metabolism
215.0559022	13.2	sn-glycero-3-Phospho-ethanolamine	2	0	3.59	Lipid metabolism
153.0899901	7.5	4-(beta-Acetylamino-ethyl)imidazole	2	2	3.06	Amino Acid Metabolism
257.1026638	12.6	sn-glycero-3-Phosphocholine	1	0	2.95	Lipid metabolism
204.0897503	11.1	L-Tryptophan	1	5	2.57	Amino Acid Metabolism

152.0333471	10.5	Xanthine	2	2	2.57	Nucleotide metabolism
158.0438878	12.6	Allantoin	2	2	2.23	Nucleotide metabolism
135.054426	9.5	Adenine	1	0	1.73	Nucleotide metabolism
149.0509534	10.9	L-Methionine	1	4	1.68	Amino Acid Metabolism
236.0795459	9.8	L-Formylkynurenine	2	1	1.64	Amino Acid Metabolism
169.0737163	7.9	Pyridoxine	1	3	1.61	Metabolism of Cofactors and Vitamins
208.0846274	10.5	L-Kynurenine	2	1	1.44	Amino Acid Metabolism

Table 6.16 Metabolites depleted in Malpighian tubules following 24 hours of desiccation stress.

Exact mass and retention time (RT) are listed with the name of the most likely isomer. Fold change indicates abundance in Malpighian tubules of desiccated flies relative to abundance in tubules of control flies.

Mass	RT	Putative metabolite	Rank	Isomers	Fold change	Pathway
180.0633576	10.6	myo-Inositol	2	56	0.12	Carbohydrate metabolism
183.0659647	12.7	Choline phosphate	2	0	0.26	Lipid metabolism
192.0634033	11.1	Quinate	2	5	0.27	Amino Acid Metabolism
166.0476796	11.6	L-Arabinonate	2	7	0.29	Carbohydrate metabolism
254.0782377	13.8	L-Arginine phosphate	2	0	0.40	Amino Acid Metabolism
125.0145762	12.9	Taurine	1	0	0.62	Lipid metabolism
103.0996119	19.3	Choline	2	0	0.67	Amino Acid Metabolism
145.0850238	13.3	4-Guanidino-butanoate	2	2	0.72	Amino Acid Metabolism

6.2.2.2 Desiccation stress significantly affects multiple metabolic pathways in Malpighian tubules

When compared to the whole fly samples, relatively few metabolites were identified in the Malpighian tubules (73 in tubules, 131 in whole flies). These can be divided into categories based on their role in metabolism and the number of metabolites identified the Malpighian tubules and involved in each type of

metabolism is shown in Figure 6.10A. When the number of metabolites identified per metabolic category is compared for Malpighian tubules and whole flies (Figure 6.4A), it can be seen that a different pattern of metabolite identification is present in each sample. In particular, a smaller proportion of the identified metabolites is involved in amino acid metabolism (58% rather than 69%). On the other hand, 10 metabolites related to carbohydrate metabolism were detected in the Malpighian tubules, while only 6 metabolites in this pathway were found in whole fly samples. There is a relatively higher proportion of metabolites identified involved in nucleotide metabolism and lipid metabolism in the Malpighian tubules than in flies. These values suggest that carbohydrate metabolism may be particularly important in the Malpighian tubules, while amino acid metabolism may be less active in this tissue than in flies as a whole.

A percentage of changed metabolites was calculated for desiccated Malpighian tubules by grouping changed metabolites into metabolism areas and dividing by the total number of metabolites identified in the dataset for each metabolic area, as shown in Figure 6.10B. As desiccated samples were compared to control samples, some of the metabolite changes identified may be due to the starvation component of desiccation exposure (see sections 2.8.2.1 and 6.2.2.4). Metabolites relating to nucleotide metabolism and metabolism of cofactors and vitamins were exclusively enriched in the Malpighian tubules following desiccation, while metabolites relating to carbohydrate metabolism were depleted. Conversely, some metabolites relating to amino acid metabolism and lipid metabolism were enriched, while others were depleted.

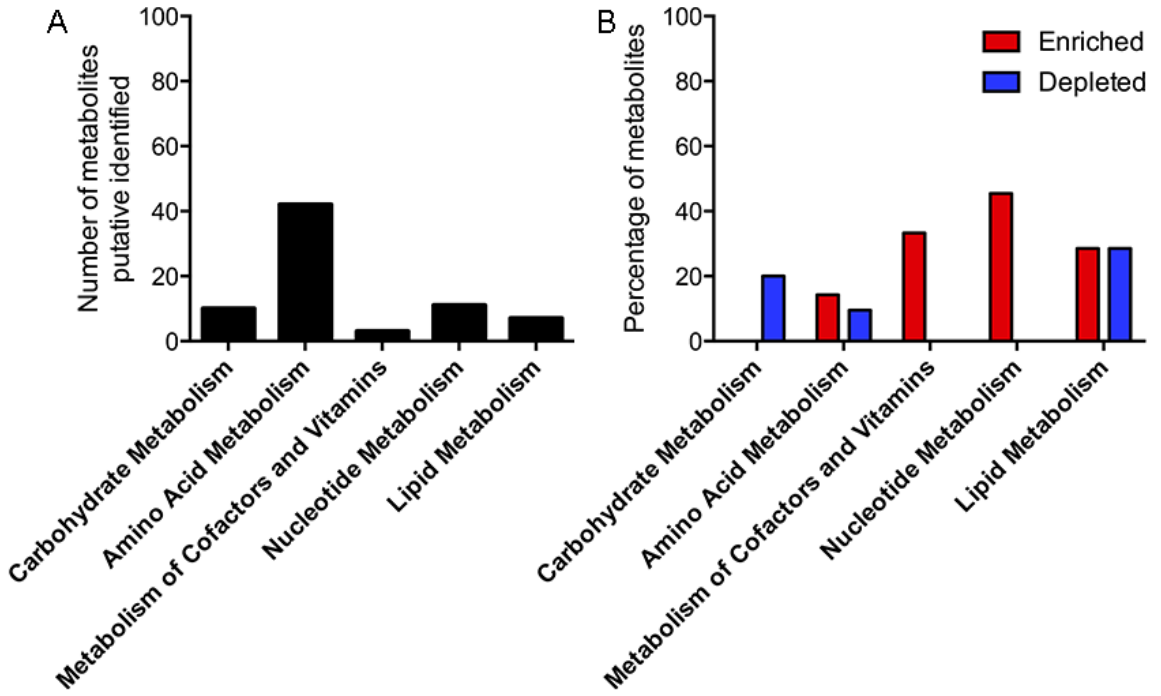

Figure 6.10 Desiccation stress affects metabolite levels in multiple metabolic pathways in the Malpighian tubules

A) The majority of metabolites identified in the Malpighian tubules is involved in amino acid metabolism. **B)** Percentage of metabolites from each metabolism area enriched or depleted following desiccation is calculated by dividing number of metabolites in each category that are either significantly higher or lower in abundance in desiccated Malpighian tubules by the number of metabolites in total identified in that category in the entire tubule dataset.

The depletion of carbohydrate metabolites in the Malpighian tubules following desiccation may be due to the starvation component of desiccation stress, as tubules from starved flies had similar decreases in the same two metabolites following a similar period of starvation (see Table 6.23; myo-Inositol and L-Arabinonate). Similarly, the enrichment of cofactor and vitamin metabolites in the tubules following desiccation may not be especially significant as it depends on changes in only one metabolite (Pyridoxine) and is based on a fold change of only 1.61. The enrichment of nucleotide metabolism metabolites, however, is particularly interesting as 5 different metabolites were found to be enriched in the tubules following desiccation. Only one of these (Allantoin), may be due to the starvation aspects of desiccation (see discussion of Table 6.23).

6.2.2.3 Effect of starvation on metabolic profile of Malpighian tubules

Changes in relative abundance of metabolites in the Malpighian tubules following mild starvation stress (24 hours) were tested statistically by comparing the relative abundance of 72 metabolites using individual two-tailed two-sample multiple t-tests as described in section 2.11.5. The rationale for the selection of the applied tests can be found in section 1.5.6. By applying a False Discovery Rate of 5% using the Benjamini and Hochberg method, the test identified eight metabolites as differing in abundance in the Malpighian tubules following starvation exposure (Table 6.17).

Table 6.17 Relative abundance of metabolites in Malpighian tubules (MT) of starved and unstressed flies compared using two-tailed two-sample Student's *t*-tests, with False Discovery Rate set at 5% using the Benjamini and Hochberg method.
Degrees of freedom of all comparisons is 13.

Putative metabolite	Control MT mean	Starved MT mean	Difference	SE of difference	t ratio	P value
myo-Inositol	45182.9	6006.38	39176.5	5278.23	7.4	<0.0001
Quinate	3563.14	1219.25	2343.89	368.289	6.4	<0.0001
Choline phosphate	1114944	566049	548895	88688.1	6.2	<0.0001
L-Arabinonate	7562.86	2454	5108.86	876.763	5.8	0.0001
Kynurenate	11849.4	22993.2	11143.8	2323.17	4.8	0.0003
Xanthine	8703	12425.8	3722.75	997.971	3.7	0.0025
Allantoin	2636.29	8267.25	5630.96	1535.58	3.7	0.0028
Urate	488794	1349164	860371	258029	3.3	0.0054

A fold change for metabolites with significantly altered relative abundance was calculated by dividing mean relative abundance in Malpighian tubules from starved flies by mean metabolite relative abundance in tubules of unstressed flies. Metabolites were evenly split into enriched and depleted metabolites, with four metabolites being enriched in the tubules following starvation (Table 6.18) and four being depleted in tubules (Table 6.19). The categories and method used for confidence ranking can be found in section 2.11.4 and is indicated in tables in the rank column.

Table 6.18 Metabolites enriched in Malpighian tubules following 24 hours of starvation stress.

Exact mass and retention time (RT) are listed with the name of the most likely isomer. Fold change indicates abundance in Malpighian tubules of starved flies relative to abundance in tubules of control flies.

Mass	RT	Putative metabolite	Rank	Isomers	Fold change	Pathway
158.0438878	12.6	Allantoin	2	2	3.14	Nucleotide metabolism
168.028253	11.0	Urate	2	0	2.76	Nucleotide metabolism
189.0424562	7.2	Kynurenate	2	5	1.94	Amino Acid Metabolism
152.0333471	10.5	Xanthine	2	2	1.43	Nucleotide metabolism

Table 6.19 Metabolites depleted in Malpighian tubules following 24 hours of starvation stress.

Exact mass and retention time (RT) are listed with the name of the most likely isomer. Fold change indicates abundance in Malpighian tubules of starved flies relative to abundance in tubules of control flies.

Mass	RT	Putative metabolite	Rank	Isomers	Fold change	Pathway
180.0633576	10.6	myo-Inositol	2	56	0.13	Carbohydrate metabolism
166.0476796	11.6	L-Arabinonate	2	7	0.32	Carbohydrate metabolism
192.0634033	11.1	Quinate	2	5	0.34	Amino Acid Metabolism
183.0659647	12.7	Choline phosphate	2	0	0.51	Lipid metabolism

6.2.2.4 Metabolic profile following desiccation differs significantly from changes following starvation

As the method used to desiccate flies involves removing both food and water, it is possible that the effect of starvation on metabolism could account for some or all of the differences in metabolite relative abundance observed after desiccation. The inclusion of Malpighian tubules from starved flies as a control sample makes it possible to determine which metabolites are altered in abundance by desiccation in a way that is different from the effects of starvation. Potential desiccation-specific metabolic changes were identified by using individual two-tailed two-sample multiple t-tests to compare relative abundance of metabolites in the Malpighian tubules following desiccation stress or starvation stress as described in section 2.11.5. The rationale for the selection of the applied tests can be found in section 1.5.6. A False Discovery

Rate of 5% was applied % using the Benjamini and Hochberg method. A total of 13 metabolites were considered to be discoveries using this approach, as shown in Table 6.20.

Table 6.20 Relative abundance of metabolites in Malpighian tubules (MT) of desiccated and starved flies compared using two-tailed two-sample Student's *t*-tests, with False Discovery Rate set at 5% using the Benjamini and Hochberg method.

The degrees of freedom of all statistical tests is 14.

Putative metabolite	P value	Starved MT mean	Desiccated MT mean	Difference	SE of difference	t ratio
Urate	<0.0001	1349164	3652733	2303569	286625	8.0
Kynurenate	<0.0001	22993	83179	60185	7582	7.9
Orotate	<0.0001	702	2069	1368	193	7.1
L-Tryptophan	<0.0001	3146869	5628447	2481578	371812	6.7
L-Arginine phosphate	<0.0001	2857	1175	1682	267	6.3
Pyridoxine	0.0001	7955	11297	3341	582	5.7
Adenine	0.0001	61518	108505	46987	8790	5.3
Xanthine	0.0004	12426	22337	9911	2115	4.7
sn-glycero-3-Phosphoethanolamine	0.0011	2374	7559	5184	1268	4.1
Inosine	0.0013	20668	35048	14380	3599	4.0
4-(beta-Acetylaminoethyl)imidazole	0.0017	8363	19072	10709	2777	3.9
Choline phosphate	0.0022	566049	293724	272325	72810	3.7
L-Formyl-kynurenine	0.0050	21956	31456	9500	2853	3.3

Enrichment in the tubules of desiccated flies relative to those of starved flies was calculated by dividing mean relative abundance in tubules from desiccated flies by mean metabolite relative abundance in tubules of starved flies. Almost all of the metabolites identified by the statistical testing were found to be enriched in the tubules of desiccated flies relative to starved flies (Table 6.21), while only two metabolites were found to be depleted (Table 6.22).

Table 6.21 Metabolites uniquely enriched in Malpighian tubules during desiccation when controlling for effect of starvation

Exact mass and retention time (RT) are listed with the name of the most likely isomer. For details of confidence ranking, see section 2.11.5. Enrichment indicates abundance in Malpighian tubules of desiccated flies relative to abundance in tubules of starved flies.

Mass	RT	Putative metabolite	Rank	Isomers	Enrichment	Pathway
189.0424562	7.2	Kynurenate	2	5	3.62	Amino Acid Metabolism
215.0559022	13.2	sn-glycero-3-Phospho-ethanolamine	2	0	3.18	Lipid metabolism
156.01703	9.3	Orotate	1	1	2.95	Nucleotide metabolism
168.028253	11.0	Urate	2	0	2.71	Nucleotide metabolism
153.0899901	7.5	4-(beta-Acetyl-aminoethyl)-imidazole	2	2	2.28	Amino Acid Metabolism
152.0333471	10.5	Xanthine	2	2	1.80	Nucleotide metabolism
204.0897503	11.1	L-Tryptophan	1	5	1.79	Amino Acid Metabolism
135.054426	9.5	Adenine	1	0	1.76	Nucleotide metabolism
268.0808697	10.4	Inosine	1	2	1.70	Nucleotide metabolism
236.0795459	9.8	L-Formyl-kynurenine	2	1	1.43	Amino Acid Metabolism
169.0737163	7.9	Pyridoxine	1	3	1.42	Metabolism of Cofactors and Vitamins

Table 6.22 Metabolites uniquely depleted in Malpighian tubules during desiccation when controlling for effect of starvation

Exact mass and retention time (RT) are listed with the name of the most likely isomer. For details of confidence ranking, see section 2.11.5. Enrichment indicates abundance in Malpighian tubules of desiccated flies relative to abundance in tubules of starved flies.

Mass	RT	Putative metabolite	Rank	Isomers	Enrichment	Pathway
254.0782377	13.8	L-Arginine phosphate	2	0	0.41	Amino Acid Metabolism
183.0659647	12.7	Choline phosphate	2	0	0.52	Lipid metabolism

Overall, fewer metabolites were identified as significantly changed in abundance when comparing tubules from desiccated flies to those from starved flies than when comparing desiccated tubules to control tubules.

6.2.2.5 Shared trends in metabolite abundance changes in desiccation and starvation

The contributions of dehydration and starvation to the overall changes in individual metabolite levels following desiccation can be separated by comparing the enrichment values of the significantly changed metabolites identified in sections 6.2.2.1, 6.2.2.2, and 6.2.2.4, as shown in Table 6.23. Almost all metabolites identified as discoveries in the comparisons detailed in sections 6.2.2.2 and 6.2.2.4 were also identified as significant when comparing desiccated to control samples. The only exception to this rule was inosine, which was only identified as changed when comparing metabolite profiles of desiccated tubules to starved tubules. Upon further inspection, it can be seen that this was due to the abundance of inosine increasing slightly (18 %) following desiccation and decreasing somewhat (30%) in abundance following starvation. In all other cases, metabolite abundance either changed in the same direction following desiccation and starvation or changed in only one condition and remained approximately constant in the other.

Table 6.23 Significant changes in abundance of metabolites in the Malpighian tubules following either desiccation or starvation stress exposure

Relative abundances that were found to be significantly different between sample sets are indicated by an asterisk to the left of the enrichment value. DMT = desiccated Malpighian tubules, CMT = control Malpighian tubules, SMT = starved Malpighian tubules

Putative metabolite	Enrichment					
	DMT/ CMT		SMT/ CMT		DMT/ SMT	
Urate	*	7.47	*	2.76	*	2.71
Kynurenate	*	7.02	*	1.94	*	3.62
Orotate	*	4.95		1.68	*	2.95
sn-glycero-3-Phosphoethanolamine	*	3.59		1.13	*	3.18
4-(beta-Acetylaminoethyl)imidazole	*	3.06		1.34	*	2.28
sn-glycero-3-Phosphocholine	*	2.95		1.13		2.61
L-Tryptophan	*	2.57		1.44	*	1.79
Xanthine	*	2.57	*	1.43	*	1.80
Allantoin	*	2.23	*	3.14		0.71
Adenine	*	1.73		0.98	*	1.76
L-Methionine	*	1.68		1.22		1.38
L-Formylkynurenine	*	1.64		1.15	*	1.43
Pyridoxine	*	1.61		1.13	*	1.42
L-Kynurenine	*	1.44		1.18		1.23
Inosine		1.18		0.70	*	1.70
4-Guanidinobutanoate	*	0.72		0.86		0.84
Choline	*	0.67		0.76		0.89
Taurine	*	0.62		0.82		0.75
L-Arginine phosphate	*	0.40		0.98	*	0.41
L-Arabinonate	*	0.29	*	0.32		0.90
Quinate	*	0.27	*	0.34		0.78
Choline phosphate	*	0.26	*	0.51	*	0.52
myo-Inositol	*	0.12	*	0.13		0.88

When comparing the metabolites that changed in abundance following desiccation to those that changed following starvation, it can be seen that 24 hours of starvation exposure did not affect the abundance of any tubule metabolites that were not also significantly affected by desiccation (Table 6.23). Indeed some of these metabolites exhibit similar enrichment in starved tubules and in desiccated tubules, suggesting that these effects on metabolite levels can be explained by the starvation component of the desiccation stress method used. This is particularly the case for metabolites that decrease in abundance

following desiccation or starvation stress. More specifically, abundance of L-arabinonate, quinate, and myo-inositol were very similar in tubules following either desiccation or starvation, when compared to unstressed controls. In contrast, L-arginine phosphate decreased significantly only in desiccated tubules, suggesting that this change is unique to the stress encountered only in the desiccation condition. Choline phosphate decreased in tubules by approximately 50% following starvation, but approximately 75% following desiccation, suggesting that metabolic processes involving this metabolite are affected in both conditions, although more strongly in desiccation.

All of the significantly changed metabolites that were enriched in starved tubules were even more abundant in desiccated tubules, apart from allantoin. This metabolite was actually more enriched in starved tubules, indicating that while this metabolite may be increased following desiccation, it is most likely due to the lack of food encountered by the flies during desiccation.

Overall, these results indicate the merit of including starvation as a control for desiccation, when the desiccation methods used require the flies to be simultaneously starved. Comparing enrichment of metabolites across these three conditions reveals changes that are unique to each stressor.

6.2.2.6 Pigment precursors are enriched in Malpighian tubules during desiccation

Tissue-specific metabolomics analysis of *D. melanogaster* has revealed that the Malpighian tubules are especially enriched in tryptophan, despite generally low abundance of amino acids in this tissue (Chintapalli et al 2013a). Moreover, downstream metabolites L-kynurenine, 3-hydroxy-L-kynurenine, hydroxykynurenate, L-formylkynurenine and 5-hydroxy-L-tryptophan were also found to be highly enriched in the tubules, a finding consistent with prior research showing that the tubules actively take up tryptophan (Sullivan et al 1980). Tryptophan metabolism is thought to be particularly active in the Malpighian tubules as tryptophan is a pigment precursor and the tubules are known to collect and process visual pigment precursors (Tearle 1991).

In the present study, tryptophan was found to be enriched in the tubules of desiccated flies relative to control flies, as was many of its downstream

metabolites (Figure 6.11). Prior studies have found changes in abundance of metabolites in this pathway in response to cold exposure and cold stress acclimation (Overgaard et al 2007, Williams et al 2014). Most of the metabolites in the tryptophan processing pathway that were previously identified as enriched in the Malpighian tubules were identified in this study as well (Chintapalli et al 2013a). The only exception was hydroxykynurenate, which was not detected. However, two additional downstream components of the pathway were identified, kynurenate and xanthurenic acid. Kynurenate was one of the most highly accumulated metabolite following desiccation identified in tubules in this study, with a 602% increase in abundance. Kynurenate was additionally found to be enriched in the tubules of starved flies, although not to the same extent as in desiccated flies (increase of 94%). The three upstream metabolites show a trend towards enrichment during starvation although this was not statistically significant. The accumulation of metabolites in the tryptophan degradation pathway shows some parallels after desiccation and starvation: in both cases, the most enriched metabolite is kynurenate, followed by tryptophan, with the remaining two linking metabolites being relatively mildly enriched.

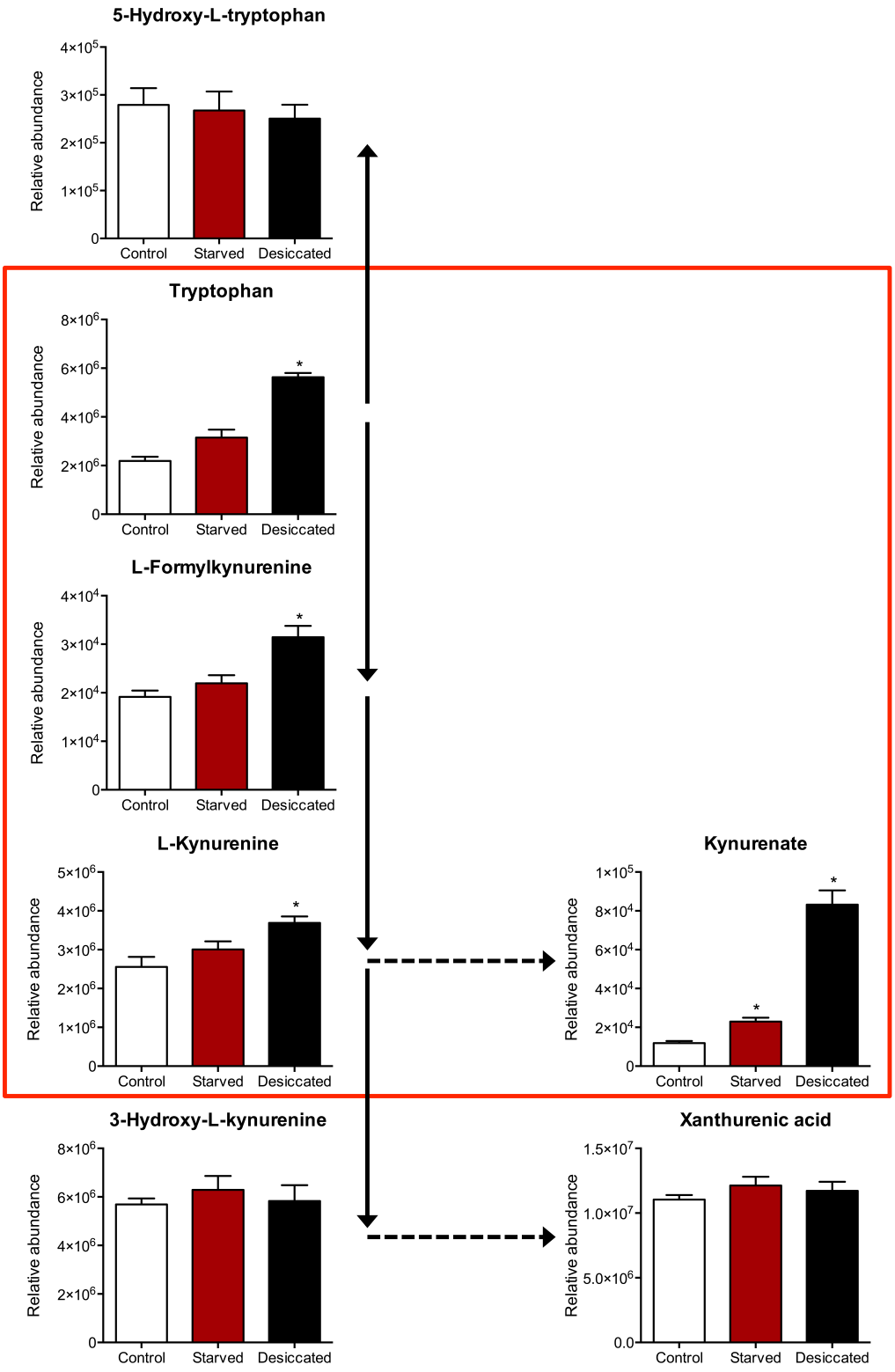

Figure 6.11 Tryptophan metabolism in the Malpighian tubules is significantly affected by desiccation stress

Relative abundance of metabolites in the tryptophan degradation pathway is shown in tubules from unstressed flies or in tubules dissected following desiccation or starvation. Arrows indicate direction of metabolism. A solid arrow indicates a direct relation, while dashed arrows indicate that a metabolic intermediate step is thought to exist, but was not detected in this experiment. The red box outlines all metabolites that are increased in abundance in desiccated tubules.

The accumulation of tryptophan and its degradation products supports the idea that the Malpighian tubules normally process these metabolites. It is likely that the metabolites accumulate due to the decreased rate of secretion known to occur after severe desiccation. The increase in some of the pathway metabolites after starvation is somewhat more surprising, although it is possible that energy shortages due to lack of nutrient input may impair tubule functioning, as the tissue is known to require abundant energy resources in order to maintain operation of the vacuolar H^+ ATPase and for K^+ conductance (Beyenbach 2001, Wu & Beyenbach 2003).

It is interesting that while kynurenate accumulates to a great extent following desiccation, 3-hydroxykynurenine does not. This could potentially be advantageous to survival as evidence indicates that kynurenate is a protective compound while 3-hydroxykynurenine can have toxic effects (Campesan et al 2011, Williams et al 2014).

The metabolomics study examining changes in levels of metabolites in the entire fly following desiccation also revealed increases in abundance of metabolites resulting from tryptophan degradation. In particular, kynurenate levels were higher in desiccated flies, as were downstream metabolites 8-methoxy-kynurenate and 4,8-dihydroxy-quinoline. However, the inter-sample variability was very high, so these results should be regarded cautiously.

6.2.2.7 Desiccation and starvation interfere with nitrogen clearance pathway

Purine degradation results in the production of xanthine and the downstream product uric acid, which can be used to form urate in salt form. Many insects take up these compounds via the Malpighian tubule for excretion, which serves as one of the main pathways of eliminating excess nitrogen (Dow 2013, O'Donnell 2009). In some insects uric acid is pumped into the tubules in a manner that is proportional to the concentration of urate in the hemolymph (O'Donnell et al 1983). Uric acid is not always excreted, but can be stored temporarily in the Malpighian tubules, sometimes as crystals (Dow & Romero 2010). As urate has strong antioxidant properties, this may protect the tissue from reactive oxygen species resulting from energy metabolism by mitochondria (Dow 2013, Hilliker et al 1992). Thus, it is evident that the tubules are a particularly important tissue

for the accumulation and excretion of waste products that are high in nitrogen. When the Malpighian tubules are not functioning properly, urate can accumulate; urate deposits were found in tubules with mutated morphology and atypical expression of the Na^+/K^+-ATPase pump (Gautam et al 2015).

Uric acid can be further metabolised into allantoin, and ultimately to ammonia, which has been found to increase in concentration in the hemolymph of desiccated blister beetles, *Cysteodemus armatus* (Cohen et al 1986). However, as accumulation of ammonia can be toxic (Withers 1992), ammonia molecules may be stored by converting glutamate to glutamine, a process that consumes one molecule of ammonia per conversion. The ratio of glutamine: glutamate can indicate the level of ammonia production occurring in a particular tissue. The Malpighian tubules have been found to have a particularly high glutamine: glutamate ratio in *D. melanogaster* relative to other tissues, presumably due to its role in ammonia production (Chintapalli et al 2013a, Chintapalli et al 2012). Accumulation of orotate (orotic acid) can also be indicative of increased levels of ammonia in a tissue and can occur as a result of urea cycle disorder, an inborn error of metabolism (Bachmann & Colombo 1980, Kesner 1965).

Interestingly, following desiccation, urate is highly enriched in the Malpighian tubules, as are its precursors xanthine and adenine and downstream metabolite allantoin, as shown in Figure 6.12. Further evidence of the accumulation of metabolites in this pathway is provided by a significantly higher ratio of glutamine: glutamate in the tubules following desiccation (M = 3.96, SD = 0.47) than in unstressed flies (M = 2.94, SD = 0.23), $t(13) = 5.230$, $p = 0.0002$ (Figure 6.13A). Many of the increases in purine degradation pathway metabolites are also observed in the tubules following starvation, although typically to a lesser extent. Likewise the ratio of glutamine: glutamate is elevated in the tubules of starved flies (M = 3.64, SD = 0.58), $t(13) = 3.006$, $p = 0.0101$. These results suggest that the tubules may be accumulating ammonia, which is additionally supported by the increase in abundance of orotic acid by 395% following desiccation. Increased ammonia load in the tubules may be a reflection of changes in the entire fly, as the whole fly glutamine: glutamate ratio following desiccation (M = 5.60, SD = 0.17) is significantly higher than in control flies (M = 2.95, SD = 0.19), $t(8) = 10.17$, $p < 0.0001$, as shown in Figure 6.13B.

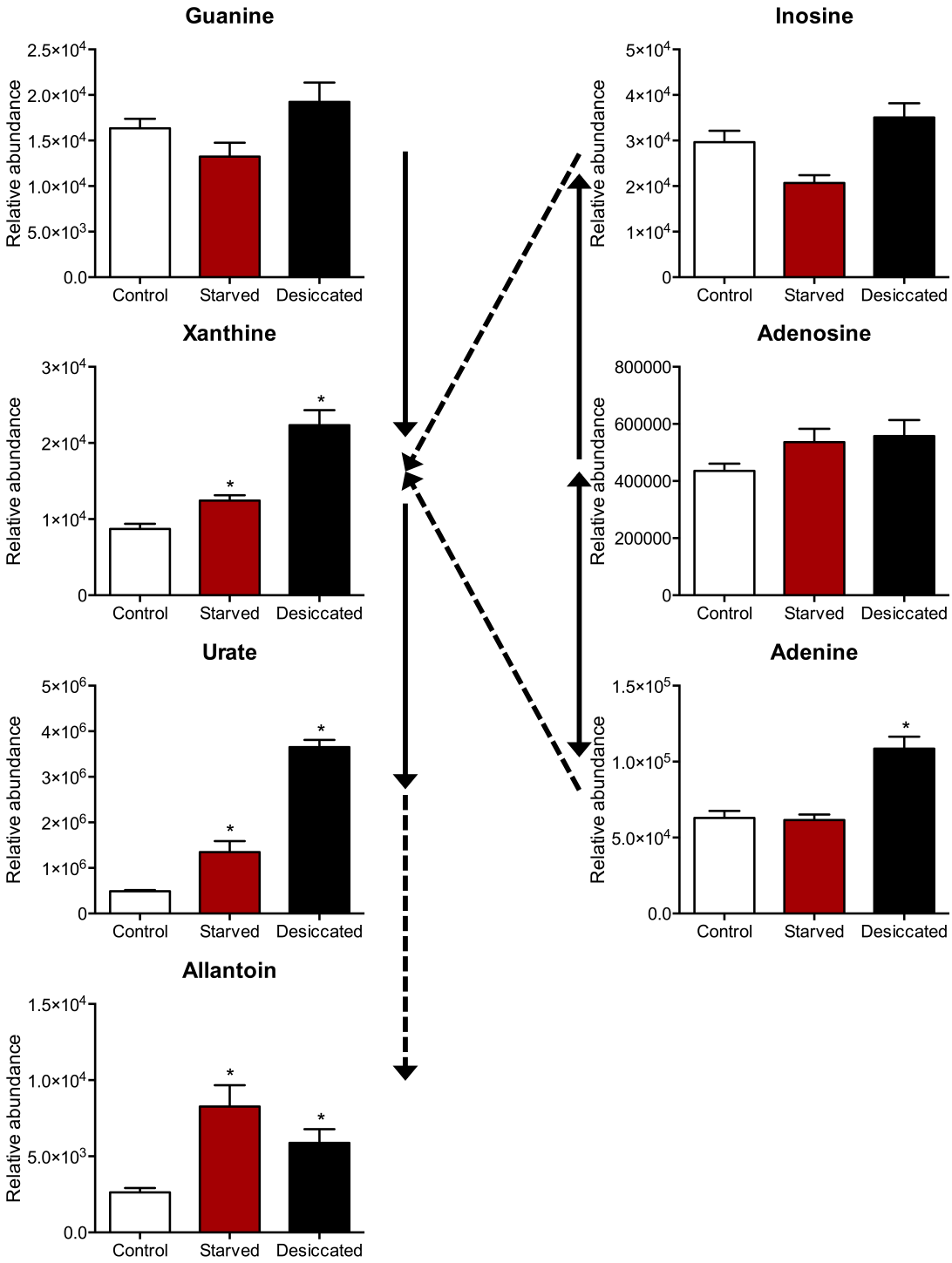

Figure 6.12 Purine metabolism in the Malpighian tubules is significantly affected by desiccation and starvation stress

Relative abundance of metabolites in the purine degradation pathway is shown in tubules from unstressed flies or in tubules dissected following desiccation or starvation. Arrows indicate direction of metabolism. A solid arrow indicates a direct relation, while dashed arrows indicate that a metabolic intermediate step is thought to exist, but was not detected in this experiment.

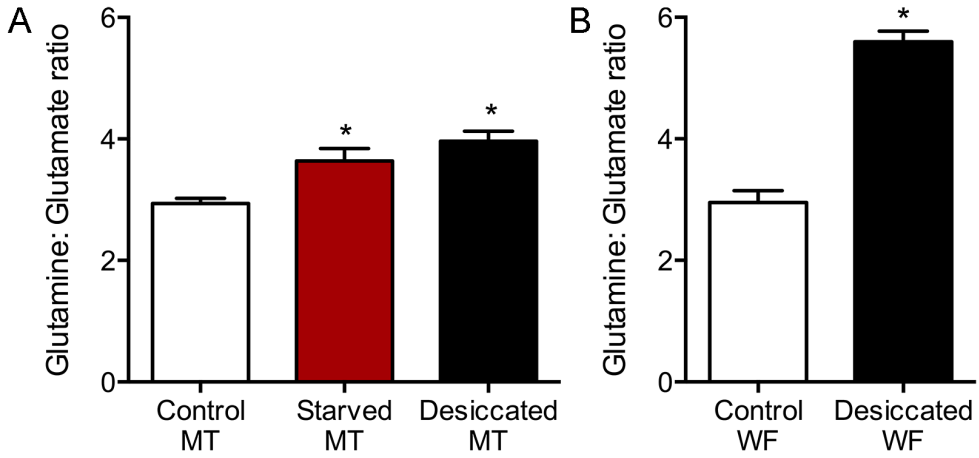

Figure 6.13 Ammonia load, as indicated by the ratio of glutamine: glutamate, is increased following desiccation and starvation stress in *D. melanogaster*

A) The ratio of glutamine: glutamate is significantly increased in the Malpighian tubules (MT) following starvation or desiccation stress. **B)** The ratio of glutamine: glutamate is significantly increased in whole fly (WF) *D. melanogaster* following desiccation stress, * $p < 0.05$ (two-sample two-tailed Student's *t*-test).

The consistently increased levels of multiple metabolites in the purine degradation pathway following desiccation indicate that there is an accumulation of metabolites that typically lead to the excretion of excess nitrogen. Insects often excrete nitrogen in highly insoluble forms like uric acid to prevent water loss, but in instances of intense dehydration, it is possible that nitrogen may be stored as uric acid rather than excreted to reduce water loss. Reductions in secretion by the tubules have previously been found to result in urate deposits (Gautam et al 2015). Alternatively, urate may be stored in the tubules during periods of stress to protect against oxidative stress. The moderate increases in some metabolites involved in purine degradation following starvation stress may likewise be due to potentially decreased energy availability to the tubules preventing normal secretion, or accumulation of urate as a protection mechanism. It additionally appears that there is a heightened burden of ammonia in the tubules following desiccation, and to a lesser extent following mild starvation exposure. This, however, may not be as high as in other tissues of the fly.

The effects of desiccation on the kynurenine pathway and purine metabolism may be connected. Changes in purine metabolism have been associated with

altered abundances of metabolites in the kynurenine pathway (Al Bratty et al 2012). Thus, it is interesting to find in the present study that the two most accumulated metabolites in the tubules following desiccation are from these two associated pathways.

6.2.2.8 Glycerophospholipid metabolism is affected by desiccation

Periods of osmotic stress can result in alterations in membrane phospholipids, and has been found to affect the levels of different kinds of glycerophospholipids (Crowe et al 1992, Holmstrup et al 2002, Tomcala et al 2006). Cold stress, and to a lesser extent desiccation stress, was found to affect thoracic muscle and fat body tissues of the insect *Pyrrhocoris apterus* such that there was an increase in glycerophosphoethanolamines (GPEtns), while simultaneously reducing the levels of glycerophosphocholines (GPChols) (Tomcala et al 2006). Likewise, in *D. melanogaster* larvae, chronic cold exposure was found to result in an increased of GPEtns and an associated decrease in levels of GPChols (Kostal et al 2011).

In the present study, only two phospholipids were detected, sn-glycero-3-phosphoethanolamine and sn-glycero-3-phosphocholine, both of which were found to significantly increase in tubules following desiccation, but not after a similar period of starvation. Choline and choline phosphate (phosphocholine), which are required for the formation of GPChols, were both found to be significantly decreased in abundance in the tubules following desiccation. Phosphocholine was also lower in abundance in tubules following starvation exposure. One possible reason why phosphocholine and choline levels may be reduced is that choline is an essential nutrient for *D. melanogaster* (Tilghman & Geer 1988). However, dietary restriction of choline has been found to result in reduced levels of GPChols (Tilghman & Geer 1988), a result that contrasts with the increase in GPChol levels found following desiccation in this study both in Malpighian tubules and in the whole fly. Clearly long-term restriction of choline intake affects metabolism differently than a short period of total food and water deprivation in *D. melanogaster*.

In the whole fly samples, increases in the levels of sn-glycero-3-phosphoethanolamine and sn-glycero-3-phosphocholine were also observed

following desiccation, although only the latter change was statistically significant due to high variability in sn-glycero-3-phosphoethanolamine levels in desiccated flies. Conversely, desiccation was not found to influence abundance of choline and phosphocholine in the fly as a whole.

Overall, these results suggest that changes take place in the composition of lipid membranes during desiccation. This is consistent with research indicating that the intensive osmotic stress of desiccation can alter the structure of lipid membranes (Holmstrup et al 2002, Levis et al 2012). It also appears that the significant decrease in choline and phosphocholine may be a tissue-specific effect of desiccation in the Malpighian tubules, as whole fly samples did not reflect similar changes.

6.2.2.9 Osmolyte levels are reduced following desiccation

The Malpighian tubules are able to transport taurine and other osmolytes via the Na^+/Cl^--dependent neurotransmitter/osmolyte transporter family (Huang et al 2002). Based on the role of this metabolite as an osmolyte, it is not surprising that the relative abundance of taurine following desiccation is significantly decreased. As liquid availability decreases, the concentration of osmolytes and ions in the lumen and cell bodies of the tubules may increase, resulting in decreased transportation of small molecules into the tubules.

6.3 Discussion

The numerous changes observed in whole fly metabolite levels following 24 hours of desiccation exposure provides evidence that the metabolism of *D. melanogaster* is greatly affected by the absence of food and water. In particular, changes were seen in the lysine degradation pathway, as well as in the levels of the activity-related neurotransmitters dopamine and acetylcholine. Many more metabolites were identified as changing in abundance, although many were not closely associated within metabolic pathways.

Far fewer metabolites were identified as changing in abundance in the Malpighian tubules after desiccation relative to the whole fly dataset, although these were found to segregate more clearly into several specific categories. In particular, tryptophan and purine degradation were disrupted, causing the

accumulation of multiple metabolites in each pathway, and evidence indicated an associated impairment of nitrogen clearance. Moreover, the glycerophospholipid balance in the tubules was altered, suggesting that restructuring of lipid membranes took place, and the level of the osmolyte taurine was found to be decreased. When considered together, these changes imply that the tubules from desiccated flies do not eliminate toxins and metabolic waste as quickly as those of unstressed flies. This is consistent with the finding that the baseline secretion rate of the Malpighian tubules of *D. melanogaster* is significantly reduced by desiccation exposure (Chapter 3). This could signify a change from normal secretory function towards water conservation. The changes observed additionally support the idea that the tubule environment has been significantly shaped by the lack of water, in that alterations in lipid membrane are associated with extreme lack of water, and a reduction in the level of osmolytes could be a result of attempting to maintain osmotic balance within the tissue in the face of greatly decreased fluid availability (Crowe et al 1992).

When the whole fly dataset and the Malpighian tubule dataset are contrasted, it is evident that analysis of a whole organism cannot sufficiently capture the nuances of metabolic changes during stress exposure and survival. Every tissue has a unique metabolite profile in *D. melanogaster,* and blending these together can make it difficult to identify metabolites that are abundant only in particular tissues (Chintapalli et al 2013a). Moreover, each tissue may respond differently to the stress such that critical changes may be overshadowed by more abundant metabolites, or opposite changes in various tissues may obscure important stress effects.

The metabolic changes observed after desiccation in the Malpighian tubule samples fit more clearly into known metabolic pathways when contrasted with the plethora of diverse changes observed in the whole fly samples. This suggests that the tubules may serve to support specific metabolic pathways. Most importantly, these data provide clear evidence that while whole-organism metabolomics may seem to be a useful time-saving measure, tissue-specific metabolomics is better suited to answer questions regarding the effect of stress on metabolism. It could even be argued that more useful information can be acquired by breaking down tissues into sub-units. In the Malpighian tubules, for

example, the posterior and anterior tubules have been found to serve unique functions (Chintapalli et al 2012), and examining these separately following desiccation may provide even more detailed insight.

Some of the changes observed in the Malpighian tubules following desiccation were also found in the whole fly dataset, suggesting either that these changes occur in more than one tissue in the fly or that even a small tissue like the tubules can affect the overall profile of the entire organism. However, in all cases, pathway analysis revealed that a greater number of metabolites from the affected pathways were identified in tubules than in the whole fly. This made pathway analysis substantially easier and more robust in the tubule samples, again providing support for the use of tissue-specific samples for metabolomic analysis of insects.

The inclusion of starvation as a control for desiccation in the Malpighian tubule samples showed that lack of water affects the metabolome of *D. melanogaster* to an extent that is significantly greater than starvation in 24 hours. All of the metabolites that changed significantly during starvation also changed significantly in desiccated flies. Several of the decreases were similar in extent following desiccation and starvation, suggesting that perhaps these decreases are due simply to the absence of food. Conversely, almost all of the metabolites that increased in abundance during starvation increased to a much greater extent following desiccation. It is interesting that several of these changes are shared given the different nature of the stressors and the much greater mortality observed during 24 hours of desiccation than during 24 hours of starvation exposure in male flies. This suggests, then, that even mild starvation stress may affect tubule functioning long before the stress exposure becomes critical or fatal. Thus the Malpighian tubules may help to adapt the fly to survive not only reduced water availability, but also situations of food scarcity.

In both datasets, a second controls was included and contrasted with the desiccated and unstressed samples. In the whole fly dataset, food was used as the second control, and in the Malpighian tubule dataset, tubules from starved flies were used to control for the effect of food deprivation during desiccation exposure. The two different controls allowed different comparisons to be made and supported the main data of the experiments in different ways. In particular,

the inclusion of food as a control alongside the whole fly dataset identified that glucose and sucrose were enriched in food, as expected, and that these metabolites are depleted in the flies in the absence of food. Additionally, at a very basic and fairly obvious level, the food data confirmed that the metabolomic profile of food differs more from flies than desiccated and unstressed flies differ from each other. Results like these that are consistent with expectations increase confidence that metabolomics is able to identify metabolites accurately and that the method is useful for determining the relative abundance of a metabolite. The starvation control, on the other hand, was able to provide information about changes that are unique to desiccation. The food control may be most useful for proof-of-principal questions, while a control like starvation for a stress experiment can be used to ask questions about the specific effect of an individual kind of stressor.

7 Conclusions and Future Work

The aim of this chapter is to summarise the main findings of the research. Evidence for the effect of desiccation stress on Malpighian tubule function is described, based on metabolomics and physiological approaches. The role of DH_{44} signalling in desiccation stress tolerance is reconciled to the experimental data involving manipulation of the DH_{44} signalling pathway. Evidence for interactions between LK and DH_{44} signalling is summarised, as are data indicating a role for peptide signalling in starvation tolerance. Finally, areas of investigation that could arise from the present work are discussed.

7.1 Conclusions

The Malpighian tubules of *D. melanogaster* are involved in desiccation tolerance (Terhzaz et al 2012, Terhzaz et al 2015b). Manipulation of diuretic hormone signals to this tissue alters survival during desiccation, as summarised in Figure 7.1. Moreover, endogenous changes in signalling pathways are observed in desiccated flies. The DH_{44} pathway, which contributes to survival of environmental stress and fluid homeostasis, may provide a target for the development of a novel insecticide mode of action (Audsley & Down 2015, Ruiz-Sanchez & O'Donnell 2015). Targets identified in *D. melanogaster* can be expected to be particularly useful for the development of products that can control populations of the invasive pest species *D. suzukii* due to the similarity in neuropeptide sequences (Audsley et al 2015). The similarity of the sequence of *D. melanogaster* DH_{44} peptide to that of insect vectors of human disease, including *Aedes aegypti* and *Anopheles gambiae*, supports the possibility that this signalling pathway could be a potential target for an insecticide in these insects as well (Schooley et al 2011).

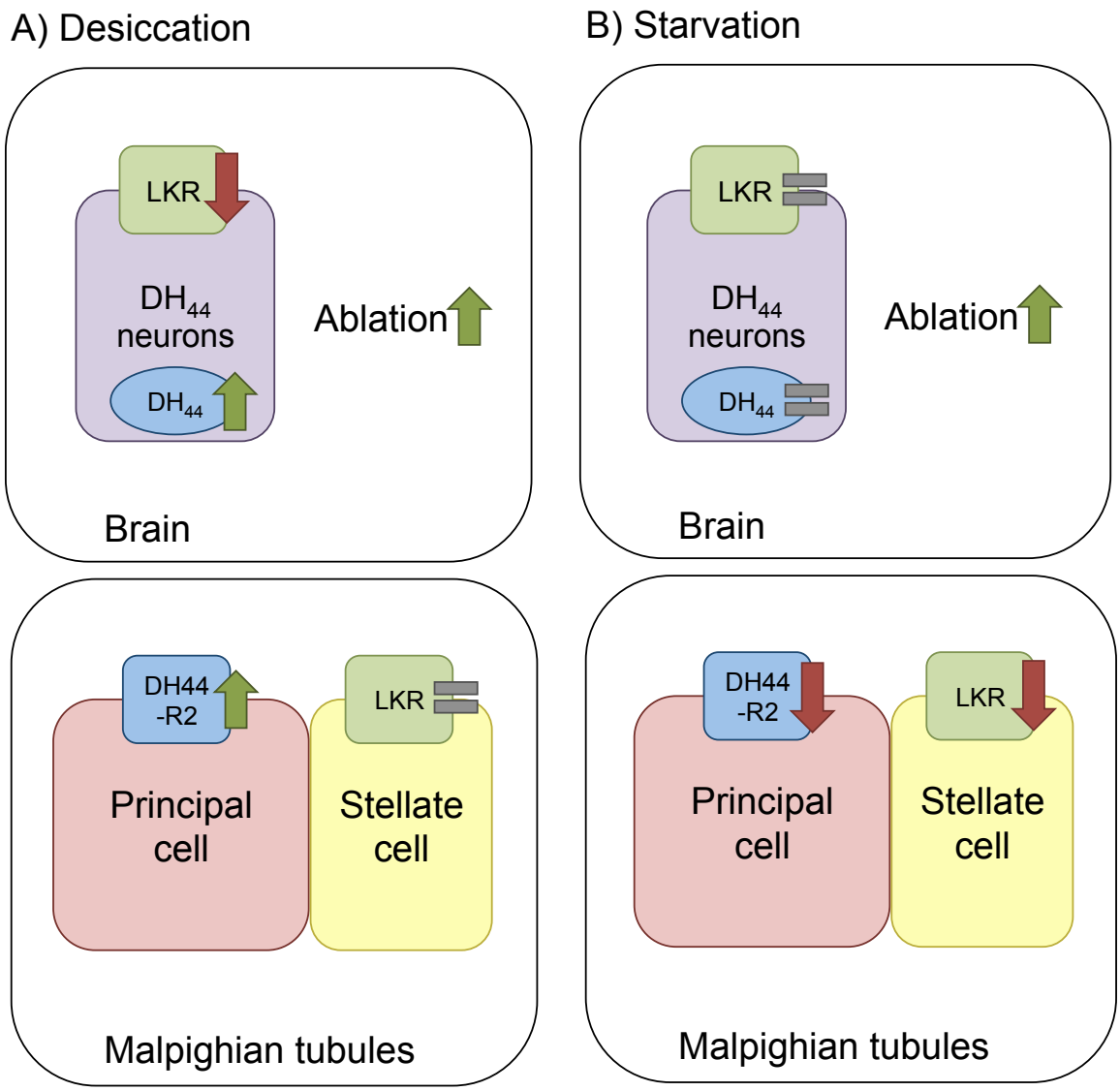

Figure 7.1 RNAi knockdown of *DH$_{44}$* and *LKR* in the DH$_{44}$ neurons, ablation of the DH$_{44}$ neurons, and knockdown of *DH44-R2* and *LKR* in the tubules affects stress survival
A) Desiccation tolerance is increased by knockdown of *DH$_{44}$* in the DH$_{44}$ neurons, ablation of the DH$_{44}$ neurons, and by knockdown of *DH44-R2* in the Malpighian tubule principal cells. Knockdown of *LKR* in the DH$_{44}$ neurons impairs desiccation survival. **B)** Starvation survival duration increases following ablation of the DH$_{44}$ neurons. Knockdown of *DH44-R2* in the Malpighian tubule principal cells or of *LKR* in stellate cells impairs survival of starvation. Green arrows indicate that manipulation (RNAi knockdown or neuron ablation) increased stress survival duration. Red arrows indicate that manipulation decreased stress survival duration. Grey equals sign indicates that manipulation did not affect survival duration.

7.1.1 The Malpighian tubules are significantly affected by desiccation stress

Metabolomics analysis of changes in metabolite abundance following desiccation in the whole fly and Malpighian tubules revealed alterations in a number of

metabolic pathways. Comparison of the two datasets indicated accumulation in the tubules of metabolites from urate degradation and tryptophan metabolic pathways. Although some of these patterns were also observed in the whole fly samples, more metabolites from these pathways were identified in the tissue-specific dataset enabling the overall trends to be more clearly distinguished. These datasets therefore indicate that stress studies in insects may be most informative when carried out in a tissue-specific manner, a conclusion that is supported by research indicating that individual *D. melanogaster* tissues exhibit distinct metabolic profiles (Chintapalli et al 2013a). Following desiccation stress, the metabolic profile of Malpighian tubules changes in a way that is distinct from that of the entire fly. Thus, while metabolic analysis of the whole organism may be the quicker option, speed may come at the consequence of obscuring interesting and informative stress-induced metabolic changes.

Physiological study of Malpighian tubule function, via Ramsay's secretion assay, indicates that tubules from desiccated flies have a reduced basal secretion rate. Moreover, after stimulation with DH_{44} peptide, the tubules did not reach the same rate of secretion as control tubules. Thus, it seems that tubule secretion is suppressed by desiccation. These data complement the findings of the metabolomic analysis, which showed accumulation of several types of metabolites that are normally cleared by the tubules following desiccation, including pigment precursors and purine degradation compounds rich in nitrogen. This accumulation may be reflective of the reduced secretion rate of the tubules following desiccation. Thus, based on both the metabolic and physiological experiments applied in this study, it is evident that the Malpighian tubules are a tissue that is significantly affected by organismal exposure to desiccation stress.

7.1.2 DH_{44} signalling modifies desiccation tolerance

Evidence that DH_{44} signalling influences *D. melanogaster* survival during desiccation emerged from studies of changes in signalling pathways in wild-type flies, and by genetically manipulating DH_{44} signalling and observing the effect on survival phenotypes. Specifically, wild-type flies had reduced *DH44-R2* gene expression and DH44-R2 protein levels in the Malpighian tubules following desiccation, when measured using RT-PCR and DH_{44}-F labelling. These findings

suggest that suppression of the DH_{44} signalling pathway may be an endogenous mechanism of desiccation tolerance in *D. melanogaster*. Genetic manipulations of the DH_{44} signalling pathway revealed that reduced levels of DH_{44} in the DH_{44} neurons are advantageous for desiccation survival, as is knockdown of DH44-R2 in the Malpighian tubules. These data are consistent with the experiment in wild-type flies as they likewise indicate that suppression of DH_{44} signalling improves desiccation tolerance. The plausibility of the results presented here is bolstered by the literature as involvement of diuretic neuropeptide signalling pathways in desiccation survival has been previously reported (Kahsai et al 2010, Terhzaz et al 2012, Terhzaz et al 2015b).

7.1.3 LK and DH_{44} signalling pathways interact

The colocalisation of LKR and DH_{44} in the pars intercerebralis of the *D. melanogaster* brain suggests the possibility of interaction between the LK and DH_{44} signalling pathways (Cabrero et al 2002). Two experiments presented in this study support this idea. Firstly, knockdown of *LKR* in the DH_{44} neurons affects desiccation tolerance in a direction that is opposite to that observed when *DH_{44}* is knocked down in these neurons. This finding is consistent with LK acting on the DH_{44} neurons via the LKR to suppress DH_{44} release. Secondly, manipulation of DH_{44} levels in the DH_{44} neurons via neuronal ablation or DH_{44} knockdown resulted in significantly reduced expression of the *LKR* gene in the Malpighian tubules. This change in gene expression supports an effect of signalling via the DH_{44} neurons on LK signalling to the Malpighian tubules. One possibility is that DH_{44} signalling suppresses LK release into circulation; if this were the case, then knocking down DH_{44} peptide would result in increased levels of circulating LK, and therefore a higher exposure of the Malpighian tubules to LK, which could result in a compensatory decrease in *LKR* expression. Overall, the results suggest that there is an interaction between LK and DH_{44} signalling. As DH_{44} signals to the principal cells in the Malpighian tubules and LK to the stellate cells, interaction between these two pathways could enable coordination of fluid homeostasis by these two cell types in renal epithelia. More experimental evidence is required, however, to validate the existence and nature of this interaction.

7.1.4 Diuretic peptide signalling to the Malpighian tubules alters starvation tolerance

Cell-type specific knockdown of *DH44-R2* and *LKR* in the Malpighian tubules had similar effects on starvation tolerance – in both cases, survival was impaired. Likewise, *LKR* expression was significantly increased following 24 hours of starvation exposure. These results suggest that peptide signalling to the tubules is important during starvation and that interference with the ability of the tubules to increase secretion rate in response to diuretic peptides impairs starvation tolerance. Secretion during starvation may be important due to the role of the Malpighian tubules in detoxification. The tubules are involved in processing and excreting the metabolic by-products created by lipid catabolism in the fat body; increased lipid metabolism during starvation may require the tubules to secrete at higher rates to clear accumulated metabolites (Marron et al 2003, Palanker et al 2009). Diuretic hormone signalling may be involved in increasing the tubule secretion rate as required during this process and interference with reception of these signals may result in the accumulation of toxic metabolites.

7.1.5 Limitations of the study

The GAL4-UAS system of genetic manipulation is a very powerful one that can enable relatively facile alterations in the expression profile of a wide variety of genes, particularly when used to drive expression of RNAi constructs (Duffy 2002). However, RNAi expression carries the risk of creating off-target or unintended effects on the cross progeny. In this study, the risk was minimised by restricting the expression of RNAi constructs using highly specific GAL4 driver lines.

The GAL4-UAS genetic manipulations used in this study were all constitutive, in that they were not triggered but were rather expressed throughout the life of the fly. This can induce the development of compensatory mechanisms (Liu et al 2015). In the present study, some of these potential mechanisms were explored by assessing gene expression and peptide stimulation of secretion rate in the Malpighian tubules of flies with manipulated DH_{44} neurons. Although changes in gene expression were found, analysis of the changes indicated that they were

unlikely to underlie the survival phenotypes observed. Conditional manipulation of the DH_{44} and LK signalling pathways during desiccation and starvation stress could be informative, particularly where no phenotype was observed. In a similar study, constitutive manipulations were found to obscure phenotypes that were later revealed via conditional manipulations (Liu et al 2015).

Due to the large divergence in survival time between male and female *D. melanogaster* during stress exposure, the study used only male flies for experiments involving stress exposure. Gender-specific differences have been observed in gene expression of receptors for neuropeptide F and sex-peptide in the Malpighian tubules, and differences in the metabolic profiles of whole fly male and female *Drosophila* have been identified (Chintapalli et al 2012, Zhang et al 2014).

7.2 Future work

The main aim of the study, to investigate the role of DH_{44} in desiccation tolerance, was satisfied in that all of the results produced indicated that DH_{44} peptide signalling is involved in desiccation survival. As with most research investigations, however, a number of lines of future inquiry arise from the work as well. These are discussed below, as are a number of approaches that could be used to extend the present work in breadth and detail.

One of the main questions arising from the present work is the role that diuretic peptides play to modify Malpighian tubule function during starvation stress. This study provided evidence of involvement of both the DH_{44} and LK signalling pathways in survival of starvation. Previous work showed tachykinin signalling to the Malpighian tubule as a starvation survival modifier, although the mechanism of this effect was not investigated (Soderberg et al 2011). Signalling in the Malpighian tubules has been implicated in the survival of a wide variety of environmental stresses, including cold, desiccation, osmotic challenge, and immune stress (Davies et al 2014, Davies et al 2012, Naikkhwah & O'Donnell 2011, Terhzaz et al 2015b). Malpighian tubule function during starvation could be explored physiologically, via a secretion assay and using metabolomics approaches. Changes in basal secretion rate and patterns of metabolite accumulation could provide insight into potential changes in tubule function

during this stressor. The involvement of LK in signalling during starvation stress could be explored by determining the secretion rate following LK stimulation of starved tubules, and by knocking down LK peptide. As LK is expressed in several tissues and cell types, if a starvation phenotype were discovered, it could be informative to knockdown LK more selectively in subsets of the LK-expressing cells (Cantera & Nassel 1992, de Haro et al 2010, Liu et al 2015).

One possible mechanism which might underlie the effects observed on starvation tolerance following knockdown of *DH44-R2* and *LKR* in the Malpighian tubules could be via indirect effects on feeding (Liu et al 2015). Although a bloating phenotype was not observed in the LKR knockdown flies, interference with the ability of the tubules to respond to diuretic peptide signals, which are induced by nutrient sensing (DH_{44}) or thought to be involved in the termination of feeding (LK), could result in a feeding phenotype (Al-Anzi et al 2010, Dus et al 2015). This could be assessed using a capillary feeder assay, which enables precise measurement of food consumption of groups of flies over time (Ja et al 2007).

The second main area of investigation suggested by the present study is further exploration of the nature of the interaction between the LK and DH_{44} signalling pathways. Based on the present research, it is hypothesised that LK and DH_{44} interact, and that furthermore, they act in a feedback loop to regulate the release of each other. In order to explore the validity of this model, a peptidomics approach could be used to evaluate changes in LK and DH_{44} levels in circulation following conditional RNAi knockdown of each peptide (Brockmann et al 2009, Predel et al 2004, Salisbury et al 2013, Schoofs & Baggerman 2003). Further work is also required to fully delineate the neuronal pathways of DH_{44} signalling. Although DH44-R1 immunocytochemical and *in situ* hybridisation has been performed, the pattern of expression of DH44-R2 in the *D. melanogaster* brain has not been investigated despite Flyatlas data indicating enriched expression in this tissue (Chintapalli et al 2007, Johnson et al 2005, Lee et al 2015). A means for LK influence on DH_{44} signalling is evident as LKR is expressed in the DH_{44} neurons. It is possible that characterisation of the DH44-R2 expression pattern in the brain may clarify a potential mechanism of DH_{44} influence on LK release.

The work presented in this thesis could be further developed both in breadth and in detail. In terms of detail, it could be interesting to perform both gene expression and metabolomic analysis on desiccated flies along a time course to determine when the observed changes occur and whether they are gradual or sudden. This would also provide a confirmation of the results presented here in that artefact changes in metabolite abundance, which can occur due to the rapid flux inherent in metabolism, would be unlikely to emerge across multiple time points. In terms of breadth, the methods presented in this thesis could be applied also to female *D. melanogaster* and to larvae in order to determine whether DH_{44} signalling is also involved in desiccation tolerance in these sample groups.

Finally, as *D. melanogaster* is a well-established model for insect disease vectors, this work could be extended to assess desiccation tolerance mechanisms in *D. suzukii* and *Aedes aegypti* (Dow 2012a, Schneider 2000). Neuroendocrine signalling appears to be conserved across *Diptera* and similarities in DH_{44} and LK function for fluid homeostasis have been observed in *Drosophila* and *Aedes* (Cabrero et al 2002, Clark et al 1998, Halberg et al 2015, Jagge & Pietrantonio 2008, Radford et al 2002, Radford et al 2004). The plausibility of shared desiccation tolerance mechanisms is also supported by the substantial similarity in tubule function across Dipteran species (Beyenbach et al 2010, Dow & Davies 2006).

List of References

Adams MD, Celniker SE, Holt RA, Evans CA, Gocayne JD, Amanatides PG, Scherer SE, Li PW, Hoskins RA, Galle RF, George RA, Lewis SE, et al. 2000. The genome sequence of *Drosophila melanogaster*. *Science* 287: 2185-2195.

Aggarwal DD. 2014. Physiological basis of starvation resistance in *Drosophila leontia*: analysis of sexual dimorphism. *Journal of Experimental Biology* 217: 1849-1859.

Al Bratty M, Chintapalli VR, Dow JA, Zhang T, Watson DG. 2012. Metabolomic profiling reveals that *Drosophila melanogaster* larvae with the y mutation have altered lysine metabolism. *FEBS Open Bio* 2: 217-221.

Al Bratty M, Hobani Y, Dow JAT, Watson DG. 2011. Metabolomic profiling of the effects of allopurinol on *Drosophila melanogaster*. *Metabolomics* 7: 542-548.

Al-Anzi B, Armand E, Nagamei P, Olszewski M, Sapin V, Waters C, Zinn K, Wyman RJ, Benzer S. 2010. The leucokinin pathway and its neurons regulate meal size in *Drosophila*. *Current Biology* 20: 969-978.

Allan AK, Du J, Davies SA, Dow JA. 2005. Genome-wide survey of V-ATPase genes in *Drosophila* reveals a conserved renal phenotype for lethal alleles. *Physiological Genomics* 22: 128-138.

Alonso A, Marsal S, Julia A. 2015. Analytical methods in untargeted metabolomics: state of the art in 2015. *Frontiers in Bioengineering Biotechnology* 3: 23.

Annesley TM. 2003. Ion suppression in mass spectrometry. *Clinical Chemistry* 49: 1041-1044.

Aplin AC, Kaufman TC. 1997. Homeotic transformation of legs to mouthparts by proboscipedia expression in *Drosophila* imaginal discs. *Mechanisms of Development* 62: 51-60.

Arnone MI, Fau DI, Gache C. 2004. Using reporter genes to study cis-regulatory elements. *Methods in Cell Biology* 74: 621-652.

Ashburner M. 1989. *Drosophila: a Laboratory Manual*. Cold Spring Harbor: Cold Spring Harbor Laboratory Press.

Audsley N, Down RE. 2015. G Protein coupled receptors as targets for next generation pesticides. *Insect Biochemistry and Molecular Biology* 67: 27-37.

Audsley N, Down RE, Isaac RE. 2015. Genomic and peptidomic analyses of the neuropeptides from the emerging pest, *Drosophila suzukii*. *Peptides* 68: 33-42.

Bachmann C, Colombo JP. 1980. Diagnostic value of orotic acid excretion in heritable disorders of the urea cycle and in hyperammonemia due to organic acidurias. *European Journal of Pediatrics* 134: 109-113.

Ballard JW, Melvin RG, Simpson SJ. 2008. Starvation resistance is positively correlated with body lipid proportion in five wild caught *Drosophila simulans* populations. *Journal of Insect Physiology* 54: 1371-1376.

Bazinet AL, Marshall KE, MacMillan HA, Williams CM, Sinclair BJ. 2010. Rapid changes in desiccation resistance in *Drosophila melanogaster* are facilitated by changes in cuticular permeability. *Journal of Insect Physiology* 56: 2006-2012.

Bellés X. 2009. Beyond *Drosophila*: RNAi in vivo and functional genomics in insects. *Annual Review of Entomology* 55: 111-128.

Benjamini Y, Hochberg Y. 1995. Controlling the false discovery rate - a practical and powerful approach to multiple testing. *Journal of the Royal Statistical Society Series B-Methodological* 57: 289-300.

Bernstein L, Anderson J, Pike MC. 1981. Estimation of the proportional hazard in two-treatment-group clinical trials. *Biometrics* 37: 513-519.

Beyenbach KW. 2001. Energizing epithelial transport with the vacuolar H(+)-ATPase. *News in Physiological Sciences* 16: 145-151.

Beyenbach KW, Skaer H, Dow JA. 2010. The developmental, molecular, and transport biology of Malpighian tubules. *Annual Review of Entomology* 55: 351-374.

Blumenthal EM. 2003. Regulation of chloride permeability by endogenously produced tyramine in the *Drosophila* Malpighian tubule. *American Journal of Physiology - Cell Physiology* 284: C718-C728.

Boom R, Sol CJ, Salimans MM, Jansen CL, Wertheim-van Dillen PM, van der Noordaa J. 1990. Rapid and simple method for purification of nucleic acids. *Journal of Clinical Microbiology* 28: 495-503.

Borland G, Smith BO, Yarwood SJ. 2009. EPAC proteins transduce diverse cellular actions of cAMP. *British Journal of Pharmacology* 158: 70-86.

Brand AH, Perrimon N. 1993. Targeted gene expression as a means of altering cell fates and generating dominant phenotypes. *Development* 118: 401-415.

Broadhurst D, Kell D. 2006. Statistical strategies for avoiding false discoveries in metabolomics and related experiments. *Metabolomics* 2: 171-196.

Brockmann A, Annangudi SP, Richmond TA, Ament SA, Xie F, Southey BR, Rodriguez-Zas SR, Robinson GE, Sweedler JV. 2009. Quantitative peptidomics reveal brain peptide signatures of behavior. *Proceedings of the National Academy of Sciences of the United States of America* 106: 2383-2388.

Bubliy OA, Kristensen TN, Kellermann V, Loeschcke V. 2012. Plastic responses to four environmental stresses and cross-resistance in a laboratory population of *Drosophila melanogaster*. *Functional Ecology* 26: 245-253.

Burger JM, Hwangbo DS, Corby-Harris V, Promislow DE. 2007. The functional costs and benefits of dietary restriction in *Drosophila*. *Aging Cell* 6: 63-71.

Burke G, Fiehn O, Moran N. 2010. Effects of facultative symbionts and heat stress on the metabolome of pea aphids. *The ISME Journal* 4: 242-252.

Cabrero P, Radford JC, Broderick KE, Costes L, Veenstra JA, Spana EP, Davies SA, Dow JA. 2002. The Dh gene of *Drosophila melanogaster* encodes a diuretic peptide that acts through cyclic AMP. *Journal of Experimental Biology* 205: 3799-3807.

Cabrero P, Richmond L, Nitabach M, Davies SA, Dow JA. 2013. A biogenic amine and a neuropeptide act identically: tyramine signals through calcium in *Drosophila* tubule stellate cells. *Proceedings of the Royal Society of London B: Biological Sciences* 280: 20122943.

Cabrero P, Terhzaz S, Romero MF, Davies SA, Blumenthal EM, Dow JA. 2014. Chloride channels in stellate cells are essential for uniquely high secretion rates in neuropeptide-stimulated *Drosophila* diuresis. *Proceedings of the National Academy of Sciences of the United States of America* 111: 14301-14306.

Campesan S, Green EW, Breda C, Sathyasaikumar KV, Muchowski PJ, Schwarcz R, Kyriacou CP, Giorgini F. 2011. The kynurenine pathway modulates neurodegeneration in a *Drosophila* model of Huntington's disease. *Current Biology* 21: 961-966.

Cannell E, Dornan AJ, Halberg KA, Terhzaz S, Dow JAT, Davies S-A. 2016. The Corticotropin-releasing factor-like diuretic hormone 44 (DH44) and kinin neuropeptides modulate desiccation and starvation tolerance in Drosophila melanogaster. *Peptides* In press

Cantera R, Hansson BS, Hallberg E, Nassel DR. 1992. Postembryonic development of leucokinin I-immunoreactive neurons innervating a neurohemal organ in the turnip moth *Agrotis segetum*. *Cell and Tissue Research* 269: 65-77.

Cantera R, Nassel DR. 1992. Segmental peptidergic innervation of abdominal targets in larval and adult dipteran insects revealed with an antiserum against leucokinin I. *Cell and Tissue Research* 269: 459-471.

Careri M, Mangia A. 2011. Trends in analytical atomic and molecular mass spectrometry in biology and the life sciences. *Analytical and Bioanalytical Chemistry* 399: 2585-2595.

Carlsson MA, Diesner M, Schachtner J, Nassel DR. 2010. Multiple neuropeptides in the *Drosophila* antennal lobe suggest complex modulatory circuits. *Journal of Comparative Neurology* 518: 3359-3380.

Cavanaugh DJ, Geratowski JD, Wooltorton JR, Spaethling JM, Hector CE, Zheng X, Johnson EC, Eberwine JH, Sehgal A. 2014. Identification of a circadian output circuit for rest:activity rhythms in *Drosophila*. *Cell* 157: 689-701.

Chahine S, O'Donnell MJ. 2011. Interactions between detoxification mechanisms and excretion in Malpighian tubules of *Drosophila melanogaster*. *Journal of Experimental Biology* 214: 462-468.

Chintapalli VR, Al Bratty M, Korzekwa D, Watson DG, Dow JA. 2013a. Mapping an atlas of tissue-specific *Drosophila melanogaster* metabolomes by high resolution mass spectrometry. *PLoS One* 8: e78066.

Chintapalli VR, Kato A, Henderson L, Hirata T, Woods DJ, Overend G, Davies SA, Romero MF, Dow JA. 2015. Transport proteins NHA1 and NHA2 are essential for survival, but have distinct transport modalities. *Proceedings of the National Academy of Sciences of the United States of America* 112: 11720-11725.

Chintapalli VR, Terhzaz S, Wang J, Al Bratty M, Watson DG, Herzyk P, Davies SA, Dow JA. 2012. Functional correlates of positional and gender-specific renal asymmetry in *Drosophila*. *PLoS One* 7: e32577.

Chintapalli VR, Wang J, Dow JA. 2007. Using FlyAtlas to identify better *Drosophila melanogaster* models of human disease. *Nature Genetics* 39: 715-720.

Chintapalli VR, Wang J, Herzyk P, Davies SA, Dow JA. 2013b. Data-mining the FlyAtlas online resource to identify core functional motifs across transporting epithelia. *BMC Genomics* 14: 518.

Chiu JC, Jiang X, Zhao L, Hamm CA, Cridland JM, Saelao P, Hamby KA, Lee EK, Kwok RS, Zhang G, Zalom FG, Walton VM, et al. 2013. Genome of *Drosophila suzukii*, the spotted wing drosophila. *G3 (Bethesda)* 3: 2257-2271.

Chomczynski P, Sacchi N. 1987. Single-step method of RNA isolation by acid guanidinium thiocyanate-phenol-chloroform extraction. *Analytical Biochemistry* 162: 156-159.

Chung H, Sztal T, Pasricha S, Sridhar M, Batterham P, Daborn PJ. 2009. Characterization of *Drosophila melanogaster* cytochrome P450 genes. *Proceedings of the National Academy of Sciences of the United States of America* 106: 5731-5736.

Cielecka-Piontek J, Zalewski P, Jelinska A, Garbacki P. 2013. UHPLC: the greening face of liquid chromatography. *Chromatographia* 76: 1429-1437.

Clark TM, Hayes TK, Beyenbach KW. 1998. Dose-dependent effects of CRF-like diuretic peptide on transcellular and paracellular transport pathways. *The American Journal of Physiology* 274: F834-F840.

Coast G, Kay II. 1994. The effects of *Acheta* diuretic peptide on isolated Malpighian tubules from the house cricket *Acheta domesticus*. *Journal of Experimental Biology* 187: 225-243.

Coast GM. 2006. Insect diuretic and antidiuretic hormones In *Handbook of Biologically Active Peptides*, pp. 157-162. California, USA: Academic Press.

Coast GM, Orchard I, Phillips JE, Schooley DA. 2002. Insect diuretic and antidiuretic hormones In *Advances in Insect Physiology*, pp. 279-409: Academic Press.

Coast GM, Webster SG, Schegg KM, Tobe SS, Schooley DA. 2001. The *Drosophila melanogaster* homologue of an insect calcitonin-like diuretic peptide stimulates V-ATPase activity in fruit fly Malpighian tubules. *Journal of Experimental Biology* 204: 1795-1804.

Cognigni P, Bailey AP, Miguel-Aliaga I. 2011. Enteric neurons and systemic signals couple nutritional and reproductive status with intestinal homeostasis. *Cell Metabolism* 13: 92-104.

Cohen AC, March RB, Pinto JD. 1986. Effects of water stress and rehydration on hemolymph volume and amino acid content in the blister beetle, *Cysteodemus armatus*. *Comparative Biochemistry and Physiology Part A: Physiology* 85: 743-746.

Colinet H, Larvor V, Laparie M, Renault D. 2012. Exploring the plastic response to cold acclimation through metabolomics. *Functional Ecology* 26: 711-722.

Connolly KJ. 1966. Locomotor activity in *Drosophila* as a function of food deprivation. *Nature* 209: 224.

Cox D, Oakes D. 1984. *Analysis of survival data: Monograph on statistics and applied probability*. USA: Chapman & Hall/CRC.

Creek DJ, Jankevics A, Breitling R, Watson DG, Barrett MP, Burgess KE. 2011. Toward global metabolomics analysis with hydrophilic interaction liquid chromatography-mass spectrometry: improved metabolite identification by retention time prediction. *Analytical Chemistry* 83: 8703-8710.

Creek DJ, Jankevics A, Burgess KE, Breitling R, Barrett MP. 2012. IDEOM: an Excel interface for analysis of LC-MS-based metabolomics data. *Bioinformatics* 28: 1048-1049.

Crowe J, Hoekstra F, Crowe L. 1992. Anhydrobiosis. *Annual Review of Physiology* 54: 579-599.

Cubbon S, Antonio C, Wilson J, Thomas-Oates J. 2010. Metabolomic applications of HILIC-LC-MS. *Mass Spectrometry Reviews* 29: 671-684.

Cunningham F, Amode MR, Barrell D, Beal K, Billis K, Brent S, Carvalho-Silva D, Clapham P, Coates G, Fitzgerald S, Gil L, Giron CG, et al. 2015. Ensembl 2015. *Nucleic Acids Research* 43: D662-D669.

Daborn PJ, Yen JL, Bogwitz MR, Le Goff G, Feil E, Jeffers S, Tijet N, Perry T, Heckel D, Batterham P, Feyereisen R, Wilson TG, et al. 2002. A single p450 allele associated with insecticide resistance in *Drosophila*. *Science* 297: 2253-2256.

Dane AD, Hendriks MM, Reijmers TH, Harms AC, Troost J, Vreeken RJ, Boomsma DI, van Duijn CM, Slagboom EP, Hankemeier T. 2014. Integrating metabolomics profiling measurements across multiple biobanks. *Analytical Chemistry* 86: 4110-4114.

Davies SA, Cabrero P, Overend G, Aitchison L, Sebastian S, Terhzaz S, Dow JA. 2014. Cell signalling mechanisms for insect stress tolerance. *Journal of Experimental Biology* 217: 119-128.

Davies SA, Cabrero P, Povsic M, Johnston NR, Terhzaz S, Dow JA. 2013. Signaling by *Drosophila* capa neuropeptides. *General and Comparative Endocrinology* 188: 60-66.

Davies SA, Huesmann GR, Maddrell SH, O'Donnell MJ, Skaer NJ, Dow JA, Tublitz NJ. 1995. CAP2b, a cardioacceleratory peptide, is present in *Drosophila* and

stimulates tubule fluid secretion via cGMP. *American Journal of Physiology* 269: R1321-R1326.

Davies SA, Overend G, Sebastian S, Cundall M, Cabrero P, Dow JA, Terhzaz S. 2012. Immune and stress response 'cross-talk' in the *Drosophila* Malpighian tubule. *Journal of Insect Physiology* 58: 488-497.

Davies SA, Terhzaz S. 2009. Organellar calcium signalling mechanisms in *Drosophila* epithelial function. *Journal of Experimental Biology* 212: 387-400.

Day JP, Wan S, Allan AK, Kean L, Davies SA, Gray JV, Dow JA. 2008. Identification of two partners from the bacterial Kef exchanger family for the apical plasma membrane V-ATPase of Metazoa. *Journal of Cell Science* 121: 2612-2619.

de Haro M, Al-Ramahi I, Benito-Sipos J, Lopez-Arias B, Dorado B, Veenstra JA, Herrero P. 2010. Detailed analysis of leucokinin-expressing neurons and their candidate functions in the *Drosophila* nervous system. *Cell and Tissue Research* 339: 321-336.

Denholm B, Hu N, Fauquier T, Caubit X, Fasano L, Skaer H. 2013. The tiptop/teashirt genes regulate cell differentiation and renal physiology in *Drosophila*. *Development* 140: 1100-1110.

Dhaliwal GS, Vikas J, Bharathi M. 2015. Crop losses due to insect pests: global and Indian scenario. *Indian Journal of Entomology* 77: 165-168.

Dieterle F, Riefke B, Schlotterbeck G, Ross A, Senn H, Amberg A. 2011. NMR and MS methods for metabonomics In *Drug Safety Evaluation*, ed. J-C Gautier, pp. 385-415: Humana Press.

Dietzl G, Chen D, Schnorrer F, Su KC, Barinova Y, Fellner M, Gasser B, Kinsey K, Oppel S, Scheiblauer S, Couto A, Marra V, et al. 2007. A genome-wide transgenic

RNAi library for conditional gene inactivation in *Drosophila*. *Nature* 448: 151-156.

Djawdan M, Rose MR, Bradley TJ. 1997. Does selection for stress resistance lower metabolic rate? *Ecology* 78: 828-837.

Donnell MJ, Aldis GK, Maddrell SHP. 1982. Measurements of osmotic permeability in the Malpighian tubules of an insect, *Rhodnius prolixus* Stal. *Proceedings of the Royal Society of London B: Biological Sciences* 216: 267-277.

Dow JA. 2009. Insights into the Malpighian tubule from functional genomics. *Journal of Experimental Biology* 212: 435-445.

Dow JA. 2012a. *Drosophila* as an experimental organism for functional genomics. In *eLS*. *John Wiley & Sons*. Chichester

Dow JA. 2012b. The versatile stellate cell - more than just a space-filler. *Journal of Insect Physiology* 58: 467-472.

Dow JA, Davies SA. 2006. The Malpighian tubule: rapid insights from post-genomic biology. *Journal of Insect Physiology* 52: 365-378.

Dow JA, Maddrell SH, Gortz A, Skaer NJ, Brogan S, Kaiser K. 1994. The malpighian tubules of *Drosophila melanogaster*: a novel phenotype for studies of fluid secretion and its control. *Journal of Experimental Biology* 197: 421-428.

Dow JA, Romero MF. 2010. *Drosophila* provides rapid modeling of renal development, function, and disease. *American Journal of Physiology - Renal Physiology* 299: F1237-1244.

Dow JAT. 2013. Excretion and salt and water regulation In *The Insects, Structure and Function*, ed. RF Chapman, pp. 547-587. Cambridge: Cambridge University Press.

Dow JT, Davies SA. 2003. Integrative physiology and functional genomics of epithelial function in a genetic model organism. *Physiological Reviews* 83: 687-729.

Duffy JB. 2002. GAL4 system in *Drosophila*: a fly geneticist's Swiss army knife. *Genesis* 34: 1-15.

Dus M, Lai JS, Gunapala KM, Min S, Tayler TD, Hergarden AC, Geraud E, Joseph CM, Suh GS. 2015. Nutrient sensor in the brain directs the action of the brain-gut axis in *Drosophila*. *Neuron* 87: 139-151.

Efetova M, Petereit L, Rosiewicz K, Overend G, Haussig F, Hovemann BT, Cabrero P, Dow JA, Schwarzel M. 2013. Separate roles of PKA and EPAC in renal function unraveled by the optogenetic control of cAMP levels in vivo. *Journal of Cell Science* 126: 778-788.

Fahy E, Sud M, Cotter D, Subramaniam S. 2007. LIPID MAPS online tools for lipid research. *Nucleic Acids Research* 35: W606-612.

Farhadian SF, Suarez-Farinas M, Cho CE, Pellegrino M, Vosshall LB. 2012. Post-fasting olfactory, transcriptional, and feeding responses in *Drosophila*. *Physiology & Behavior* 105: 544-553.

Feala JD, Coquin L, McCulloch AD, Paternostro G. 2007. Flexibility in energy metabolism supports hypoxia tolerance in *Drosophila* flight muscle: metabolomic and computational systems analysis. *Molecular Systems Biology* 3: 99.

Fischer JA, Giniger E, Maniatis T, Ptashne M. 1988. GAL4 activates transcription in *Drosophila*. *Nature* 332: 853-856.

Folk DG, Bradley TJ. 2003. Evolved patterns and rates of water loss and ion regulation in laboratory-selected populations of *Drosophila melanogaster*. *Journal of Experimental Biology* 206: 2779-2786.

Folk DG, Han C, Bradley TJ. 2001. Water acquisition and partitioning in *Drosophila melanogaster*: effects of selection for desiccation-resistance. *Journal of Experimental Biology* 204: 3323-3331.

Foray V, Desouhant E, Voituron Y, Larvor V, Renault D, Colinet H, Gibert P. 2013. Does cold tolerance plasticity correlate with the thermal environment and metabolic profiles of a parasitoid wasp? *Comparative Biochemistry and Physiology Part A: Molecular & Integrative Physiology* 164: 77-83.

Friggi-Grelin F, Coulom H, Meller M, Gomez D, Hirsh J, Birman S. 2003. Targeted gene expression in *Drosophila* dopaminergic cells using regulatory sequences from tyrosine hydroxylase. *Journal of Neurobiology* 54: 618-627.

Galili G, Tang G, Zhu X, Gakiere B. 2001. Lysine catabolism: a stress and development super-regulated metabolic pathway. *Current Opinion in Plant Biology* 4: 261-266.

Gangisetty O, Reddy DS. 2009. The optimization of TaqMan real-time RT-PCR assay for transcriptional profiling of GABA-A receptor subunit plasticity. *Journal of Neuroscience Methods* 181: 58-66.

Gauch S, Hermann R, Feuser P, Oelmüller U, Bastian H. 1998. Isolation of total RNA using silica-gel based membranes In *Molecular Tools for Screening Biodiversity*, ed. A Karp, P Isaac, D Ingram, pp. 67-70: Springer Netherlands.

Gautam NK, Verma P, Tapadia MG. 2015. Ecdysone regulates morphogenesis and function of Malpighian tubules in *Drosophila melanogaster* through EcR-B2 isoform. *Developmental Biology* 398: 163-176.

Gauthier M. 2010. State of the art on insect nicotinic acetylcholine receptor function in learning and memory In *Insect Nicotonic Acetylcholine Receptors*, ed. SH Thany, pp. 97-115. USA: Landes Bioscience.

Geminard C, Rulifson EJ, Leopold P. 2009. Remote control of insulin secretion by fat cells in *Drosophila*. *Cell Metabolism* 10: 199-207.

Gibbons D, Morrissey C, Mineau P. 2015. A review of the direct and indirect effects of neonicotinoids and fipronil on vertebrate wildlife. *Environmental Science and Pollution Research* 22: 103-118.

Gibbs AG, Chippindale AK, Rose MR. 1997. Physiological mechanisms of evolved desiccation resistance in *Drosophila melanogaster*. *Journal of Experimental Biology* 200: 1821-1832.

Gibbs AG, Gefan E. 2009. Physiological adaptation in laboratory environments In *Experimental Evolution: Concepts, Methods, and Applications of Selection Experiments*, ed. T Garland, MR Rose. Berkeley and Los Angeles: University of California Press.

Gibbs AG, Matzkin LM. 2001. Evolution of water balance in the genus *Drosophila*. *Journal of Experimental Biology* 204: 2331-2338.

Gibbs AG, Reynolds LA. 2012. *Drosophila* as a model for starvation: evolution, physiology, and genetics In *Comparative Physiology of Fasting, Starvation, and Food Limitation*, ed. MD McCue, pp. 37-51: Springer Berlin Heidelberg.

Gilleard JS, Woods DJ, Dow JA. 2005. Model-organism genomics in veterinary parasite drug-discovery. *Trends in Parasitology* 21: 302-305.

Goenaga J, Fanara J, Hasson E. 2013. Latitudinal variation in starvation resistance is explained by lipid content in natural populations of *Drosophila melanogaster*. *Evolutionary Biology* 40: 601-612.

Guillot C, Lecuit T. 2013. Mechanics of epithelial tissue homeostasis and morphogenesis. *Science* 340: 1185-1189.

Halberg KA, Terhzaz S, Cabrero P, Davies SA, Dow JA. 2015. Tracing the evolutionary origins of insect renal function. *Nature Communications* 6: 6800.

Hall JC. 2003. Genetics and molecular biology of rhythms in *Drosophila* and other insects. *Advances in Genetics* 48: 1-280.

Harbison ST, Chang S, Kamdar KP, Mackay TF. 2005. Quantitative genomics of starvation stress resistance in *Drosophila*. *Genome Biology* 6: R36.

Hariharan R, Hoffman JM, Thomas AS, Soltow QA, Jones DP, Promislow DE. 2014. Invariance and plasticity in the *Drosophila melanogaster* metabolomic network in response to temperature. *BMC Systems Biology* 8: 139.

Hasko G, Deitch EA, Szabo C, Nemeth ZH, Vizi ES. 2002. Adenosine: a potential mediator of immunosuppression in multiple organ failure. *Current Opinion in Pharmacology* 2: 440-444.

Hayward SA, Rinehart JP, Denlinger DL. 2004. Desiccation and rehydration elicit distinct heat shock protein transcript responses in flesh fly pupae. *Journal of Experimental Biology* 207: 963-971.

Hector CE, Bretz CA, Zhao Y, Johnson EC. 2009. Functional differences between two CRF-related diuretic hormone receptors in *Drosophila*. *Journal of Experimental Biology* 212: 3142-3147.

Hege DM, Stanewsky R, Hall JC, Giebultowicz JM. 1997. Rhythmic expression of a PER-reporter in the Malpighian tubules of decapitated *Drosophila*: evidence for a brain-independent circadian clock. *Journal of Biological Rhythms* 12: 300-308.

Hentze JL, Carlsson MA, Kondo S, Nassel DR, Rewitz KF. 2015. The neuropeptide allatostatin A regulates metabolism and feeding decisions in *Drosophila*. *Scientific Reports* 5: 11680.

Herrewege Jv, David JR. 1997. Starvation and desiccation tolerances in *Drosophila*: Comparison of species from different climatic origins. *Écoscience* 4: 151-157.

Hilliker AJ, Duyf B, Evans D, Phillips JP. 1992. Urate-null rosy mutants of *Drosophila melanogaster* are hypersensitive to oxygen stress. *Proceedings of the National Academy of Sciences of the United States of America* 89: 4343-4347.

Ho CS, Lam CW, Chan MH, Cheung RC, Law LK, Lit LC, Ng KF, Suen MW, Tai HL. 2003. Electrospray ionisation mass spectrometry: principles and clinical applications. *The Clinical Biochemist Reviews* 24: 3-12.

Hoffmann AA, Harshman LG. 1999. Desiccation and starvation resistance in *Drosophila*: patterns of variation at the species, population and intrapopulation levels. *Heredity* 83: 637-643.

Hoffmann AA, Parsons PA. 1989. Selection for increased desiccation resistance in *Drosophila melanogaster*: additive genetic control and correlated responses for other stresses. *Genetics* 122: 837-845.

Hoffmann AA, Parsons PA. 1993. Direct and correlated responses to selection for desiccation resistance: a comparison of *Drosophila melanogaster* and *D. simulans*. *Journal of Evolutionary Biology* 6: 643-657.

Holmstrup M, Hedlund K, Boriss H. 2002. Drought acclimation and lipid composition in *Folsomia candida*: implications for cold shock, heat shock and acute desiccation stress. *Journal of Insect Physiology* 48: 961-970.

Houchmandzadeh B, Wieschaus E, Leibler S. 2002. Establishment of developmental precision and proportions in the early *Drosophila* embryo. *Nature* 415: 798-802.

Houslay MD. 2010. Underpinning compartmentalised cAMP signalling through targeted cAMP breakdown. *Trends in Biochemical Sciences* 35: 91-100.

Hsouna A, Lawal HO, Izevbaye I, Hsu T, O'Donnell JM. 2007. *Drosophila* dopamine synthesis pathway genes regulate tracheal morphogenesis. *Developmental Biology* 308: 30-43.

Huang X, Huang Y, Chinnappan R, Bocchini C, Gustin MC, Stern M. 2002. The *Drosophila* inebriated-encoded neurotransmitter/osmolyte transporter: dual roles in the control of neuronal excitability and the osmotic stress response. *Genetics* 160: 561-569.

Huey RB, Suess J, Hamilton H, Gilchrist GW. 2004. Starvation resistance in *Drosophila melanogaster*: testing for a possible 'cannibalism' bias. *Functional Ecology* 18: 952-954.

Idborg H, Zamani L, Edlund PO, Schuppe-Koistinen I, Jacobsson SP. 2005. Metabolic fingerprinting of rat urine by LC/MS Part 1. Analysis by hydrophilic interaction liquid chromatography-electrospray ionization mass spectrometry. *Journal of Chromatography B: Journal of Chromatography B: Analytical Technologies in the Biomedical and Life Sciences* 828: 9-13.

Iijima K, Zhao L, Shenton C, Iijima-Ando K. 2009. Regulation of energy stores and feeding by neuronal and peripheral CREB activity in *Drosophila*. *PLoS One* 4: e8498.

Ja WW, Carvalho GB, Mak EM, de la Rosa NN, Fang AY, Liong JC, Brummel T, Benzer S. 2007. Prandiology of *Drosophila* and the CAFE assay. *Proceedings of the National Academy of Sciences of the United States of America* 104: 8253-8256.

Jagge CL, Pietrantonio PV. 2008. Diuretic hormone 44 receptor in Malpighian tubules of the mosquito *Aedes aegypti*: evidence for transcriptional regulation paralleling urination. *Insect Molecular Biology* 17: 413-426.

Jandera P. 2008. Stationary phases for hydrophilic interaction chromatography, their characterization and implementation into multidimensional chromatography concepts. *Journal of Separation Science* 31: 1421-1437.

Jenett A, Rubin GM, Ngo TT, Shepherd D, Murphy C, Dionne H, Pfeiffer BD, Cavallaro A, Hall D, Jeter J, Iyer N, Fetter D, et al. 2012. A GAL4-driver line resource for *Drosophila* neurobiology. *Cell Reports* 2: 991-1001.

Jennings BH. 2011. *Drosophila* – a versatile model in biology & medicine. *Materials Today* 14: 190-195.

Jess S, Kildea S, Moody A, Rennick G, Murchie AK, Cooke LR. 2014. European Union policy on pesticides: implications for agriculture in Ireland. *Pest Management Science* 70: 1646-1654.

Johnson EC, Bohn LM, Taghert PH. 2004. *Drosophila* CG8422 encodes a functional diuretic hormone receptor. *Journal of Experimental Biology* 207: 743-748.

Johnson EC, Shafer OT, Trigg JS, Park J, Schooley DA, Dow JA, Taghert PH. 2005. A novel diuretic hormone receptor in *Drosophila*: evidence for conservation of CGRP signaling. *Journal of Experimental Biology* 208: 1239-1246.

Kahsai L, Kapan N, Dircksen H, Winther AM, Nassel DR. 2010. Metabolic stress responses in *Drosophila* are modulated by brain neurosecretory cells that produce multiple neuropeptides. *PLoS One* 5: e11480.

Kamleh MA, Dow JA, Watson DG. 2009. Applications of mass spectrometry in metabolomic studies of animal model and invertebrate systems. *Briefings in Functional Genomics and Proteomics* 8: 28-48.

Kamleh MA, Hobani Y, Dow JA, Watson DG. 2008. Metabolomic profiling of *Drosophila* using liquid chromatography Fourier transform mass spectrometry. *FEBS Letters* 582: 2916-2922.

Kanehisa M, Goto S, Sato Y, Kawashima M, Furumichi M, Tanabe M. 2014. Data, information, knowledge and principle: back to metabolism in KEGG. *Nucleic Acids Research* 42: D199-205.

Kanehisa M, Sato Y, Kawashima M, Furumichi M, Tanabe M. 2016. KEGG as a reference resource for gene and protein annotation. *Nucleic Acids Research* 44: D457-462.

Kaneko M, Hall JC. 2000. Neuroanatomy of cells expressing clock genes in *Drosophila*: transgenic manipulation of the period and timeless genes to mark the perikarya of circadian pacemaker neurons and their projections. *Journal of Comparative Neurology* 422: 66-94.

Kaplan EL, Meier P. 1958. Nonparametric estimation from incomplete observations. *Journal of the American Statistical Association* 53: 457-481.

Kaufmann N, Mathai JC, Hill WG, Dow JA, Zeidel ML, Brodsky JL. 2005. Developmental expression and biophysical characterization of a *Drosophila melanogaster* aquaporin. *American Journal of Physiology - Cell Physiology* 289: C397-407.

Kennerdell JR, Carthew RW. 2000. Heritable gene silencing in *Drosophila* using double-stranded RNA. *Nature Biotechnology* 18: 896-898.

Kesner L. 1965. The effect of ammonia administration on orotic acid excretion in rats. *Journal of Biological Chemistry* 240: 1722-1724.

Kim HK, Choi YH, Verpoorte R. 2010. NMR-based metabolomic analysis of plants. *Nature Protocols* 5: 536-549.

Klowden MJ. 2008. Excretory systems In *Physiological Systems in Insects*, pp. 403-431. California, USA: Academic Press.

Kostal V, Korbelova J, Rozsypal J, Zahradnickova H, Cimlova J, Tomcala A, Simek P. 2011. Long-term cold acclimation extends survival time at 0 degrees C and modifies the metabolomic profiles of the larvae of the fruit fly *Drosophila melanogaster*. *PLoS One* 6: e25025.

Koštál V, Šimek P, Zahradníčková H, Cimlová J, Štětina T. 2012. Conversion of the chill susceptible fruit fly larva (*Drosophila melanogaster*) to a freeze tolerant organism. *Proceedings of the National Academy of Sciences of the United States of America* 109: 3270-3274.

Kristensen TN, Overgaard J, Hoffman AA, Nielsen NC, Malhotra A. 2012. Inconsistent effects of developmental temperature acclimation on low-temperature performance and metabolism in *Drosophila melanogaster*. *Evolutionary Ecology Research* 14: 821-837.

Laye MJ, Tran V, Jones DP, Kapahi P, Promislow DE. 2015. The effects of age and dietary restriction on the tissue-specific metabolome of *Drosophila*. *Aging Cell* 14: 797-808.

Leader DP, Burgess K, Creek D, Barrett MP. 2011. Pathos: a web facility that uses metabolic maps to display experimental changes in metabolites identified by mass spectrometry. *Rapid Communications in Mass Spectrometry* 25: 3422-3426.

Lee D, O'Dowd DK. 1999. Fast excitatory synaptic transmission mediated by nicotinic acetylcholine receptors in *Drosophila* neurons. *The Journal of Neuroscience* 19: 5311-5321.

Lee G, Park JH. 2004. Hemolymph sugar homeostasis and starvation-induced hyperactivity affected by genetic manipulations of the adipokinetic hormone-encoding gene in *Drosophila melanogaster*. *Genetics* 167: 311-323.

Lee KM, Daubnerova I, Isaac RE, Zhang C, Choi S, Chung J, Kim YJ. 2015. A neuronal pathway that controls sperm ejection and storage in female *Drosophila*. *Current Biology* 25: 790-797.

Lei Z, Huhman DV, Sumner LW. 2011. Mass spectrometry strategies in metabolomics. *Journal of Biological Chemistry* 286: 25435-25442.

Lepre CA, Moore JM, Peng JW. 2004. Theory and applications of NMR-based screening in pharmaceutical research. *Chemical Reviews* 104: 3641-3676.

Levenson JM, Roth TL, Lubin FD, Miller CA, Huang IC, Desai P, Malone LM, Sweatt JD. 2006. Evidence that DNA (cytosine-5) methyltransferase regulates synaptic plasticity in the hippocampus. *Journal of Biological Chemistry* 281: 15763-15773.

Levis NA, Yi SX, Lee RE, Jr. 2012. Mild desiccation rapidly increases freeze tolerance of the goldenrod gall fly, *Eurosta solidaginis*: evidence for drought-induced rapid cold-hardening. *Journal of Experimental Biology* 215: 3768-3773.

Lewis SE, Smallman BN. 1956. The estimation of acetylcholine in insects. *The Journal of Physiology* 134: 241-256.

Life Technologies. 2012. Amplification efficiency of TaqMan® Gene Expression Assays (Application Note): Assays tested extensively for qPCR efficiency. Life Technologies Corporation

Lima SQ, Miesenbock G. 2005. Remote control of behavior through genetically targeted photostimulation of neurons. *Cell* 121: 141-152.

Liu Y, Luo J, Carlsson MA, Nassel DR. 2015. Serotonin and insulin-like peptides modulate leucokinin-producing neurons that affect feeding and water homeostasis in *Drosophila*. *Journal of Comparative Neurology* 523: 1840-1863.

Livak KJ, Schmittgen TD. 2001. Analysis of relative gene expression data using real-time quantitative PCR and the 2(-Delta Delta C(T)) Method. *Methods* 25: 402-408.

Lopez-Arias B, Dorado B, Herrero P. 2011. Blockade of the release of the neuropeptide leucokinin to determine its possible functions in fly behavior: chemoreception assays. *Peptides* 32: 545-552.

Luan Z, Quigley C, Li HS. 2015. The putative Na+/Cl--dependent neurotransmitter/osmolyte transporter inebriated in the *Drosophila* hindgut is essential for the maintenance of systemic water homeostasis. *Scientific Reports* 5: 7993.

Ma Y, Creanga A, Lum L, Beachy PA. 2006. Prevalence of off-target effects in *Drosophila* RNA interference screens. *Nature* 443: 359-363.

MacPherson MR, Lohmann SM, Davies SA. 2004. Analysis of *Drosophila* cGMP-dependent protein kinases and assessment of their in vivo roles by targeted expression in a renal transporting epithelium. *Journal of Biological Chemistry* 279: 40026-40034.

Maddrell SHP. 1981. The functional design of the insect excretory system. *Journal of Experimental Biology* 90: 1-15.

Malmendal A, Overgaard J, Bundy JG, Sorensen JG, Nielsen NC, Loeschcke V, Holmstrup M. 2006. Metabolomic profiling of heat stress: hardening and recovery of homeostasis in *Drosophila*. *American Journal of Physiology - Regulatory, Integrative and Comparative Physiology* 291: R205-212.

Malmendal A, Sorensen JG, Overgaard J, Holmstrup M, Nielsen NC, Loeschcke V. 2013. Metabolomic analysis of the selection response of *Drosophila melanogaster* to environmental stress: are there links to gene expression and phenotypic traits? *Naturwissenschaften* 100: 417-427.

Mamai W, Mouline K, Blais C, Larvor V, Dabire KR, Ouedraogo GA, Simard F, Renault D. 2014. Metabolomic and ecdysteroid variations in *Anopheles gambiae* s.l. mosquitoes exposed to the stressful conditions of the dry season in Burkina Faso, West Africa. *Physiological and Biochemical Zoology* 87: 486-497.

Marcombe S, Darriet F, Tolosa M, Agnew P, Duchon S, Etienne M, Yp Tcha MM, Chandre F, Corbel V, Yebakima A. 2011. Pyrethroid resistance reduces the efficacy of space sprays for dengue control on the island of Martinique (Caribbean). *PLoS Neglected Tropical Diseases* 5: e1202.

Marko MA, Chipperfield R, Birnboim HC. 1982. A procedure for the large-scale isolation of highly purified plasmid DNA using alkaline extraction and binding to glass powder. *Analytical Biochemistry* 121: 382-387.

Marron MT, Markow TA, Kain KJ, Gibbs AG. 2003. Effects of starvation and desiccation on energy metabolism in desert and mesic *Drosophila*. *Journal of Insect Physiology* 49: 261-270.

Matzkin LM, Markow TA. 2009. Transcriptional regulation of metabolism associated with the increased desiccation resistance of the cactophilic *Drosophila mojavensis*. *Genetics* 182: 1279-1288.

Matzkin LM, Watts TD, Markow TA. 2009. Evolution of stress resistance in *Drosophila*: interspecific variation in tolerance to desiccation and starvation. *Functional Ecology* 23: 521-527.

Michaud MR, Benoit JB, Lopez-Martinez G, Elnitsky MA, Lee RE, Jr., Denlinger DL. 2008. Metabolomics reveals unique and shared metabolic changes in response to heat shock, freezing and desiccation in the Antarctic midge, *Belgica antarctica*. *Journal of Insect Physiology* 54: 645-655.

Michaud MR, Denlinger DL. 2007. Shifts in the carbohydrate, polyol, and amino acid pools during rapid cold-hardening and diapause-associated cold-hardening in flesh flies (*Sarcophaga crassipalpis*): a metabolomic comparison. *Journal of*

Comparative Physiology B: Biochemical, Systems, and Environmental Physiology 177: 753-763.

Morrow AL, Lagomarcino AJ, Schibler KR, Taft DH, Yu Z, Wang B, Altaye M, Wagner M, Gevers D, Ward DV, Kennedy MA, Huttenhower C, et al. 2013. Early microbial and metabolomic signatures predict later onset of necrotizing enterocolitis in preterm infants. *Microbiome* 1: 13.

Muller C, Schafer P, Stortzel M, Vogt S, Weinmann W. 2002. Ion suppression effects in liquid chromatography-electrospray-ionisation transport-region collision induced dissociation mass spectrometry with different serum extraction methods for systematic toxicological analysis with mass spectra libraries. *Journal of Chromatography B: Journal of Chromatography B: Analytical Technologies in the Biomedical and Life Sciences* 773: 47-52.

Nagatsu T, Levitt M, Udenfriend S. 1964. Tyrosine hydroxylase. The initial step in norepinephrine biosynthesis. *Journal of Biological Chemistry* 239: 2910-2917.

Naikkhwah W, O'Donnell MJ. 2011. Salt stress alters fluid and ion transport by Malpighian tubules of *Drosophila melanogaster*: evidence for phenotypic plasticity. *Journal of Experimental Biology* 214: 3443-3454.

Nation JL. 2015a. Neurophysiology In *Insect Physiology and Biochemistry*, pp. 285-308. USA: CRC Press.

Nation JL. 2015b. Nutrition In *Insect Physiology and Biochemistry*, pp. 75-98. USA: CRC Press.

Neckameyer WS, Weinstein JS. 2005. Stress affects dopaminergic signaling pathways in *Drosophila melanogaster*. *Stress* 8: 117-131.

Neven LG. 2000. Physiological responses of insects to heat. *Postharvest Biology and Technology* 21: 103-111.

Ni JQ, Liu LP, Binari R, Hardy R, Shim HS, Cavallaro A, Booker M, Pfeiffer BD, Markstein M, Wang H, Villalta C, Laverty TR, et al. 2009. A *Drosophila* resource of transgenic RNAi lines for neurogenetics. *Genetics* 182: 1089-1100.

Nitabach MN, Wu Y, Sheeba V, Lemon WC, Strumbos J, Zelensky PK, White BH, Holmes TC. 2006. Electrical hyperexcitation of lateral ventral pacemaker neurons desynchronizes downstream circadian oscillators in the fly circadian circuit and induces multiple behavioral periods. *The Journal of Neuroscience* 26: 479-489.

Nkuipou-Kenfack E, Duranton F, Gayrard N, Argiles A, Lundin U, Weinberger KM, Dakna M, Delles C, Mullen W, Husi H, Klein J, Koeck T, et al. 2014. Assessment of metabolomic and proteomic biomarkers in detection and prognosis of progression of renal function in chronic kidney disease. *PLoS One* 9: e96955.

O'Donnell MJ. 2009. Too much of a good thing: how insects cope with excess ions or toxins in the diet. *Journal of Experimental Biology* 212: 363-372.

O'Donnell MJ, Dow JA, Huesmann GR, Tublitz NJ, Maddrell SH. 1996. Separate control of anion and cation transport in malpighian tubules of *Drosophila Melanogaster*. *Journal of Experimental Biology* 199: 1163-1175.

O'Donnell MJ, Maddrell SHP, Gardiner BOC. 1983. Transport of uric acid by the Malpighian tubules of *Rhodnius prolixus* and other insects. *Journal of Experimental Biology* 103: 169-184.

O'Donnell MJ, Rheault MR, Davies SA, Rosay P, Harvey BJ, Maddrell SH, Kaiser K, Dow JA. 1998. Hormonally controlled chloride movement across *Drosophila* tubules is via ion channels in stellate cells. *The American Journal of Physiology* 274: R1039-1049.

O'Kane CJ, Gehring WJ. 1987. Detection in situ of genomic regulatory elements in *Drosophila*. *Proceedings of the National Academy of Sciences of the United States of America* 84: 9123-9127.

O'Kane C. 2011. *Drosophila* as a model organism for the study of neuropsychiatric disorders In *Molecular and Functional Models in Neuropsychiatry*, ed. JJ Hagan, pp. 37-60: Springer Berlin Heidelberg.

Oliveira CM, Auad AM, Mendes SM, Frizzas MR. 2014. Crop losses and the economic impact of insect pests on Brazilian agriculture. *Crop Protection* 56: 50-54.

Oliver SG, Winson MK, Kell DB, Baganz F. 1998. Systematic functional analysis of the yeast genome. *Trends in Biotechnology* 16: 373-378.

Olsen JV, de Godoy LM, Li G, Macek B, Mortensen P, Pesch R, Makarov A, Lange O, Horning S, Mann M. 2005. Parts per million mass accuracy on an Orbitrap mass spectrometer via lock mass injection into a C-trap. *Molecular & Cellular Proteomics* 4: 2010-2021.

Olsson K-E, Saltin B. 1970. Variation in total body water with muscle glycogen changes in man. *Acta Physiologica Scandinavica* 80: 11-18.

Overgaard J, Malmendal A, Sorensen JG, Bundy JG, Loeschcke V, Nielsen NC, Holmstrup M. 2007. Metabolomic profiling of rapid cold hardening and cold shock in *Drosophila melanogaster*. *Journal of Insect Physiology* 53: 1218-1232.

Overgaard J, Sørensen JG. 2008. Rapid thermal adaptation during field temperature variations in *Drosophila melanogaster*. *Cryobiology* 56: 159-162.

Palanker L, Tennessen JM, Lam G, Thummel CS. 2009. *Drosophila* HNF4 regulates lipid mobilization and beta-oxidation. *Cell Metabolism* 9: 228-239.

Park D, Veenstra JA, Park JH, Taghert PH. 2008. Mapping peptidergic cells in *Drosophila*: where DIMM fits in. *PLoS One* 3: e1896.

Parker CE, Warren MR, Mocanu V. 2010. Mass spectrometry for proteomics In *Neuroproteomics*, ed. O Alzate. Florida: CRC Press.

Patti GJ, Yanes O, Siuzdak G. 2012. Innovation: metabolomics: the apogee of the omics trilogy. *Nature Reviews Molecular Cell Biology* 13: 263-269.

Pauling L, Robinson AB, Teranishi R, Cary P. 1971. Quantitative analysis of urine vapor and breath by gas-liquid partition chromatography. *Proceedings of the National Academy of Sciences of the United States of America* 68: 2374-2376.

Pedersen KS, Kristensen TN, Loeschcke V, Petersen BO, Duus JO, Nielsen NC, Malmendal A. 2008. Metabolomic signatures of inbreeding at benign and stressful temperatures in *Drosophila melanogaster*. *Genetics* 180: 1233-1243.

Pfaffl MW. 2001. A new mathematical model for relative quantification in real-time RT-PCR. *Nucleic Acids Research* 29: e45.

Pfeiffer BD, Jenett A, Hammonds AS, Ngo TT, Misra S, Murphy C, Scully A, Carlson JW, Wan KH, Laverty TR, Mungall C, Svirskas R, et al. 2008. Tools for neuroanatomy and neurogenetics in *Drosophila*. *Proceedings of the National Academy of Sciences of the United States of America* 105: 9715-9720.

Poupardin R, Riaz MA, Vontas J, David JP, Reynaud S. 2010. Transcription profiling of eleven cytochrome P450s potentially involved in xenobiotic metabolism in the mosquito *Aedes aegypti*. *Insect Molecular Biology* 19: 185-193.

Predel R, Wegener C, Russell WK, Tichy SE, Russell DH, Nachman RJ. 2004. Peptidomics of CNS-associated neurohemal systems of adult *Drosophila melanogaster*: a mass spectrometric survey of peptides from individual flies. *Journal of Comparative Neurology* 474: 379-392.

Prestrelski SJ, Tedeschi N, Arakawa T, Carpenter JF. 1993. Dehydration-induced conformational transitions in proteins and their inhibition by stabilizers. *Biophysical Journal* 65: 661-671.

Price DP, Schilkey FD, Ulanov A, Hansen IA. 2015. Small mosquitoes, large implications: crowding and starvation affects gene expression and nutrient accumulation in *Aedes aegypti*. *Parasites & Vectors* 8: 252.

Prince GJ, Parsons PA. 1977. Adaptive behaviour of *Drosophila* adults in relation to temperature and humidity. *Australian Journal of Zoology* 25: 285-290.

Radford JC, Davies SA, Dow JA. 2002. Systematic G-protein-coupled receptor analysis in *Drosophila melanogaster* identifies a leucokinin receptor with novel roles. *Journal of Biological Chemistry* 277: 38810-38817.

Radford JC, Terhzaz S, Cabrero P, Davies SA, Dow JA. 2004. Functional characterisation of the *Anopheles* leucokinins and their cognate G-protein coupled receptor. *Journal of Experimental Biology* 207: 4573-4586.

Ramniwas S, Kajla B. 2013. Dehydration tolerance: a mode of adaptation in two related *Drosophila* species of the repleta subgroup from western Himalayas. *Ethology Ecology & Evolution* 27: 17-28.

Ramsay JA. 1954. Active transport of water by the Malpighian tubules of the stick insect, *Dixippus-morosus* (Orthoptera, Phasmidae). *Journal of Experimental Biology* 31: 104-113.

Ranson H, Burhani J, Lumjuan N, Black WC. 2010. Insecticide resistance in dengue disease vectors. *TropIKAnet Journal* 1

Reagan JD. 1995. Functional expression of a diuretic hormone receptor in baculovirus-infected insect cells: evidence suggesting that the N-terminal region of diuretic hormone is associated with receptor activation. *Insect Biochemistry and Molecular Biology* 25: 535-539.

Reyes-DelaTorre A, Peña-Rangel MR, Riesgo-Escovar JR. 2012. Carbohydrate metabolism in *Drosophila*: reliance on the disaccharide trehalose In

Carbohydrates - Comprehensive Studies on Glycobiology and Glycotechnology, ed. C-F Chang: InTech.

Riemensperger T, Isabel G, Coulom H, Neuser K, Seugnet L, Kume K, Iche-Torres M, Cassar M, Strauss R, Preat T, Hirsh J, Birman S. 2011. Behavioral consequences of dopamine deficiency in the *Drosophila* central nervous system. *Proceedings of the National Academy of Sciences of the United States of America* 108: 834-839.

Rion S, Kawecki TJ. 2007. Evolutionary biology of starvation resistance: what we have learned from *Drosophila*. *Journal of Evolutionary Biology* 20: 1655-1664.

Roberts LD, Souza AL, Gerszten RE, Clish CB. 2012. Targeted metabolomics. *Current Protocols in Molecular Biology* Chapter 30: Unit 30 32 31-24.

Rosay P, Davies SA, Yu Y, Sozen MA, Kaiser K, Dow JA. 1997. Cell-type specific calcium signalling in a *Drosophila* epithelium. *Journal of Cell Science* 110 (Pt 15): 1683-1692.

Rota-Stabelli O, Blaxter M, Anfora G. 2013. *Drosophila suzukii*. *Current Biology* 23: R8-9.

Roth TL, Lubin FD, Funk AJ, Sweatt JD. 2009. Lasting epigenetic influence of early-life adversity on the BDNF gene. *Biological Psychiatry* 65: 760-769.

Rothman KJ. 1990. No adjustments are needed for multiple comparisons. *Epidemiology* 1: 43-46.

Rubin GM, Spradling AC. 1982. Genetic transformation of *Drosophila* with transposable element vectors. *Science* 218: 348-353.

Ruiz-Sanchez E, O'Donnell MJ. 2015. The insect excretory system as a target for novel pest control strategies. *Current Opinion in Insect Science* 11: 14-20.

Rutledge RG, Cote C. 2003. Mathematics of quantitative kinetic PCR and the application of standard curves. *Nucleic Acids Research* 31: e93.

Ryan D, Robards K. 2006. Analytical chemistry considerations in plant metabolomics. *Separation & Purification Reviews* 35: 319-356.

Sacktor B. 1965. Energetics and the respiratory metabolism of muscular contraction In *The Physiology of Insects*, ed. M Rockstein, pp. 483-580. New York: Academic Press.

Salisbury JP, Boggio KJ, Hsu YW, Quijada J, Sivachenko A, Gloeckner G, Kowalski PJ, Easterling ML, Rosbash M, Agar JN. 2013. A rapid MALDI-TOF mass spectrometry workflow for *Drosophila melanogaster* differential neuropeptidomics. *Molecular Brain* 6: 60.

Sambrook J, Russell D. 2001. *Molecular cloning: a laboratory manual*. Cold Spring Harbor, N.Y., USA: Cold Spring Harbor Laboratory Press.

Sarup P, Pedersen SM, Nielsen NC, Malmendal A, Loeschcke V. 2012. The metabolic profile of long-lived *Drosophila melanogaster*. *PLoS One* 7: e47461.

Sarup P, Sorensen JG, Kristensen TN, Hoffmann AA, Loeschcke V, Paige KN, Sorensen P. 2011. Candidate genes detected in transcriptome studies are strongly dependent on genetic background. *PLoS One* 6: e15644.

Saville DJ. 1990. Multiple comparison procedures: the practical solution. *The American Statistician* 44: 174-180.

Scheltema RA, Jankevics A, Jansen RC, Swertz MA, Breitling R. 2011. PeakML/mzMatch: a file format, Java library, R library, and tool-chain for mass spectrometry data analysis. *Analytical Chemistry* 83: 2786-2793.

Schmidt PS, Matzkin L, Ippolito M, Eanes WF. 2005. Geographic variation in diapause incidence, life-history traits, and climatic adaptation in *Drosophila melanogaster*. *Evolution* 59: 1721-1732.

Schmidt-Nielsen K. 1997. Energy metabolism In *Animal Physiology: Adaptation and Environment*, pp. 169-214. Cambridge: Cambridge University Press.

Schmittgen TD, Livak KJ. 2008. Analyzing real-time PCR data by the comparative C(T) method. *Nature Protocols* 3: 1101-1108.

Schneider CA, Rasband WS, Eliceiri KW. 2012. NIH Image to ImageJ: 25 years of image analysis. *Nature Methods* 9: 671-675.

Schneider D. 2000. Using *Drosophila* as a model insect. *Nature Reviews Genetics* 1: 218-226.

Schoofs L, Baggerman G. 2003. Peptidomics in *Drosophila melanogaster*. *Briefings in Functional Genomics and Proteomics* 2: 114-120.

Schooley DA, Horodyski FM, Coast GM. 2011. Hormones controlling homeostasis in insects In *Insect Endocrinology*, pp. 366-429. California, USA: Academic Press.

Schwasinger-Schmidt TE, Kachman SD, Harshman LG. 2012. Evolution of starvation resistance in *Drosophila melanogaster:* measurement of direct and correlated responses to artificial selection. *Journal of Evolutionary Biology* 25: 378-387.

Seger C, Sturm S. 2007. Analytical aspects of plant metabolite profiling platforms: current standings and future aims. *Journal of Proteome Research* 6: 480-497.

Seinen E, Burgerhof JG, Jansen RC, Sibon OC. 2011. RNAi-induced off-target effects in *Drosophila melanogaster*: frequencies and solutions. *Briefings in Functional Genomics* 10: 206-214.

Sharmila Bharathi N, Prasad NG, Shakarad M, Joshi A. 2003. Variation in adult life history and stress resistance across five species of *Drosophila*. *Journal of Genetics* 82: 191-205.

Sisodia S, Singh BN. 2010. Resistance to environmental stress in *Drosophila ananassae*: latitudinal variation and adaptation among populations. *Journal of Evolutionary Biology* 23: 1979-1988.

Smith CA, Want EJ, O'Maille G, Abagyan R, Siuzdak G. 2006. XCMS: processing mass spectrometry data for metabolite profiling using nonlinear peak alignment, matching, and identification. *Analytical Chemistry* 78: 779-787.

Snart CJP, Hardy ICW, Barrett DA. 2015. Entometabolomics: applications of modern analytical techniques to insect studies. *Entomologia Experimentalis et Applicata* 155: 1-17.

Soderberg JA, Birse RT, Nassel DR. 2011. Insulin production and signaling in renal tubules of *Drosophila* is under control of tachykinin-related peptide and regulates stress resistance. *PLoS One* 6: e19866.

Sofia Hernandez C, Gonzalez E, Whittembury G. 1995. The paracellular channel for water secretion in the upper segment of the Malpighian tubule of *Rhodnius prolixus*. *Journal of Membrane Biology* 148: 233-242.

Sorensen JG, Nielsen MM, Loeschcke V. 2007. Gene expression profile analysis of *Drosophila melanogaster* selected for resistance to environmental stressors. *Journal of Evolutionary Biology* 20: 1624-1636.

Sozen MA, Armstrong JD, Yang M, Kaiser K, Dow JA. 1997. Functional domains are specified to single-cell resolution in a *Drosophila* epithelium. *Proceedings of the National Academy of Sciences of the United States of America* 94: 5207-5212.

Sperlagh B, Doda M, Baranyi M, Hasko G. 2000. Ischemic-like condition releases norepinephrine and purines from different sources in superfused rat spleen strips. *Journal of Neuroimmunology* 111: 45-54.

Steele JE. 1981. The role of carbohydrate metabolism in physiological function In *Energy Metabolism in Insects*, ed. RGH Downer, pp. 101-116. New York: Springer US.

Stergiopoulos K, Cabrero P, Davies SA, Dow JA. 2009. Salty dog, an SLC5 symporter, modulates *Drosophila* response to salt stress. *Physiological Genomics* 37: 1-11.

Stinziano JR, Sove RJ, Rundle HD, Sinclair BJ. 2015. Rapid desiccation hardening changes the cuticular hydrocarbon profile of *Drosophila melanogaster*. *Comparative Biochemistry and Physiology Part A: Molecular & Integrative Physiology* 180: 38-42.

Sugahara K, Zhang J Fau - Kodama H, Kodama H. 1994. Liquid chromatographic-mass spectrometric analysis of N-acetylamino acids in human urine. *Journal of Chromatography B: Biomedical Sciences and Applications* 657: 15-21.

Sullivan DT, Bell LA, Paton DR, Sullivan MC. 1980. Genetic and functional analysis of tryptophan transport in Malpighian tubules of *Drosophila*. *Biochemical Genetics* 18: 1109-1130.

Taghert PH, Nitabach MN. 2012. Peptide neuromodulation in invertebrate model systems. *Neuron* 76: 82-97.

Tautenhahn R, Cho K, Uritboonthai W, Zhu Z, Patti GJ, Siuzdak G. 2012. An accelerated workflow for untargeted metabolomics using the METLIN database. *Nature Biotechnology* 30: 826-828.

Taylor RC, Webb Robertson BJ, Markillie LM, Serres MH, Linggi BE, Aldrich JT, Hill EA, Romine MF, Lipton MS, Wiley HS. 2013. Changes in translational

efficiency is a dominant regulatory mechanism in the environmental response of bacteria. *Integrative Biology* 5: 1393-1406.

Tearle R. 1991. Tissue specific effects of ommochrome pathway mutations in *Drosophila melanogaster*. *Genetics Research* 57: 257-266.

Teets NM, Denlinger DL. 2013. Physiological mechanisms of seasonal and rapid cold-hardening in insects. *Physiological Entomology* 38: 105-116.

Teets NM, Peyton JT, Colinet H, Renault D, Kelley JL, Kawarasaki Y, Lee RE, Jr., Denlinger DL. 2012. Gene expression changes governing extreme dehydration tolerance in an Antarctic insect. *Proceedings of the National Academy of Sciences of the United States of America* 109: 20744-20749.

Telonis-Scott M, Gane M, DeGaris S, Sgro CM, Hoffmann AA. 2012. High resolution mapping of candidate alleles for desiccation resistance in *Drosophila melanogaster* under selection. *Molecular Biology and Evolution* 29: 1335-1351.

Telonis-Scott M, Guthridge KM, Hoffmann AA. 2006. A new set of laboratory-selected *Drosophila melanogaster* lines for the analysis of desiccation resistance: response to selection, physiology and correlated responses. *Journal of Experimental Biology* 209: 1837-1847.

Tepass U, Tanentzapf G, Ward R, Fehon R. 2001. Epithelial cell polarity and cell junctions in *Drosophila*. *Annual Review of Genetics* 35: 747-784.

Terhzaz S, Cabrero P, Brinzer RA, Halberg KA, Dow JA, Davies SA. 2015a. A novel role of *Drosophila* cytochrome P450-4e3 in permethrin insecticide tolerance. *Insect Biochemistry and Molecular Biology* 67: 38-46.

Terhzaz S, Cabrero P, Chintapalli VR, Davies SA, Dow JA. 2010. Mislocalization of mitochondria and compromised renal function and oxidative stress resistance in *Drosophila* SesB mutants. *Physiological Genomics* 41: 33-41.

Terhzaz S, Cabrero P, Robben JH, Radford JC, Hudson BD, Milligan G, Dow JA, Davies SA. 2012. Mechanism and function of *Drosophila* capa GPCR: a desiccation stress-responsive receptor with functional homology to human neuromedinU receptor. *PLoS One* 7: e29897.

Terhzaz S, O'Connell FC, Pollock VP, Kean L, Davies SA, Veenstra JA, Dow JA. 1999. Isolation and characterization of a leucokinin-like peptide of *Drosophila melanogaster*. *Journal of Experimental Biology* 202: 3667-3676.

Terhzaz S, Overend G, Sebastian S, Dow JA, Davies SA. 2014. The *D. melanogaster* capa-1 neuropeptide activates renal NF-kB signaling. *Peptides* 53: 218-224.

Terhzaz S, Teets NM, Cabrero P, Henderson L, Ritchie MG, Nachman RJ, Dow JA, Denlinger DL, Davies SA. 2015b. Insect capa neuropeptides impact desiccation and cold tolerance. *Proceedings of the National Academy of Sciences of the United States of America* 112: 2882-2887.

Thomas A, Lee PJ, Dalton JE, Nomie KJ, Stoica L, Costa-Mattioli M, Chang P, Nuzhdin S, Arbeitman MN, Dierick HA. 2012. A versatile method for cell-specific profiling of translated mRNAs in *Drosophila*. *PLoS One* 7

Tilghman JA, Geer BW. 1988. The effects of a choline deficiency on the lipid composition and ethanol tolerance of *Drosophila melanogaster*. *Comparative Biochemistry and Physiology Part C: Comparative Pharmacology and Toxicology* 90: 439-444.

Tomcala A, Tollarova M, Overgaard J, Simek P, Kostal V. 2006. Seasonal acquisition of chill tolerance and restructuring of membrane glycerophospholipids in an overwintering insect: triggering by low temperature, desiccation and diapause progression. *Journal of Experimental Biology* 209: 4102-4114.

Treherne JE, Willmer PG. 1975. Hormonal control of integumentary water-loss: evidence for a novel neuroendocrine system in an insect (*Periplaneta americana*). *Journal of Experimental Biology* 63: 143-159.

Ueno T, Tomita J, Kume S, Kume K. 2012. Dopamine modulates metabolic rate and temperature sensitivity in *Drosophila melanogaster*. *PLoS One* 7: e31513.

Van Coster RN, Gerlo EA, Giardina TG, Engelke UF, Smet JE, De Praeter CM, Meersschaut VA, De Meirleir LJ, Seneca SH, Devreese B, Leroy JG, Herga S, et al. 2005. Aminoacylase I deficiency: A novel inborn error of metabolism. *Biochemical and Biophysical Research Communications* 338: 1322-1326.

Van Wielendaele P, Dillen S, Marchal E, Badisco L, Vanden Broeck J. 2012. CRF-like diuretic hormone negatively affects both feeding and reproduction in the desert locust, *Schistocerca gregaria*. *PLoS One* 7: e31425.

Vanden Broeck J. 2001. Neuropeptides and their precursors in the fruitfly, *Drosophila melanogaster*. *Peptides* 22: 241-254.

Vogel C, Marcotte EM. 2012. Insights into the regulation of protein abundance from proteomic and transcriptomic analyses. *Nature Reviews Genetics* 13: 227-232.

Walsh DB, Bolda MP, Goodhue RE, Dreves AJ, Lee J, Bruck DJ, Walton VM, Neal SD, Zalom FG. 2011. *Drosophila suzukii* (Diptera: Drosophilidae): Invasive Pest of Ripening Soft Fruit Expanding its Geographic Range and Damage Potential. *Journal of Integrated Pest Management* 2: G1-G7.

Wang J, Kean L, Yang J, Allan AK, Davies SA, Herzyk P, Dow JA. 2004. Function-informed transcriptome analysis of *Drosophila* renal tubule. *Genome Biology* 5: R69.

Want EJ, Nordstrom A, Morita H, Siuzdak G. 2007. From exogenous to endogenous: the inevitable imprint of mass spectrometry in metabolomics. *Journal of Proteome Research* 6: 459-468.

Waters JC. 2009. Accuracy and precision in quantitative fluorescence microscopy. *The Journal of Cell Biology* 185: 1135-1148.

Watson DG. 2013. A rough guide to metabolite identification using high resolution liquid chromatography mass spectrometry in metabolomic profiling in metazoans. *Computational and Structural Biotechnology Journal* 4: e201301005.

Wessing AD, Eichelberg D. 1978. *Malpighian tubules, rectal papillae and excretion*. London: Academic Press.

Wieczorek H, Putzenlechner M, Zeiske W, Klein U. 1991. A vacuolar-type proton pump energizes K+/H+ antiport in an animal plasma membrane. *Journal of Biological Chemistry* 266: 15340-15347.

Williams AE, Rose MR, Bradley TJ. 2004. The respiratory pattern in *Drosophila melanogaster* selected for desiccation resistance is not associated with the observed evolution of decreased locomotory activity. *Physiological and Biochemical Zoology* 77: 10-17.

Williams CM, Watanabe M, Guarracino MR, Ferraro MB, Edison AS, Morgan TJ, Boroujerdi AF, Hahn DA. 2014. Cold adaptation shapes the robustness of metabolic networks in *Drosophila melanogaster*. *Evolution* 68: 3505-3523.

Williams JB, Lee RE, Jr. 2011. Effect of freezing and dehydration on ion and cryoprotectant distribution and hemolymph volume in the goldenrod gall fly, *Eurosta solidaginis*. *Journal of Insect Physiology* 57: 1163-1169.

Wishart DS, Jewison T, Guo AC, Wilson M, Knox C, Liu Y, Djoumbou Y, Mandal R, Aziat F, Dong E, Bouatra S, Sinelnikov I, et al. 2013. HMDB 3.0--The human metabolome database in 2013. *Nucleic Acids Research* 41: D801-807.

Withers PC. 1992. *Comparative animal physiology*. New York: Saunders College Publishing.

World Health Organisation. 2012. Dengue and severe dengue: fact sheet N°117.

Wu DS, Beyenbach KW. 2003. The dependence of electrical transport pathways in Malpighian tubules on ATP. *Journal of Experimental Biology* 206: 233-243.

Wu G. 2009. Amino acids: metabolism, functions, and nutrition. *Amino Acids* 37: 1-17.

Xu K, Zheng X, Sehgal A. 2008. Regulation of feeding and metabolism by neuronal and peripheral clocks in *Drosophila*. *Cell Metabolism* 8: 289-300.

Xue R, Lin Z, Deng C, Dong L, Liu T, Wang J, Shen X. 2008. A serum metabolomic investigation on hepatocellular carcinoma patients by chemical derivatization followed by gas chromatography/mass spectrometry. *Rapid Communications in Mass Spectrometry* 22: 3061–3068.

Yellman C, Tao H, He B, Hirsh J. 1997. Conserved and sexually dimorphic behavioral responses to biogenic amines in decapitated *Drosophila*. *Proceedings of the National Academy of Sciences of the United States of America* 94: 4131-4136.

Zhang R, Zhang T, Korzekwa D, Al-Johani S, A.T. Dow J, G. Watson D. 2014. A comparison of the metabolome of male and female *Drosophila melanogaster*. *Current Metabolomics* 2: 174-183.

Zhao Y, Bretz CA, Hawksworth SA, Hirsh J, Johnson EC. 2010. Corazonin neurons function in sexually dimorphic circuitry that shape behavioral responses to stress in *Drosophila*. *PLoS One* 5: e9141.

Zubarev RA, Makarov A. 2013. Orbitrap mass spectrometry. *Analytical Chemistry* 85: 5288-5296.